CHEMICAL INVESTIGATIONS OF MARINE CYANOBACTERIA. THE SEARCH FOR NEW ANTICANCER AGENTS FROM THE SEA.

A DISSERTATION SUBMITTED TO THE GRADUATE DIVISION OF THE UNIVERSITY OF HAWAI'I IN PARTIAL FULFILLMENT OF THE REQUIREMENTS FOR THE DEGREE

DOCTOR OF PHILOSOPHY

IN

CHEMISTRY

AUGUST 2003

By
Philip Williams

Dissertation Committee:

Richard E. Moore, Chairperson
Thomas K. Hemscheidt
Katja Michael
Marcus A. Tius
Michael Cooney

Acknowledgments

I would like to thank Professor Richard E. Moore for the opportunity to participate in his research group, and for his support and guidance over the last few years. I would also like to thank my other committee members for their interest in my development, their availability, and their criticisms. A special thanks to Professor Thomas K. Hemscheidt for his continued interest in my development as a scientist, despite the fact I still have not yet read a novel that was written by Joseph Conrad. Thanks also to our collaborators Valerie Paul and Thomas Corbett for the collecting and the screening of the extracts, respectively. Former members of the Moore group, Julie Becker and Dr. Dietmar Hoffmann, also deserve my thanks for the multitude of smiles they brought to my face during the times we shared. A special thanks to my former lab mate Dr. Hendrik Luesch for his comments, his ability to make me laughter, and his stereo that sustained me in the year following his departure.

This work could not have been completed without the assistance of many people. Dr. George Harrigan, Dr. Adrian Franke, Laurie Cluster, and Mike Burger, all provided valuable mass spectrometry data. I am grateful to Mike Lieberman, Sue Mooberry, and especially Georgia Tien for the bioassay data. Finally, I shall forever be in debt to Wesley Yoshida for his advice on many of the compounds in this dissertation, for his friendship, and for the vast stream of NMR data he has provided me with.

Abstract

Eighteen strains of marine cyanobacteria belonging to the genera *Symploca* and *Lyngbya,* which showed activity against multidrug resistant solid tumors, were examined for cytotoxins. This resulted in the isolation and identification of 11 known and 15 new secondary metabolites from extracts collected in Micronesia. The structures of these metabolites were determined through a variety of NMR techniques (TOCSY, HMBC, HSQC, COSY, ROESY, and NOESY) and/or chemical degradation. Most of the compounds isolated were of mixed peptide-polyketide biogenesis.

The two most potent cytotoxins discovered were the depsipeptides palau'amide and lyngbyastatin 3. The latter was shown to be a potent microfilament disruptor, but was poorly tolerated in vivo. Chemical degradation of the latter series of compounds demonstrated they were mixtures of epimers in the acid sensitive 4-amino-3-oxo-2,2-dimethylpentanoic acid unit, and not single compounds as recently suggested.

Lyngbyastatin 3 and lyngbyabellin D are analogues of compounds isolated from the sea hare *Dolabella auricularia.* The isolation of lyngbyastatin 3 and lyngbyabellin D from marine cyanobacteria supports the proposal that many of the compounds isolated from this sea hare are of cyanobacterial origin.

Table of Contents

List of Figures/Illustrations

List of Figures/Illustrations

List of Abbreviations

Å	ångström
$[\alpha]^T_D$	specific optical rotation at 589 nm and temperature T in °C
Ac	acetyl
AD	asymmetric dihydroxylation
Adhpa	4-amino-2,2-dimethyl-3-hydroxypentanoic acid
Ahp	3-amino-6-hydroxypiperidone
Ahppa	4-amino-3-hydroxy-5-phenylpentanoic acid
Amha	3-amino-2-methylhexanoic acid
AMO	3-amino-2-methyl-7-octynoic acid
Amu	atomic mass units
Apa	3-aminopentanoic acid
BBr_3	boron tribromide
BPO	bromoperoxidase
Bn	benzyl
Br	broad
c	concentration in g/100 mL
°C	degrees Celsius
C_8	octyl
C_{18}	octadecyl
C38	colon adenocarcinoma C38
calcd	calculated
COSY	correlation spectroscopy

C-terminus	carboxyl terminus
1D	one-dimensional
2D	two-dimensional
3D	three-dimensional
d	doublet
D	configurational descriptor (Fisher system)
δ	chemical shift (in ppm)
D. auricularia	*Dolabella auricularia*
DCC	1,3-dicyclohexanecarbodiimide
dd	doublet of doublets
ddd	doublet of doublet of doublets
Dddd	5,7-dihydroxy-2,6-dimethyldodec-2-en-11-ynoic acid
DEPT	distortionless excitation by polarization transfer
DG	distance geometry
Dhmp	2,3-dihydroxy-3-methylpentanoic acid
DMAP	4-(dimethylamino)pyridine
DMSO	dimethyl sulfoxide
dq	doublet of quartets
dt	doublet of triplets
DTT	dithiothreitol
E	entegen (descriptor in Cahn-Ingold-Prelong system)
EC_{50}	effective concentration 50 %
EDCI	1-(dimethylaminopropyl)-3-ethylcarbodiimide

ESI	electrospray ionization
Et	ethyl
FAB	fast atom bombardment
FABMS	fast atom bombardment mass spectrometry
FDLA	1-fluoro-2,4-dinitrophenyl-5-leucinamide
GC	gas chromatography
H_{ax}	methylene proton in the axial position of a 6-membered ring
H_{eq}	methylene proton in the equatorial position of a 6-membered ring
Hex	hexyl
Hiva	hydroxyisovaleric acid
HMBC	heteronuclear multiple bond correlation
HMQC	heteronuclear multiple quantum coherence
HPLC	high performance liquid chromatography
HR-FABMS	high-resolution FABMS
HR-MALDI	high-resolution MALDI
HR-MS	high-resolution MS
HSQC	heteronuclear single quantum coherence
$H\text{-}X_D$	downfield proton of the diastereotopic methylene X
$H\text{-}X_U$	upfield proton of the diastereotopic methylene X
Hz	hertz
Ibu	4-amino-2,2-dimethyl-3-oxo-pentanoic acid
IC_{50}	inhibitory concentration 50 %
i-Pr	isopropyl

IR	infrared
^nJ	coupling constant via *n* bonds
KB	human nasopharyngeal cell line KB
KHMDS	potassium hexamethyldisilazane, potassium bis(trimethylsilyl)amide
L	configurational descriptor (Fisher system)
L	leukemia
L1210	murine leukemia 1210
L. bouillonii	*Lyngbya bouillonii*
LC	liquid chromatography
LDA	lithium diisopropylamide
L. majuscula	*Lyngbya majuscula*
m	multiplet
M^+	molecular ion
MALDI	matrix-assisted laser desorption ionization
MAP	3-amino-2-methylpentanoic acid
m-CBPA	*meta*-chloroperoxybenzoic acid
Me	methyl
MeCN	acetonitrile
MHz	megahertz
MPA	α-methoxyphenylacetic acid
MS	mass spectrometry
MS/MS	Tandem mass spectrometry
MTPA	α-methoxy-α-trifluorophenylacetic acid

m/z	mass/charge
n-Bu	*n*-butyl
NMR	nuclear magnetic resonance
NOE	nuclear Overhauser effect
NOESY	nuclear Overhauser effect spectroscopy
NRPS	non-ribosomal peptide synthetase
N-terminus	amino terminus
ODS	octadecyl silane
PCC	pyridinium chlorochromate
PDC	pyridinium dichromate
ppm	part per million
q	quartet
qd	quartet of doublets
QD	Latin *quaque die*, daily
R	rectus (descriptor in Cahn-Ingold-Prelog system)
R_f	retention factor
RP	reversed phase
ROESY	rotating frame nuclear Overhauser effect spectroscopy
s	singlet
S	sinister (descriptor in Cahn-Ingold-Prelog system)
SAM	*S*-adenosylmethionine
S. hydnoides	*Symploca hydnoides*
sp.	species (singular)

spp.	species (plural)
ST	solid tumor
t	triplet
T/C	tumor burden of treated group/tumor burden of control group, in % (measurement of tumor growth inhibition)
TFA	trifluoroacetic acid
THF	tetrahydrofuran
thz	thiazole
TOCSY	total correlation spectroscopy
TOF	time of flight
t_R	retention time
TSCl	*p*-toluenesulphonyl chloride
UV	ultraviolet
vis	visible
Z	zusammen (descriptor in Cahn-Ingold-Prelong system)

1.1 INTRODUCTION

1.1.1 Marine Natural Products

Man and Nature have had a complex relationship throughout the development of human culture. For most of man's history, the study of Nature and medicine were, for all practical purposes, synonymous fields of knowledge. The shaman, or witch doctor, treated illnesses armed with a combination of spiritualism and knowledge of the pharmacological properties of the surrounding flora. Even today approximately 80 % of the world's population still relies primarily on these traditional medicines for their health care.[1]

The discovery of penicillin from *Penicillium notatum* in the 1940s ushered in the "Golden Age" of antibiotics and intensified investigations into Nature as a source of novel bioactive agents. Since then terrestrial microorganisms have proven to be a prolific source of structurally diverse bioactive metabolites and have yielded some of the most important products of the drug industry, including the penicillins, aminoglycosides, tetracyclines, cephalosporins, and other classes of antibiotics that have revolutionized modern science.[1]

Serious investigations into natural products from marine organisms started in the middle of the twentieth-century. The first notable discovery was the isolation of the C-nucleosides spongouridine and spongothymidine from the Caribbean sponge *Cryptotheca crypta* in the early 1950s.[2] Studies on synthetic analogues of these compounds eventually led to the development of cytosine arabinoside as a clinically useful anticancer agent approximately 15-years later.[3] Several more drug candidates derived from marine sources

are currently in cancer clinical trials (Table 1), signaling the great potential for drug discovery from the ocean.

Table 1. Marine-Derived Experimental Anticancer Agents[3]

Metabolite	Organism	Group	Location
Didemnin B	Tunicate	*Tridemnum solidum*	Caribbean
Bryostatin 1	Bryozoan	*Bugula neritina*	Gulf of California
Ecteinascidin-743	Tunicate	*Ecteinascidia turbinate*	Caribbean
Halichondrin B	Sponge	*Halichondria okadai*	Okinawa
Dolastatin 10	Nudibranch	*Dolabella auricularia*	Indian Ocean
Halomon	Red alga	*Portieria hornemannii*	Philippines
Aplidine	Tunicate	*Aplidium albicans*	Mediterranean
Aplyronine A	Nudibranch	*Aplysia kurodai*	Japan
Kahalalide F	Mollusk	*Elysia rufescens*	Hawaii
Mycaperoxide B	Sponge	*Mycale* sp.	Thailand
Thiocoraline	Actinomycete	*Micromonospora marina*	Mozambique Strait
Granulatimide	Tunicate	*Didemnum granulatum*	Brazil

As of 2001, over 13,000 secondary metabolites have been identified[4] and approximately 300 patents[5] issued on bioactive marine natural products. The majority of these compounds have been discovered in extracts of invertebrates such as sponges, mollusks, bryozoans, and tunicates, but since the middle of the 1980s mounting evidence has suggested that marine microorganisms, such as bacteria, fungi, and cyanobacteria, might be the true producers of many of these compounds.[6] This has been suggested to be the case with the sea hare isolate dolastatin 10 (Table 1) since a recent collection of the cyanobacterium *Symploca* sp. afforded this compound in approximately 10^4 times higher yield than obtained from the nudibranch.

The discovery that microorganisms may be responsible for many of these compounds was significant for a number of reasons. Field-collected samples of the natural producer have often yielded only a milligram of each cytotoxin. Even this minute amount often was many orders of magnitude greater than was available from organisms that acquire the compounds through diet.[7] This disparity has led to collections of large quantities of invertebrates, which could have had devastating ecological effects,[8] in order to isolate sub-milligram quantities of chemical agents that were more readily available from microorganisms. Also, culturing of these microorganisms, currently possibly in 1-10 % of the cases, provides a relatively inexpensive solution to the demand for large quantities of these agents needed for clinical trials.

1.1.2 Importance of Cyanobacteria

Cyanobacteria are an ancient and diverse group of microorganisms that are known to be the evolutionary origin of chloroplasts,[9] which are found in all plants and eukaryotic algae. They are able to inhabit and thrive in an incredible variety of environments, in part because of their ability to produce a rich range of secondary metabolites. In fact it is estimated that the genes responsible for the production of these secondary metabolites utilize approximately 10 % of the cyanobacterial genome.[10] The exact reason for this is unknown, but since only organisms that do not have an immune system are prolific producers of secondary metabolites, one hypothesis is that the secondary metabolites provide an alternative defense mechanism and thus an evolutionary edge over the competition.[11]

Historically, the secondary metabolites from cyanobacteria have been associated with the poisoning of cattle and humans,[12] but the medicinal qualities of cyanobacteria

were recognized as early as 1500 BC, when *Nostoc* species were used to treat gout, fistula, and several forms of cancer.[13] Investigations, over the last few decades, have shown that cyanobacterial metabolites exhibited a broad array of biological activities, including antibiotic, antiviral, antifungal, anticancer, and a wide variety of proteinase-inhibiting activity.[4] A high proportion of these metabolites possesses the ability to interfere with the assembly of protein polymers in eukaryotic cells, such as tubulin or actin, and a significant number appears to produce toxins which specifically target mammalian ion channels, often voltage-gated sodium channels.[10] The preponderance of these compounds that had either anticancer (40 %) or cytotoxic (20 %) activity likely reflects the research emphasis of the laboratories of Moore[12] and Gerwick.[10]

An unusual feature of cyanobacterial secondary metabolites is the frequency with which nitrogen is incorporated. Terpenoids, acetogenins, and compounds of mixed biosynthesis are the major classes of secondary metabolites found in many marine organisms, especially algae and coelenterates. By comparison, an amazing 40-60 % of the compounds isolated from cyanobacteria contain nitrogen.[14] The predominant metabolic theme of these nitrogen-containing cyanobacterial metabolites is the integration of peptide and polyketide biosynthetic pathways, usually through the linking of polyketides to amino acids by amide or ester bonds or the use of amino acids as starter units for polyketide extension.[10]

1.1.3 Research Objectives/Strategy

In the early 1960s, Barnett Rosenberg and his coworkers at Michigan State conducted a series of experiments designed to determine the effects of electrical current on the growth of *Escherichia coli* cells. They observed that the bacteria formed long

filaments, but that the cells did not divide. After a year of frustration, the source of this bacterial inhibition was attributed to the "inert" platinum electrodes, specifically *cis*-diamminedichloroplatinum (II). The discovery of cisplatin led to a series of platinum-containing agents for the treatment of cancers with sales amounting to approximately a half billion dollars in 1998.

While this made for a good story, such serendipity could not be counted on to provide novel medicines. Thus the primary goal of this research was to explore the potential of marine cyanobacteria to provide inspiration for the development of new medicines, particularly in the area of oncology. At the inception of this project, in the early 1990s, agents that were effective against solid-growing tumors such as cancers of the breast, lung, colon, and pancreas, which account for approximately 85 % of cancer fatalities, were in desperate shortage.[15] Even today only two compounds, bleomycin and doxorubicin, out of the 93 currently approved[16] for clinical use, are broadly effective against solid tumors.[1] The discovery of new therapeutic agents effective against solid-tumors remains of critical importance.

Drug resistance generally develops quite rapidly if a cure is not achieved.[17] For example in the case of the antibiotic penicillin, by 1947, just four years after the start of mass production, penicillin-resistant strains of *Staphylococcus aureus* had appeared.[18] With neoplastic cells, the development of drug resistance is almost inevitable, but surprisingly it is virtually never seen in normal cells.[19] If anything, the tolerance of normal cells to chemotherapy declines with time, so that increasing the dosage to combat a growing resistance in the cancer cells produces a disproportionately small increase in

efficacy. This is a never-ending battle. Thus, the second group of tumors that the extracts were screened against was multi-drug resistant tumors (MDR).

To restate, the principal goal of this research was to identify new cytotoxic secondary metabolites from marine cyanobacteria that might serve as a scaffold for the development of drugs with antitumor activity against solid and/or multi-drug resistant tumors, and to elucidate the structure of these natural products.

To this end, collaborations were established with Dr. Valerie J. Paul at the University of Guam Marine Laboratory and Dr. Thomas H. Corbett at Wayne State University. During the three years of this project, represented by this dissertation, approximately 220 varieties of cyanobacteria were collected by Dr. Paul and assayed in Dr. Corbett's laboratory. Samples that displayed significant activity in Dr. Corbett's laboratory, defined in terms of their zone of inhibition in a disk diffusion assay, were re-collected on a larger scale and sent to Hawaii for fractionation.

Samples of marine filamentous cyanobacteria were collected from a variety of locations around Micronesia. In general, no specific criteria governed which strains of cyanobacteria were collected and prescreened, though a disproportionate number of samples were obtained from around Guam due to the convenience. Only field-collected samples of cyanobacteria were examined and no attempt was made to culture any of the samples. The primary reason for relying exclusively on field-collected strains was to examine as diverse a population of cyanobacteria as possible. A secondary factor in this decision was the low success rate for culturing marine microbes (1 to 10 %).[4] Even if successfully cultivated, no guarantee existed that the same metabolites, seen in wild varieties, would be expressed in cultured strains if there were a lack of appropriate

environmental cues. The diversity that field-collected samples offered was essential for identifying new pharmacophores.

This method of prescreening was based on the selective cytotoxicity of the extracts. The degree of selective cytotoxicity, potency, and number and types of solid tumors in which this in vitro selectivity was obtained, determined the advancement of the agent. A zone of inhibition greater than 6.5 mm (250 zone units), when compared to the control, signified the extract was selective towards that particular cell line and was found to be a critical indicator in predicting the efficacy of the extract during in vivo trials in mice.[20]

The assay worked as follows (Figure 1). The crude extract was absorbed onto a 6.0-mm paper disk that was then placed on an agar plate containing the cell lines. The cytotoxicity of the extract was evaluated against five tumors: a murine leukemia (L1210); a murine solid tumor (colon adenocarcinoma C38, pancreatic ductal adenocarcinoma P03, or mammary adenocarcinoma M16); a multidrug-resistant (MDR) murine solid tumor (mammary adenocarcinoma M17); a human solid tumor (H15, H116, H125), and a normal healthy cell line (fibroblast L-929). Agents that displayed a zone differential ($Z_{\text{Solid Tumor}} - Z_{\text{Leukemia}}$) greater than or equal to 250 units were classified as solid tumor selective and if the opposite were true ($[Z_{\text{Leukemia}} - Z_{\text{Solid Tumor}}] \geq 250$) they were categorized as leukemia selective. Finally, if a greater than 250 units differential existed between either the solid tumor or leukemia cell line and the normal cells ($[Z_{\text{Solid Tumor}} - Z_{\text{Normal}}]$ or $[Z_{\text{Leukemia}} - Z_{\text{Normal}}] \geq 250$), the sample was classified as "tumor selective". Fulfilling any one of these three conditions garnered the extract a high priority to be re-collected and fractionated. An extract that eliminated 250 units of either the solid or the

leukemia tumors, but with an absolute magnitude of $Z_{Solid\ Tumor} - Z_{Leukemia}$ less than 250 units was termed "equally active".[15]

Extracts that were "equally active" or "leukemia selective" were subsequently evaluated in the Valeriote assay,[15] a comparison of the cytotoxicity of the agent against a murine lymphocytic leukemia (L1210) and stem cells of hematopoietic tissue from murine bone marrow (CFU-GM). A medium priority was assigned to those extracts that were leukemia selective in both the Corbett and Valeriote assays.[15]

This means of prioritizing samples was most likely to give erroneous results when the observed cytotoxicity was due to the presence of multiple biologically active compounds. For example, one particular extract of the cyanobacterium *Scytonema mirabile* was equally active and assigned a low priority, but fractionation of this extract yielded 28 different cytotoxins, including tolytoxin, tantazole B, and mirabimide E. When these three pure compounds were tested in the Corbett assay, all displayed solid tumor selectivity and were advanced to in vivo trials in mice.[21]

Despite this difficulty, the prescreen remained an effective means of prioritizing samples. In general, only 0.2 % of the extracts displayed solid tumor selectivity, 1 % leukemia selectivity, and 1-5 % eliminated tumor cells more effectively than healthy cells (tumor selective).[21] This allowed for a reasonable number of extracts to be examined each year.

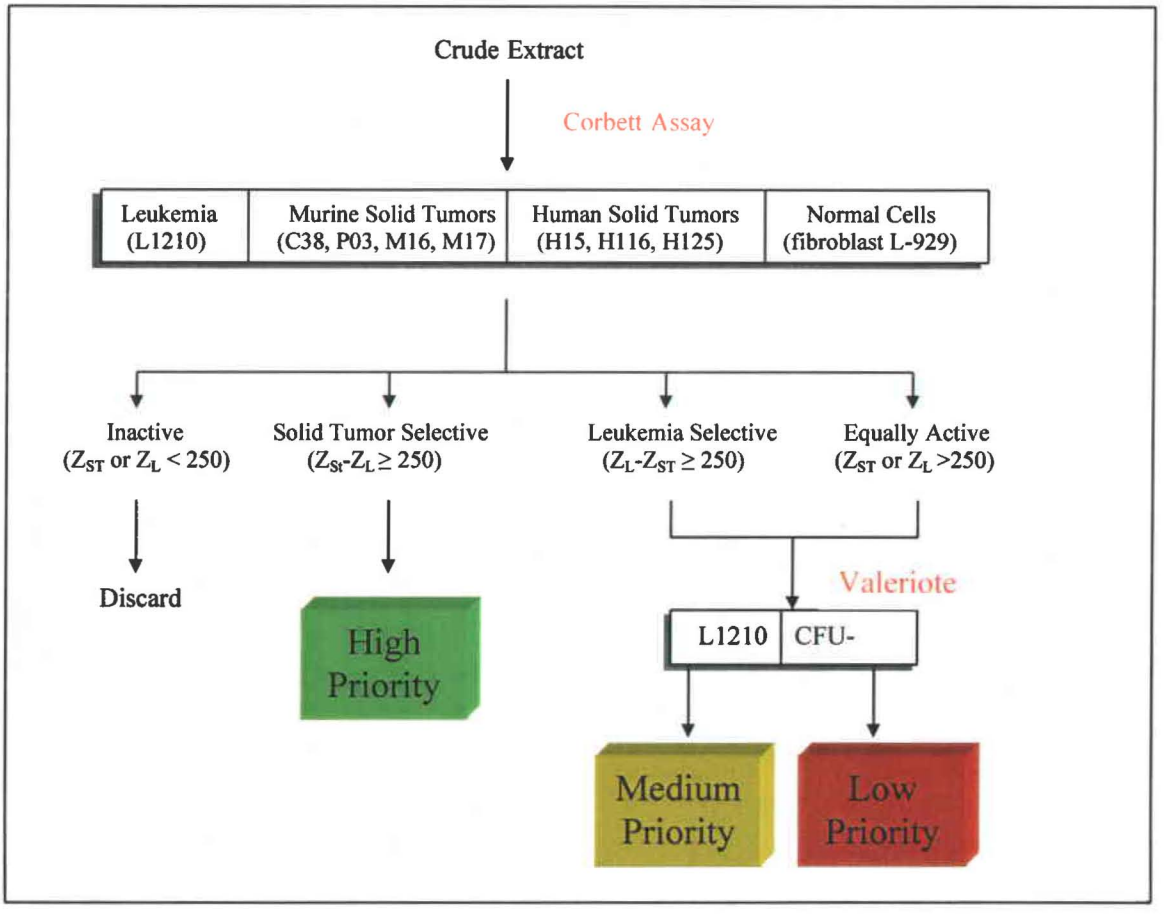

Figure 1. Prioritization of Extracts from Cyanobacteria.

Following the prescreening, promising cyanobacteria were re-collected and sent to Hawaii for cytotoxicity-guided fractionation. Two cell lines were used during this process: KB (human nasopharyngeal) and LoVo (human colon adenocarcinoma) cell lines.

This dissertation describes the results of fractionating several of the extracts screened during the last three years. Chapter 1.2 describes the results from the genus *Symploca* while Chapter 1.3 describes the secondary metabolites isolated from collections of the genus *Lyngbya*.

1.2 CYTOTOXINS FROM *SYMPLOCA*

1.2.1 Overview of *Symploca* Metabolites

Prior to the 1990s there were only a few scattered reports of the chemistry and biological activity of the *Symploca* genus in the literature. The first mentioned an extract of *Symploca muscorum*, collected near Enewetak Atoll, that was active in vivo against a P-388 leukemia model,[22] while another reported that extracts of Palauan strains of *Symploca* spp. were inactive.[23] During the 1980s it was found that cultured *Symploca muscorum* produces geosmin, a long chain alcohol that is often responsible for the undesirable earthy flavor in fish,[24] and dihydrochalcone-glucosides were isolated as the sweet principles of another strain of *Symploca*.[25]

Table 2. Compounds Isolated from the Extracts of *Symploca* spp. Examined

Strain Designation	Genus	Compounds	Collection Site
VP727	*Symploca*	Micromides A & B Apramides A, B, & G	Fingers Reef, Guam
VP643	*Symploca*	Tasiamides A & B Tasipeptins A & B Tasihalides A & B	Short Drop-off, Palau

During the past five years, extracts examined at the University of Hawaii have suggested that this genus may produce more bioactive compounds than previously thought. Recent collections of *Symploca* spp. from Hawaii, Guam, and Palau have afforded the malevamides[26] and the symplostatins.[27] These compounds were notable because the symplostatins and one of the malevamides were structurally related to the dolastatins, two of which were evaluated in clinical trials as anticancer agents.[28] One of the compounds in clinical trials, dolastatin 10 , was isolated from a strain of *Symploca* in a yield that was many orders of magnitude larger than was available from the sea hare

Dolabella auricularia.[29] The discovery of these compounds from cyanobacteria strongly supported the hypothesis that the sea hare acquired many of the dolastatins through its diet.[6]

Table 3. Corbett Assay Data for the *Symploca* spp. Investigated

Extract	Leukemia (L1210)	Murine Solid (C38)[b]	Human Solid (H15)[c]	Fibroblast	
VP727 (1/250)[a]	300	460	700	0-600	Solid tumor selective
VP643 (1/250)[a]	440-480	800-850	880	0-900	Solid tumor selective

[a] Dilution [b] Colon solid tumor [c] Colon multidrug resistant tumor

Two varieties of *Symploca*, VP643 and VP727, were investigated during the course of this research. Both collections displayed solid-tumor selectivity in the Corbett assay at high dilutions (Table 3). Fractionation of each collection yielded an array of cytotoxins (Table 2), including three known compounds {apramide A, B, and G (**1.1-1.3**)}.[30] The isolation and the structure elucidation of the new compounds are presented in this chapter.

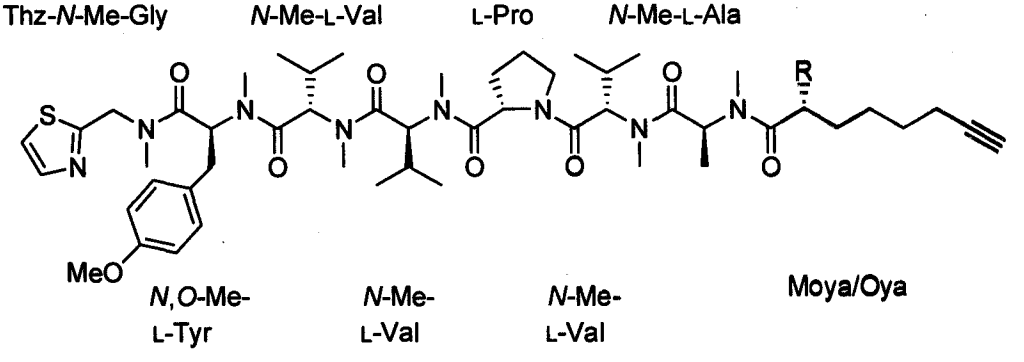

Apramide A (**1.1**) R = Me
Apramide B (**1.2**) R=H

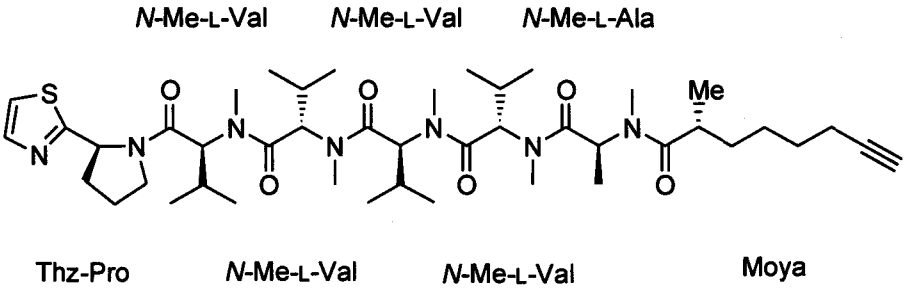

Apramide G (**1.3**)

1.2.2 Micromide A (1.4)

Micromide A (**1.4**) was isolated from a strain of *Symploca* collected off the coast of Guam in the Spring of 2001. This lipopeptide was structurally related to the apramides, three of which (**1.1-1.3**) were also isolated from this extract. The most notable structural difference between micromide A, which had an IC_{50} value of 0.26 μM against KB cells, and the apramides was the replacement of the oct-7-ynoic acid with a 3-methoxyhexanoic acid unit.

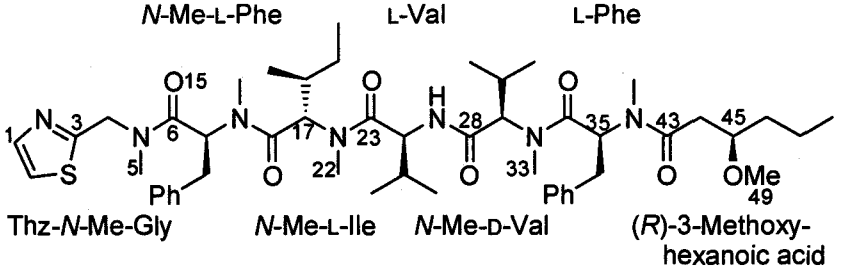

Micromide A (**1.4**)

1.2.2.1 Isolation and Structure Elucidation

The lipophilic extract of VP727 was separated by successive gel permeation and C_{18} chromatography followed by repeated reversed-phase HPLC to afford micromide A (**1.4**, 1.7 mg) in 0.12 % yield, based on the mass of the crude extract.

The initial spectral data of the amorphous powder showed UV/vis and IR absorptions at 225 nm and 1680 cm^{-1}, respectively, suggesting that **1.4** was a peptide containing a heteroaromatic ring. High-resolution MALDI-TOF established the elemental composition of the optically active compound as $C_{49}H_{73}N_7O_7S$, despite the presence of only forty-four carbon signals in the ^{13}C NMR spectrum. Distinctive carbon resonances at δ_C 136.8, 135.9, 129.3, 128.5, 128.4, 126.9, and 126.6, suggested the presence of two monosubstituted phenyl rings and brought the total carbon count deduced from the ^{13}C NMR spectrum into agreement with the mass spectrometry data. This also accounted for

eight of the seventeen double bond equivalents implied by the molecular formula. Based on the number of sp^2 carbons and their chemical shifts, the remaining degrees of unsaturation could be ascribed to seven carbonyl equivalents, one carbon-carbon double bond, and one more ring.

Examination of the spectral data recorded in $CDCl_3$ (Table 4) established a series of partial structures. In conjunction with the UV/vis and MS data, a pair of doublets at δ_H 7.64 and 7.26 in the HSQC spectrum with $^1J_{CH}$ correlations to sp^2 carbon signals at δ_C 142.0 and 120.1 suggested the presence of a thiazole ring. HMBC correlations to a carbon at δ_C 165.6 (C-3) from a pair of diastereotopic methylene protons (H-4) expanded this fragment into a thiazole-glycine unit. A second fragment was constructed starting from an oxygenated methine at δ_H 3.45 (C-45). A series of $^{2,3}J_{CH}$ correlations from this proton (H-45) to C-43, C-44, C-46, and C-49 revealed the structural core of this unit. Further HMBC cross-peaks from a methyl triplet (H-48) to C-47 and C-46 established this last unusual moiety as 3-methoxyhexanoic acid. The remaining fragments, assembled from COSY and HMBC correlations, consisted of one isoleucine, two valine, and two phenylalanine units.

The sequence of **1.4** was determined through HMBC correlations. Two fragments, (Thz-*N*-Me-Gly)-(*N*-Me-Phe)-(*N*-Me-Ile)-Val (C-1 through C-27) and (*N*-Me-Val)-Phe (C-28 through C-40), were constructed by HMBC correlations from the *N*-methylamide proton signals. In particular, cross-peaks were observed from H-5 to C-4 and C-6, from H-15 to C-7 and C-16, and from H-22 to C-17 and C-23. HMBC correlations from the secondary amide proton signals provided the remaining connectivities needed to establish unambiguously the planar structure depicted.

Table 4. NMR Spectral Data for Micromide A (**1.4**) in $CDCl_3$

Unit	C/H no.	δ_H [a] (*J* in Hz)	δ_C [b,c]	^1H-^1H COSY	HMBC[d,e]
N-Me-Gly-Thiazole	1	7.64, d (3.3)	142.0, d	2	
	2	7.26, d (3.3)	120.1, d	1	
	3		165.6, s		4
	4	4.88, d (-15.1)	48.9, t	4_b	5
		4.38, d (-15.1)			
	5	2.56, s	34.8, q		4
N-Me-Phe	6		169.8, s		4, 5, 7
	7	5.34, dd (10.4, 4.2)	53.8, d	8	8, 15
	8	3.11, dd (-13.1, 10.4)	35.1, t	7	7
		2.22, dd (-13.1, 4.2)			
	9		136.8, s		8, 11/13
	10/14	7.02, d (7.7)	129.3, d		8, 14/10
	11/13	7.22, t (7.7)	128.5, d		12, 13/11
	12	7.13, t (7.7)	126.9, d		
	15	2.94, s	30.8, q		7
N-Me-Ile	16		171.4, s		7, 15, 17
	17	5.22, d (10.9)	57.0, d	18	21, 22
	18	2.19, m	33.3, d	17, 19, 21	17
	19	1.24, m	23.9, t	18, 20	20, 21
		1.00, m		18, 20	
	20	0.87, t (6.6)	10.9, q	19	
	21	0.84, d (6.0)	15.4, q	18	17
	22	3.24, s	30.3, q		17
Val	23		171.3, s		22, 24
	24	4.77, dd (8.3, 4.1)	54.0, d	24-NH, 25	26, 27
	24-NH	6.95, d (8.3)		24	
	25	1.88, m	30.5, d	24, 26, 27	24, 26, 27
	26	0.93, d (6.9)	19.9, q	25	24, 27
	27	0.81, d (6.8)	16.9, q	25	24, 26
N-Me-Val	28		170.0, s		24-NH, 24, 29
	29	4.65, d (11.2)	62.4, d	30	31, 32, 33
	30	2.34, m	25.0, d	29, 31, 32	31, 32
	31	1.01, d (6.4)	19.8, q	30	32
	32	0.84, d (5.9)	18.7, q	30	30, 31
	33	2.90, s	30.7, q		29
Phe	34		171.6, s		33, 35
	35	5.19, ddd (8.0, 7.2, 6.0)	50.1, d	36	36
	35-NH	6.82, d (8.0)			
	36	3.22, dd (-13.5, 6.0)	36.9, t	35	
		2.80, dd (-13.5, 7.2)			
	37		135.9, s		36, 39/42
	38/42	6.83, d (7.9)	129.3, d		36, 40
	39/41	7.12, t (7.9)	128.4, d		
	40	7.17, t (7.9)	126.6, d		
3-methoxyhexanoic acid	43		170.5, s		35-NH, 44, 45
	44	2.30, d (6.1)	40.7, t	45	45
	45	3.45, m	77.4, d	44, 46	44, 49
	46	1.40, m	35.4, t	45	44, 45, 48
		1.28, m			
	47	1.27, m	18.3, t	48	48
	48	0.86, t (6.6)	14.1, q	47	
	49	3.27, s	56.6, q		45

[a] Recorded at 500 MHz. [b] Recorded at 125 MHz. [c] Multiplicity deduced from HSQC.
[d] Protons showing long-range correlation with indicated carbon. [e] If not indicated otherwise, correlations were observed for $^nJ_{CH} = 7$ Hz.

1.2.2.2 Stereochemistry

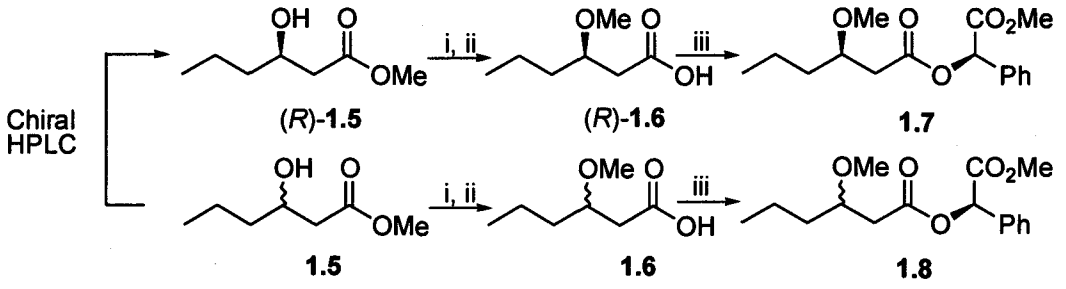

(i) Dimethyl sulfate, KOH, Et_3N, Petroleum Ether; (ii) 0.5 N KOH, MeOH; (iii) DCC, DMAP, Methyl D-Mandelate

Figure 2. Synthesis of (Methyl D-Mandelate) 3-Methoxyhexanoate

The absolute stereochemistry of the units in **1.4** was determined by a combination of chiral and RP-HPLC. Ozonolysis and acid hydrolysis liberated the amino acid-derived centers in **1.4** that were analyzed by chiral HPLC. This established the configuration of the stereocenters derived from *N*-Me-L-Ile, *N*-Me-L-Phe, *N*-Me-D-Val, L-Val, and L-Phe. To determine the configuration of the polyketide-derived moiety, 3-methoxyhexanoic acid, we initially envisioned demethylation of **1.4** and subsequent analysis of this product as the (*R*)- and (*S*)-Mosher's derivatives. Despite the clean conversion of the model compound, attempted demethylation of **1.4** with BBr_3 in CH_2Cl_2[31] afforded neither the desired product nor starting material, thus forcing a more circuitous route with the remaining 0.5 mg of **1.4** (Figure 2).

Racemic methyl 3-hydroxyhexanoate (**1.5**) was resolved on a chiral column and the enantiomers were identified based on comparison of their optical rotations with the reported values.[32] The alcohols were subsequently methylated in petroleum ether with dimethyl sulfate, potassium hydroxide and a catalytic amount of triethylamine,[33] before saponification of the methoxyesters. Unfortunately, attempts to resolve these

methoxyacids (**1.6**) on the OD and OJ chiral columns that were available to us failed, but separation of these compounds was achieved as their methyl D-mandelate derivatives (**1.7**, **1.8**) by C_{18} HPLC. The remaining quantity of **1.4** was therefore hydrolyzed with 6 N HCl at 118 °C for 24 h and the residue exhaustively extracted with CH_2Cl_2. Subsequent derivatization of this residue with methyl D-mandelate, followed by purification and analysis by C_{18} HPLC established the configuration of C-45 to be *R*. Thus the absolute stereochemistry of **1.4** is 7*S*,17*S*,18*S*,24*S*,29*R*,35*S*,45*R*.

1.2.3 Micromide B (1.9)

Micromide B (**1.9**) was isolated from the same collection as **1.4**. It was slightly less cytotoxic against KB cells with an IC_{50} value of 1.2 μM. This lipopeptide contains the simplest example of a 4-amino-3-hydroxyacid, which in this case was likely formed by condensation of acetate to glycine with subsequent reduction. These amino acid-derived units are relatively rare in marine organisms.

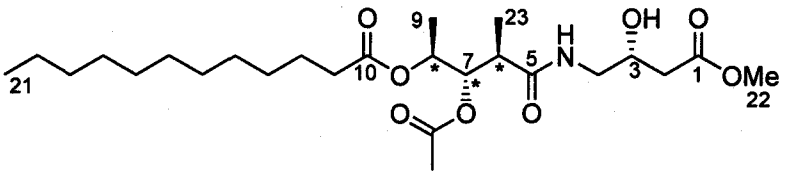

Micromide B (**1.9**)*

1.2.3.1 Isolation and Structure Elucidation

Examination of the Sephadex LH-20 fractions from the crude extract of VP727 led to the isolation of micromide B (**1.9**, 1.7 mg, 0.12 % of the dry extract weight). High-resolution FABMS established the molecular formula of **1.9** as $C_{25}H_{45}NO_6$ based on a pseudo-molecular ion peak at 488.3225 ($[M + H]^+$ 0.2 mDa error), and revealed four degrees of unsaturation. These could be accounted for by the ^{13}C NMR spectrum which contained four carbonyl signals (δ_C 173.3, 173.1, 172.6, and 170.3). From the proton NMR spectrum, it was apparent that **1.9** contained one acetate (δ_H 2.11), one secondary amide (δ_H 6.17), one methoxy (δ_H 3.72), and two methyl proton signals (δ_H 1.23 and 1.17). These fragments were expanded with the aid of the 2D NMR data (Table 5) to provide the gross structure depicted for **1.9**.

---

* Only the relative stereochemistry of these centers has been determined. The absolute configuration remains unassigned.

Table 5. NMR Spectral Data for Micromide B (**1.9**) in $CDCl_3$

C/H no.	δ_H [a] (*J* in Hz)	δ_C [b,c]	^1H-^1H COSY	HMBC [d,e]
1		172.6, s		2, 22
2	2.50, dd (4.3, 2.1)	38.6, t	3	3
3	4.14, m	67.1, d	3, 4a	2, 4a
4	3.62, ddd (-11.6, 7.4, 4.4)	44.5, t	3, 4b, NH	2
	3.08, ddd (-11.6, 7.4, 4.4)		4a, NH	
NH	6.17, t (4.4)		4	
5		173.1, s		4b, NH, 7, 23
6	2.55, p (7.1)	42.4, d	7, 23	7, 23
7	5.25, dd (7.1, 4.4)	74.1, d	6, 8	6, 9, 8, 23
8	5.00, qd (6.5, 4.4)	69.5, d	7, 9	6, 7, 9
9	1.23, d (6.5)	14.4, q	8	7, 8
10		173.3, s		8, 11
11	2.26, t (7.4)	34.4, t	12	12
12	1.58, m	24.8, t	11, 13	11
13	1.20, m	24.0, t	12	
14	1.20, m	29.6, t[f]		
15	1.20, m	29.6, t[f]		
16	1.20, m	29.5, t[f]		
17	1.20, m	29.3, t[f]		
18	1.20, m	29.3, t[f]		
19	1.20, m	31.9, t		21
20	1.21, m	22.6, t	21	21
21	0.87, t (6.9)	14.1, q	20	
22	3.72, s	52.0, q		
23	1.17, d (7.1)	13.5, q	6	6, 7
24		170.3, s		7, 25
25	2.11, s	20.8, q		

[a] Recorded at 500 MHz. [b] Recorded at 125 MHz. [c] Multiplicity deduced from HSQC.
[d] Protons showing long-range correlation with indicated carbon. [e] If not indicated otherwise, correlations were observed for $^nJ_{CH}$ = 7 Hz. [f] These carbon signals may be interchanged.

1.2.3.2 Stereochemistry

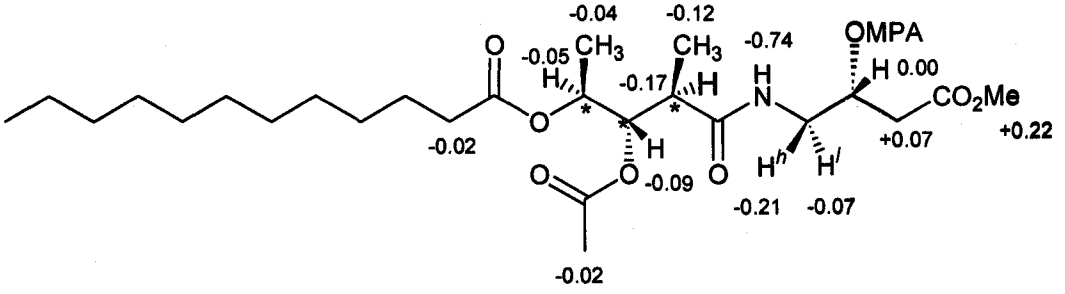

Figure 3. $\Delta\delta$ ($\delta_R - \delta_S$) values in ppm for the MPA esters of Micromide B (**1.9**).

To establish the configuration of C-3, **1.9** was derivatized with α-methoxyphenylacetic acid (MPA). Preparation of the (*R*)- and the (*S*)-MPA derivatives and comparison of the δ_H values (Figure 3) indicated that C-3 possessed the *R* absolute configuration.[34]

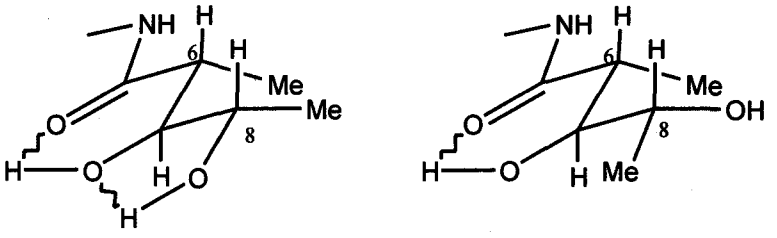

6R,7S*,8S**

1.10

6R, 7S*,8R**

Figure 4. Possible Configurations of the 3,4-Dihydroxy-2-methylpentamide

To determine the relative stereochemistry between C-6 and C-7, **1.9** was saponified with barium hydroxide in methanol. In the resulting adduct H-7 displayed two large couplings ($^3J_{H\text{-}6/H\text{-}7} = 9.5$ and $^3J_{H\text{-}7/H\text{-}8} = 7.7$ Hz) when the proton NMR spectrum was recorded in CD_3CN (See experimental section for ^1H NMR data). Since rotation around C-6 and C-7 would be restricted by hydrogen bonding between the hydroxy group on C-7 and the amide carbonyl, the large coupling between H-6 and H-7 was indicative of an *anti* relationship between the two protons.[35] Furthermore calculated energies of hydrogen bonding between various groups suggested that the hydroxy group on C-7 in this adduct acts simultaneously as an intramolecular hydrogen donor and acceptor (**1.10**), to lock the conformation of this unit (Figure 4).[36] If this was the case, then only the **6*S**,7*R**,8*R**** stereochemistry explained the large coupling constants.[37] Attempts to verify the relative stereochemistry of the *vic*-diol by NOE experiments failed because the limited amount of

material did not provide any NOE correlations. Thus the relative stereochemistry of C-7/C-8 must be regarded as tentative.

1.2.3.3 Comments on the Micromide-Containing Collection

Micromides A (**1.4**) and B (**1.9**) are part of an ever-increasing class of lipopeptides that have been isolated from marine cyanobacteria. The most common of these metabolites are the malyngamides, characterized by a (-)-7-methoxy-4(*E*)-enoic acid moiety of varying length that is appended through an amide linkage to a functionalized cyclohexane ring (cf. **1.34**).[10] Micromide A (**1.4**) contains structural features common to many cyanobacterial metabolites, including *N*-methylated amino acids, a D-amino acid, and a modified cysteine unit in the form of a thiazole ring. It should be noted that despite the structural similarity between micromide A and the apramides, the IC_{50} of the former compound against KB cells was an order of magnitude greater than that of any member of the latter series.

Despite the comparatively simple structures of the micromides, these compounds might be of pharmacological interest. In recent years simple lipopeptides have been implicated in a variety of biological roles, including the regulation of cellular signaling.[38] Micromide B (**1.9**), therefore, may potentially be useful as a tool to probe these interactions.

The apramides (**1.1-1.3**) were originally isolated from an earlier collection of VP417 (cf. section 1.3.3). One puzzling fact surrounding the apramides was the inconsistency with which they appeared over the eight years of the re-collections of VP417 examined. This phenomenon was originally explained as arising from the elimination or modification of the gene cluster responsible for the biosyntheses of the

apramides. The isolation of some members of this structural family from other strains of *Symploca* and *Lyngbya* (cf. section 1.3.1) suggested, however, that the initial collections may have been an assemblage of cyanobacteria and not a single species as originally thought. Subsequent analysis of the partial sequence of the 16S rRNA gene revealed that apparently homogenous re-collections of VP417 consisted of at least two different strains, which likely belonged to the same species (Genbank Accession nos. AY049750 and AY049751).[39] Varying degrees of contamination over the eight years VP417 was collected might explain why the apramides were only isolated from the earlier re-collections.

1.2.3 Tasiamide A (1.11)

Tasiamide A (**1.11**) was isolated from a large re-collection of the cyanobacterium designated VP643 made during a drift dive at Short Drop-off in Palau. The prefix of the trivial name of **1.11** and all subsequent compounds isolated from this collection was derived from the Chamorroan word "tasi" meaning ocean. Tasiamide (**1.11**) was cytotoxic against KB cells with an IC_{50} value of 0.55 μM.

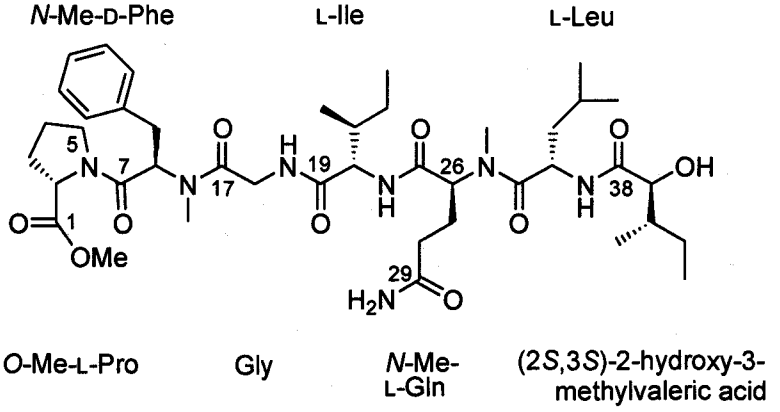

Tasiamide A (**1.11**)

1.2.3.1 Isolation and Structure Elucidation*

VP643, a *Symploca* sp. collected at Short Drop-off in Palau, was repeatedly extracted with a 4:1 mixture of CH_3CN-CH_2Cl_2 to afford a total of 2.67 g of lipophilic extract. Subsequent solvent partitioning and purification by silica gel, C_8 and repeated HPLC yielded tasiamide A (**1.11**) as an amorphous powder (2.1 mg, 0.08 % dry extract weight).

---

* Reproduced in part with permission from Williams, P. G.; Yoshida, W. Y.; Moore, R. E.; Paul, V. J. *J. Nat. Prod.* **2002**, *65*, 1336-1339. Copyright (2002) American Chemical Society.

Table 6. NMR Spectral Data for Tasiamide A (**1.11**) in $CDCl_3$

C/H no.	^{15}N-HSQC[a]	δ_H[b] (*J* in Hz)	δ_C[c, d]	COSY[b]	HMBC[e,f]	ROESY[b]
1			172.5, s		2, 3, 6	
2		4.39, dd (8.7, 6.4)	58.9, d	3a, 3b	3, 4	3
3		2.12, m	28.8, t		2, 4, 5	
		1.87, m				
4		1.93, m	24.9, t	3a		
		1.81, m		3a		
5		3.36, m	46.8, t	4a, 4b	3	3, 8
		3.29, m		4a, 4b		
6		3.72, s	52.3, q			
7			167.9, s		8, 9a, 9b	
8		5.52, dd (8.7, 6.8)	56.3, d	9a, 9b	16	5, 9, 11
9		3.29, dd (-13.5, 8.7)	35.1, t	8, 9b	8	4, 11
		2.82, dd (-13.5, 6.8)		8, 9a	8	
10			136.8, s		8, 9a, 9b, 12	
11/15		7.22, d (7.5)	129.4, d	12	9a, 9b, 11, 13	
12/14		7.26, dd (7.5, 7.1)	128.4, d	11, 13	12	
13		7.20, t (7.1)	126.8, d	12	11	
16		2.96, s	29.7, q		8	
17			167.6, s		16, 18	
18		4.07, dd (-17.5, 4.8)	41.1, t	18a, NH-Gly		16, 23, 24, NH-Gly
		3.82, dd (-17.5, 3.6)		18b, NH-Gly		16, 23, 24, NH-Gly
NH-Gly	-270.9	6.96, dd (4.8, 3.6)		18a, 18b		21
19			171.4, s		18, 20, NH-Gly	
20		4.31, dd (8.9, 6.4)	57.7, d	21, NH-Ile	24	8, NH-Gly
21		1.84, m	37.1, d	22, 24	20	NH-Gly
22		1.41, m	24.7, t	21, 22b, 23	20, 21, 23, 24	
		1.11, m		22a, 23		
23		0.87, t (7.6)	11.3, q	22	22	
24		0.88, d (6.8)	15.6, q	21	20, 22	
NH-Ile	-264.0	7.05, d (8.9)		20		
25			169.7, s		20, 26, 27, NH-Ile	
26		5.06, dd (7.5, 7.3)	56.2, d	27a, 27b	27, 30	3, 27, 30, NH-Ile
27		2.31, m	22.9, t	26, 27b, 28a, 28b	26	30
		2.00, m		27a, 28a, 28b		30
28		2.23, m	32.2, t	27b, 28b	26	
		2.19, m		28a		
29			174.1, s		27, 28	
29- NH	-276.4	5.89, br s				29-NHb
	-276.4	5.57, br s				29-NHa, 18b, 38
30		3.18, s	31.0, q		26	27a, 27b, 33, 34, 36
31			174.4, s		26, 30, 32	
32		4.97, dt (8.4, 7.3)	47.1, d	33, NH-Leu	34	33, 34
33		2.23, m	41.0, t		32, 34, 35, 36	30
		1.60, m				
34		1.60, m	24.9, d	35	33	30
35		0.96, d (6.4)	22.1, q	34	34, 36	30
36		0.95, d (7.1)	23.0, q	34	34	30
NH-Leu	-260.4	7.12, d (8.4)		32		
37			174.0, s		38, NH-Leu	
38		3.94, d (3.9)	76.5, d	39	40, 42	39, 40a, 42, NH-Leu
39		1.84, m	38.3, d	40, 42	38, 40	
40		1.46, m	23.7, t	39, 40b, 41	39, 41, 42	
		1.23, m		39, 40a	38, 39	
41		0.90, t (7.3)	11.8, q	40a	40	
42		0.97, d (6.9)	15.5, q	39	38, 40	

[a] Recorded at 50 MHz. [b] Recorded at 500 MHz. [c] Recorded at 125 MHz. [d] Multiplicity deduced from HSQC.[e] Protons showing long-range correlation with indicated carbon. [f] If not indicated otherwise, correlations were observed for $^{n}J_{CH}$ = 7 Hz.

The initial examination of the spectral data revealed many of the basic substructures that comprise **1.11**. The optically active powder ($[\alpha]^{21}_D$ +15° *c* 0.4, $CHCl_3$) displayed IR bands at 1737 and 1643 cm^{-1} that were characteristic of ester and amide carbonyl vibrations, respectively. The UV/vis spectrum of **1.11** contained an absorbance at 254 nm indicating a phenyl chromophore. HR-FABMS provided a molecular ion peak at *m/z* 852.4833 ($[M + Na]^+$ Δ 0.8 mmu) that established the molecular formula for **1.11** as $C_{42}H_{67}N_7O_{10}$. The ^1H NMR data, recorded in $CDCl_3$ (Table 6), revealed seven α-proton signals between 3.94 and 5.52 ppm while the ^{13}C NMR spectrum showed eight carbonyl signals. Five amide proton signals in the form of two broad singlets (δ_H 5.57, 5.89), two doublets (δ_H 7.05, 7.12) and one doublet of doublets (δ_H 6.96) were visible in the ^1H NMR spectrum. The two broad singlets suggested a primary amide, while the doublet of doublets was reminiscent of the coupling pattern of an amide proton in a glycine unit. Other distinctive structural features consisted of two *N*-methylamides (δ_H 2.96 and 3.18) and one methoxy group (δ_H 3.72).

Analysis of the data from the HMBC and COSY experiments (Table 6) established the remaining fragments. Spin systems that corresponded to *N*-methylphenylalanine, glycine, isoleucine, leucine, and 2-hydroxy-3-methylvaleric acid residues were readily identified. The latter was easily distinguished from isoleucine by the downfield chemical shift of C-38 (δ_C 76.5). Another amino acid residue that was either glutamine or glutamic acid was identified based on COSY (H-26/H-27 and H-27/H-28) and HMBC (H-27 to C-25 and C-29) correlations. The two broad exchangeable proton signals at 5.57 and 5.87 ppm, along with the lack of a proton signal indicative of a carboxylic acid at 10 ppm in the ^1H NMR spectrum, suggested the presence of a *N*-Me-

Gln unit. This was confirmed by a ^{15}N-HSQC experiment (Table 6) which indicated that these two protons (δ_H 5.89 and 5.57) were attached to the same amide nitrogen at -276.4 ppm.[40]

The six remaining carbons were assembled to form the last amino acid residue. A linear chain was constructed based on HMBC correlations to C-1 from H-2, H-3, and H-6, and from COSY correlations between H-3/H-4 and H-4/H-5. The downfield carbon chemical shift of the terminus of this linear chain (C-5, δ_C 46.8) indicated that this carbon was attached to a nitrogen atom and suggested that this residue was either *O*-methylproline or *O*-methylornithine. Careful consideration of all the fragments, along with the degrees of unsaturation implied by the molecular formula, indicated that the final residue was proline.

The HMBC data provided the majority of the peptide sequence. Correlations from the *N*-methylamide signal at δ_H 2.96 (H-16) to C-8 and C-17 connected the nitrogen of phenylalanine to the carbonyl of glycine. Cross-peaks from the second *N*-methylamide signal (H-30) to C-26 and C-31 established the glutamine-leucine linkage. The majority of the remaining sequence was obtained from HMBC correlations from the amide proton signals of glycine, isoleucine, and leucine to C-19, C-25, and C-37 respectively. The *O*-methylproline-*N*-methylphenylalanine linkage was discerned by a ROESY experiment that showed strong cross-peaks between H-5 and the α-proton signal of Phe (H-8).

The FAB mass spectrum of **1.11** provided support for the amino acid sequence in the expanded structure (Figure 5). Key fragmentations included *m/z* 348, 291, and 128 from the cleavage of the amide bond between glycine and isoleucine followed by sequential loss of glycine and *N*-Me-Phe respectively. Key "N-terminus" containing

fragments at *m/z* 483, 370, and 228, resulted from cleavage of the same glycine-isoleucine amide bond and loss of isoleucine and glutamine respectively. Cleavage of the proline-phenylalanine bond resulted in a prominent *m/z* of 701 supporting the location of the proline unit.

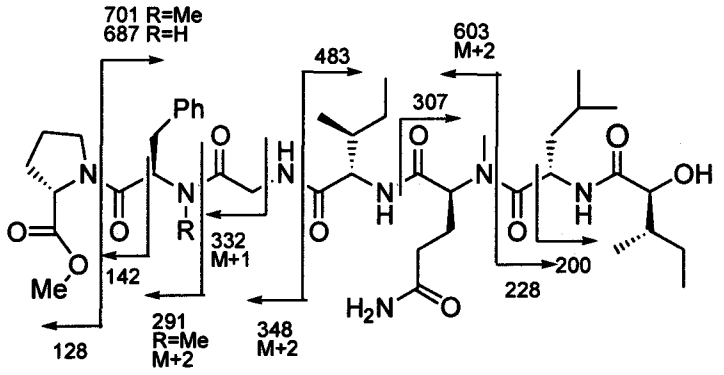

Figure 5. FABMS Fragmentations of Tasiamide A (**1.11**).

1.2.3.2 Stereochemistry

The absolute stereochemistry of **1.11** was deduced after chiral HPLC analysis of the degradation products of the acid hydrolyzate. The HPLC chromatogram from the hydrolyzate was compared with authentic standards to establish the stereochemistry of the amino acid-derived units as L-Pro, *N*-Me-D-Phe, L-Ile, L-Leu and L-2-hydroxy-3-methylvaleric acid. The *N*-Me-L-Gln unit was detected as *N*-Me-L-Glu by chiral HPLC after acid hydrolysis.

1.2.3.3 Comments on Tasiamide A (1.11)

It is the structural simplicity of **1.11** that makes it unusual for a cyanobacterial metabolite. The biosynthesis of **1.11** likely involves just non-ribosomal peptide synthetases with no contribution from polyketide biosynthetic machinery, which is atypical for these organisms. Only the *N*-methylation and the presence of a D-amino acid suggested that **1.11** was a cyanobacterial metabolite. At the time of publication, the

closest structurally related metabolite to **1.11** was the linear peptide malevamide A,[26] isolated from a Hawaiian *Symploca* sp., which shared the amino acid sequence from *O*-methylproline through isoleucine.

Tasiamide A (**1.11**) is only the third example of a glutamine-containing peptide from marine cyanobacteria.[41] The vast majority of marine cyanobacterial peptides and depsipeptides contain only hydrophobic amino acids.[10] This contrasts sharply with freshwater cyanobacterial metabolites that are traditionally rich in polar amino acid residues, e.g. microcystin-LR, a well-known compound from freshwater cyanobacteria, contains three polar amino acid residues: methyl aspartic acid, glutamic acid, and arginine.[42] The reason for this difference is unknown.

1.2.4 Tasiamide B (1.12)

Tasiamide B (**1.12**) was isolated from the aqueous extract of VP643. Structurally **1.12** is similar to tasiamide A (**1.11**) and was named in a manner that reflected this relationship. Tasiamide B was distinguished by the unusual amino acid, 4-amino-3-hydroxy-5-phenylpentanoic acid (Ahppa) residue. The IC_{50} value for **1.12** against KB cells was 0.83 μM.

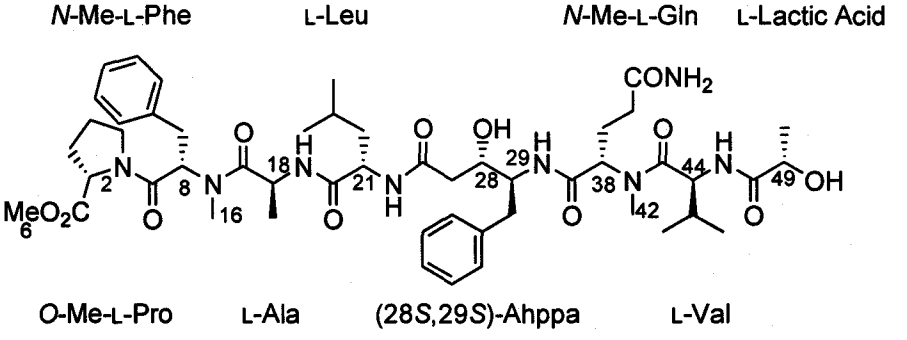

Tasiamide B (**1.12**)

1.2.4.1 Isolation and Structure Elucidation

The freeze-dried *Symploca* sp. VP643 was extracted with 30 % aqueous ethanol after initial extraction with 4:1 CH_3CN/CH_2Cl_2. Bioactivity-guided fractionation of the aqueous extract by Sephadex LH-20 and repeated reversed-phase HPLC afforded 2.6 mg of **1.12**, in 0.13 % yield based on the crude aqueous extract.

Inspection of the carbon, proton, and mass spectral data laid the framework for the structure determination of **1.12**. The elemental composition of **1.12** was deduced as $C_{50}H_{74}N_8O_{12}$ (18 units of unsaturation) based on a high-resolution pseudo-molecular ion peak at *m/z* 1001.5347 ($[M + Na]^+$, Δ 2.9 mDa). The proton spectrum of **1.12** recorded in $CDCl_3$ indicated the existence of two conformers in a ratio of approximately 5:1, but the signals were well enough dispersed to interpret those from the major conformer.

Table 7. NMR Spectral Data for the Major Conformer of Tasiamide B (**1.12**) in $CDCl_3$

Unit	C/H no.	δ_H[a] (*J* in Hz)	δ_C[b, c]	^1H-^1H COSY	HMBC[d,e]
O-Me-Pro	1		172.6, s		2, 3, 6
	2	4.43, t (6.7)	59.2, d		3, 4
	3	2.22, m	28.8, t	2, 4	2, 5
		1.83, m		2	
	4	1.91, m	25.3, t		2, 3, 5
		1.81, m			
	5	3.42, ddd (10.9, 6.9, 4.5)	46.9, t	4, 5b	3
		3.25, m		4, 5a	
	6	3.75, s	52.3, q		
N-Me-Phe	7		168.1, s		8
	8	5.63, dd (9.1, 6.7)	55.6, d		9, 16
	9	3.20, dd (-14.8, 6.7)	34.7, t	8	8, 11
		2.95, dd (-14.8, 9.1)			
	10		136.7, s		8
	11/15	7.20, d (7.8)	129.5, d	12/14	
	12/14	7.23, dd (8.0, 7.8)	128.4, d	11/15, 13	
	13	7.18, t (8.0)	126.7, d	12/14	
	16	3.06, s	31.8, q		8
Ala	17		172.4, s		16, 18, 19
	18	4.69, p (7.1)	45.2, d	18-NH, 19	19, 18-NH
	18-NH	6.98, d (7.1)		18	
	19	0.82, d (7.1)	17.3, q	18	18
Leu	20		171.7, s		18-NH, 21
	21	4.32, q (7.9)	51.9, d	21-NH, 22	22
	21-NH	7.35, d (7.9)		21	
	22	1.48, m	41.0, t	21, 23	21, 23
	23	1.56, m	24.7, d	22, 24, 25	24, 25
	24	0.88, d (6.4)	22.9, q	23	23
	25	0.86, d (6.2)	21.9, q	23	23
Ahppa	26		171.6, s		21-NH, 27
	27	2.42, dd (-14.6, 9.3)	40.7, t	28	
		2.29, dd (-14.6, 4.4)			
	28	4.02, ddd (9.4, 4.4, 2.4)	69.4, d	27, 29	27, 29, 30
	29	4.16, dddd (8.9, 7.1, 6.5, 2.4)	53.8, d	28, 29-NH, 30	27, 30
	29-NH	7.10, d (7.1)			
	30	2.94, dd (-14.1, 6.5)	37.2, t	29	29, 32
		2.84, dd (-14.1, 8.9)		29	
	31		137.9, s		30
	32/36	7.20, d (7.8)	129.0, d	33/35	30
	33/35	7.23, dd (8.0, 7.8)	128.2, d	32/36, 34	
	34	7.18, t (8.0)	126.4, d	33/35	
N-Me-Gln	37		169.9, s		29-NH, 38, 39
	38	4.97, m	55.9, d	39	42
	39	2.13, m	22.9, t	38	
		1.83, m			
	40	2.15, m	31.2, t		39
	41		175.5, s		39, 40
	41-NH	6.52, br s			
		6.37, br s			
	42	2.82, s	30.9, q		
Val	43		173.4, s		42, 44
	44	4.47, t (7.6)	54.0, d	45	44-NH, 45, 46, 47
	44-NH	7.23, d (7.6)		44	
	45	1.94, m	30.4, d		
	46	0.95, d (6.7)	17.8, q	45	44
	47	0.93, d (7.1)	19.3, q	45	44
Lactic Acid	48		176.2, s		44-NH, 49
	49	4.15, q (6.9)	68.7, d	50	50
	50	1.39, d (6.9)	20.8, q	49	49

[a] Recorded at 500 MHz. [b] Recorded at 125 MHz. [c] Multiplicity deduced from HSQC.
[d] Protons showing long-range correlation with indicated carbon. [e] If not indicated otherwise, correlations were observed for $^nJ_{CH}$ = 7 Hz.

The ^{13}C NMR spectrum showed only 46 resonances for the major conformer; therefore, in accord with the mass spectrometry data, elements of symmetry had to be present in some part of the molecule. Signals in the proton and carbon NMR spectra allowed us to attribute this symmetry to the presence of two monosubstituted phenyl rings, which accounted for eight of the double bond equivalents. Among the other resonances present in the ^{13}C NMR spectrum were nine carbonyls (δ_C >168), two amide type *N*-methyl groups (δ_H 3.06, 2.82), and two oxygen- and seven nitrogen-bearing methines (δ_C 69.4, 68.7, 59.2, 55.9, 55.6, 54.0, 53.8, 51.9, 45.2).

Further NMR analysis (Table 7) established several of the amino acids. COSY and HMBC experiments established the presence of alanine, leucine, valine, *N*-methylphenylalanine, and *N*-methylglutamine units. Two primary amide proton signals (δ_H 6.52 and 6.37) distinguished this latter possibility from *N*-methylglutamic acid, despite the lack of HMBC correlations from these exchangeable proton signals to the ε-carbonyl (C-41). Another unit was assembled into a lactic acid residue based on a COSY correlation between the methyl group at δ_H 1.39 (H-50) and the methine quartet at δ_H 4.15 (H-49), which showed a $^1J_{CH}$ coupling to one of the oxygen-bearing methines (δ_C 68.7) in the HSQC spectrum. The second carbinol proton signal (H-28) showed COSY cross-peaks to a methine proton signal at δ_H 4.16 (H-29) and methylene proton signals at δ_H 2.42 and 2.29 (H-27). HMBC correlations from H-27 to C-26, from H-30 to C-29, and from H-30 to C-31, indicated that this fragment was 4-amino-3-hydroxy-5-phenylpentanoic acid (Ahppa). Further analysis of the COSY spectrum established an isolated chain (C-2 to C-5) consisting of one methine and three pairs of diastereotopic proton signals. A HMBC correlation between the methine proton (H-2) and the carbonyl

at δ_C 172.6 (C-1) established that this was an α-amino acid, while the proton and carbon chemical shifts (δ_H 3.42, 3.25, and δ_C 46.9) for the other end of this moiety (C-5) indicated a nitrogen-bearing methylene. Based on the molecular formula this unit was *O*-methylproline. Thus **1.12** was composed of the following fragments: Ala, Leu, Val, *N*-Me-Phe, *N*-Me-Gln, lactic acid, Ahppa, and *O*-Me-Pro.

The sequence of these fragments was determined by HMBC and ROESY correlations. Cross-peaks from the secondary amide proton signals to the adjacent carbonyls connected the amino acid units into two fragments: Ala-Leu-Ahppa-(*N*-Me-Gln) and Val-Lactic acid. These two fragments were joined by a HMBC correlation between the *N*-methylamide signal of Gln (H-42) and the carboxy terminus of valine (C-43). A similar correlation from the *N*-methylamide signal of *N*-Me-Phe (H-16) appended it to the alanine terminus of this linear chain (C-17), while a ROESY correlation from H-5 of proline to H-8 confirmed the attachment of the final unit, *O*-methylproline, to the carboxy terminus of *N*-methylphenylalanine (C-7).

1.2.4.2 Stereochemistry

The absolute configurations of the amino acid-derived units in **1.12** were determined by chiral HPLC of the hydrolyzate. Comparison of the components of the hydrolyzate with authentic standards indicated stereocenters derived from L-Pro, *N*-Me-L-Phe, L-Ala, L-Leu, L-Val, and L-lactic acid. The configuration of the glutamine-derived center was determined by the presence of *N*-Me-L-Glu in the hydrolyzate.

There are few reports of naturally occurring γ-amino-β-hydroxy acids in the literature and no general method has been developed for determining the configuration of the chiral centers. However, reports in the literature indicated that 4-amino-3-hydroxy-5-

methylheptanoic acid, found in the didemnins, underwent an epimerization at C-3 via an acid-catalyzed dehydration/hydration sequence, and that significant quantities of the intermediate α,β-unsaturated acid existed after prolonged hydrolysis.[43] This suggested that the absolute configuration of C-29 could be determined by acid hydrolysis and subsequent ozonolysis, with oxidative workup, to D-Phe or L-Phe. Treatment of **1.12** in this manner did not afford any significant amount of phenylalanine. Instead the hydrolyzate contained a peak, presumably derived from the ozonolysis of phenylalanine, which co-eluted with L-aspartic acid that proved the configuration of C-29.[44] To relate the configuration of vicinal centers C-28 and C-29, we attempted to prepare an oxazolidinone derivative by treatment of **1.12** with triphosgene. This failed and so instead we prepared the (*R*)- and (*S*)-methoxyphenylacetic acid (MPA) derivatives.[45] Unfortunately, the (*R*)-MPA adduct decomposed upon purification over silica, leaving only the (*S*)-MPA derivative.

It has been reported that the absolute configuration of a secondary alcohol can be determined from the ^{1}H NMR spectra of a single MPA derivative. In these techniques two proton spectra are recorded under different conditions, e.g. before and after the addition of a barium (II) salt[46] or at two different temperatures.[47] The net shielding or deshielding experienced by the protons reflects the different conformational equilibrium under the two set of conditions for the MPA group, i.e. the methoxy group is *syn*-periplanar or *anti*-periplanar to the carbonyl. In essence, the *anti*-periplanar conformer acts as the second MPA derivative that is needed to determine the absolute configuration. Unfortunately, when these techniques were applied to (*S*)-MPA-**1.12** positive $\Delta\delta_H$ values were obtained for all the protons adjacent to the derivatized alcohol, rather than one side

displaying positive $\Delta\delta_H$ values and other side negative ones as is expected. It appears that any differences in the chemical shifts of the peptide were determined primarily by a change in the overall conformation of in **1.12** which overwhelmed the contribution of the MPA group.

Even though the stereochemistry of C-28 could not be determined by chemical means, NMR analysis pointed to a 28*S*,29*S* stereochemistry for the Ahppa unit. Inspection of the ^{1}H NMR data in the literature for synthetic 4-amino-3-hydroxy-5-phenylpentanoic acid units and related compounds (Table 8) suggested that the chemical shifts and the coupling constants for the C-2 methylene protons (C-27 in **1.12**), recorded in $CDCl_3$, were indicative of the C-3/C-4 relative stereochemistry, i.e. the downfield methylene proton signal (H-2) generally showed a larger coupling with H-3 when the configuration is 3*S**,4*S** and the smaller coupling when 3*R**,4*S**.[48,49] In our case, the downfield H-27 signal (δ_H 2.42) showed a larger proton coupling ($J_{H\text{-}27/H\text{-}28}$ = 9.4 Hz) to H-28, suggesting a 28*S*,29*S* configuration. The same conclusion was reached by a modeling study on the (L-Gln)-Ahppa-(L-Leu) tripeptide fragment (Figure 6). Regardless of the stereochemistry of the Ahppa unit, the preferred conformation placed the Ahppa carbonyl (C-26) oxygen and the secondary amide proton (29-NH) on the same face on the molecule where both were hydrogen bonded to the secondary alcohol group on C-28. These results implied that the conformation of the Ahppa unit was locked.[50] Assuming this hydrogen bonding was occurring in **1.12**, then only a 28*S*,29*S* stereochemistry was consistent with the proton-proton coupling constants and all of the ROESY correlations observed around these stereocenters. Specifically cross-peaks were observed between H-27_u/H-29, H-27_u/H-28, H-28/ H-32, H-29/H-36, and H-28/H-30_u. Low energy conformers

could not be found for the tripeptide fragment containing a 28*R*,29*S*-Ahppa unit that were in agreement with the proton-proton coupling constants and the observed NOE correlations. Based on these considerations, a *S* configuration was tentatively assigned for C-28.

Table 8. Synthetic γ-Amino-β-hydroxy Acid Units

3*R**,4*S**	$\delta_{H\text{-}2}$ (*J* in Hz)	3*S**,4*S**	$\delta_{H\text{-}2}$ (*J* in Hz)
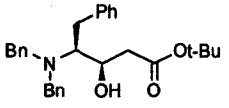	2.63 (16.3, 2.5) 2.22 (16.3, 10.1)[51]	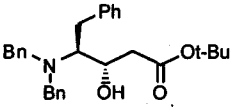	2.40 (16.0, 9.5) 2.04 (16.0, 2.4)[51]
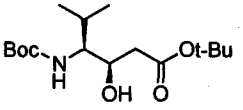	2.52 (16.5, 2.9) 2.38 (16.5, 8.9)[51]	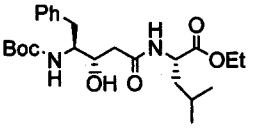	2.54 (15.3, 9.8) 2.28 (15.3, 3.1)[52]
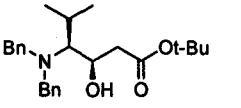	2.64 (16.0, 2.1) 2.32 (16.0, 10.6)[51]	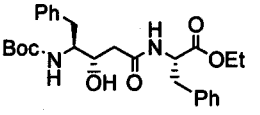	2.38 (15.0, 9.0) 2.19 (15.0, 4.0)[52]
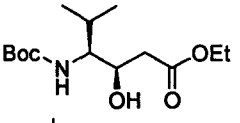	2.58 (16.6, 2.9) 2.47 (16.6, 9.1)[53]	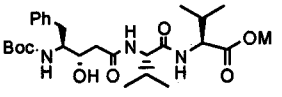	2.55 (14.9, 9.5) 2.32 (14.9, 3.0)[52]
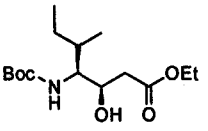	2.60 (16.7, 2.7) 2.48 (16.7, 9.1)[43]	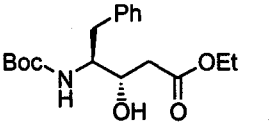	2.59 (16.8, 9.9) 2.37 (16.8, 2.6)[54]
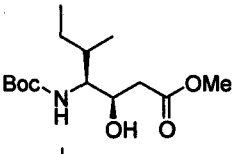	2.60 (16.5, 2.7) 2.42 (16.5, 8.7)[43]	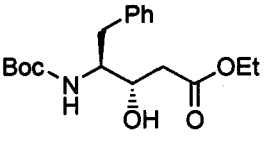	2.57 (16.8, 10.2) 2.38 (16.8, 2.6)[55]
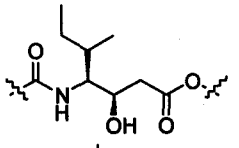	3.24 (17.0) 2.61 (17.0, 10.5)[43]	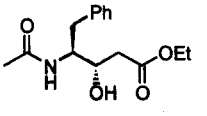	2.57 (17.3, 10.3) 2.38 (17.3, 3.0)[55]
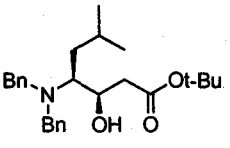	2.48 (16.2, 2.9) 2.29 (16.2, 10.0)[51]	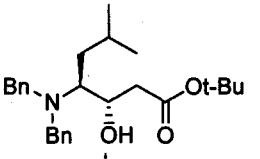	2.34 (15.6, 7.9) 2.27 (15.6, 3.4)[51]
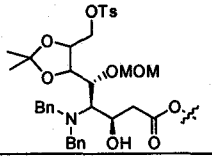	2.84 (16.1, 2.6) 2.45 (16.1, 10.3)[56]	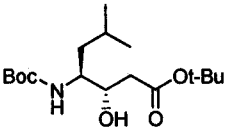	2.48 (16.8, 10.1) 2.35 (16.8, 2.7)[51]

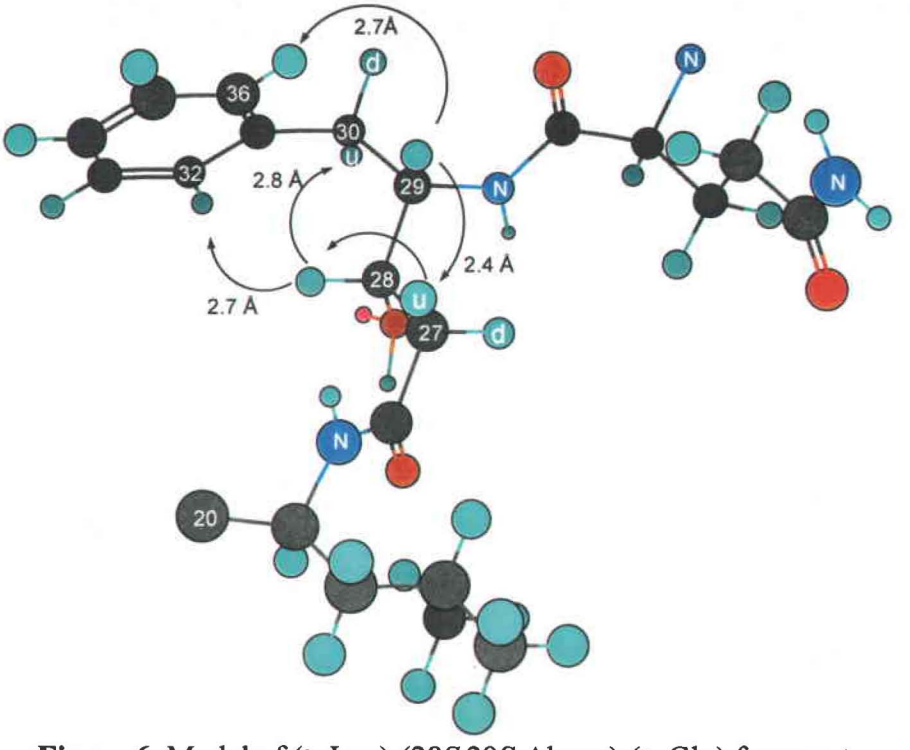

Figure 6. Model of (L-Leu)-(28*S*,29*S*-Ahppa)-(L-Gln) fragment

1.2.4.3 Comments on Tasiamide B (1.12)

The main difference between the tasiamide A (**1.11**) and B (**1.12**) was the incorporation of an Ahppa unit into **1.12**. This was the first time that this modified amino acid residue has been found in a metabolite from a marine cyanobacterium,[57] although it has been identified as part of the freshwater cyanobacterial metabolite hapalosin.[58] The Ahppa unit has been found in acid protease inhibitors from *Candida*[59] and *Streptomyces*[60] spp. and has been widely utilized in the field of peptidomimetics. Other, related δ-amino-β-hydroxyacids from marine cyanobacteria include valine and proline derivatives in lyngbyabellin D (cf. section 1.3.3) and symplostatin 1,[61] respectively. The incorporation of modified amino acids formed by a combination of polyketide synthases and non-ribosomal peptide synthetases is a common theme among cyanobacterial metabolites[10] and is one of the reasons investigations into these organisms remain so fruitful.

1.2.5 Tasipeptins A (1.13) and B (1.14)

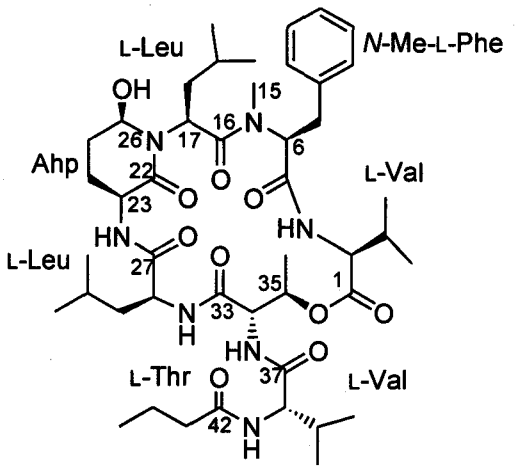

Tasipeptin A (**1.13**)

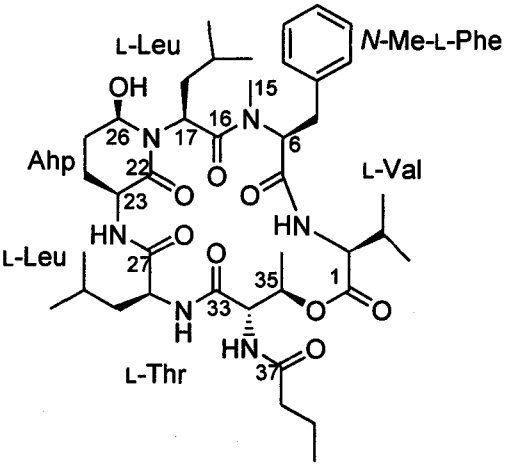

Tasipeptin B (**1.14**)

Tasipeptin A (**1.13**) and B (**1.14**) were isolated from the aqueous extract of VP643. They differ from the other metabolites in this collection by the incorporation of a 3-amino-6-hydroxy-piperidone ring. Both were cytotoxic towards KB cells with IC_{50} values of 0.93 and 0.82 μM, respectively.

1.2.5.1 Isolation and Structure Elucidation*

Solvent partitioning and gel permeation chromatography of the aqueous extract of *Symploca* sp. VP643 yielded several fractions that displayed cytotoxicity. One such fraction after further purification by repeated reversed-phase HPLC provided 4.3 and 2.2 mg of tasipeptins A (**1.13**) and B (**1.14**) in 0.24 % and 0.12 % yield, respectively, based on the mass of the crude aqueous extract.

Table 9. NMR Spectral Data for Tasipeptin A (**1.13**) in $CDCl_3$

Unit	C/H no.	δ_H[a] (*J* in Hz)	δ_C[b, c]	^1H-^1H COSY[a,d]	HMBC[d,e]	ROESY[a]
Val	1		172.5, s		3, 35	
	2	4.57, dd (7.9, 4.7)[f]	57.4, d	2-NH[f]	4, 5	
	2-NH	6.96, d (7.8)		2[f]		
	3	2.15, m	31.1, d	3[f]		
	4	0.92, d (6.6)	18.9, q	3		
	5	0.87, d (6.7)	18.1, q	3		15, 36
N-Me-Phe	6		169.6, s		2-NH, 7	
	7	5.40, dd (11.5, 2.5)	62.0, d	8	15	17
	8	3.45, dd (-14.3, 2.5)	34.0, t	7		
		2.91, dd (-14.3, 11.5)		7		
	9		137.1, s		7, 8	
	10/14	7.27, d (7.0)	129.1, d	11	8	
	11/13	7.18, t (7.0)	129.2, d	10, 12		
	12	7.22, t (7.0)	126.9, d	11		
	15	2.89, s	31.0, q		7	4
Leu	16		174.0, s		15, 17	
	17	4.84, dd (10.9, 4.2)	49.6, d	18		7
	18	1.68, m	37.4, t	17	17, 20 ,21	26
		0.33, m		17		17
	19	0.97, m	24.2, d		20, 21	20, 21
	20	0.46, d (6.5)	21.6, q	19	21	17
	21	0.68, d (6.6)	23.6, q	19	20	
Ahp	22		170.2, s		17, 26	
	23	4.53, ddd (12.7, 8.0, 5.6)[f]	50.6, d	23-NH[f]	23-NH, 24_{ax}	
	23-NH	7.23, d (8.0)		23[f]		
	24_{ax}	2.43, qd (12.7, 2.2)	21.8, t	23, 25_{eq}	23-NH, 25_{ax}	24_{eq}, 25_{ax}, 23-NH
	24_{eq}	2.05, m				24_{ax}
	25_{eq}	2.04, m	29.5, t	26		26
	25_{ax}	1.83, td (13.5, 2.9)		24_{ax}, 26		26
	26	5.14, br d (5.0)	74.9, d			18, 25, 26-OH
	26-OH	4.32, br d (5.0)		26		26
Leu-2	27		171.2, s		23-NH, 29a	
	28	4.48, br dd (9.4, 7.9)[f]	52.1, d	28-NH[f], 29a		
	28-NH	6.41, d (7.9)		28[f]	30	34
	29	1.91, ddd (-13.5, 9.4, 4.1)	38.8, t	29b	28	
		1.57, m		29a		
	30	1.53, m	24.7, t			
	31	0.90, d (6.1)	23.3, q	30	30, 32	
	32	0.83, d (6.6)	21.1, q	30	29, 30	
Thr	33		168.8, s		28-NH, 34, 35	
	34	4.74, d (9.2)	55.0, d	34-NH, 35	35	28-NH, 35, 36
	34-NH	6.92, d (9.2)		34		38
	35	5.49, q (6.4)	71.6, d	34	1, 36	34, 36
	36	1.32, d (6.4)	18.3, q	35		4, 34, 35
Val	37		172.4, s		34, 34-NH	
	38	4.47, t (8.1)[f]	58.5, d	38-NH[f], 39		
	38-NH	6.36, d (8.1)		38[f]		43
	39	1.24, m	31.4, d			
	40	0.96, d (7.4)	19.2, q		38	
	41	0.95, d (7.2)	18.1, q		38	
Butanoic	42		173.5, s		38-NH, 43, 44	
	43	2.35, t (7.1)	38.3, t	44	44, 45	38-NH, 44
	44	1.71, m	19.2, t	43, 45		43
	45	0.98, t (6.8)	13.3, q	44		38-NH

[a] Recorded at 500 MHz. [b] Recorded at 125 MHz. [c] Multiplicity deduced by HSQC. [d] Protons showing long-range correlation with indicated carbon. [e] Correlations were observed for $^nJ_{CH}$ = 7 Hz. [f] Confirmed by 1D-TOCSY experiments on the appropriate 2° amide proton.

Tasipeptin A (**1.13**) was a colorless amorphous powder whose UV/vis spectrum showed end absorptions only. Examination of the ^1H, ^{13}C NMR, and HSQC spectra of

1.13 recorded in $CDCl_3$ (Table 9) indicated fourteen sp^2 carbons, thirteen methines, seven methylenes and eleven methyl groups in accordance with a molecular weight of 892.5140 established by MADLI-TOF ($C_{45}H_{71}N_7O_{10}Na$, Δ 1.5 mmu). Based on chemical shifts, eight of the fourteen sp^2 carbons were carbonyls (δ_c 174.0, 173.5, 172.5, 172.4, 171.2, 170.2, 169.6, and 168.8) and the remainder constituted a monosubstituted phenyl ring (δ_c 137.1, 129.2, 129.1, and 126.9). This accounted for a total of twelve of the fourteen degrees of unsaturation implied by the molecular formula, with the remaining two double bond equivalents in the form of rings. The thin-film IR spectrum of **1.13** suggested a depsipeptide with vibrations characteristic of amides, esters, and hydroxyl groups at 1643, 1731, and 3291 cm^{-1} respectively. These conclusions were corroborated by five signals for exchangeable protons — one hydroxyl and four secondary amide proton signals— deduced by the lack of correlations in the HSQC spectrum.

Irradiation of the secondary amide proton signals of **1.13** in a 1D TOCSY experiment established the presence of one threonine, two leucine, and two valine residues. Subsequent irradiation of the α-proton signal at δ_H 5.40 (H-7) showed transfer to a pair of geminal methylene proton signals with a -14.3 Hz coupling (H-8). The magnitude of this proton-proton coupling denoted an adjacent π system and revealed that this unit was phenylalanine. Finally, irradiation of the alcohol proton signal (26-OH) and the secondary amide proton signal at δ_H 7.23 (23-NH) in two separate TOCSY experiments established the final fragment as the modified amino acid, 3-amino-6-hydroxy-piperidone (Ahp).

The remaining protons were assigned based on the COSY spectrum that showed a methylene multiplet at δ_H 1.71 (H-44) that had cross-peaks to a methyl triplet at δ_H 0.98

(H-45) and to a methylene triplet at δ_H 2.35 (H-43). This aliphatic chain was expanded into a butyric acid moiety by HMBC correlations between the carbonyl signal at 173.5 ppm and both methylenes (H-43, H-44).

The sequence of **1.13** was determined primarily by $^2J_{CH}$ HMBC correlations between the 2° amide proton signals and the corresponding carbonyl carbons. Specifically cross-peaks between C-27/23-NH, C-33/28-NH, C-37/34-NH, C-42/38-NH, and C-6/2-NH established two partial fragments: Ahp-Leu-Thr-Val-Butyrate and Val-Phe. The latter unit was expanded based on HMBC cross-peaks from H-15 to carbons within the Phe unit (C-7) and the other Leu residue (C-16). Finally, $^3J_{CH}$ correlations between H-17 and C-22 of the Ahp unit and between C-1 and H-35 unambiguously established the cyclic structure of **1.13**.

The NMR signals of **1.14** (Table 10) were almost superimposable on those of **1.13** and this suggested a minor variation in the gross structure. High-resolution mass spectrometry data of the optically active ($[\alpha]^{21}_D$ -13° *c* 0.7, MeOH) amorphous powder **1.14** revealed a molecular formula of $C_{40}H_{62}N_6O_9$ (MNa^+ 793.4454) indicating a smaller compound than **1.13**. Analysis of the one-dimensional TOCSY data clearly established all the isolated spin systems and indicated that one of the valine residues had been eliminated in **1.14**, which accounted for all of the differences in the molecular formula. Once again HMBC correlations from the *N*-methylamide and the 2° amide proton signals provided two fragments, Val-(*N*-Me-Phe)-Leu and Ahp-Leu-Thr-Butyrate that could be linked by HMBC cross-peaks (H-17/C-22, H-17/C-26) to form a linear chain. Finally, a HMBC correlation between C-1 and H-35 of threonine confirmed the cyclic nature of **1.14**.

1.2.5.2 Stereochemistry

The stereochemistry of all the proteogenic and *N*-methylated amino acids was determined by chiral HPLC analysis of the acid hydrolyzate of **1.13**, which contained diagnostic peaks for L-Thr, L-Val, L-Leu, and *N*-Me-L-Phe. PCC oxidation of **1.13** prior to acid hydrolysis and chiral HPLC analysis led to L-glutamic acid from the Ahp unit. The absolute stereochemistry of C-23 in the Ahp unit was therefore *S*. Analysis of the $^{2,3}J_{HH}$ coupling constants, obtained through one-dimensional TOCSY and selective decoupling experiments, established the relative stereochemistry around the piperidone ring. Two large $^{3}J_{HH}$ couplings to H-23 and the small $^{3}J_{HH}$ couplings to H-26 indicated an axial and equatorial orientation, respectively, for these protons. Therefore the absolute configuration of the Ahp moiety was 23*S*,26*R*.

The absolute configuration of **1.14** was deduced in a manner analogous to **1.13** leading us to conclude the tasipeptins had the same stereochemistry for all remaining units (2*S*,7*S*,17*S*,23*S*,26*R*,28*S*,34*S*,35*R*).

Table 10. NMR Spectral Data for Tasipeptin B (**1.14**) in $CDCl_3$

Unit	C/H no.	δ_H[a] (*J* in Hz)	δ_C[b, c]	^1H-^1H COSY	HMBC[d,e]	ROESY[a]
Val	1		172.4, s		3, 35	
	2	4.57, dd (7.2, 4.7)[f]	57.3, d	2-NH[f]	3, 4, 5	
	2-NH	6.94, d (7.2)		2[f]		7, 15
	3	2.13, m	31.1, d	2[f]		
	4	0.89, d (6.6)	18.8, q		3	
	5	0.86, d (6.7)	18.1, q		3	
N-Me-Phe	6		169.5, s		2-NH, 7	
	7	5.41, dd (8.9, 2.4)	62.1, d	8	15	2-NH
	8	3.45, dd (-14.7, 2.5)	33.9, t	7		17
		2.90, dd (-14.7, 8.9)		7		
	9		137.1,s		8, 11	
	10/14	7.27, d (5.9)	129.0, d	11	8, 10	
	11/13	7.19, t (7.4)	129.3, d	10, 12	11, 12	
	12	7.22, t (6.0)	126.8, d	11		
	15	2.86, s	31.0, q		7	
Leu	16		174.0,s		15, 17	
	17	4.82, t (9.5)	48.5, d	18b		7
	18	1.69, m	37.4, t	18b	17, 20, 21	
		0.31, dt (10.4, 9.5)				
	19	0.99, m	24.2, d	18b	20, 21	
	20	0.46, d (6.5)	21.7, q	19		17
	21	0.69, d (6.6)	23.6, q	19		
Ahp	22		170.3, s		17, 26	
	23	4.55, ddd (11.6, 8.4, 3.5)[f]	50.6, d	23-NH[f]		
	23-NH	7.21, d (8.8)		23[f]		24_{ax}
	24_{ax}	2.45, qd (11.6, 2.2)	21.8, t	23[f], 25	23	NH-23, 24_{eq}, 25_{eq}
	24_{eq}	2.04, m		25		
	25_{eq}	2.01, m	29.5, t	24	23	
	25_{ax}	1.85, td (13.5, 2.9)		24[f]		26
	26	5.10, br d (5.0)	74.8, d	25, 26-OH	17	26
	26-OH	4.42, br d (5.0)		26		
Leu-2	27		171.4,s		23-NH	
	28	4.50, br dd (8.3, 9.3)[f]	51.9, d	28-NH[f]		23
	28-NH	6.65, d (8.3)				29b, 34, 35
	29	1.97, ddd (-14.1, 9.3, 4.4)	39.2,t	28[f]	31, 32	26
		1.57, m				26
	30	1.53, m	24.7, t			
	31	0.90, d (6.6)	23.2, q	30	29a	
	32	0.85, d (6.6)	21.3, q	30	29a	
Thr	33		169.3, s		34, 28-NH	
	34	4.85, d (9.2)	54.7, d	34-NH[f]	36	28-NH, 34-NH
	34-NH	6.75, d (9.2)				38
	35	5.50, q (6.4)	71.8, d		36	34
	36	1.30, d (6.4)	18.2, q	35		34
Butanoic	37		174.1, s		34-NH, 38, 39	
	38	2.35, t (7.1)	38.3, t	39	39, 40	
	39	1.71, m	19.2, t	38, 40	38	
	40	0.98, t (6.8)	13.3, q	39		

[a] Recorded at 500 MHz. [b] Recorded at 125 MHz. [c] Multiplicity deduced by HSQC. [d] Protons showing long range correlation with indicated carbon. [e] Correlations were observed for $^nJ_{CH}$ = 7 Hz. [f] Confirmed by 1D-TOCSY experiments on the appropriate 2° amide proton.

1.2.5.3 Comments on Tasipeptins A (1.13) and B (1.14)

Tasipeptins A and B display many characteristics typical of many cyanobacterial metabolites. Features such as *N*-methylation, the incorporation of polyketide units and modified amino acids are biosynthetic signatures of cyanobacteria and probably serve to

enhance the biological efficacy. To date, the unusual Ahp unit has appeared in approximately fifty secondary metabolites isolated primarily from terrestrial and marine cyanobacteria (*Microcystis*,[62] *Oscillatoria*,[63] *Anabaena*,[64] *Nostoc*,[65] *Microchaete*,[66] *Scyonema*,[67] *Lyngbya*,[68] and *Symploca* spp.), although this moiety has also appeared in natural products from the terrestrial bacterium *Streptomyces resistomicificus*.[69] Surprisingly, regardless of the source, all known Ahp-containing metabolites share the same basic structure of a 19-membered ring constructed from six amino acids cyclized through the alcohol oxygen of threonine, or in one case 3-hydroxy-4-methylproline. Most of the variations are located in the side chains that are attached to the amino terminus of threonine. Also, the sequence of the six amino acids which comprise the macrocycle is to a large extent conserved in the form of cyclo(L-Val/Ile-*N*-Me-L-Phe/Tyr[70]-X_1-(3*S*,6*R*)-Ahp-X_2-L-Thr) with X_1 a hydrophobic L-amino acid (Leu, Ile, Val and Phe) or in a few cases Thr. The identity of X_2 appears to play a crucial role in determining the biological activity since compounds which possess a nonpolar amino acid in this position are often reported to be inhibitors of chymotrypsin while those with polar residues generally inhibit trypsin but have little effect on chymotrypsin.[71,72,73] A crystal structure of a complex between trypsin and an Ahp-containing compound (A90720A; X_1=L-Leu, X_2=L-Arg) indeed showed that the guanadinium provided a number of key hydrogen bonds within the specificity pocket, while hydrogen bonds around the Ahp unit defined the elliptical shape of A90720A.[74]

1.2.6 Tasihalides A (1.15) and B (1.16)

Tasihalides A (**1.15**) and B (**1.16**) were isolated from the extracts of the Palauan cyanobacterium designated VP643. It was surprising that tasihalide A, which appeared to be the more polar of the two compounds, was isolated only from the lipophilic extract, while tasihalide B was isolated from the polar extract. The reason for this discrepancy was unclear. The simplest explanation, that **1.16** was an artifact, seemed unlikely given that readily apparent acylating agents, such as ethyl acetate or ammonium acetate, were not used during the isolation.

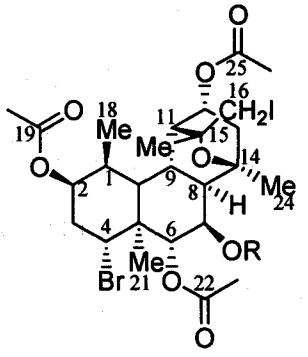

Tasihalide A (**1.15**) R = H
Tasihalide B (**1.16**) R = Ac

The tasihalides are unusual for two main reasons. First, the ring system in **1.15** and **1.16** has not been found in other diterpenes. Secondly, these compounds represent the first example of the incorporation of iodine into a cyanobacterial secondary metabolite. Unfortunately, both compounds did not display cytotoxicity against KB or LoVo cell lines.

1.2.5.1 Isolation and Structure Elucidation

Tasihalide A (**1.15**) was isolated from the lipophilic extract of the cyanobacterium designated VP643. After repeated extraction with 4:1 CH_3CN:CH_2Cl_2, the residue was separated by a combination of solvent partitioning, silica chromatography, and repeated

reversed-phase HPLC. Final purification of **1.15** was achieved on an Ultracarb 30 ODS with 70 % aqueous CH_3CN (t_R 19.6 min) to afford 0.8 mg of an optically active oil {$[\alpha]^{23}_D$ -18° (*c* 0.6, MeOH)} in 3.4 x 10^{-2} % yield.

Inspection of the richly detailed proton and carbon NMR spectra (Table 11), along with IR and UV/vis data, set the framework for the gross structure determination. The ^{13}C NMR spectrum revealed that **1.15** was composed of 26 carbons that could be further divided into seven methyl, three methylene, ten methine, and six quaternary carbon signals. The three carbonyl signals were ascribed to acetate groups based on the methyl singlets at δ_H 2.21, 2.13, and 2.08. The attachment of these acetate groups to the carbon skeleton also accounted for three of the six oxygenated sp^3-carbons (δ_C 76.8, 76.6, 73.4, 73.9, 69.8, and 68.8). The number of carbons that remained (20) suggested, from a biosynthetic perspective, that **1.15** was a diterpene formed from four isoprene units. The NMR spectrum of **1.15** revealed a single signal indicative of an exchangeable proton at δ_H 2.15 that was attributed to an alcohol proton on account of the 3501 cm^{-1} vibration in the IR spectrum. The chemical shifts and coupling constants for the methylene signals were also noteworthy. Surprisingly, the proton NMR spectrum revealed two pairs of methylene proton signals that possessed geminal coupling constants with an absolute magnitude greater than 15 Hz. A geminal coupling constant of this size is usually indicative of a methylene directly attached to a π-system, which, given that all the sp^2 carbons were present in the form of acetates, was not possible in **1.15**. The third set of methylene proton signals comprised an AB system at δ_H 3.27 and 3.10 that showed a $^1J_{CH}$ of 150 Hz to a carbon which resonated at δ_C 15.3. This unusual combination of values was indicative of a heavy-atom effect and indicated that either bromine or iodine was

attached to this carbon.[75] The presence of iodine in **1.15** was confirmed by the UV/vis spectrum, recorded in MeOH, which showed an n-σ^* transition at 254 nm characteristic of this halide.

Difficulties arose in obtaining a clear-cut molecular ion peak for **1.15**. FAB and MALDI-TOF mass spectrometry failed to provide useful data under a variety of conditions, but pseudo-molecular ion peaks at *m/z* 707 and 709 [M + Na] were eventually obtained by ESI. These two ions had an isotope pattern in a 1:1 ratio that indicated that bromine was incorporated into **1.15**. The fragmentation of the 709 ion peak was followed in a series of MS/MS experiments which provided ions at *m/z* 627, 499, 439, and 383 from loss of HBr^{81}, HI and two successive McLafferty rearrangements that resulted in the elimination of two molecules of acetic acid (-60). The elemental composition of **1.15** was therefore $C_{26}H_{37}O_8BrI$ as confirmed by a high-resolution ESI peak $[M + NH_4]^+$ at *m/z* 702.1154 (2.1 mDa error).

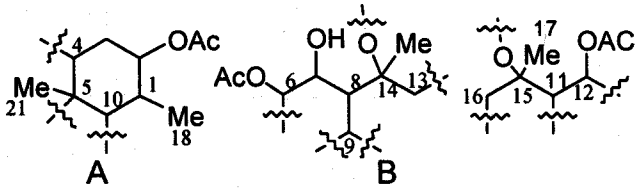

Figure 7. Partial Fragments of Tasihalide A (**1.15**).

The structure of **1.15** was elucidated from the 2D NMR data (Table 11). Analysis of the COSY and HMBC data, recorded in $CDCl_3$ at 500 MHz, established three fragments (Figure 7). The proton and carbon chemical shifts of fragments A, B, and C suggested that the halides were attached to C-4 and C-16. The iodine was connected to C-16 (δ_C 15.3) and the bromine to C-4 (δ_C 54.5) based on the carbon chemical shifts in

accordance with literature values.[75] An HMBC correlation from H-21 to C-6 and a COSY cross-peak from H-9 to H-10 established the C-5/C-6 and C-9/C-10 junctions, respectively. Fragment C was linked to this unit by a COSY correlation from H-12 to H-13 and a HMBC cross-peak to C-10 from H-9. The two downfield carbons (C-14 and C-15) were connected via an ether linkage to account for the remaining oxygen atom and the final degree of unsaturation required by the molecular formula.

Table 11. NMR Spectral Data for Tasihalide A (**1.15**) in $CDCl_3$

C/H no.	δ_H[a] (*J* in Hz)	δ_C[b,c]	^{1}H-^{1}H COSY	HMBC[d,e]	NOESY
1	2.40, qd (7.3, 3.6)	33.1, d	2, 18	3ax, 3eq, 10, 18	
2	5.04, br s	73.9, d	1, 3ax, 3eq	3ax, 3eq, 18	1, 3ax, 3eq, 18
3ax	2.53, ddd (-15.4, 11.5, 4.8)	39.0, t	2, 3eq, 4	4	21
3eq	2.49, ddd (-15.4, 5.5, 1.7)		2, 3ax, 4		
4	5.34, dd (11.5 5.5)	54.5, d	3ax, 3eq	2, 3ax, 3eq, 6, 10, 21	3eq, 9, 13ax
5		45.3, s		3ax, 3eq, 4, 6, 9, 21	
6	5.50, d (3.1)	76.6, d	7	7, 7-OH, 8, 21	7-OH, 21
7	4.05, br s	69.8, d	6, 7-OH, 8	6, 7-OH	7-OH, 8, 24
7-OH	2.15, d (1.5)		7		
8	1.71, d (11.1	47.2, d	9, 13eq	6, 7, 7-OH, 9, 10, 11, 13eq, 13ax, 24	7, 10. 24
9	2.93, t (11.1)	28.8, d	8, 10	5, 7, 8, 10, 11, 12	4, 7-OH
10	2.37, dd (11.1 3.5)	51.0, d	9	1, 2, 6, 8, 9, 18, 21	
11	2.94, d (4.9)	37.0, d	12, 13eq	9, 13eq, 16b, 17	12, 17, 18
12	5.34, t (4.9)	68.8, d	11, 13eq, 13ax	9, 11, 13ax	11, 13eq, 16a
13eq	2.36, dd (-15.6 4.9)	50.0, t	8, 13b	8, 11, 24	12, 13ax, 16a
13ax	1.47, d (-15.6)		13eq		7-OH, 12, 13eq, 24
14		73.4, s		8, 12, 13eq, 13ax, 24	
15		76.8, s		9, 11, 12, 16a, 16b, 17	
16a	3.27, dd (-10.2, 1.1)	15.3, t	16b, 17	11, 17	12, 13eq, 16b
16b	3.10, d (-10.2)		16a		16a, 17
17	1.70, br s	26.4, q	16a	11, 16a, 16b	10, 18
18	1.16, d (7.3)	17.9, q	1	1, 2	1, 2, 10, 11, 20
19		171.1, s		2, 20	
20	2.21, s	22.1, q			
21	1.10, s	19.2, q		4, 6, 10	1, 3ax, 6, 10
22		169.5, s		6, 23	
23	2.08, s	21.0, q			
24	1.12, s	21.2, q		13eq, 13ax	7, 7-OH, 8, 13eq
25		169.9, s		12, 26	
26	2.13, s	21.7, q			

[a] Recorded at 500 MHz. [b] Recorded at 125 MHz. [c] Multiplicity deduced by HSQC. [d] Protons showing long range correlation with indicated carbon. [e] Correlations were observed for $^nJ_{CH}$ = 7 Hz.

A related compound, tasihalide B (**1.16**, 0.8 mg), was isolated from the 30 % aqueous EtOH extract of the cyanobacterium. The proton NMR spectrum of **1.16** was nearly identical to **1.15** except for the downfield shift of H-7 and the presence of an extra methyl singlet at δ_H 2.17. HR-ESI established a molecular formula of $C_{28}H_{44}NO_9BrI$

based on a $[M + NH_4]^+$ of 744.1246 (0.7 mDa error) for the peracetylated analogue **1.16**. NMR analysis (Table 12) confirmed the gross structure to be otherwise identical to **1.15**.

Table 12. NMR Spectral Data for Tasihalide B (**1.16**) in $CDCl_3$

C/H no.	δ_H[a] (*J* in Hz)	δ_C[b,c]	^1H-^1H COSY	HMBC[d,e]	ROSEY
1	2.40, m	33.1, d			
2	5.06, br s	73.8, d	3	18	3, 18, 20, 21
3	2.59, m	39.0, t	2		2
	2.40, m		2		2
4	5.10, dd (7.3, 5.1)	52.8, d		21	9, 28
5		45.9, s		21	
6	5.53, d (3.0)	73.9, d	7	21	7, 21, 26
7	5.13, dd (2.6, 1.3)	69.6, d	6, 8		6, 8, 24
8	1.85, d (11.1, 1.3)	45.5, d	9		7, 10, 13b, 24
9	2.91, dd (11.1, 10.5)	31.1, d	8, 10		4, 17
10	2.39, d (10.5)	50.3, d	9	18, 21	8
11	2.96, d (4.7)	37.0, d	12	16a, 17	12, 17
12	5.33, dd (8.6, 4.9)	68.6, d	11, 13	11, 13b	11, 13a, 16a
13	2.33, dd (-15.5, 8.4)	45.4, t	12, 13b		12, 16a
	1.47, d (-15.5)		12, 13a		8, 24
14		72.7, s		24	
15		76.4, s		16a, 17	
16	3.25, dd (-10.2, 1.0)	15.3, t	16b	17	12, 13a
	3.09, d (-10.2)		16a		17
17	1.70, s	26.3, q			9, 11, 16b, 20, 28
18	1.17, d (7.1)	17.8, q			2, 9
19		171.2, s		20	
20	2.25, s	22.24, q			2, 17, 21
21	1.09, s	18.5, q			3, 6, 9, 20
22		168.7, s		23	
23	2.10, s	21.0, q			
24	1.03, s	22.16, q			7, 8, 13b
25		169.8, s		26	
26	2.13, s	21.7, q			6
27		169.2, s		28	
28	2.17, s	21.4, q			4, 17

[a] Recorded at 500 MHz. [b] Recorded at 125 MHz. [c] Multiplicity deduced by HSQC. [d] Protons showing long range correlation with indicated carbon. [e] Correlations were observed for $^nJ_{CH}$ = 7 Hz.

1.2.5.2 Stereochemistry

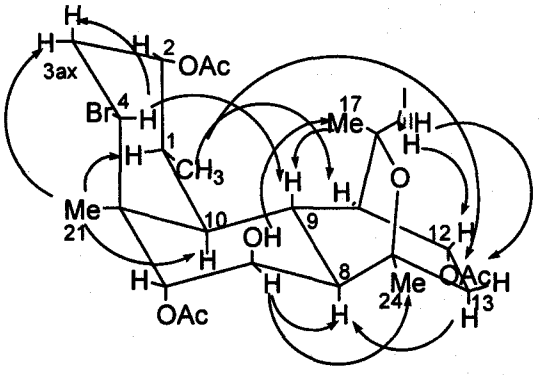

Figure 8. Key ROESY Correlations Observed in Tasihalide A (**1.15**).

The relative stereochemistry of the ring system in **1.15** was established by analysis of proton-proton coupling constants and ROESY correlations (Figure 8). A large proton-proton coupling between H-3_{ax} and H-4 ($^3J_{H\text{-}3ax/H\text{-}2}$ = 11.5) established the axial orientation of both these protons. Likewise a small proton-proton coupling between H-3_{ax} and H-2 ($J_{H\text{-}2/H\text{-}3ax}$ = 4.5) established this latter proton was in an equatorial position. Three other protons H-8, H-9, and H-10 were also assigned axial configurations based on large proton-proton couplings. ROESY correlations from H-4 to H-9 and from H-21 to H-1 indicated that the A/B ring junction was *cis*, while the axial position of H-8 and H-9, determined from coupling constants, indicated that the B/C ring junction was *trans*. The configuration of the B-ring with respect to the oxabicyclic systems was elucidated from ROESY cross-peaks from H-8 and H-16 to H-13. The relative configuration of **1.16** was determined by a similar analysis.

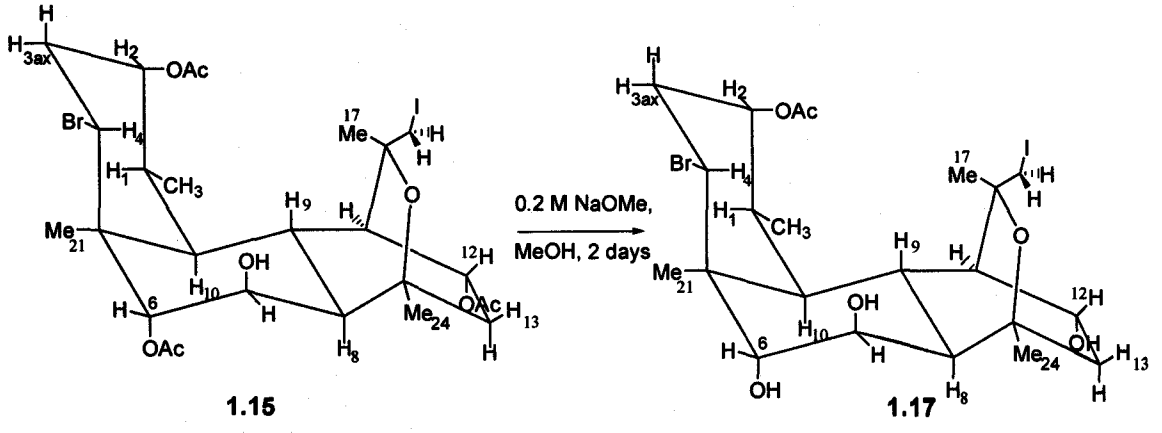

Figure 9. Degradation of **1.15.**

Although this required the preparation of a suitable derivative, determining the absolute configuration of **1.15** by circular dichroism seemed the most viable option of all the possible alternatives. Inspection of a model suggested that the hydroxyl groups on C-6 and C-12 were the least hindered and perhaps the acetate groups at these centers could

be replaced with more appropriate chromophores. Deacetylation of **1.15** (Figure 9) with sodium methoxide proceeded smoothly and yielded the triol **1.17**, but two subsequent attempts to derivatize C-6 and C-12 have so far been unsuccessful. The treatment of **1.17** with an excess of anisoyl chloride and a stoichiometric amount of DMAP in pyridine for two days at room temperature and at 70 °C have resulted only in recovered **1.17**. Thus, the absolute configuration of the tasihalides remains unassigned.

1.2.5.3 Comments on the Tasihalides.

Numerous halogenated natural products have been isolated from terrestrial and marine organisms. [76] Given the relatively high concentration of halides in ocean water (0.5 M in Cl^-, 0.1mM in Br^-, 1 μM in I^-)[77] it is not surprising that marine natural products incorporate these atoms more frequently than secondary metabolites from terrestrial sources. But of the approximately 3000 halogenated natural products known, less than 100 contain iodine[78] and half of these compounds are simple hydrocarbons of less than eight carbons.[79,80] Examples of more complex iodine-containing metabolites include the depsipeptides geodiamolides[81] and doliculide (iodotyrosines), iodinated nucleosides,[82] lukianol B,[83] and the structurally intriguing calicheamicin.[84] The placement of iodine in the tasihalides is unusual, though. It is one of the few examples of a structurally complex molecule in which this halide is attached to a sp^3 rather than a sp^2 carbon. Tasihalides A and B are, to our knowledge, also the first examples of iodine incorporation into a marine diterpene.

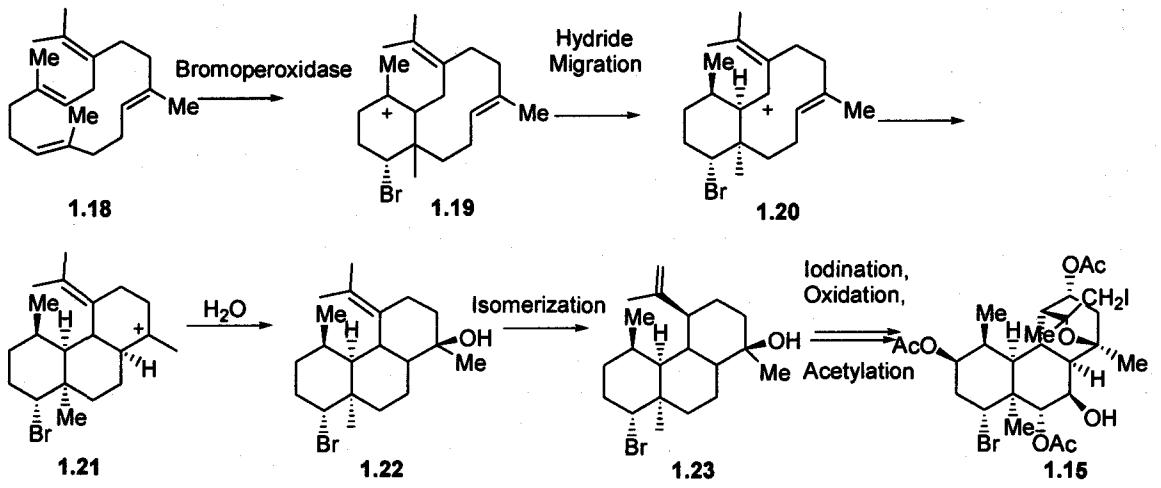

Figure 10. Possible Biosynthesis of the Tasihalides.

The tasihalides also appear to be the first examples of this structural core in a natural product. It is the formation of an oxabicyclic system in the C-ring that makes the carbon skeleton of **1.15** and **1.16** unusual. The structures most closely related to **1.15** and **1.16** are synthetic tricyclic compounds, lacking the oxabicyclic system, which are formed by treatment of cembrane diterpenes with electrophiles.[85] This makes it tempting to speculate that **1.15** and **1.16** arise from the cyclization of an oxygenated cembrane diterpene initiated by a bromoperoxidase (BPO) halogenation. Such haloperoxidase mediated electrophilic cyclizations have been demonstrated *in vitro* using bromoperoxidases cloned from red algae (Rhodophyta).[86,87] Two general types of peroxidases have been identified: vanadium bromoperoxidases and FeHeme bromoperoxidases. The latter are capable of generating both electrophilic and radical species while the former are much more common and only generate an electrophilic halogenating agent (Br^+ or I^+). A cationic biosynthetic scheme[88] based on a hypothetical intermediate is shown in Figure 10.

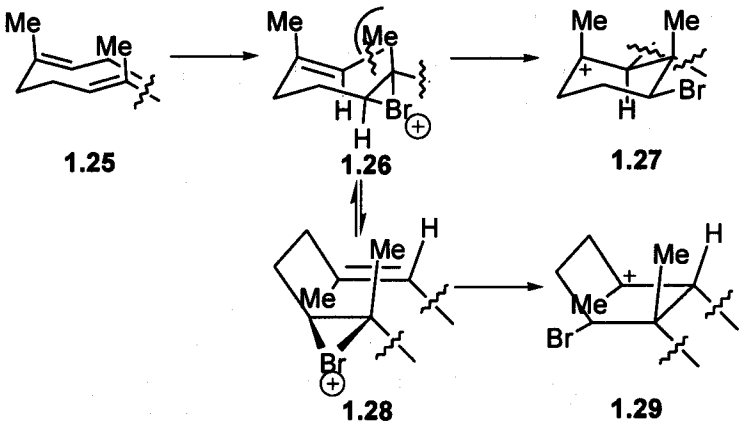

Figure 11. Formation of A-B ring system.

The *cis* stereochemistry of the A/B-ring system[89] would be consistent with a peroxidase-catalyzed cyclization. After formation of the bromonium ion, the chair-like transition state (**1.26**) that would lead to a *trans* ring junction (**1.27**) would be destabilized by a 1,3-syndiaxial interaction (Figure 11). The corresponding twist-boat transition state (**1.28**) that would lead to a *cis* ring junction (**1.29**) does not have this unfavorable steric strain.[90]

The hydride shift, which would be required to convert **1.19** to **1.20**, could occur via either two successive 1,2-hydride shifts or a single 1,3-hydride shift.[91] The latter would retain the *cis*-ring junction but would be problematic for stereochemical reasons. For example, if the A-ring were in a chair conformation, the vacant *p* orbital would point directly at the methylene protons (Figure 12). This alignment would facilitate hydride transfer, but would result in a final product with the hydrogen in the equatorial position in the A-ring rather than the axial position as seen in **1.15**.[92] Conversely, a mechanism involving two successive 1,2-hydride shifts[93] would circumvent these stereoelectronic problems, but would generate a carbocation at the A/B ring junction (C-10) after the first

1,2-hydride shift. The binding pocket of the enzyme would have to control the stereochemistry of the A/B ring junction to produce the thermodynamically less favored *cis* junction.

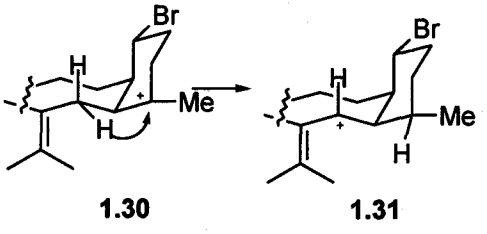

1.30 **1.31**

Figure 12. Stereochemical Outcome of 1,3-Hydride Migration

The configurations of the remaining centers would be consistent with thermodynamically controlled conditions (Figure 13). After formation of the A/B ring junction and hydride migration, the remaining two rings could be cyclized via a *trans*-decalin system to generate a 3° carbocation that could be trapped by water. The axial position of the alcohol would be consistent with placement of the larger group in the equatorial position. The formation of the trans B/C ring junction would generate an unfavorable steric interaction between the methyl and isopropenyl substituents on the A- and C-rings, respectively. This interaction could be alleviated by double bond isomerization placing the isopropenyl group in the equatorial position. Subsequent conversion to the twist-boat conformation would be necessary to cyclize the final ring system. In the isomerization to the terminal double, the protonation would have to occur from the *pro-S* face, as proposed, since this would result in a chair conformation. Addition of a proton from *pro-R* face would result in a twist-boat conformation, in which conversion to a chair conformation with an axial isopropenyl group would require that

the two groups with the unfavorable steric interaction to be initially brought closer together.

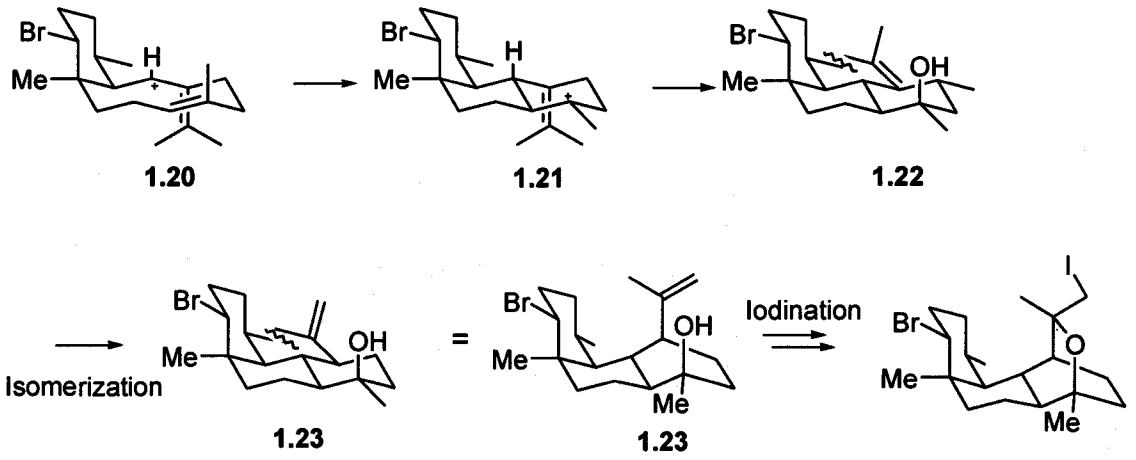

Figure 13. Hypothetical Biosynthesis of the Tasihalides.

1.3 CYTOTOXINS FROM *LYNGBYA*

1.3.1 Overview of *Lyngbya* Metabolites

Table 13. Cytotoxins Isolated from the Extracts of *Lyngbya* spp. Investigated

Strain Designation	Genus and Species	Compounds	Collection Site
VP680	*Lyngbya confervoides*	Obyanamide	Obyan Bay, Saipan
VP755	*Lyngbya* sp.	Ulongapeptin Palau'amide	Ulong Channel, Palau
VP417	*Lyngbya* sp.	15-Norlyngbyapeptin A Lyngbyabellin D	Apra Harbor, Guam
NIH199, 154, 143	*Lyngbya majuscula*	Lyngbyastatin 3 Ibu-epilyngbyastatin 3	Apra Harbor, Guam
VP637	*Lyngbya majuscula*	Lyngbyastatin 1 Ibu-epilyngbyastatin 1 Dolastatin 12 Ibu-epidolastatin 12	Apra Harbor, Guam
VP664	*Lyngbya* sp.	Apramides A, B, & G	Guam
NIH288	*Lyngbya* sp.	Lyngbyic Acid	Guam
VP694	*Lyngbya majuscula*	Malyngamide C	Palau
VP557	*Lyngbya majuscula*	Oscillatoxin A Debromoaplysiatoxin A	Guam

In tropical and sub-tropical areas, the most frequently encountered cyanobacteria belong to the genus *Lyngbya*.[12] As a consequence, this genus accounts for more than 30 % of all the natural products that have been isolated from marine cyanobacteria.[10] During this research, eleven of the sixteen strains of *Lyngbya* examined yielded cytotoxins (Table 13). Of these eighteen secondary metabolites, eleven were known compounds, four were analogues of known compounds (15-norlyngbyapeptin A, lyngbyabellin D, lyngbyastatin 3, and Ibu-epilyngbyastatin 3), and three were new structures (obyanamide, ulongapeptin, and palau'amide).

Table 14. Corbett Assay Data for the *Lyngbya* spp. Investigated

Extract	Leukemia (L1210)	Murine Solid (C38)[b]	Human Solid (H15)[c]	Fibroblast
VP680	400-500	700	800	800
VP755	600	430	600	580
VP417	N/A	N/A	N/A	N/A
NIH199 (1/25)[a]	440	780	820	0-200
NIH154 (1/4)[a]	0-80	380	440-550	0-550
NIH143	650	850	750	220-250
VP637 (1/100)[a]	370	600	380	300-500
VP664	320	450	440	160-430
NIH288	N/A	N/A	N/A	N/A
VP694	N/A	N/A	N/A	N/A
VP557	550	390	400-460	300-500

[a] Dilution [b] Colon solid tumor [c] Colon multidrug resistant tumor

Of the known compounds re-isolated, several are noteworthy for a variety of reasons. For example, during the summer months of 1980, 86 cases of severe contact dermatitis were reported from various beaches on the windward side of Oahu.[94] The source of the dermatitis was traced to filaments of *Lyngbya majuscula* that had broken loose from the sea floor during heavy surf and later came into contact with swimmers. Isolation of the major inflammatory agents from this cyanobacterium led to the discovery of the oscillatoxins and aplysiatoxins (**1.32**, **1.33**).[95] Further biological evaluation of these toxins indicated that the aplysiatoxins were potent tumor promoters at nanomolar concentrations.[95] At that time, only two other classes of compounds displayed such potent activity: the phorbol esters, found in a variety of terrestrial organisms, and lyngbyatoxin, from *Lyngbya majuscula* found on the south shore of Oahu. It has been suggested that the presence of strains of *Lyngbya*, which produce these toxins, in the coastal waters of Hawaii and their mistaken consumption as seaweed were two of the factors which contributed to people in Hawaii having the highest rate of gastrointestinal cancer in the world during the late 70s and mid-80s.[12]

Malyngamide C (**1.34**) was one of the other known compounds isolated. The malyngamides are one of the largest classes of cyanobacterial metabolites. They are characterized by a lyngbyic acid unit (**1.35**) connected to a six-membered ring via an amide bond. There are currently 23 analogues known, having been isolated from a variety of organisms around the globe. Despite the prevalence of these compounds, their ecological significance and biological function are currently unknown.

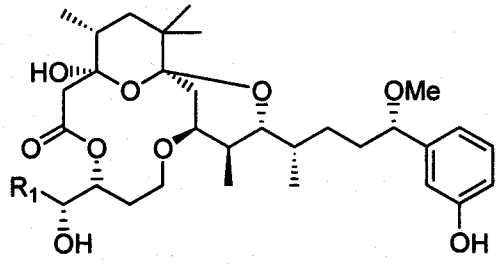

Oscillatoxin A R = H (**1.32**)
Debromoaplysiatoxin R= Me (**1.33**)

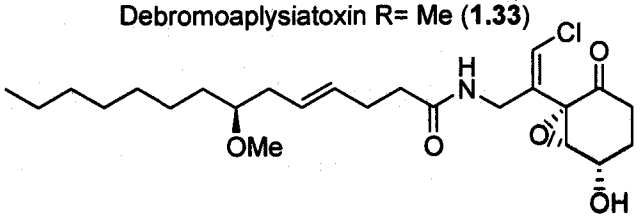

Malyngamide C (**1.34**)

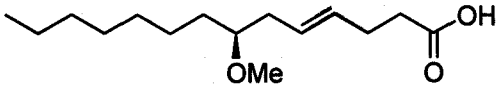

Lyngbyic Acid (**1.35**)

1.3.2 15-Norlyngbyapeptin A (1.36)

One of the best-characterized strains of *Lyngbya* can be found in Palau and Guam.[96] This field-collected cyanobacterium, easily identifiable by the presence of a small shrimp[97] within the algal mat, produces an extraordinary array of secondary metabolites. Collections of this cyanobacterium made over the last ten years have yielded eight distinct classes of metabolites, consisting of some twenty-six different compounds.[96,98]

Several large re-collections of this cyanobacterium from Guam were undertaken during the Spring of 2002 to facilitate further biological evaluation of two of these cytotoxins, the apratoxins and the lyngbyabellins. Fractionation of this extract provided 15-norlyngbyapeptin A (**1.36**) in a yield of 3×10^{-4} %. An IC_{50} value of 1.3 μM was obtained for **1.36** against KB cells.

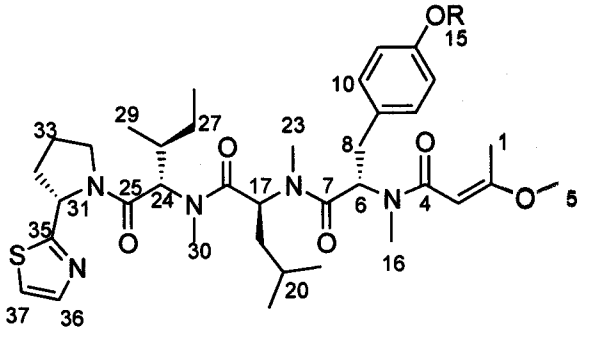

15-Norlyngbyapeptin A R=H (**1.36**)
Lyngbyapeptin A R=Me (**1.37**)

1.3.2.1 Isolation and Structure Elucidation*

Table 15. NMR Spectral Data for 15-Norlyngbyapeptin A (**1.36**) in $CDCl_3$

C/H no.[a]	δ_H[b] (*J* in Hz)	δ_C[c]
1	2.18, s	19.1, q
2		170.4, s
3	5.17, s	90.4, d
4		167.9, s
5	3.64, s	55.0, q
6	5.81, dd (9.7, 5.2)	54.3, d
7		169.5, s
8	3.24, dd (-12.9, 9.7)	34.7, t
	2.68, dd (-12.9, 5.2)	
9		129.0, s
10/14	7.14, d (8.5)	130.7, d
11/13	6.67, d (8.5)	115.2, d
12		154.5, s
15	5.60, br s	
16	3.00, s	29.9, q
17	5.44, dd (9.4, 5.5)	51.7, d
18		171.2, s
19	1.63, ddd (-14.4, 9.4, 5.0)	37.9, t
	1.51, ddd (-14.4, 9.1, 5.5)	
20	1.30, m	23.4, d
21	0.94, d (6.4)	22.3, q
22	0.92, d (6.7)	24.5, q
23	2.80, s	30.2, q
24	4.97, d (11.2)	58.0, d
25		169.9, s
26	1.92, m	33.4, d
27	0.98, m	23.4, t
	0.75, m	
28	0.74, t (6.5)	10.2, q
29	0.83, d (6.7)	15.0, q
30	2.59, s	30.2, q
31	5.43, dd (9.4, 5.5)	58.4, d
32	2.33, m	31.5, t
	2.17, m	
33	2.12, m	24.3, t
	1.96, m	
34	3.94, m	47.4, t
	3.75, m	
35		171.7, s
36	7.67, d (3.3)	142.1, d
37	7.22, d (3.3)	118.0, d

[a] The numbering system for lyngbyapeptin A (**1.37**) has been adopted.[99a]
[b] Recorded at 500 MHz. [c] Recorded at 125 MHz.

The molecular formula of 15-norlyngbyapeptin A (**1.36**) was determined to be $C_{36}H_{53}N_5O_6S$ by high-resolution FABMS (*m/z* $[M+Na]^+$ 706.3649, +3.5 mmu error), which was consistent with the ^1H and ^{13}C NMR data (Table 15). The richly detailed proton spectrum displayed a characteristic pattern of resonances that suggested that **1.36** belonged to the family of metabolites known as the lyngbyapeptins,[9699] viz. a pair of vicinal thiazole protons (δ_H 7.67, 7.22), a pair of aromatic doublets (δ_H 7.14, 6.67), a vinyl singlet (δ_H 5.17), three *N*-methylamide signals (δ_H 3.00, 2.80, 2.59), and a methyl enol ether singlet at 3.64 ppm. Conspicuously absent from both the proton and carbon NMR data were the signals for the aromatic methoxy group on the tyrosine unit (C-15). The loss of this methyl ether explained the longer retention time of **1.36** relative to lyngbyapeptin A (**1.37**) during silica chromatography and the 14 amu difference between **1.36** and **1.37**. The strong similarity between the spectral data of **1.36** and **1.37**, in conjunction with fragments observed during FABMS, suggested the same amino acid sequence (Figure 14). Fragments derived from the sequential loss of Thz-pro, *N*-Me-Ile, and *N*-Me-Leu gave rise to major ion peaks at *m/z* 530, 403, and 276 respectively.

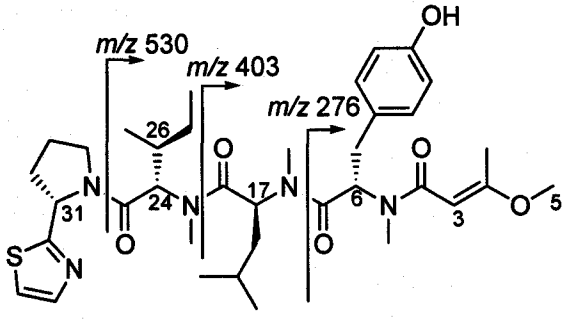

Figure 14. FABMS Fragmentation of 15-Norlyngbyapeptin (**1.36**).

1.3.2.2 Stereochemistry

The absolute stereochemistry of the amino acid-derived units in **1.36** was determined by chiral HPLC after ozonolysis and acid hydrolysis. Comparison with

authentic standards established the stereochemistry as 6*S*,17*S*,24*S*,26*S*,31*S*, analogous to lyngbyapeptin A (**1.37**).[99] The configuration of the C-2/C-3 double bond was *E*, since irradiation of H-3 (δ_H 5.17) showed a NOE to the adjacent methoxy proton signal (H-5).

1.3.2.3 Comments on 15-Norlyngbyapeptin A (1.36)

The most unusual structural feature of lyngbyapeptin A and 15-norlyngbyapeptin A is the proline-thiazole unit. In fact, these compounds are one of the few examples of secondary metabolites from marine cyanobacteria that contain a thiazole ring at the carboxy terminus of proline.[100] Generally, proline residues are not modified in marine cyanobacterial metabolites.[10] It is interesting to note that the other two members of this structural family, lyngbyapeptin B and C, have replaced this proline-thiazole unit with an alanine-thiazole moiety. Traditionally, amino acids are more likely to be substituted by units with the same hydrophobicity or polarity, i.e. neutral, acidic or basic, since this involves little modification to the enzyme. According to the model of NRPS substrate-binding pockets, substitution of proline by alanine would require the exchange of three of the eight core amino acid residues in the binding pocket (alanine to glutamine, glycine to methionine, and cysteine to histidine).[101,102] This means at least 6 of the 24 DNA base pairs that encode for these eight key positions must be modified.[103] The scale of these modifications suggests a single organism cannot be responsible for the production of all the lyngbyapeptins. The isolation of **1.36** and **1.37** only from Guamanian collections and lyngbyapeptin B and C from Palauan collections corroborate this hypothesis.

1.3.3 Lyngbyabellin D (1.38)

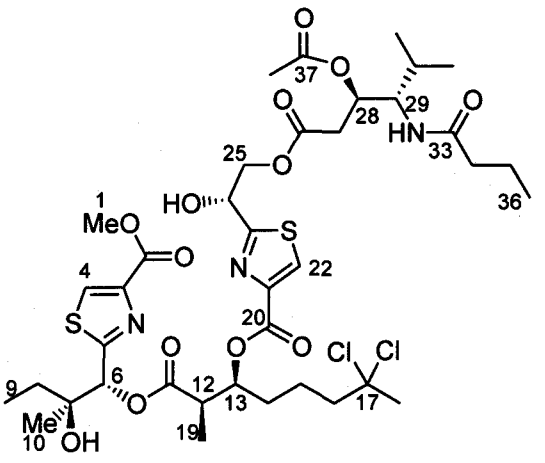

Lyngbyabellin D (**1.38**)

Of all the compounds isolated from VP417, the potency of the apratoxins[98] and the lyngbyabellins (**1.33-1.35**)[96] are particularly noteworthy. The latter were analogues of dolabellin (**1.42**),[104] a sea hare isolate, and their isolation further supported the proposal that many of the dolastatins were of cyanobacterial origin.[6] Lyngbyabellin A[105] was also a nanomolar microfilament disrupter and a related compound, hectochlorin, displayed an unique profile of cytotoxicity by the COMPARE algorithm, which suggests that this class of compounds may have a novel mode of action.[106]

Further examination of VP417 led to the isolation of lyngbyabellin D (**1.38**) in 3×10^{-4} % yield, based on the dry weight of the extract. Lyngbyabellin D (**1.38**) was the largest member of this structural family isolated, and displayed an IC_{50} value of 0.1 μM against the KB cell line.

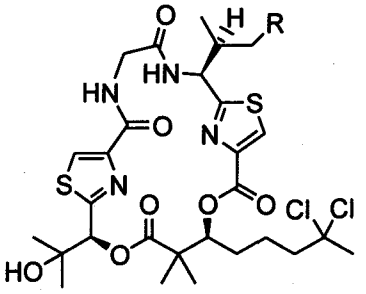

Lyngbyabellin A R =Me (**1.39**)
Lyngbyabellin B R= H (**1.40**)

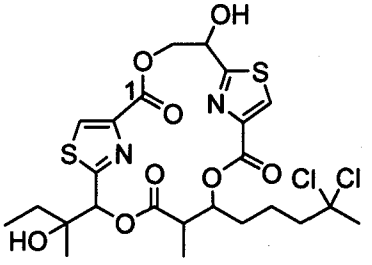

Lyngbyabellin C (**1.41**)

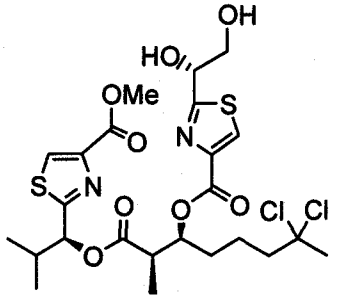

Dolabellin (**1.42**)

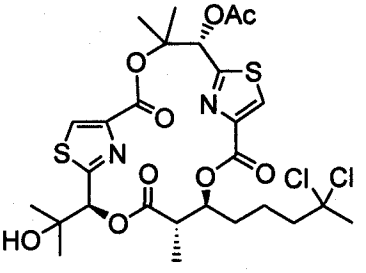

Hectochlorin (**1.43**)

1.3.3.1 Isolation and Structure Elucidation*

The molecular formula of **1.38** was established as $C_{38}H_{55}Cl_2N_3O_{13}S_2$ by high-resolution MALDI-TOF, which indicated twelve degrees of unsaturation. These could be ascribed to six carbonyls, two carbon-carbon double bonds, two carbon-heteroatom double bonds, and two rings. The downfield singlets at δ_H 8.22 and 8.17 (H-22, H-4), in conjunction with the MS data, indicated the presence of two 2-alkylthiazole-4-

---

* Reproduced in part with permission from Williams, P. G.; Luesch, H.; Yoshida, W. Y.; Moore, R. E.; Paul, V. J *J. Nat. Prod.* **2003**, *5*, 595-598. Copyright (2003) American Chemical Society.

carboxylate rings which were consistent with the UV absorption at 223 nm. These resonances, plus the unusual quaternary carbon at δ_C 90.1 (C-17) and the downfield methyl singlet at δ_H 2.12 (H-18), implied that many of the abnormal structural features characteristic of this class of metabolites were still intact. Based on the fragments already identified, it was clear that **1.38** was linear, bearing a closer relationship to dolabellin (**1.42**)[104] rather than the cyclic lyngbyabellins (**1.39-1.41**)[96] and hectochlorin (**1.43**).[99]

Analysis of the two-dimensional NMR data of **1.38** rapidly led to the identification of several fragments including an acetate, a butyric acid, a 2-(1,2-dihydroxyethyl)thiazole-4-carboxylate unit, and a methyl 2-(1,2-dihydroxy-2-methylbutyl)thiazole-4-carboxylate unit. This latter unit was present in another member of this family, but its stereochemistry had not been determined due to the paucity of material.[96] A 7,7-dichloro-3-hydroxy-2-methyloctanoic acid fragment was also easily sequenced. These fragments accounted for a total of $C_{31}H_{43}Cl_2N_2O_{11}S_2$.

On the basis of a HMBC correlation from H-25 to C-26, the remaining $C_7H_{12}NO_2$ was clearly attached to the β-hydroxyl group of the glyceric acid-derived moiety via an ester linkage. The secondary amide proton signal at δ_H 5.47 (29-NH) showed a strong COSY correlation to H-29, which in turn showed three vicinal couplings ($^3J_{H\text{-}29/29\text{-}NH}$ = 11.8, $^3J_{H\text{-}29/H\text{-}28}$ = 8.4, $^3J_{H\text{-}29/H\text{-}30}$ = 3.2 Hz). Using HMBC and COSY correlations, this fragment was expanded into a modified valine unit (C-26 to C-32). A $^1J_{CH}$ from H-28 to a downfield carbon at 70.3 ppm indicated that this carbon was oxygenated, while a COSY correlation to the methylene protons (H-27) and two HMBC correlations to carbonyls at δ_C 170.6 and δ_C 169.5 (C-37, C-26) from H-28 established the acetylated structure depicted.

Table 16. NMR Spectral Data for Lyngbyabellin D (**1.38**) in $CDCl_3$

C/H no.	δ_H[a] (*J* in Hz)	δ_C[b,c]	^{1}H-^{1}H COSY	HMBC[d,e]
1	3.95, s	52.5, q		
2		161.7, s		1
3		145.9, s		4
4	8.17, s	128.8, d		
5		167.4, s		4, 6
6	6.22, s	76.9, d		8, 10
7		74.4, s		6, 8, 9, 10
8	1.78, q (7.4)	31.5, t	9	9, 10
9	0.934, t (7.4)	8.1, q		
10	1.06, s	21.58, q		
11		170.9, s		6, 12, 19
12	2.98, dq (7.1, 6.9)	43.8, d	12, 19	19
13	5.41, m	74.7, d	12, 14	19
14	1.78, m	31.7, t	13	15
	1.67, m			
15	1.85, m	21.56, t		16
16	2.24, m	49.0, t	15	18
	2.20, m		15	
17		90.1, s		18
18	2.12, s	37.4, q		
19	1.25, d (7.1)	13.6, q	12	12
20		160.9, s		
21		146.7, s		22
22	8.22, s	129.1, d		
23		172.8, s		22, 24-OH, 25
24	5.25, ddd (8.7, 5.5, 3.3)	69.6, d	24-OH, 25	24-OH, 25
24-OH	5.60, d (5.5)		24	
25	4.56, dd (-11.3, 3.3)	68.1, t	24, 25b	
	4.44, dd (-11.3, 8.7)		24, 25a	
26		169.5, s		25, 27
27	2.71, dd (-15.5, 5.7)	36.5, t	28	
	2.63, dd (-15.5, 5.7)		28	
28	5.11, dt (8.4, 5.7)	70.3, d	27, 29	27
29	4.25, ddd (11.8, 8.4, 3.2)	54.4, d	28, 29-NH, 30	27, 31, 32
29-NH	5.47, d (11.8)		29	
30	1.93, m	27.6, d	29, 31, 32	31, 32
31	0.930, d (7.1)	20.2, q	30	32
32	0.84, d (6.9)	16.0, q	30	31
33		173.7, s		34, 35
34	2.20, t (7.4)	38.9, t	35	35, 36
35	1.67, m	19.2, t	34, 36	34, 36
36	0.95, t (7.4)	13.7, q	35	34, 35
37		170.6, s		28, 38
38	2.08, s	21.0, q		

[a] Recorded at 500 MHz. [b] Recorded at 125 MHz. [c] Multiplicity deduced by HSQC. [d] Protons showing long range correlation with indicated carbon. [e] Correlations were observed for $^nJ_{CH}$ = 7 Hz.

1.3.3.2 Stereochemistry

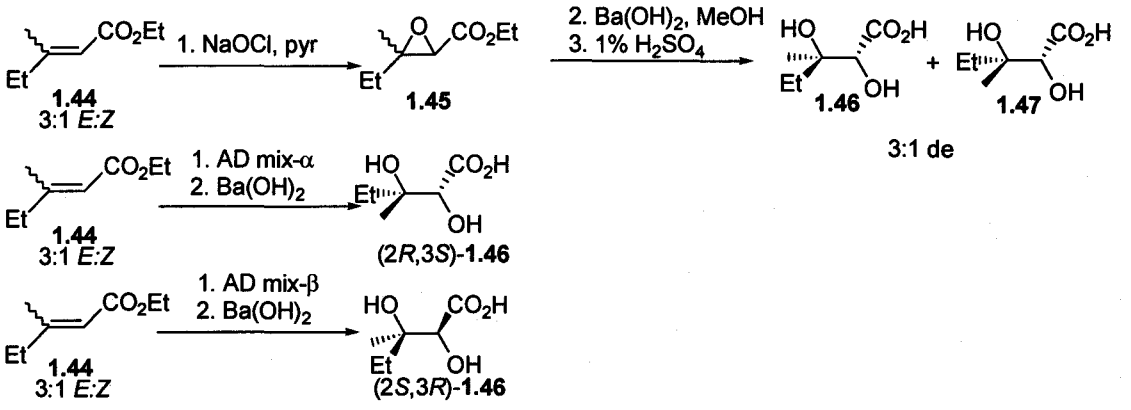

Figure 15. Synthesis of α,β-Dihydroxy-β-methylpentanoic Acid Standards.

The configuration of **1.38** was determined by analysis of the degradation products. Ozonolysis and base hydrolysis liberated C-5 through C-10 as 2,3-dihydroxy-3-methylpentanoic acid (Dhmp) and C-23 through C-25 as glyceric acid. Dhmp standards were prepared by diastereoselective and enantiospecific routes (Figure 15). First, a mixture of all four diastereomers was synthesized by epoxidation[107] of a 3:1 mixture of *E:Z* ethyl 3-methyl-2-pentenoate[108] (**1.44**). Subsequent acid-catalyzed ring opening, with nucleophilic attack on the epoxide occurring adjacent to the carbonyl afforded **1.46** and **1.47**. Comparison of this mixture (**1.46**, **1.47**), after deprotection, with the ozonized base hydrolyzate of **1.38**, established the *threo* relative stereochemistry for this unit (**1.46**, 2*R**,3*S**), since it contained a peak that co-eluted with the synthetic standard derived from epoxidation of the *Z*-enoate. Asymmetric dihydroxylation with AD-α and AD-β mixtures of the α,β-unsaturated ester provided enantiomerically pure (2*R*,3*S*)- and (2*S*,3*R*)-**1.46** respectively from the *trans* olefin.[109] Subsequent chiral HPLC established

the absolute stereochemistry of the Dhmp and the glyceric acids as shown in **1.38**, viz. 6*R*,7*S*,24*R*. The configuration of C-6 was opposite of that found in the α,β-dihydroxy-β-methylbutanoic acid of lyngbyabellin A (**1.39**) and hectochlorin (**1.43**). The configuration at C-24 was identical to the glyceric acid unit in dolabellin (**1.42**), but opposite to that of the corresponding dihydroxy acid unit found at this position in hectochlorin (**1.43**).

The relative stereochemistry of the polyketide-derived β-hydroxy acid was determined to be 12*R**,13*S** by comparison of coupling constants and chemical shifts with other members of this family. Specifically H-12 exhibited two large couplings of approximately 7 Hz, almost identical to the ones for dolabellin, whose configuration was determined by synthesis.[104,110] The absolute stereochemistry of C-13 is probably *S*, since despite the numerous structural and stereochemical variations, **1.39**, **1.40**, **1.42**, and **1.43** all have the *S* absolute configuration at the β-position of the polyketide chain.[104,105,106]

The stereochemistry of the γ-amino-β-hydroxy acid residue in **1.38** was determined by a combination of techniques. First, the relative stereochemistry of H-28 and H-29 was determined by a NOE correlation between 29-NH and H-27. Using NOE correlations to determine the configuration around these centers was possible owing to a large $^{3}J_{\text{H-29/H-28}}$ value (8.4 Hz).[111] Then the absolute configuration of C-29 was determined by acid hydrolysis and subsequent ozonolysis, with oxidative workup to L-valine as determined by chiral HPLC. The stereochemical assignment of lyngbyabellin D (**1.38**) was therefore 6*R*,7*S*,12*R*,13*S*,24*R*,28*S*,29*S*.

1.3.3.3 Comments on Lyngbyabellin D (1.38)

One significance of the isolation of the lyngbyabellins from cyanobacteria is to further the hypothesis that many of the dolastatins, originally isolated from the sea hare

Dolabella auricularia, are acquired by the mollusk through its diet.[6] In the case of lyngbyabellin D, the stereochemistry of the β-hydroxy and the glyceric acid-derived moieties are identical to those found in the sea hare isolate dolabellin and opposite in configuration to the corresponding stereocenters in the other cyanobacterial metabolites.

The structure of lyngbyabellin D (**1.38**) suggested that dolabellin may not be an artifact of the isolation procedure. This had been suggested based on the preferential methanolysis of the C-1 to C-25 ester linkage in lyngbyabellin C (**1.41**).[96] In the case of lyngbyabellin D (**1.38**), the methyl ester at C-1 cannot arise from methanolysis of the C-1/C-25 ester linkage since C-25 is derivatized with the γ-amino-β-hydroxyacid.[112] This suggests that the methyl ester at C-1 of **1.38** arises via the biosynthetic machinery of the cyanobacterium, most likely by *S*-adenosylmethionine (SAM) methylation of the acid. Evidently, this organism is able to produce concurrently both cyclic and acyclic analogues of these compounds with a variety of stereochemical configurations, a tactic which, if these metabolites are antifeedants, may provide an evolutionary advantage by delaying the development of detoxification mechanisms by predators.[113]

It is also interesting to note, that α,β-dihydroxy-β-methylpentanoic acid, contained within **1.38** is the penultimate intermediate in isoleucine biosynthesis. Therefore the configuration of this unit depicted in **1.38** is likely the stereochemistry produced by the primary metabolism of this cyanobacterium. Subsequent dehydration and transamination would adjust the stereochemistry of these vicinal centers as required to produce either D- or L-Ile.

1.3.4 Obyanamide (1.48)

Obyanamide (**1.48**) was isolated from a strain of the marine cyanobacterium *Lyngbya confervoides* collected from Saipan, Commonwealth of the Northern Mariana Islands. Obyanamide (**1.48**) exhibited moderate cytotoxicity against KB cells with IC_{50} value of 0.98 μM.

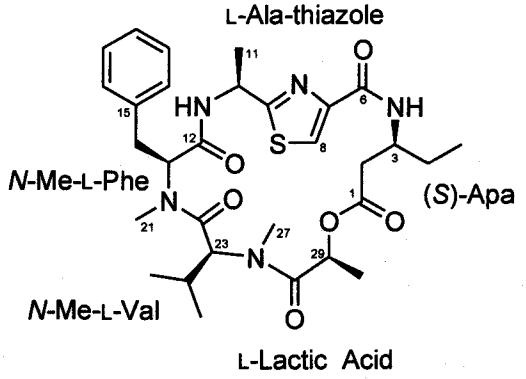

Obyanamide (**1.48**)

1.3.4.1 Isolation and Structure Elucidation*

The lipophilic extract of VP680 showed slight solid tumor selectivity in the Corbett assay.[114] Solvent partitioning of this extract followed by Si gel chromatography and repeated reversed phase HPLC, yielded **1.48** as a white amorphous powder.

---

* Reproduced in part with permission from Williams, P. G.; Yoshida, W. Y.; Moore, R. E.; Paul, V. J *J. Nat. Prod.* **2002**, *65*, 29-31. Copyright (2001) American Chemical Society.

Table 17. NMR Spectral Data for Obyanamide (**1.48**) in $CDCl_3$

C/H no.	δ_H[a] (*J* in Hz)	δ_C[b,c]	^1H-^1H COSY	HMBC[d,e]
3-aminopentanoic acid				
1		170.4, s		H-2, H-29
2	2.74, dd (-11.8, 5.0)	39.1, t	H-3	
	2.38, dd (-11.8, 3.0)			
3	4.36, m	47.6, d	H-2, 3-NH, H-4	H-4, H-5
3-NH			H-3	
4	1.63, m	26.2, t	H-3, H-5	H-2, H-5
5	1.05, t (7.4)	11.3, q	H-4	H-4
Ala-Thz				
6		160.4, s		H-8
7		149.0, s		H-8
8	7.98, s	123.2, d		
9		170.1, s		H-8, H-11, 10-NH
10	5.04, q (7.6)	48.3, d	10-NH, H-11	10-NH, H-11
10-NH	7.90, d (7.6)		H-10	
11	1.42, d (7.6)	24.1, q	H-10	
N-Me-Phe				
12		168.2, s		10-NH
13	5.42, dd (8.2, 6.9)	60.9, d	H-14	H-14, H-21
14	3.25, dd (-13.7, 8.2)	37.2, t	H-13	
	2.87, dd (-13.7, 6.9)			
15		137.0, s		H-14
16/20	7.17, d (7.9)	128.9, d	H-17	H-14
17/19	7.21, dd (7.9, 7.2)	129.4, d	H-16, H-18	
18	7.08, t (7.2)	127.1, d	H-17	
21	3.085, s	29.1, q		H-16
N-Me-Val				H-13
22		169.8, s		H-21, H-23, H-13
23	5.06, d (10.2)	57.9, d	H-24	H-26, H-25, H-27
24	2.28, m	27.6, t	H-23, H-25, H-26	H-23
25	0.84, d (6.6)	18.5, q	H-24	H-26
26	0.48, d (6.6)	18.6, q	H-24	H-25
27	3.094, s	29.9, q		H-23
Lactic Acid				
28		173.2, s		H-27, H-30
29	5.20, q (6.9)	67.9, d	H-30	H-30
30	1.23, d (6.9)	16.0, q	H-29	H-29

[a] Recorded at 500 MHz. [b] Recorded at 125 MHz. [c] Multiplicity deduced by HSQC. [d] Protons showing long range correlation with indicated carbon. [e] Correlations were observed for $^nJ_{CH}$ = 7 Hz.

HR-FABMS analysis established the molecular formula for **1.48** as $C_{30}H_{41}N_5O_6S$, which indicated 13 degrees of unsaturation. Inspection of the ^{13}C NMR spectrum showed 14 sp^2 carbons in the form of four carbon-carbon double bonds and six carbon-heteroatom double bonds, which accounted for ten degrees of unsaturation. The remaining three degrees of unsaturation must then be in the form of rings. The IR spectrum revealed that **1.48** contained both amide (1628 cm^{-1}) and ester bonds (1734 cm^{-1}), indicating it was in fact a peptolide. This peptidic nature was further supported by

the presence of two amide (δ_H 9.11, 7.90) and two *N*-methylamide proton signals (δ_H 3.085, 3.094) in the ^{1}H NMR spectrum. The COSY, HSQC and HMBC data, summarized in Table 17, suggested the presence of *N*-methylvaline, *N*-methylphenylalanine, and 3-aminopentanoic acid (Apa) fragments. The low-field resonance for C-29 (δ_C 67.9) and the corresponding proton (δ_H 5.20) indicated that the acyloxy group was attached to this carbon. A COSY correlation to H-30 and a HMBC cross-peak to C-1 from H-29 along with a HMBC correlation from H-30 to C-28 expanded this particular fragment into a lactic acid moiety, which was attached to the β-amino acid (Apa) unit via an ester linkage. The downfield singlet in the ^{1}H NMR spectrum at δ_H 7.98 as well as the sp^2 carbon resonances at 123.2, 149.0, 160.4, and 170.1 ppm were characteristic of a 2-alkylthiazole-4-carboxylic acid unit (C-6 to C-9).[115] HMBC correlations to C-9 and C-10 from H-11 and to C-9 from H-8 connected the remaining carbons to form an Ala-thiazole fragment.

As always, HMBC couplings from the *N*-methyl groups were quite informative in sequencing the peptolide. From the *N*-methylamide signal at 3.085 ppm (H-21), HMBC cross-peaks to the signals for the α-carbon of phenylalanine (C-13) and to the carbonyl carbon of valine (C-22) were visible. This clearly indicated that the *N*-Me-Phe nitrogen was attached to the *N*-Me-Val carbonyl. Similarly the *N*-methylamide signal at δ 3.094 (H-27) showed HMBC correlations to the signal for the α carbon of the valine (C-23) and to the carbonyl carbon of the lactic acid fragment (C-28). Finally, a HMBC correlation between the δ 7.90 amide proton of the Ala-thiazole moiety (10-NH) and C-12 of the *N*-Me-Phe residue firmly established the connection of the Ala nitrogen to the *N*-Me-Phe

carbonyl. Since one degree of unsaturation remained, **1.48** had to be cyclic with the amine of the Apa attached to the cysteine-derived carbonyl of the thiazole ring.

1.3.4.2 Stereochemistry

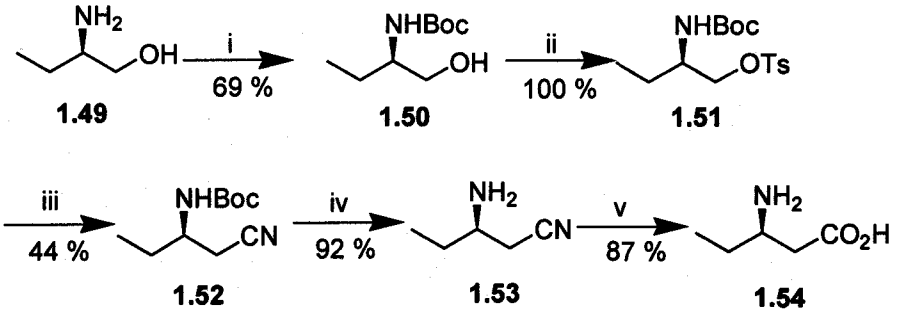

(i) Boc_2O, t-BuOH, H_2O; (ii) TsCl, pyridine; (iii) NaCN, DMSO; (iv) TFA; (v) 6 N HCl.

Figure 16. Synthesis of (*R*)-3-Aminopentanoic Acid.

The absolute stereochemistry of **1.48** was established by analysis of the degradation products. Obyanamide was subjected to ozonolysis followed by acid hydrolysis, and the product mixture was analyzed by HPLC on a chiral column [Chirex phase 3126 (D)]. Comparison of the components of the hydrolyzate with authentic amino acid standards established an L configurations of the all the amino acids. Pure L- and D-lactic acid standards were prepared from alanine[116] and chiral TLC and chiral HPLC determined the L-stereochemistry of this unit. Due to the limited amount of material available, determination of the final stereocenter at C-3 necessitated the synthesis of (*R*)- and (*S*)-3-aminopentanoic acid (Figure 16). Commercially available (*R*)- and (*S*)-2-aminobutanol served as the chiral starting block for the five step synthesis. Boc protection and tosylation of the amino alcohol followed by sodium cyanide substitution

(**1.52**) and acid hydroylsis provided the necessary standards (**1.54**). A comparison of the hydrolyzate mixture and these standards showed no sign of the (*R*)–Apa under a variety of solvent strengths and flow rates. Conversely a peak co-eluting with the (*S*)-Apa standard was clearly evident.

1.3.4.3 Comments on Obyanamide (1.48)

Obyanamide (**1.48**) is a new depsipeptide containing two *N*-methyl amino acids, an Ala-thiazole unit and a β-amino acid. β-amino acid fragments are not uncommon in marine cyanobacterial metabolites. Structurally related units include the (2*S*,3*R*)-3-amino-2-methyl-pentanoic acid found in majusculamide C,[117] dolastatin 11,[118] dolastatin 12,[119] and lyngbyastatin 1.[119] Similarly, dolastatin 16[120] possesses a 3-amino-2,4-dimethylpentanoic acid fragment of unknown stereochemistry, while dolastatin D[121] has a (2*R*,3*R*)-3-amino-2-methylbutanoic acid unit.

Obyanamide (**1.48**) was the first compound reported from *L. confervoides*. Subsequently another class of depsipeptides from this species, lobocyclamides A-D,[122] was identified, which like **1.48** contain a long chain β-amino acid. Since then a Palauan collection of *L. majuscula* has afforded ulongamides A-F[123] that have a strong structural similarity to **1.48**. In fact, the sequence of ulongamide A differs from **1.48** just by the reversal of the *N*-Me-Val and *N*-Me-Phe residues. This variation has a negligible effect on the cytotoxicity, as both compounds had IC_{50} value of approximately 1 μM against KB cells.

Interestingly, ulongamide F was inactive against KB cells at 10 μM, which suggested that either the aromatic amino acid residue or the *N*-methylation adjacent the hydroxy acid was important for the cytotoxicity.

1.3.5 Ulongapeptin (1.55)

Ulongapeptin (**1.55**), a cyclic depsipeptide, was isolated from a Palauan strain of the marine cyanobacterium *Lyngbya*. Ulongapeptin (**1.55**) was cytotoxic against KB cells at an IC_{50} of 0.64 μM.

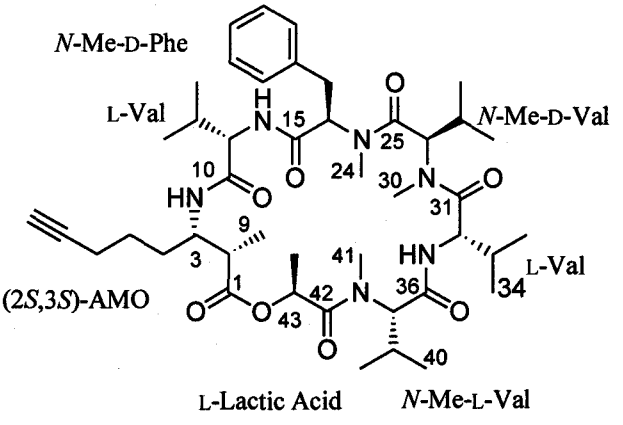

Ulongapeptin (**1.55**)

1.3.5.1 Isolation and Structure Elucidation*

Lyophilized VP755 was extracted with a 1:1 mixture of methanol/ethyl acetate and the resulting concentrate fractionated by normal and reversed-phase chromatography to afford 1.1 mg of ulongapeptin (**1.55**) in 9.9 x 10^{-2} % yield after RP-HPLC.

Ulongapeptin (**1.55**) had a molecular weight of 808 Da based on FABMS pseudo-molecular ion peaks at *m/z* 809, 831, and 847 for $[M + H]^+$, $[M + Na]^+$, and $[M + K]^+$ respectively. HR-MALDI, in conjunction with the proton and carbon spectral data,

---

* Reproduced in part with permission from Williams, P. G.; Yoshida, W. Y.; Quon, M. K.; Moore, R. E.; Paul, V. J *J. Nat. Prod.* **2003**, *5*, 651-654. Copyright (2003) American Chemical Society.

established an elemental composition for the amorphous powder as $C_{44}H_{68}N_6O_8$. From the proton and carbon spectral data, 13 sp^2 carbons, in the form of seven carbonyls and three carbon-carbon double bonds, constituted ten of the 14 degrees of unsaturation implied by the molecular formula of **1.55**. According to the ^1H NMR data, the six nitrogens were accounted for by three secondary amide (δ_H 6.19, 8.18, 8.24) and three tertiary *N*-methylamide groups (δ_H 2.75, 2.90, 3.40). In addition to a broad band at 1654 cm^{-1} for amide carbonyls, the IR spectrum showed a strong vibration at 1727 cm^{-1} characteristic of an ester moiety. The eight oxygens were therefore located in one ester and six amide carbonyl groups, which suggested that **1.55** was a depsipeptide that consisted of one hydroxy and six amino acid units.

One-dimensional TOCSY experiments enabled us to identify the amino acids that constituted **1.55**. Excitation of the 2° amide proton signals at δ_H 8.18 (32-NH) and 8.24 (11-NH) produced spectra with signals for protons that were either directly- or relay-coupled to these NH groups and suggested the presence of two valine units. Likewise excitation of the doublets at δ_H 3.95 (H-37) and 4.90 (H-26) generated spectra consistent with two more valine units whose nitrogens were part of tertiary amide groups. Analysis of the HMBC spectra showed $^3J_{CH}$ cross-peaks from the methyl singlets at δ_H 3.40 (H-30) and 2.75 (H-41) to C-26 and C-37, respectively, which verified this conclusion and thereby expanded these fragments into two *N*-Me-Val units. Another unit was generated starting from the α-proton signal at 4.99 ppm (H-16) that showed $^3J_{HH}$ couplings to a pair of geminal doublet of doublets at 3.90 and 2.53 ppm (H-17). This fragment was expanded into a *N*-methylphenylalanine unit via HMBC correlations to C-18 from H-17 and H-20, and to the α-carbon (C-16) from the methylamide signal at δ_H 2.90 (H-24).

Table 18. NMR Spectral Data for Ulongapeptin (**1.55**) in $CDCl_3$

C/H no.	δ_H[a] (*J* in Hz)	δ_C[b,c]	$^1H - ^1H$ COSY	HMBC[d,e]	ROESY
AMO					
1		177.7, s		2, 9	
2	2.82, qd (7.0, 3.6)	41.8, d	3, 9	9	3, 9
3	4.27, m	49.4, d	2, 3-NH, 4	9	2, 9
3-NH	6.19, d (10.1)		3		4, 11-NH
4	1.59, m	33.0, t	3, 4b	2, 3	2, 3-NH, 5, 6, 19
	1.30, m		4a		
5	1.28, m	24.1, t		3	4a
6	2.18, m	17.7, t	5, 8		
	2.02, m		5, 8		
7		83.9, s			
8	1.98, t (2.6)	68.9, d	6		
9	1.13, d (7.0)	14.7, q	2		2, 3, 13
Val					
10		171.4, s		3-NH, 11	
11	4.28, t (10.2)	61.2, d	11-NH, 12		13, 14
11-NH	8.24, d (10.2)		11		3-NH, 16
12	1.62, m	31.8, d	11, 13, 14	11, 13, 14	13, 14
13	0.97, d (6.7)	19.5, q	12	12, 14	9, 11, 12, 14
14	0.78, d (6.6)	20.3, q	12	11, 12, 13	11, 12, 13, 24
N-Me Phe					
15		167.5, s		11, 16, 17b, 11-NH	
16	4.99, dd (11.5, 1.9)	62.0, d	17	17a, 17b, 24	11-NH, 17b, 26
17	3.90, dd (-13.2, 11.5)	35.8, t	16, 17b		17b, 24
	2.53, dd (-13.2, 1.9)		16, 17a		17a, 19, 28
18		137.6, s		17, 20	
19/23	7.26, d (7.4)	129.4, d	20	17, 19, 21	4, 17b, 28
20/22	7.30, dd (7.4, 6.0)	128.6, d	19, 21		
21	7.25, t (6.0)	126.7, d		19	
24	2.90, s	29.2, q			14, 17a
N-Me-Val					
25		170.9, s		16, 24, 26	
26	4.90, d (10.9)	58.4, d	27	28, 29, 30	16, 28, 29
27	2.39, m	28.5, d	26, 28, 29	28, 29	30
28	1.07, d (6.5)	20.1, q	27	27, 29	17b, 19, 27
29	0.94, d (6.4)	19.6, q	27	26, 27, 28	26, 30, 35
30	3.40, s	31.6, q		26	27, 29, 32, 35
Val					
31		175.7, s		26, 30, 32	
32	4.76, t (9.4)	54.6, d	32-NH, 33	34, 35	30, 34, 35
32-NH	8.18, d (9.4)		32		37
33	2.06, m	31.2, d	32	32, 34, 35	34, 35
34	0.87, d (6.7)	18.6, q	33	32, 35	32, 33
35	0.84, d (6.8)	19.7, q	33	34	29, 35
N-Me-Val					
36		167.6, s		32, 32-NH, 37	
37	3.95, d (10.5)	66.5, d	38	39, 40, 41	32-NH, 39, 40, 43
38	2.46, m	26.1, d	37, 39, 40	37, 40	38, 40, 41
39	1.03, d (6.3)	20.7, q	38	37, 38, 40	37
40	0.87, d (6.7)	19.2, q	38	37, 38, 39	38, 44
41	2.75, s	29.3, q		37	34, 38, 40
Lac					
42		170.7, s		37, 41, 44	
43	5.45, q (6.6)	66.4, d	44	44	37, 44
44	1.50, d (6.6)	17.7, q	43	43	40, 43

[a] Recorded at 500 MHz. [b] Recorded at 125 MHz. [c] Multiplicity deduced by HSQC. [d] Protons showing long range correlation with indicated carbon. [e] Correlations were observed for $^nJ_{CH} = 7$ Hz.

The two isolated spin systems that remained were assigned as follows. Irradiation of the methine quartet at δ_H 5.45 (H-43) in a 1D-TOCSY experiment showed magnetization transfer to a methyl doublet at δ_H 1.50 (H-44) to form a 2-carbon unit. A $^1J_{CH}$ cross-peak obtained from the HSQC spectra connected this downfield methine to a carbon signal at δ_C 66.4 (C-43); a chemical shift suggestive of a carbinol and hence a lactic acid moiety. An initial one-dimensional TOCSY experiment on the final secondary amide proton signal at δ_H 6.19 (3-NH) gave correlations to a nitrogen-bearing methine at δ_H 4.27 (H-3), a methyl doublet (H-9), a quartet of doublets at δ_H 2.82 (H-2), and the proton signals for H-4. These diagnostic resonances implied an α-methyl-β-amino acid unit common in cyanobacterial metabolites.[10] A second TOCSY experiment with a longer mixing time showed the secondary amide proton (3-NH) was relay-coupled to the terminal alkyne proton at δ_H 1.98 (H-8). Considering all the fragments previously identified and the constraints imposed by the molecular formula, this had to be a C_8 unit, viz. a 3-amino-2-methyl-7-octynoic acid unit.

With the molecular formula satisfied, the gross structure was assembled via HMBC correlations. Cross-peaks from the amide proton signals to C-10, C-15, and C-36 established the sequences (AMO)-(Val)-(*N*-Me-Phe) [C-1 to C-24] and (Val)-(*N*-Me-Val) [C-31 to C-41]. These two fragments were linked by $^3J_{CH}$ correlations from the *N*-methylamide signals to the remaining units. Specifically, cross-peaks to C-25 from H-24, to C-31 from H-30, and to C-42 from H-41 connected all of these fragments into a linear chain, i.e. (AMO)-(Val)-(*N*-Me-Phe)-(*N*-Me-Val)-(Val)-(*N*-Me-Val)-(Lactic acid). HMBC[124] and ROESY experiments failed to show any correlations which supported a connection between C-1 of the AMO unit and the lactic acid oxygen, but given the ester

carbonyl vibration in the IR at 1727 cm^{-1} and the degrees of unsaturation required by the molecular formula, ulongapeptin had to be the cyclic depsipeptide **1.55**.

1.3.5.2 Stereochemistry

The absolute configuration of **1.55** was established by analysis of the degradation products. A small sample of **1.55** was hydrogenated to reduce the terminal alkyne and then hydrolyzed with 6 N HCl to liberate the amino acids. These were analyzed by chiral HPLC and the retention times compared with authentic standards. The proteogenic amino acids and the hydroxy acid were shown to all have the L configuration. Of the *N*-methylated amino acids, the phenylalanine-derived unit was clearly D, but both enantiomers of *N*-methylvaline were encountered in an equal amount. Hydrolysis of **1.55** at a lower temperature (90 °C) gave the same result and confirmed the presence of both enantiomers of *N*-Me-Val in **1.55**.

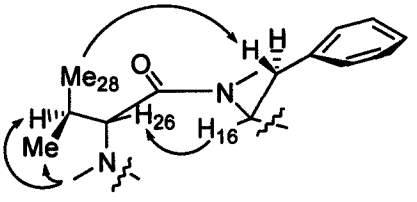

Figure 17. Key ROESY Correlations around C-26.

Analysis of the ROESY data, suggested a D configuration around C-26 (Figure 17). Specifically, a cross-peak from H-16 to H-26 indicated a *cis* geometry of the amide bond between these two units, while a correlation between H-17b and H-28 revealed that the side chains of these units were on the same face of the molecule. Molecular modeling of this dipeptide fragment indicated that both stereocenters must have the same absolute

configuration in order to explain these cross-peaks. Similar correlations between the lactic acid moiety and the adjacent *N*-Me-Val unit were in line with this conclusion and further suggested an L configuration around C-37.[125]

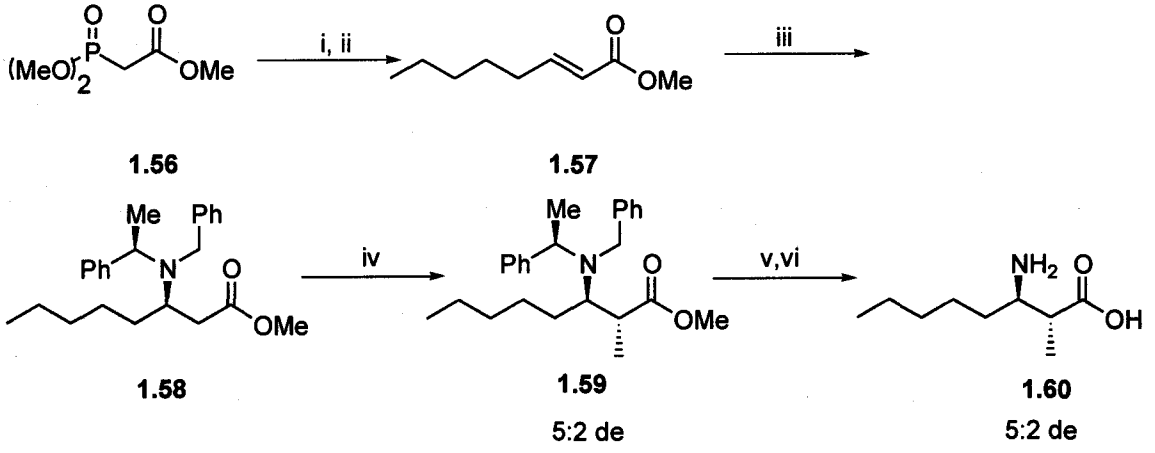

(i) *n*-BuLi, THF; (ii) hexanal; (iii) *n*-BuLi, THF (*R*)-*N*-Benzyl-α-methylbenzylamine; (iv) KHMDS, MeI; (v) H_2, 20 % Pd/C; (vi) 6 N HCl.

Figure 18. Synthesis of (2*R*,3*R*)-AMO.

The α-methyl-β-amino acid was synthesized as a 5:2 mixture of C-2 diastereomers (2*R*,3*R* and 2*S*,3*R*) as shown in Figure 18. The Horner-Wadsworth-Emmons elongation of hexanal produced a 1:1 mixture of *E*:*Z* methyl oct-2-enoate, which was easily separated by flash chromatography. Michael addition of *N*-benzyl-α-methylbenzylamine to *trans*-**1.57** afforded **1.58** after purification.[126] Subsequent methylation produced a mixture of diastereomers[127] that were separated after deprotection (1.60) as their 1-fluoro-2,4-dinitrophenyl-leucinamide derivatives (FDLA) to afford the (2*R*,3*R*)- and (2*S*,3*R*)-AMO standards. The enantiomers of the other two standards [(2*S*,3*S*) and (2*R*,3*S*)] were prepared by derivatization of the synthetic reaction mixture

with DL-FLDA and subsequent separation of the four resulting peaks by HPLC.[128] Comparison with the L-FDLA derivatized hydrogenated hydrolyzate established the absolute configuration of the 3-amino-2-methyl-7-octynoic acid as 2*S*,3*S* under standard Marfey conditions.

1.3.5.3 Comments on Ulongapeptin (1.55)

The trivial name of **1.55** has been assigned after the collection site of the cyanobacterium. Ulong channel has proven to be a rich source of interesting metabolites including the lyngbyabellins (**1.38-1.41**),[33] and the apramides (**1.1-1.3**).[30] Both classes of compounds possess C_8 units similar to **1.55**. The AMO unit found in **1.55** has been previously identified in the mollusk metabolite onchidin.[129] Such α-methyl-β-amino acid units frequently occur in cyanobacterial metabolites and their appearance in compounds isolated from other marine organisms has often been suggested as being indicative of either a dietary or a symbiotic relationship between the two organisms.[6]

The structure of **1.55** is an excellent example of the metabolic themes of cyanobacteria. Four of the five amino acid-derived units are valine, which is the most commonly encountered amino acid in cyanobacterial compounds, and half of these valine units are *N*-methylated, a percentage which mirrors that found in the literature.[10] The presence of two amino acids, which have been epimerized to a D configuration, is unusual though, since over 90 % of amino acids incorporated into cyanobacterial metabolites have an L configuration.[10]

1.3.6 Palau'amide (1.61)

Bioassay-guided fractionation of the lipophilic extract of a *Lyngbya* sp. from Palau has yielded palau'amide (**1.61**). This was the most potent cytotoxin isolated from the strains of marine cyanobacteria examined. The IC_{50} value of **1.61** against KB cells was 13 nM.

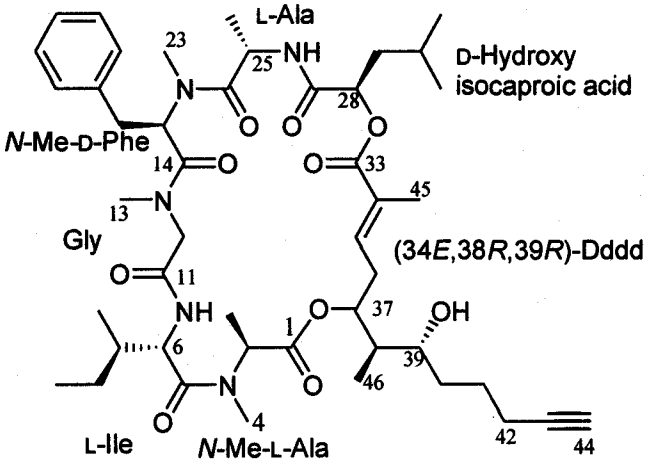

Palau'amide (**1.61**)

1.3.6.1 Isolation and Structure Elucidation

In the spring of 2000, a strain of *Lyngbya* was collected from Ulong Channel, Palau. Since the lipophilic extract of these dark reddish-brown clumps was slightly solid tumor selective, the cyanobacterium was re-collected for further study. Bioassay-guided fractionation of the lipophilic extract provided palau'amide (**1.61**) in 0.2 % yield (2.8 mg).

Table 19. Spectral Data for the Major Conformer of Palau'amide (**1.61**) in MeOH-d_3

Unit	C/H no.	δ_H [a] (J in Hz)	δ_C [b,c]	^{1}H-^{1}H COSY	HMBC [d,e]
N-Me-Ala	1		171.7, s		2, 3
	2	3.84, q (6.7)	61.3, d	3	4
	3	1.44, d (6.7)	13.8, q	2	
	4	3.36, s	39.0, q		2
Ile	5		172.6, s		4, 6
	6	4.89, t (9.6)	53.9, d	6-NH, 7	7, 10
	6-NH	8.17, d (9.6)		6	
	7	1.87, m	38.8, d		
	8	1.84, m	25.5, t		9, 10
		1.32, m		9	
	9	0.94, t (7.4)	10.9, q		7
	10	0.88, d (6.6)	11.5, q	7	7
N-Me-Gly	11		170.6, s		6-NH, 6, 12
	12	4.18, d (-18.7)	52.7, t	12_U	13
		3.13, d (-18.7)		12_D	
	13	2.87, s	36.8, q		12
N-Me-Phe	14		172.4, s		12, 13, 15, 16
	15	5.43, dd (9.9, 5.5)	55.2, d	16	16, 23
	16	3.01, dd (-14.5, 9.9)	35.9, t	15	18/22
		2.95, dd (-14.5, 5.5)		15	
	17		138.3, s		16
	18/22	7.14, d (6.9)	130.7, d		16, 20
	19/21	7.18, t (6.9)	129.1, d		
	20	7.16, t (6.9)	127.5, d		18/22
	23	3.01, s	30.7, q		15
Ala	24		174.9, s		15, 23, 25, 26
	25	4.47, p (6.8)	46.4, d	25-NH, 26	26
	25-NH	8.57, d (6.8)		25	
	26	0.82, d (6.8)	15.3, q	25	25, 25-NH
Hica	27		173.8, s		25-NH, 28
	28	4.91, dd (12.0, 9.8)	74.2, d	29	
	29	1.79, m	41.9, t	28, 29_u, 30	
		1.51, m		28, 29_d, 30	
	30	1.37, m	30.6, t	31, 32	
	31	0.95, d (6.6)	23.8, q	30	32
	32	0.92, d (6.0)	21.7, q	30	31
Dddd	33		169.9, s		35, 45
	34		146.5, s		45
	35	6.84, t (6.7)	141.7, d	36, 45	45
	36	2.83, ddd (-15.2, 6.7, 3.7)	29.3, t	35, 36_u 37	
		2.46, ddd (-15.2, 6.7, 5.9)		35, 36_u, 37	
	37	4.93, ddd (6.7, 5.9, 3.7)	76.2, d	36, 38	46
	38	1.79, qdd (7.0, 6.7, 5.6)	43.3, d	37, 39, 46	46
	39	3.49, ddd (8.8, 5.6, 2.0)	73.0, d	40	46
	40	1.58, m	33.7, t	39, 41_d	39
		1.41, m			
	41	1.65, m	26.0, t	42	42
		1.48, m		40_u	
	42	2.19, td (7.2, 3.6)	18.8, t	41, 44	
	43		85.0, s		42
	44	2.20, t (3.6)	70.0, d	44	42
	45	1.93, br s	12.9, q	35	35
	46	0.85, d (7.0)	15.9, q	38	

[a] Recorded at 500 MHz. [b] Recorded at 125 MHz. [c] Multiplicity deduced by HSQC. [d] Protons showing long range correlation with indicated carbon. [e] Correlations were observed for $^nJ_{CH}$ = 7 Hz.

High-resolution mass spectrometry produced a $[M + Na]^+$ ion at 874.5003 that afforded a molecular formula of $C_{46}H_{69}N_5O_{10}$ (0.1 mDa error). The proton and carbon NMR data, recorded in $CDCl_3$, of the apparently chromatographically homogeneous material revealed a complex mixture of conformers (1:1:0.3:0.3). By changing the solvent to MeOH-d_3 (Table 19) the conformational ratio improved to an acceptable level (2:1:0.1) and provided reasonably well-dispersed signals. Examination of the ^1H NMR spectrum of **1.61** recorded in MeOH-d_3 indicated that it was a peptide containing both aliphatic and aromatic residues. The ^{13}C NMR spectrum contained seven carbonyls, five of which were amides based on the presence of two secondary amide (δ_H 8.17, 8.57) and three *N*-methylamide proton signals (δ_H 2.87, 3.01, 3.36). Two degrees of unsaturation were assigned to a terminal alkyne based on the characteristic carbon chemical shifts (δ_C 85.0, 70.0) and a diagnostic 250 Hz $^1J_{CH}$ from δ_C 70.0 (C-44) to a proton signal at δ_H 2.20 (H-44).[130] Based on the carbon NMR data, the seven remaining double bond equivalents were assigned to five carbon-carbon double bonds and two rings.

COSY, HMBC and TOCSY experiments determined the individual units which comprised **1.61**. TOCSY experiments, which produced spectra with signals that were directly- or relay-coupled to the secondary amide protons, established the presence of Ala and Ile units. HMBC correlations to the tertiary *N*-methylamide signals provided the starting point for the elucidation of the *N*-Me-Ala, *N*-Me-Phe, and *N*-Me-Gly units. A TOCSY experiment on the doublet of doublets at δ_H 4.91 (H-28) showed relay-transfer to three multiplets (δ_H 1.79, 1.51, 1.37) and two doublet methyl proton signals (δ_H 0.95, 0.92) that suggested a leucine-derived unit. The downfield chemical shift of the α-carbon

C-28 (δ_C 74.2) clearly indicated that this was the acyloxy carbon of an ester linkage, i.e. the final amino acid-derived unit was 2-hydroxyisocaproic acid.

Table 20. NMR Spectral Data for Conformer A of Palau'amide (**1.61**) in $CDCl_3$

Unit	C/H no.	δ_H[a] (*J* Hz)	δ_C[b,c]	^{1}H-^{1}H COSY	HMBC[d,e]	ROESY
N-Me-Ala	1		169.5, s		2, 3, 37	
	2	4.50, q (6.9)	54.6, d	3	3, 4	6, 7, 8_d
	3	1.39, d (6.9)	14.1, q	2	2	
	4	2.51, s	27.7, q		2	
Ile	5		170.5, s		4, 6	
	6	5.15, dd (9.6, 4.2)	53.2, d	6-NH, 7	7, 8, 10	2
	6-NH	7.10, d (9.6)		6		7, 8_u, 13
	7	1.69, m	38.4, d	6, 10	9, 10	
	8	1.46, m	23.4, t			
		1.25, m		9		
	9	0.852, t (7.2)	12.3, q			
	10	0.892, d (6.6)	16.5, q			
N-Me-Gly	11		168.1, s		6, 6-NH, 12	
	12	4.95, d (-17.1)	51.0, t	12_u	13	
		3.10, d (-17.1)		12_d		
	13	2.60, s	35.8, q		12_d	6-NH, 15
N-Me-Phe	14		173.2, s		13, 15, 16	
	15	5.23, dd (10.5, 6.1)	55.7, d	16	16_d, 23	
	16	3.21, dd (-13.2, 10.5)	35.5, t	15, 16_u	18/22	13
		3.09, dd (-13.2, 6.1)		15, 16_d		15
	17		136.7, s		16,19/21	
	18/22	7.14, d (7.1)	129.5, d		16, 18/22, 20	15
	19/21	7.20, dd (7.1, 6.3)	128.0, d		19/21	13, 16
	20	7.15, t (6.3)	126.5, d		18/22	
	23	3.20, s	31.5, q		15	25
Ala	24		172.9, s		23, 25, 26	
	25	5.09, dq (9.9, 6.6)	44.9, d	25-NH, 26	26	23
	25-NH	8.05, d (9.9)		25		25, 26, 29_u
	26	1.20, d (6.6)	16.5, q		25	
Hica	27		169.7, s		25, 28, 29	
	28	5.53, dd (8.4, 3.7)	71.7, d	29	29_u	25-NH
	29	1.96, ddd (-13.8, 9.8, 3.7)	40.9, t	28	31, 32	28
		1.73, ddd (-13.8, 8.4, 4.4)		28		28
	30	1.57, m	24.43, d	29_d, 31, 32	28, 31, 32	
	31	0.939, d (6.4)	21.7, q	30	32	
	32	0.902, d (6.5)	23.1, q	30	31	
Dddd	33		166.5, s		28, 45	
	34		130.5, s		35, 36_d, 45	
	35	6.52, br d (11.8)	139.0, d	36	36_d, 45	37
	36	3.03, dt (-15.1, 11.8)	30.9, t	35, 36_u, 37		
		2.20, dd (-15.1, 3.3)		35, 36_d, 37		
	37	5.27, dt (11.8, 3.3)	76.8, d	36, 38	36_d, 46	35, 36_u, 38, 46
	38	1.93, m (8.3, 7.0, 3.3)	42.4, d	37, 39, 46	46	37
	39	3.52, m (8.3)	72.1, d	38, 40	46	36_u, 40, 41_d, 46
	40	1.61, m	31.4, t	39, 40_u	39	37
		1.46, m		39, 40_d, 41_d		
	41	1.75, m	24.1, t			
		1.62, m		42		
	42	2.23, td (6.0, 2.6)	18.2, t	41, 44		
	43		84.3, s		41, 42	
	44	1.954, t (2.6)	68.6, d	42	42	
	45	1.75, br s	12.2, q	35		
	46	0.971, d (7.0)	13.4, q		37	36_d, 37, 39, 40

[a] Recorded at 500 MHz. [b] Recorded at 125 MHz. [c] Multiplicity deduced by DEPT. [d] Protons showing long range correlation with indicated carbon. [e] Correlations were observed for $^nJ_{CH}$ = 7 Hz.

Table 21. NMR Spectral Data for Conformer B of Palau'amide (**1.61**) in $CDCl_3$

Unit	C/H no.	δ_H[a] (*J* in Hz)	δ_C[b,c]	^1H-^1H COSY	HMBC[d,e]	ROESY
N-Me-Ala	1		170.1, s		2, 3	
	2	3.59, q (7.1)	60.1, d	3	3, 4	
	3	1.51, d (7.1)	13.6, q	2	2	4
	4	3.34, s	38.3, q		2	3, 6, 6-NH
Ile	5		171.2, s		2, 4, 6	
	6	4.86, t (9.7)	52.2, d	6-NH, 7	10	7, 8
	6-NH	7.81, d (9.6)		6		12, 35
	7	1.98, m	37.2, d		6, 9, 10	
	8	1.84, m	24.40, t		6	
		1.44, m				
	9	0.979, t (7.5)	10.4, q			
	10	0.896, d (6.7)	14.9, q		6	
N-Me-Gly	11		168.6, s		6-NH, 6, 12	16_d
	12	4.06, d (-18.1)	51.1, t	12_u	13	15
		3.19, d (-18.1)		12_d		15
	13	2.97, s	36.7, q		12_d	
N-Me-Phe	14		169.6, d		12, 13, 15, 16_u	
	15	5.45, dd (10.8, 5.4)	53.7, d	16	16, 23	12_d, 18/22
	16	3.12, dd (-14.9, 10.8)	34.8, t	15, 16_u	15, 18/22	15
		3.02, dd (-14.9, 5.4)		15, 16_d		15
	17		135.9, s		16, 19/21	
	18/22	7.192, d (6.4)	129.0, d		16, 18/22, 19/21, 20	15, 16
	19/21	7.31, dd (6.6, 6.4)	128.7, d		19/21	
	20	7.28, t (6.6)	127.4, d		18/22	
	23	2.955, s	29.9, q		15	25
Ala	24		173.0, s		15, 23, 26	
	25	4.60, dq (8.6, 7.1)	44.5, d	25-NH, 26	26	23, 26
	25-NH	6.26, d (8.6)		25		25, 26, 28
	26	0.760, d (7.1)	16.1, q	25	25	
Hica	27		171.4, s		28, 29_d	
	28	4.70, dd (10.1, 3.9)	73.3, d	29	29	
	29	1.87, ddd (-14.5, 10.1, 4.9)	40.7, t	28	28, 31, 32	
		1.47, m		28, 30		
	30	1.78, m	24.6, d	29_u, 31, 32	28	
	31	0.936, d (6.7)	23.1, q	30		
	32	0.894, d (6.5)	21.6, q	30		
Dddd	33		168.3, s		28, 45	
	34		128.4, s		35, 36_u, 45	
	35	6.84, dd (6.6, 6.2)	139.8, d	36, 45	45	
	36	2.88, ddd (-16.7, 6.2, 3.8)	28.4, t	35, 36_u		
		2.39, ddd (-16.7, 9.0, 6.6)		35, 36_d		
	37	4.82, ddd (9.0, 5.2, 3.8)	75.5, d	36, 38	40_d, 46	
	38	1.72, ddd (8.5, 6.4, 5.2)	42.1, d		46	6, 36_d, 37, 40, 46_u
	39	3.61, m (8.5)	71.5, d	38, 40_u	40_u, 46	
	40	1.75, m	33.9, t		39	
		1.44, m		41_u		
	41	1.80, m	24.38, t			
		1.62, m		40_u		
	42	2.22, td (6.7, 2.5)	18.0, t	41, 44		
	43		84.1, s			
	44	1.955, t (2.5)	68.9, d	42	41, 42	
	45	1.88, br s	12.6, q	35	42	
	46	0.818, d (6.4)	10.7, q			36_u, 37, 39, 40_d, 41_u

[a] Recorded at 500 MHz. [b] Recorded at 125 MHz. [c] Multiplicity deduced by DEPT. [d] Protons showing long range correlation with indicated carbon. [e] Correlations were observed for $^nJ_{CH}$ = 7 Hz.

The structure of the remaining $C_{14}H_{21}O_3$ was assembled as follows. Chemical shift considerations indicated that the last unassigned sp^2 proton signal (δ_H 6.84, H-35) was the β-proton of an α,β-unsaturated ester bearing an α-methyl group (δ_H 1.93, H-45). The methylene group (H-36) adjacent to H-35 was easily identified by a geminal proton-proton coupling constant of -15.2 Hz. These methylene proton signals showed COSY cross-peaks to a oxygenated methine proton at δ_H 4.93 (H-37), whose proton chemical shift indicated an ester linkage to this oxygen. HMBC correlations from a methyl doublet (H-46) to C-37, C-38, and C-39 established this 1,3-dihydroxy-2-methylpropyl subunit. The remainder of this fragment was elucidated by a long-range COSY correlation from the terminal alkyne proton (H-44) to H-42 and HMBC cross-peaks from H-39 and H-42 to C-40 and C-41 respectively. The polyketide unit was therefore 5,7-dihydroxy-2,6-dimethyldodec-2-en-11-ynoic acid (Dddd).

The sequence of **1.61** was established by HMBC correlations. Cross-peaks from the tertiary *N*-methylamide proton signals (H-4, H-13, H-23) to the adjacent carbonyls (C-5, C-14, C-24) established two fragments: (*N*-Me-Ala)-(Ile) and (*N*-Me-Gly)-(*N*-Me-Phe)-(Ala). Correlations from the secondary amide proton signals (6-NH and 25-NH) to C-11 and C-27 linked these two units in a linear chain with the 2-hydroxyisocaproic acid appended to the amino terminus of *N*-Me-Ala. The carboxy terminus of the Dddd unit (C-33) was linked to the hydroxyisocaproic acid and the carboxy terminus of alanine (C-1) was linked to C-37. The latter (C-37) was chosen over the other secondary alcohol in the Dddd unit (C-39) based on the proton chemical shifts of the two centers (δ_H 4.93 vs 3.49). Although no HMBC or ROESY correlations, in MeOH-d_3, supported these linkages, the molecular formula necessitated the cyclic structure depicted. Later, both of these

connections (C-1/C-37 and C-28/C-33) would be confirmed by HMBC correlations observed in $CDCl_3$ (vide infra).

1.3.6.2 Stereochemistry

Several techniques were used to determine the stereochemistry of **1.61**. The amino acid-derived units were determined by chiral HPLC of the acid hydrolyzate. Comparison with authentic samples established the presence of L-Ala, L-Ile, *N*-Me-L-Ala, *N*-Me-D-Phe, and D-hydroxyisocaproic acid.

The geometry of the α,β-unsaturated ester was determined by an NOE experiment. Irradiation of H-36 revealed the close spatial proximity of H-45 and established an *E* configuration of the double bond.

We had initially hoped to determine the relative configuration of the diol unit via *J*-based analysis techniques,[111] but HETLOC and HSQMBC spectra, with an adequate signal-noise ratio needed to determine the carbon-hydrogen coupling constants, could not be obtained due to the limited amount of material. Analysis of the proton-proton couplings observed in MeOH-d_4 indicated the $^3J_{HH}$ were of an intermediate magnitude ($^3J_{H\text{-}37/H\text{-}38}$ = 6.7 Hz, $^3J_{H\text{-}38/H\text{-}39}$ = 5.6 Hz), which were perhaps the result of an interconverting mixture of rotamers around these stereocenters.[111] We sought to change this ratio and increase the magnitude of these coupling constants, which would allow us to determine the configuration through NOE experiments, but cooling the sample from 15 to -50 °C resulted in only a minimal increase in the magnitude of these coupling constants.

Analysis of the ^1H NMR data recorded in other solvents revealed that in $CDCl_3$ (Table 20, Table 21) the major conformers of **1.61** had a large proton-proton coupling

($^3J_{H\text{-}38/H\text{-}39}$ ca. 8.3 Hz) between H-38 and H-39. Subsequent NOE experiments (Figure 19) indicated that the methyl group on C-38 and the hydroxy group on C-39 were *anti*. Changing solvents did not increase the magnitude of the coupling constant between H-37 and H-38 to above 8 Hz, so the relative configuration of H-37/H-38 would have to be determined by chemical manipulations.

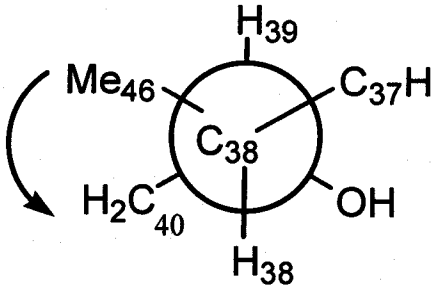

Figure 19. NOE Correlation around C-38/39.

Owing to the limited amount of material, the absolute configuration of C-39 was determined prior to degrading **1.61**. To this end, the MPA derivatives were prepared and purified by silica chromatography. The chemical shifts of the protons in the Dddd units were determined by 1D TOCSY experiments in MeOH-d_4 at 50 °C.[131] Comparison of the $\Delta\delta^{RS}$ values for the MPA derivatives of **1.61** established the *R* absolute configuration of C-39 (Figure 20).

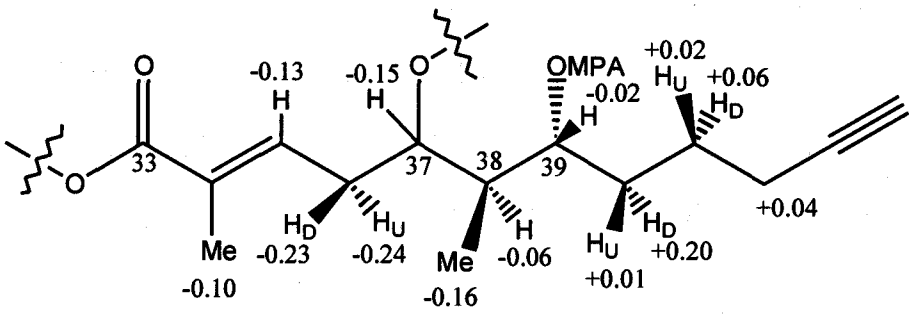

Figure 20. $\Delta\delta$ ($\delta_R - \delta_S$) for the MPA Derivatives of Palau'amide in MeOH-d_4 at 50 °C.

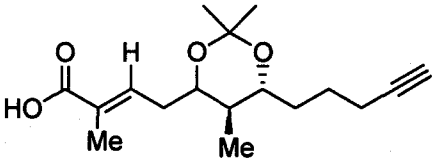

1.62

Next we attempted to determine the stereochemistry of C-37 via the acetonide derivative **1.62** by comparing $^3J_{H\text{-}5/H\text{-}6}$ constants with the literature values for 2-methyl-1,3-diols.[132] Since all of the available sample of **1.61** had been converted to the MPA derivatives, this first required the cleavage of the ester linkage at C-37 and removal of the MPA groups from C-39 to provide the free hydroxy groups. Three attempts were made to isolate this fragment. First, the acid hydrolyzate of **1.61**, used to determine the amino acid stereochemistry, was exhaustively extracted with CH_2Cl_2. Inspection of the ^1H NMR spectrum of this extract showed no sign of the most distinctive signals expected for this unit, i.e. the β-proton signal of the α,β-unsaturated acid or the terminal alkyne proton signal. There was also no sign of these proton signals in the residue after methanolysis of the MPA adduct using sodium methoxide. This last result was surprising since methanolysis of similar polyketide-derived units in other natural products had been reported in the literature with satisfactory yields.[133] The final attempt involved cleavage

of the ester linkages by DIBAL reductions, which would have also reduced the terminal alkyne. Once again, no proton signals corresponding to the polyketide-derived unit could be identified in the ^{1}H NMR spectra of the HPLC fractions from the reaction mixture. Due to these difficulties the stereochemistry of C-37 remains unassigned.

1.3.6.3 Comments on Palau'amide (1.61)

Palau'amide (**1.61**) displayed strong cytotoxicity against KB cells with an IC_{50} value of 13nM. Compounds that display a similar level of activity in this assay are the lyngbyabellin, lyngbyastatins, and majusculamide C, while cryptophycin 1, recently in phase II trials, has an IC_{50} of 10 pM.

Palau'amide (**1.61**) was likely formed by a combination of the polyketide and the non-ribosomal peptide biosynthetic machinery and in this regard was a typical cyanobacterial metabolite. The degree of functionalization in the polyketide chain was unusual for marine cyanobacterial depsipeptides, which rarely have heteroatoms incorporated after the β-position.

Analysis of the NMR data indicated the locations of conformational differences. Comparison of the major conformers of **1.61** in $CDCl_3$ revealed approximately a full ppm difference in the proton chemical shifts of H-4. Analysis of the ROESY correlations around this stereocenter established a *cis*-amide bond between *N*-Me-Ala and Ile in conformer A, while conformer B had cross-peaks consistent with a *trans*-amide bond in this position.[134] Specifically, conformer A gave cross-peaks from H-2 to H-6 and H-3 to H-4, while conformer B showed a strong correlation between H-4 and H-6 in $CDCl_3$. Also the configuration of the amide bond between Gly and *N*-Me-Phe is opposite in the two major conformers, with a *trans*-amide bond in conformer A and a *cis*-amide bond in

conformer B.[135] The similarity between the chemical shifts of conformer B in $CDCl_3$ and the major conformer of **1.61** in MeOH-d_3 suggests a predominance of 4-*trans*-13-*cis*-amide bonds in this latter solvent. This conclusion was supported by ROESY correlations observed in MeOH-d_3 from H-4 to H-6 and from H-13 to H-15.

1.3.7 Lyngbyastatin 3 (1.63)

Lyngbyastatin 3 (**1.63**) was isolated from three collections of *Lyngbya* (NIH199, 154, 143) in yields ranging from 0.3 to 0.8 % of the dry extract. This compound was similar to a series of known metabolites (**1.64-1.67**) that were discovered in the extracts of the cyanobacteria *Lyngbya* sp. and the sea hare *Dolabella* sp. Two unusual amino acids (3-amino-2-methylpentanoic acids [MAP] and 4-amino-3-oxo-2,2-dimethylpentanoic acid [Ibu]) are usually incorporated in the structures of these metabolites. Lyngbyastatin 3 (**1.63**) was the first member of this structural class to incorporate a different β-amino acid, viz. a 3-amino-2-methylhexanoic acid (Amha).

In 1998, we reported the isolation and biological evaluation of samples of lyngbyastatin 1 (**1.64**) and dolastatin 12 (**1.65**), from a *Lyngbya majuscula/Schizothrix calcicola* assemblage.[119] The structure determinations of these cyanobacterial samples were hampered by the extensive signal broadening and doubling observed in the NMR spectra. This phenomenon had not been observed in the NMR spectra of majusculamide C (**1.66**)[117] and dolastatin 11 (**1.67**)[118] from cyanobacteria or the sample of dolastatin 12 (**1.65**)[118] isolated from the sea hare. Based on epimerization experiments on **1.66**, we concluded that the unusual spectral broadness observed in the cyanobacterial samples of **1.64** and **1.65** was due to these samples being mixtures of diastereomers arising from epimerization of the acid-sensitive Ibu unit. Synthetic studies have now established the *S* configuration for the Ibu unit of dolastatin 11[136] (**1.67**) and more recently have suggested that the Ibu units of the cyanobacterial metabolites **1.64** and **1.65** have an *R* configuration. In other words, *R*-Ibu-**1.65** had been isolated from the cyanobacteria

whereas *S*-Ibu-**1.65** had been isolated from the sea hare.[137] Degradation of these natural products (**1.63-1.66**) has proven that the cyanobacterial samples of **1.63 – 1.65** are mixtures of Ibu epimers [*R* (major) and *S* (minor)], whereas the structurally related majusculamide C (**1.66**) is a single diastereomer having the *S*-Ibu unit.

1.3.7.1 Isolation and Structure Elucidation

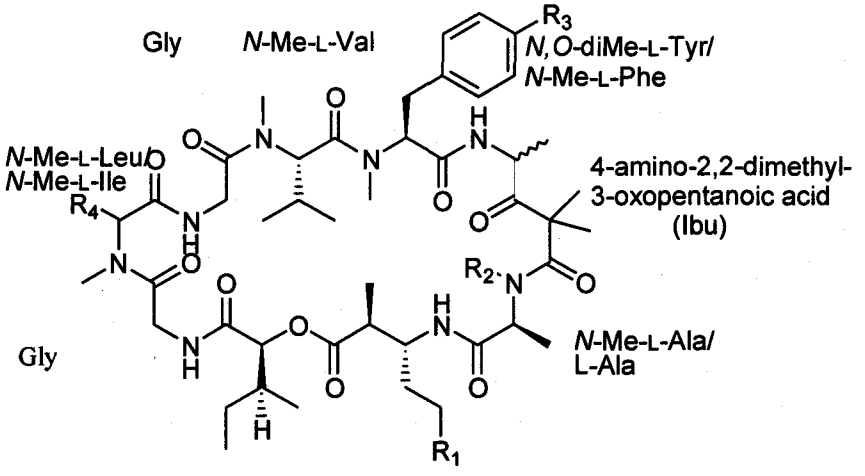

Lyngbyastatin 3	(**1.63**) R_1 = Me	R_2 = Me	R_3 = OMe	R_4 = *i*-Bu
Lyngbyastatin 1	(**1.64**) R_1 = H	R_2 = Me	R_3 = OMe	R_4 = *i*-Bu
Dolastatin 12	(**1.65**) R_1 = H	R_2 = Me	R_3 = H	R_4 = *i*-Bu
Majusculamide C	(**1.66**) R_1 = H	R_2 = H	R_3 = OMe	R_4 = *sec*-Bu
Dolastatin 11	(**1.67**) R_1 = H	R_2 = H	R_3 = OMe	R_4 = *i*-Bu

Lyngbyastatin 3 (**1.63**) was isolated by bioassay-guided fractionation of the weakly solid tumor selective,[20] but highly cytotoxic (even at 1/100 dilution) extracts of NIH143, 154 and 199. The biological activity of **1.63** was almost identical to **1.64** with an IC_{50} value against KB cells for **1.63** of 32 nM.

Very few structural features could be elucidated from the spectral data of **1.63**. A series of 2D NMR and 1D TOCSY experiments were largely unsuccessful due to the extensive signal broadening and doubling in the ^1H and ^{13}C NMR spectra of the apparently chromatographically homogeneous material. Variable temperature NMR

experiments between 70 and -20 °C in a variety of solvents with and without LiCl[138] failed to alter the conformational ratio as to ameliorate the situation. These experiments did indicate that **1.63** contained at least eight amino acids, based on four *N*-methylamide and four secondary amide proton signals. Lyngbyastatin 3 (**1.63**) was likely a depsipeptide based on the prominent vibrations at 1729 and 1637 cm^{-1} in the thin-film IR spectrum that indicated ester and amide functionalities, respectively.

These physical characteristics suggested that **1.63** was related to the known *L. majuscula* metabolite lyngbyastatin 1 (**1.64**). While the IR, UV, and ^1H NMR spectra of **1.63** and **1.64** were virtually identical, a comparison of the two samples by reversed-phase HPLC[139] indicated that **1.63** was more lipophilic than **1.64**. This difference in polarity was attributed to an additional methylene (δ_C 20.7) in **1.63** as revealed by a DEPT experiment in CD_3CN at 70 °C and confirmed by high-resolution mass spectrometry.

A small sample of **1.63** was hydrolyzed to determine if one of the α-amino acids was modified. Chiral HPLC analysis of the acid hydrolyzate confirmed **1.63** contained the same amino acids as **1.64**. Peaks due to glycine, *N,O*-dimethyl-L-tyrosine, *N*-methyl-L-valine, *N*-methyl-L-leucine, *N*-methyl-L-alanine, and L-2-hydroxy-3-methylvaleric acid were identified. Also both glycine residues were still incorporated, since alanine was not present in the hydrolyzate. This left two possibilities. The additional CH_2 in **1.63** had to be incorporated as a modified form of either the 4-amino-2,2-dimethyl-3-oxopentanoic acid (Ibu) or the 3-amino-2-methylpentanoic acid (MAP) moieties found in **1.64**.

Analysis of the derivatized acid hydrolyzate of **1.63** by chiral GC-MS[140] established the location of the methylene. The GC-MS chromatogram did not show a

peak corresponding to the derivatized (2*S*,3*R*)-3-amino-2-methylpentanoic acid unit (**1.68**, *m/z* 319) found in lyngbyastatin 1 (**1.64**). A synthetic standard[141] of this MAP unit exhibited two predominant fragmentation pathways (Figure 21). In the first pathway, successive homolytic cleavage of the aliphatic side chain adjacent to the amide bond (**1.71**), McLafferty rearrangement (**1.74**), and decarboxylation (**1.76**) generated *m/z* 290, 248, and 204, respectively. In the second pathway, cleavage around the ester linkage in **1.68** produced ion peaks at *m/z* 260 (**1.70**) and 204 (**1.73**) where the side chain is still intact. Analysis of the hydrolyzate revealed a derivative (**1.69**, *m/z* 333) in which all fragments derived from cleavage adjacent to the amide linkage were accounted for (**1.71**, **1.74**, and **1.76**). Two new ions, at *m/z* 274 (**1.72**) and 218 (**1.75**), established that the methylene was part of the aliphatic side chain of a 3-amino-2-methylhexanoic acid (Amha) unit, which has been found in three other natural products, viz. malevamide B,[26] ulongamides A-F,[123] and kulokekahilide-1.[142]

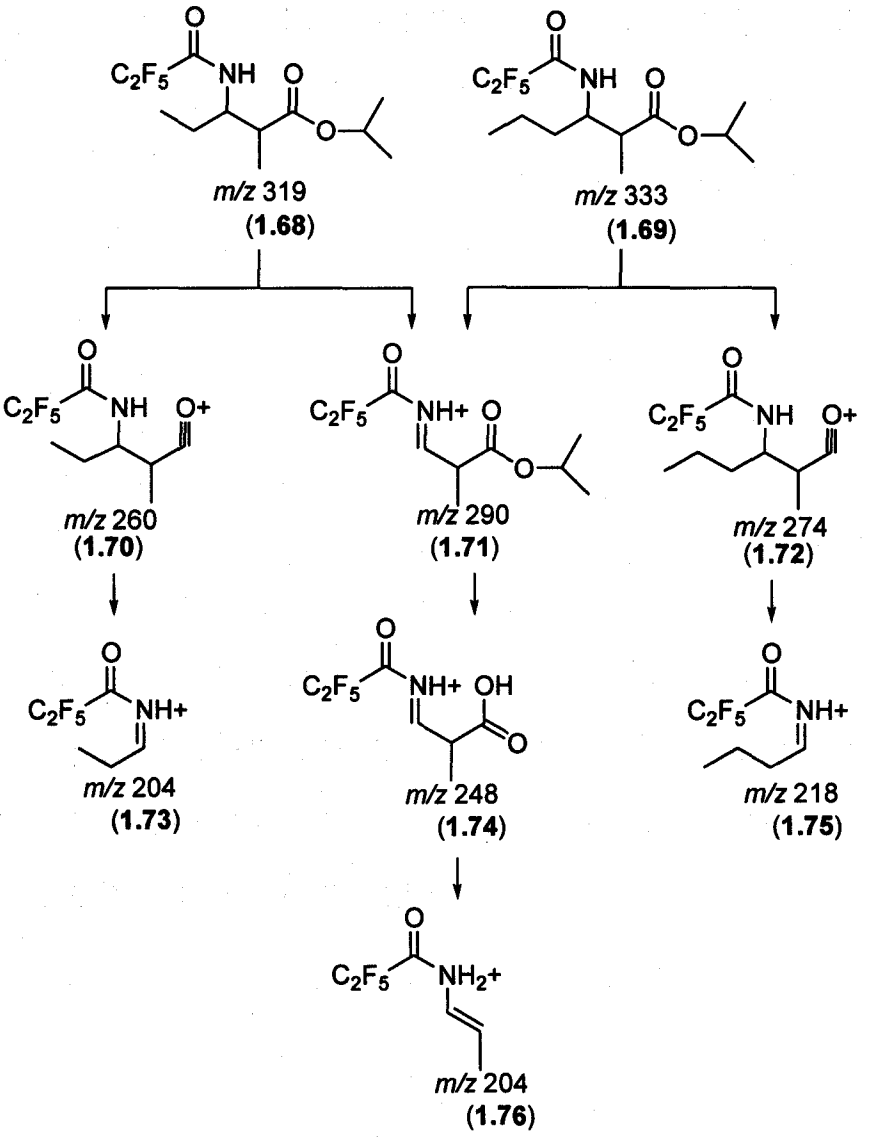

Figure 21. GC/MS Fragmentations of the Amha Unit (**1.69**) in **1.63** and the Synthetic MAP (**1.68**).

1.3.7.2 Stereochemistry

The stereochemistry of the α-amino acid units in **1.63** was determined by chiral HPLC. Comparison with authentic standards established the configuration of the α-amino

and α-hydroxy acids in **1.63** as *N,O*-dimethyl-L-tyrosine, *N*-methyl-L-valine, *N*-methyl-L-leucine, *N*-methyl-L-alanine, and L-2-hydroxy-3-methylvaleric acid.

Synthetic standards were prepared to establish the relative configuration of the Amha unit. We initially attempted to prepare the *syn*-α-alkyl-β-amino acids by the Michael addition of (*R*)-(+)-*N*-benzyl-*N*-α-methylbenzylamine to ethyl 2-methylhex-2(*E*)-enoate.[143] The reaction proved problematic and yielded less than 10 % of the desired product on numerous attempts. Since the same reaction using methyl crotonate as a substrate proceeded smoothly (over 80 % yield), it was suspected that the α-methyl group was significantly affecting the rate of the 1,4-addition, thus allowing the reaction to proceed via an undesired pathway. It was also evident that the 1,2-addition of the *N*-benzyl-*N*-α-methylbenzylamine was not occurring to a significant degree based on NMR analysis of the reaction products. It became clear that the γ-deprotonation was the competing pathway, when deuterium incorporation was observed in the α,β-unsaturated acid after quenching with D_2O.

The problem of γ-deprotonation was circumvented by performing the Michael addition on the unsubstituted ester and subsequent methylation to prepare the *anti*-α-alkyl-β-amino acids.[144] The Michael addition of (*R*)-(+)-*N*-benzyl-*N*-α-methylbenzylamine to ethyl hex-2(*E*)-enoate afforded the enantiomerically pure adduct **1.78** in 50 % yield (Figure 22). Treatment of **1.78** with potassium hexamethyldisilazane (KHMDS) and an excess of iodomethane gave **1.79**. The resulting 3:1 mixture of diastereomers[145] was then hydrogenated and hydrolyzed to afford (2*S*,3*R*)- and (2*R*,3*R*)-**1.80**. Half of this mixture was then separated as their L-(1-fluoro-2,4-dinitrophenyl)-5-leucinamide (FDLA) derivatives.[146] Derivatization of the remaining amount of **1.80** with

D-FDLA and subsequent HPLC separation produced standards equivalent to (2*R*,3*S*)- and (2*S*,3*S*)-**1.80**.[128,147,148] Comparison by LC-MS of these standards with the L-FDLA derivatized hydrolyzate established the 2*S*,3*R* configuration of the β-amino acid unit in **1.63**.[149]

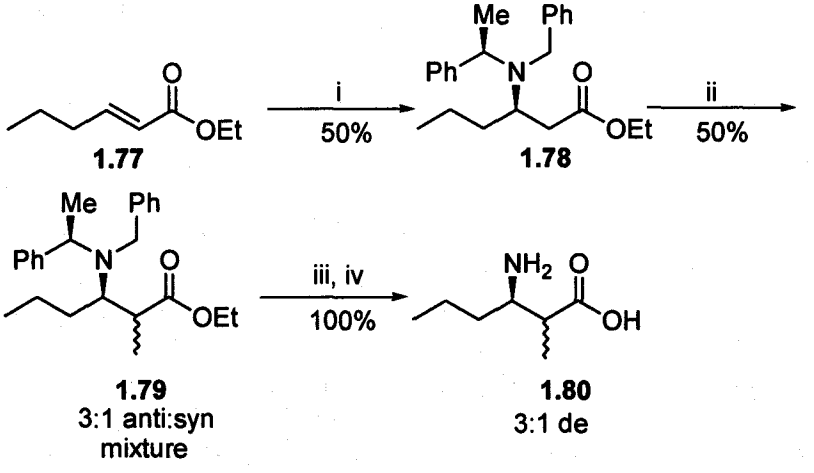

(i) *n*-BuLi, THF, (*R*)-*N*-benzyl-*N*-methylbenzylamine; (ii) KHMDS, MeI; (iii) H_2, 20 % Pd/C; (iv) 6 N HCl.

Figure 22. Synthesis of α-Methyl-β-amino Acid Standards.

Next, we turned our attention to the configuration of the Ibu units in **1.63** - **1.66**. We attempted to effect a Baeyer-Villiger oxidation on **1.63** or its methanolysis product, which would allow the configuration of the Ibu unit to be deduced from the presence of L- or D-alanine after acid hydrolysis. Unfortunately, these efforts were unsuccessful using *m*-CPBA, peracetic acid, trifluoroperacetic acid, and hydrogen peroxide. Presumably the failure of the first three is due to the steric congestion around the ketone. Reductive deoxygenation[150] also did not yield the desired product, perhaps again due to the steric congestion around the ketone. An attempted Beckmann rearrangement of an oxime derivative also failed to yield alanine upon treatment with acid. Due to these difficulties, we decided instead to reduce the ketone with sodium borohydride.

Synthetic standards of the reduced Ibu unit, 4-amino-2,2-dimethyl-3-hydroxypentanoic acid (Adhpa), were prepared as shown in Figure 23. The β-ketoester (**1.89**) was prepared by the 1,1′-carbonyldiimidazole activated coupling of *N*-Boc-L-Ala to the enolate of benzyl acetate following a procedure developed during the synthesis of dolastatin 11 (**1.67**).[136] The initial attempts to couple these two fragments resulted in yields of less than 10 %. Inspection of the crude reaction mixture suggested that self-condensation of the benzyl acetate was responsible for the erosion in the yield of the desired product. The amount of time the benzyl acetate was stirred with LDA was reduced from 1 h to 5 min to provide **1.89** in approximately the same yield (52 %) as reported in the literature (55 %).[136] This compound was subsequently dimethylated with NaH and MeI.[136,] The gem-dimethyl adduct (**1.90**) was isolated in 17 % yield by silica chromatography and eluted after the major product (53 %), (4*S*)-*N*-Boc-3-oxo-2,2,4-trimethyl-γ-lactam (**1.91**).[151] Reduction of **1.90** with $NaBH_4$ provided a mixture of epimeric alcohols (**1.92**). The relative configurations of the minor and major reduction products of **1.92** were not established conclusively, but $NaBH_4$ reductions on related amino acid-derived ketoesters generally occur via a chelation controlled mechanism which suggests that the 3*R*,4*S* diastereomer is the major product.[152] The residue from this borohydride reduction was subsequently deprotected to afford a mixture of (3*R*,4*S*)- and (3*S*,4*S*)-**1.93** (Adhpa). Derivatization with L- and DL-FDLA and HPLC analyses of these mixtures established the elution order of the standards.[153,154]

$NaBH_4$ reduction of the natural products produced derivatives[155] that could be degraded to liberate Adhpa (**22**) from which the configurations of the Ibu units could be determined. The reductions of **1.63-1.65** afforded two products apiece (**1.82-1.87**) after

HPLC purification of each reaction mixture, while the reduction of **1.66** produced a single adduct (**1.81**) (Table 22). All of the reaction products were identified by HR-MS and the major reduction products of lyngbyastatin 3 and dolastatin 12 were also characterized by NMR (Table 23 and Table 24). In general, the ^{1}H NMR spectra of the major reduction products were characterized by a methine doublet (J = 6.4 Hz) at approximately δ_H 3.34 coupled only to the alcohol proton (δ_H 5.43). The minor reduction products each appeared to be mixtures of two compounds as the HSQC spectra of each

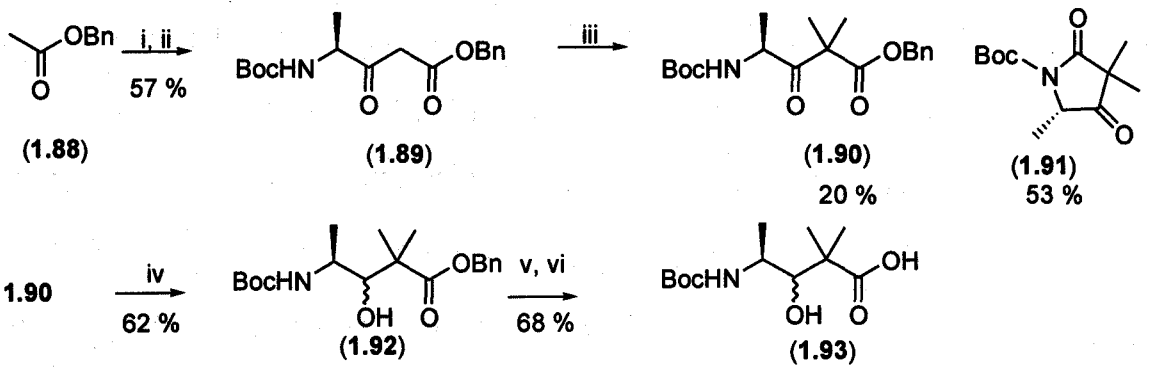

(i) LDA; (ii) *N*-Boc-L-Ala, 1,1'-carbonyldiimidazole; (iii) 2 eq. NaH, 18 eq. MeI; (iv) $NaBH_4$; (vi) H_2, Pd/,C; (vi) TFA.

sample showed two protons at approximately δ_H 3.3 that correlated to carbons at approximately 80 ppm.

Figure 23. Synthesis of the 4-Amino-3-hydroxy-2,2-dimethylpentanoic Acid Standards.

Acid hydrolysis of the reduction products of **1.63-1.66** and comparison with the Adhpa synthetic standards (**1.93**) by Marfey analysis established the configuration of the Ibu units in the cyanobacterial metabolites. As shown in Table 22, the reduction of the samples of **1.63-1.66** produced adducts that contained Adhpa units in which the configuration of C-4 was derived from both *R*- and *S*-Ibu, with the latter stereochemistry found in the minor products (**1.82**, **1.84**, **1.86**) in all three cases. Conversely, the

reduction of majusculamide C (**1.66**) produced an adduct (**1.81**) which only contained an Adhpa unit derived from *S*-Ibu. It should be noted that only those samples which had broad NMR spectra (**1.63-1.65**) produced reduction products corresponding to *both R*- and *S*-Ibu units.

Table 22. Stereochemistry of the Cyanobacterial Metabolites.

Cyanobacterial Sample	Broad NMR Spectra	Reduction product(s)	Ibu Configuration Determined[a]
Lyngbyastatin 3 (**1.63**)	Yes	**1.83** (major)	*R* (major) = Lyngbyastatin 3
		1.82 (minor)	*S* (minor) = Ibu-epilyngbyastatin 3
Lyngbyastatin 1 (**1.64**)	Yes	**1.85** (major)	*R* (major) = Lyngbyastatin 1
		1.84 (minor)	*S* (minor) = Ibu-epilyngbyastatin 1
Dolastatin 12 (**1.65**)	Yes	**1.87** (major)	*R* (major) = Ibu-epidolastatin 12
		1.86 (minor)	*S* (minor) = Dolastatin 12
Majusculamide C (**1.66**)	No	**1.81**	*S*

[a] This is the configuration at C-4 of Adhpa that was detected in the L-FDLA derivatized hydrolyzate of the reduction products.

It is unlikely these mixtures are artifacts of the reduction process. In a control experiment, dolastatin 12 (**1.65**) was reduced in MeOH-d_4 and the purified reaction products were analyzed by mass spectrometry. A comparison of the minor reduction products from the original and deuterium reduction experiments showed only an 8 % increase in the signal intensity of the $(M + 1 + H)^+$ ion relative to the $(M + H)^+$ ion peak in the latter.[156] The magnitude of this deuterium incorporation suggests that very little enolization occurs during the reduction and that the (*S*)-Ibu-**1.65** is present in the original sample.

Table 23. NMR Spectral Data for **1.83** in $CDCl_3$

Unit	C/H no.	δ_H[a] (*J* in Hz)	δ_C[b,c]	$^1H-^1H$ COSY	HMBC[d,e]
Amha	1		173.6, s		2, 7, 48
	2	2.82, m	43.5, d	3, 7	
	3	3.89, m	52.5, d	2, 3-NH, 4	2
	3-NH	7.68, d (7.9)		3	
	4	1.38, m	24.2, t		6
		1.20, m		3	
	5	1.22, m	19.9, t		6
	6	0.86, t (6.4)	13.7, q		
	7	1.25, d (7.2)	14.9, q	2	
N-Me-Ala	8		170.9, s		9, 10
	9	5.14, q (6.9)	54.6, d	10	11
	10	1.38, d (6.9)	14.2, q	9	
	11	3.09, s	32.2, q		9
Adhpa	12		178.0, s		11, 14, 17, 18
	13		46.2, s		17, 18
	14	3.36, d (6.4)	81.3, d	14-OH	16, 17, 18
	14-OH	5.43, d (6.4)		14	
	15	4.24, dq (8.6, 6.7)	44.6, d	15-NH, 16	16
	15-NH	6.04, d (8.6)		15	
	16	1.04, d (6.7)	21.2, q	15	
	17	1.26, s	26.3, q		
	18	1.27, s	22.8, q		
N,O-diMe-Tyr	19		168.5, s		15, 20, 21
	20	4.78, dd (10.2, 4.5)	60.8, d	21	21, 29
	21	2.96, dd (-17.7, 10.2)	34.8, t	20	
		2.90, dd (-17.7, 4.5)		20	
	22		128.4, s		21
	23/27	7.12, d (8.2)	130.3, d	24/26	21, 23/27, 25
	24/26	6.81, d (8.2)	114.3, d	23/27	22, 24/26, 25
	25		158.7, s		28
	28	3.74, s	55.3, q		
	29	2.93, s	29.3, q		20
N-Me-Val	30		169.5, s		29, 31
	31	4.61, d (10.7)	58.4, d	32	33, 34
	32	2.16, m	26.8, d	31, 33, 34	31, 33, 34
	33	0.62, d (6.7)	18.0, q	32	34
	34	0.18, d (6.9)	18.2, q	32	33
	35	2.87, s	29.9, q		31
Gly	36		169.2, s		35, 37
	37	4.22, dd (-18.9, 7.2)	41.5, t	37_u, 37-NH	
		4.10, d (-18.9)		37_d	
	37-NH	7.09, d (7.2)		37_d	
N-Me-Leu	38		169.9, s		37, 39, 40
	39	5.32, dd (9.5, 4.5)	54.1, d	40	
	40	1.72, m	36.6, t	39, 41	42, 43
		1.66, m		39, 41	
	41	1.36, m	24.6, d	40	
	42	0.98, d (6.2)	23.3, q	41	
	43	0.88, d (7.3)	21.9, q	41	
	44	2.92, s	29.4, q		
Gly	45		169.0, s		44, 46
	46	4.46, dd (-18.1, 7.1)	41.2, t	46-NH	
		3.81, dd (-18.1, 1.7)		46-NH	
	46-NH	7.27, dd (7.1, 1.7)		46	
HMVA	47		168.9, s		46, 48
	48	5.15, d (4.3)	77.7, d	49	
	49	2.04, m	37.0, d	48, 50, 52	48
	50	1.58, m	30.5, t	49	48
		1.20, m		49	
	51	0.90, t (7.3)	11.4, q	50	
	52	0.95, d (6.2)	15.0, q	49	48

[a] Recorded at 500 MHz. [b] Recorded at 125 MHz. [c] Multiplicity deduced by HSQC. [d] Protons showing long range correlation with indicated carbon. [e] Correlations were observed for $^nJ_{CH}$ = 7 Hz.

Table 24. NMR Spectral Data for **1.87** in $CDCl_3$

Unit	C/H no.	δ_H[a] (*J* in Hz)	δ_C[b,c]	$^1H-^1H$ COSY	HMBC[d,e]
Map	1		173.6, s		2, 3, 6
	2	2.89, m	42.5, d	3, 6	6
	3	3.74, m	54.4, d	2, 3-NH, 4	2, 4, 5
	3-NH	7.73, d (7.1)		3	
	4	1.66, m	21.6, t	3, 4_u, 5	2
		1.18, m		3, 4_d, 5	
	5	0.89, t (6.6)	11.5, q	4	4
	6	1.25, d (8.2)	14.9, q	2	2
N-Me-Ala	7		171.1, s		3, 8, 9
	8	5.18, q (6.9)	54.5, d	9	9, 10
	9	1.38, d (6.9)	14.2, q	8	
	10	3.08, s	32.2, q		
Adhpa	11		178.0, s		10, 13, 16, 17
	12		46.2, s		13, 16, 17
	13	3.35, d (5.6)	81.1, d	13-OH	15, 16, 17
	13-OH	5.44, d (5.6)		13	
	14	4.23, dq (8.1, 6.7)	44.6, d	14-NH, 15	15
	14-NH	6.05, d (8.1)		14	
	15	1.04, d (6.7)	21.3, q	14	14
	16	1.24, s	26.1, q		
	17	1.27, s	22.7, q		
N-Me-Phe	18		168.4, s		14, 19
	19	4.85, dd (10.4, 4.4)	60.8, d	20	20, 27
	20	3.05, dd (-14.3, 4.4)	34.8, t	19	19
		2.97, dd (-14.3, 10.4)		19	
	21		136.5, s		20, 23/25
	22/26	7.20, d (7.6)	129.3, d	23/25	
	23/25	7.26, t (7.6)	128.9, d	22/26, 24	
	24	7.20, d (7.6)	127.1, d	23/25	
	27	2.92, s	29.3, q		19
N-Me-Val	28		169.5, s		19, 27, 29
	29	4.60, d (10.4)	58.4, d	30	30, 31, 32
	30	2.12, m	26.8, d	29, 31, 32	29, 31, 32
	31	0.60, d (6.7)	18.0, q	30	
	32	0.09, d (6.4)	18.1, q	30	
	33	2.86, s	29.0, q		29
Gly	34		169.2, s		33, 35
	35	4.46, dd (18.1, 7.1)	41.2, t	35_u	
		3.81, d (18.1)		35_d	
	35-NH	7.23, d (7.1)		35_d	
N-Me-Leu	36		169.9, s		35, 37, 38
	37	5.32, dd (9.9, 4.2)	54.5, d	38	39, 42
	38	1.75, ddd (-14.6, 10.4, 4.2)	36.6, t	37, 38_u, 39	37
		1.61, ddd (-14.6, 9.9, 4.0)		37, 38_d, 39	
	39	1.34, m	24.6, d		37, 38
	40	0.93, d (6.6)	23.3, q		38
	41	0.86, d (6.4)	21.8, q		38
	42	2.91, s	29.3, q		
Gly	43		168.9, s		37, 42, 44
	44	4.19, d (17.1)	41.4, t	44_u	
		3.99, dd (17.1, 5.2)		44_d, 44-NH	
	44-NH	7.06, d (5.2)		44_u	
HMVA	45		169.1, s		44, 46
	46	5.15, d (4.7)	77.8, d	47	47, 48, 50
	47	2.04, m	36.9, d	46, 48, 50	
	48	1.49, m	24.2, t	47, 48_u	
		1.19, m		48_d	
	49	0.88, t (7.4)	11.3, q	48_d	48_u
	50	0.92, d (6.9)	15.0, q	47	48_d

[a] Recorded at 500 MHz. [b] Recorded at 125 MHz. [c] Multiplicity deduced by HSQC. [d] Protons showing long range correlation with indicated carbon. [e] Correlations were observed for $^nJ_{CH}$ = 7 Hz.

1.3.7.3 Comments on the Lyngbyastatins

These results indicate that our cyanobacterial samples of dolastatin 12 and lyngbyastatin 1 and 3 are mixtures of two Ibu-epimers. The configuration of the major Ibu-epimer in each of the three mixtures is *R*. The relative amounts of the two epimers, as determined by HPLC analysis after borohydride reduction, was 4:1 for both lyngbyastatin 1 (**1.64**) and dolastatin 12 (**1.65**), but 2:1 for lyngbyastatin 3 (**1.61**). The samples of **1.64** and **1.65** had both been isolated from the same collection of *L. majuscula*, but the sample of lyngbyastatin 3 (**1.63**) had been obtained from several different collections of *L. majuscula* from Apra Harbor.[157] Since the collections were subjected to slightly different isolation procedures, this variation in the ratio of **1.63** might be due to some epimerization during the isolation. The plausibility of this event is supported by the molecular modeling of lyngbyastatin 1 (**1.64**) and Ibu-epi-**1.64** (data not shown), which suggests that the *S* configuration for the Ibu unit is thermodynamically favored.[137]

The broadness in the NMR spectra of the cyanobacterial samples of **1.63**, **1.64**, and **1.65** is likely due to a combination of factors. The presence of a minor diastereomer obviously may lead to an apparent broadening of the spectra. However, it has also been suggested that the *R*- and *S*-Ibu diastereomers probably have appreciably different amounts of *cis* and *trans* conformers around the (Ibu)-(*N*-Me-Ala) bond. Also, in the case of the *R*-Ibu compounds, the overall shape of the *cis* and *trans* conformers differs significantly.[137] All of these factors likely contribute to the unusual degree of line broadening in the NMR spectra.

It has been proposed, that dolastatin 11 (**1.67**) and 12 (**1.65**) arise in the sea hare from feeding on cyanobacteria.[118] The isolation of another dolastatin analogue, lyngbyastatin 3 (**1.63**), from a cyanobacterium further supports this proposal. The stereochemical differences in the Ibu units of the compounds isolated from cyanobacteria and sea hares may be caused by epimerization of the *R* to the thermodynamically favorable *S*-Ibu configuration in the digestive gut of the sea hare or during the lengthy isolation procedure used in Pettit's lab. It is also quite possible that the cyanobacterium eaten by the sea hare produces dolastatin 12 with only the (*S*)-Ibu unit, analogous to what is found in majusculamide C.

Lyngbyastatin 3 (**1.63**) showed similar biological activity to lyngbyastatin 1 (**1.64**). Both compounds completely depolymerized the microfilament network at a concentration of 100 nM (Figure 24). The efficacy of lyngbyastatin 3 was evaluated *in vivo* against two early stage adenocarcinomas (Table 25, Table 26). In general, the compound was poorly tolerated in mice with only marginal or no antitumor activity (T/C % >42).

Table 25. Effects of Lyngbyastatin 3 Against Adenocarcinoma #38 in Female Mice

Treatment	Drug Route	Schedule	Total Dose (mg/kg)	Drug Deaths	Median Tumor burden in mg on day 14 (range)	T/C %	Antitumor Activity
No treatment	---	---	---	---	768 (708-1375)	---	---
Lyngbyastatin 1	IV	QD 3-11	13	0/4	832 (526-1393)	93	Inactive
Dolastatin 12	IV	QD 3-11	7.5	2/4	822 (732-911)	92	Inactive (toxic)
Lyngbyastatin 3	IV	QD 3-6	4.0	0/3	723 (283-1067)	92	Inactive

Table 26. Effects of Lyngbyastatin 3 Against Adenocarcinoma #16/C in Female Mice

Treatment	Drug Route	Schedule	Total Dose	Drug Deaths	Median Tumor burden in mg on day 14 (range)	T/C %	Antitumor Activity
No treatment	---	---	---	---	1300 (926-2777)	---	---
Lyngbyastatin 1	IV	QD 1-9	11.7	0/5	776 (663-1380)	61	Inactive
Dolastatin 12	IV	QD 1-8	6.4	0/5	1100 (478-1613)	86	Inactive
Lyngbyastatin 3	IV	QD 1-5	5.0	0/6	1655 (932-2643)	>100	Inactive

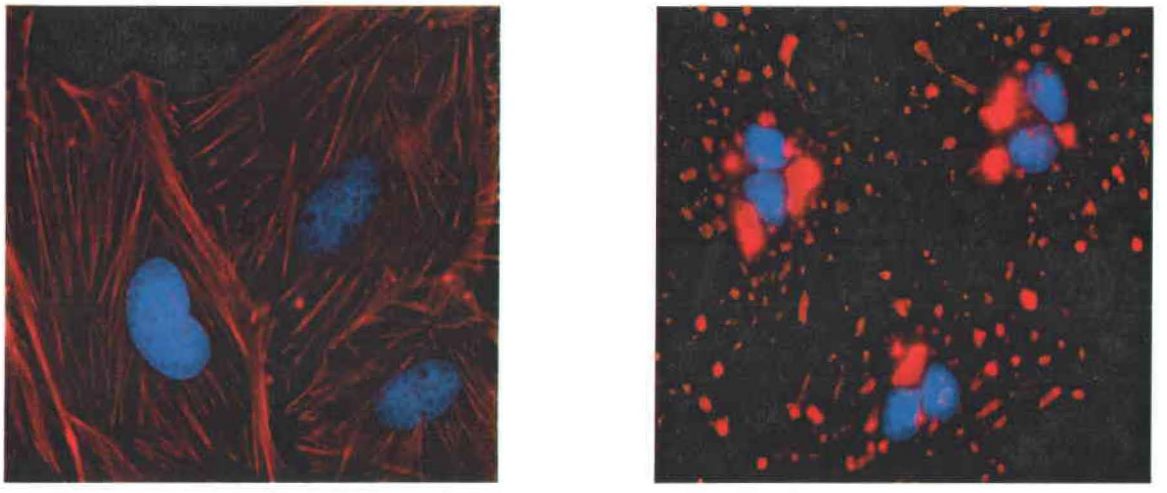

Figure 24. Microfilament-disrupting effects of lyngbyastatin 3 (**1.52**). The micofilament network in A-10 cells when treated with the control (left) or a 100 nM solution of lyngbyastatin 3 (**1.63**) (right) and visualized with rhodamine-phalloidin. Binucleated cells can be seen in blue when visualized with 4,6-diamidino-2-phenylindole.

1.4 Conclusion

Several new cytotoxins were discovered by the bioassay-guided fractionation of various collections of the marine cyanobacteria *Symploca* and *Lyngbya.* Most of these compounds were peptides or depsipeptides that incorporated modified amino acids and/or polyketide-derived residues. The most difficult part of the structure determination of the natural products was often determining the stereochemistry of these modified units. The most frequently encountered stereochemical problem in cyanobacterial metabolites is determining the absolute and relative configurations of α-methyl-β-amino acids. A streamlined procedure for the analysis of this unit that combined both synthesis and chemical derivatization was developed and applied during the stereochemical determination of ulongapeptin and lyngbyastatin 3. Chemical degradation of several members of the latter structural family has also proven that the cyanobacterial samples are mixtures of Ibu-epimers, except for majusculamide C which is a single compound.

Lyngbyabellin D and tasiamide B contained γ-amino-β-hydroxyacid units, which are rarely incorporated into cyanobacterial metabolites. A procedure for degradation of this unit, via the α,β-unsaturated acid, to the α-amino acid was demonstrated for lyngbyabellin D and micromide B. A simple method of relating the configuration of the two vicinal centers in this unit has yet to be found. Development of a chiral NMR database or the advent of more sensitive *J*-based NMR methods would be an effective solution to this problem in cases where a limited amount of material is available.

These unusual structural features seen in cyanobacterial metabolites likely serve to enhance the chemical stability and biological effectiveness of these metabolites. Unfortunately, due to the limited amount of material in all but one case, further biological

evaluation of the compounds isolated was precluded. Lyngbyastatin 3, an analogue of lyngbyastatin 1, was demonstrated to be a potent microfilament disruptor, but displayed marginal or nil antitumor activity in vivo at non-toxic dosages. Against KB cells, only the depsipeptide palau'amide was more cytotoxic than lyngbyastatin 3. Given this potent activity, palau'amide would be a candidate for in vivo testing if more of the compound was available. This paucity of material in general prevented the screening of the isolated metabolites for a wider range of biological activities, but other potential pharmacological uses for these secondary metabolites may appear when we develop a better understanding of their ecological roles.

Clearly, cyanobacteria produce a large number of secondary metabolites. But despite producing many compounds, the actual structural diversity is often small since most of these metabolites are peptides and depsipeptides. From this perspective the limited biosynthetic diversity is a liability for drug discovery from cyanobacteria. On the other hand, within these boundaries, the structural variation of the metabolites produced is impressive, as amino acid residues are frequently swapped (e.g. Leu to Val), modified (e.g. methylations, oxidations, reductions, dehydrations), or combined with polyketide residues. The number of natural analogues generated by this combinatorial approach in some cases allows the rapid assessment of the structure activity relationships, which could expedite the development of cyanobacterial compounds as drugs.

From the results of this dissertation it is difficult to evaluate whether the Corbett assay is the best method of prescreening cyanobacterial extracts. The presence of several cytotoxins with the crude cyanobacterial extracts can cause mixed results in the prescreening process and result in inaccurate prioritization of extracts. Too many

competing modes of actions are evaluated in the same assay. As initial screen it still is useful, but perhaps should be followed by more specific mechanism based assays. Unfortunately the hierarchy and even the identity of the factors involved in tumor promotion and growth are poorly understood, making it difficult to decide which inhibitors would be the most useful. This is one area where the natural product chemists will have to wait for the molecular biologists.

In general there are still some serious obstacles to the development of drugs from marine sources, most of which fundamentally center on the issue of supply. The most obvious are the low growth rates of the organisms, the small quantities of each of secondary metabolites produced, and their complex structures, which in many cases realistically prevent large amounts of these compounds being produced by chemical synthesis.[158] The first two are problems that do hamper the development of drugs from cyanobacteria, but the third is less of an issue compared to other organisms. In all likelihood cyanobacterial drug candidates would be peptides and depsipeptides that can be synthesized from amino acid subunits. The fact that many of these subunits are available as enantiomerically pure starting material eliminates many of the concerns which plague chemical synthesis about controlling the stereochemical outcome of reactions. These factors should make synthesis of drugs from cyanobacteria more economically viable for a pharmaceutical company and increase the odds that cyanobacteria may one day be an important source of new biomedical leads.

1.5 EXPERIMENTAL SECTION

1.5.1 General

1.5.1.1 Spectral Analysis

Routine NMR Analysis. ^{1}H, ^{13}C NMR and 2D NMR experiments on the natural products were carried out on Varian Unity Inova 400/500 spectrometers or on a GE Omega 500 spectrometer, operating at 400/500 MHz and 100/125 MHz respectively. The NMR spectra of the synthetic materials were obtained at 300 and 75 MHz using a GE QE-300 spectrometer or a Varian 300. NMR spectra were referenced to the appropriate residual solvent signal (δ_H 7.26, δ_C 77.0 for $CDCl_3$ and δ_H 3.30, δ_C 49.0 for MeOH-$d_{3/4}$) with chemical shifts reported in δ units (ppm). Multiplicities are as indicated in the list of abbreviations. The HMQC and HSQC experiments were optimized for $^{1}J_{CH}$ = 140 Hz and HMBC experiments for $^{3}J_{CH}$ = 7 or 4 Hz. Mixing times for the ROESY and NOESY experiments were 500 ms and generally 180 ms for the 1D TOCSY experiments.

Mass Spectrometric Analysis. HRMS were generally performed at the UCR Mass Spectrometry Facility at the Department of Chemistry, University of California at Riverside. These spectra were recorded in the positive mode by either FAB or MALDI-TOF on VG-ZAB and DE-STR mass spectrometers respectively. The high-resolution ESI spectra were recorded in the positive mode at Pharmacia Corporation, Chesterfield, MO. The LC/MS and MS/MS were performed on a quadrupole ion trap mass spectrometer (model LCQ, Thermo Finnigan Corp., San Jose, California). MS/MS was carried out by infusing the analyte dissolved in methanol directly into the electrospray ionization unit with a mass screening covering the range of 80-1000 amu. In these cases, the capillary temperature was held at 200 °C, sheath nitrogen flow was set at 60 corresponding to

approximately 60 psi. The ESI source needle voltage was set at 4.5 kV leading to an average current of 80μA, and the capillary voltage was set at +10 V.

IR, UV, CD, and Optical Rotations. The UV spectra were determined on a Hewlett-Packard 8453 spectrophotometer and the IR spectra were recorded on a Perkin-Elmer 1600 FTIR instrument as a film on a NaCl disk. The optical rotations were measured on a Jasco-DIP-700 polarimeter at the sodium D line (589 nm). CD measurements were recorded on a JASCO J-600 Spectropolarimeter.

1.5.1.2 General Chemical Procedures

Normal-phase column chromatography was performed on silica gel, 200-425 mesh, from Fisher Scientific, and reversed-phase flash columns were performed with ODS-coated silica gel, YMC-ODS-A. Gel filtration was carried out on Sephadex LH-20 available from Sigma. Polygram Sil G/UV254 precoated plates (0.25 mm) from Macherey-Nagel were used for most thin layer chromatography, except for the chiral TLC, which was performed on Chiralplates from Macherey-Nagel. Isocratic HPLC separations were performed on a Beckman 110B apparatus coupled to an Applied Biosystems 759A absorbance detector. Gradient separations used a Shimadzu system consisting of LC-10AT VP Solvent Delivery Modules, a SPD-M10A VP Diode Photodiode Array Detector, and a SCL-10A VP System Controller. The following HPLC columns were used: Ultracarb 5 ODS 30 (5 μm, 250 x 10 mm, Phenomenex), Econosil C_{18} (10 μm, 250 x 10 mm, Alltech), Econosil C_8 (10 μm, 250 x 10 mm, Alltech), YMC-Pack ODS-AQ-323 (5 μm, 250 x 10 mm, YMC), Bondclone 10 C_{18} (10 μm, 300 x 7.8 mm, Phenomenex), Phenosphere Silica (5 μm, 150 x 4.6 mm, Phenomenex), and Econosil CN (10 μm, 250 x 10 mm, Alltech). For the isocratic HPLC systems the

detection was at 220 nm, while the gradients had photodiode array (PDA) detection. Chiral HPLC analyses were performed on the following columns: Chirex phase 3126 (D)-Penicillamine (250 x 4.6 mm, Phenomenex), CHIRALPAK MA(+) (50 x 4.6 mm, Diacel Chemicals Ind., Ltd.), and Chiral OD gold (250 x 10 mm, Phenomenex). The analyte was detected at 254 nm when using the first two columns and at 220 nm with the third. Exact chromatographic conditions are specified in the corresponding experimental sections. Solvents used for HPLC were generally distilled and filtered before use, while dry solvents were prepared by distillation over calcium hydride. All synthetic yields are unoptimized. Racemic methyl 3-hydroxyhexanoate was purchased from CTC Organics. Commercially available amino and hydroxy acids were obtained from Sigma or Aldrich. Lactic acid was obtained by diazotization of alanine.[159] *N*-methyltyrosine and the diastereomers of *N*-methylisoleucine were prepared by H. Luesch and F. D. Horgen, Department of Chemistry, University of Hawaii at Manoa. Chiral GC/MS was done on a Chirasil-Val column (25 μm x 0.25 m, Alltech) with an initial pressure of 12 psi.

1.5.2 Biological Material

1.5.2.1 *Symploca* Collections

The cyanobacterium VP727 was collected in the Spring of 2001 in Guam at Finger's Reef. The cyanobacterium VP643 was collected at Short Drop-off in Palau during May of 2000. V. J. Paul and E. Cruz-Rivera of the University of Guam Marine Research Station identified the samples as *Symploca* spp. Vouchers are maintained in formalin at UOG or the Smithsonian Marine Research Station, Ft. Pierce, FL.

1.5.2.2 *Lyngbya* Collections

The dark reddish-black clumps of cyanobacterium, designated VP680, were collected at Obyan Bay, Saipan in 1999. The cyanobacteria, designated NIH199, NIH154, and NIH143, were collected on the Tokai Maru shipwreck in Apra Harbor. Several collections of *Lyngbya* sp. (VP417), from Finger's Reef, Apra Harbor, Guam, were carried out from February to April 2002 and combined for a total weight of 300 g. Dark reddish-black clumps of cyanobacterium were collected from Ulong Channel in Palau and designated VP755. VP664, NIH288, and NIH139 were all collected from the coastal waters around Guam, while VP 694 was collected from the coastal waters around Palau. Vouchers are maintained in formalin at the University of Guam Marine Laboratory or the Smithsonian Marine Research Station. The organisms were identified as indicated in Table 13 by V. J. Paul.

1.5.3 Extraction and Isolation

1.5.3.1 Isolation of *Symploca* Metabolites

Extraction and Isolation of VP727. The cyanobacterium was exhaustively extracted with 4:1 CH_3CN:CH_2Cl_2 to afford 1.23 g of lipophilic extract. After initial partitioning between hexane and 80 % aqueous MeOH, the organic residue from a second partitioning with *n*-BuOH and water was loaded onto a Sephadex LH-20 column (360 x 20 mm) and eluted with 5 % MeOH in $CHCl_3$. The bioactive fraction eluting between 120 and 140 mL was further purified by C_{18} chromatography and the two fractions eluting with 50 and 70 % CH_3CN combined. Separation by RP-HPLC [Ultracarb ODS 30, 250 x 10 mm, 70 % aqueous CH_3CN, flow rate 3 mL/min, detection at 254 nm] afforded apramide A (**1.1**, t_R 22 min, 1.3 mg), apramide B (**1.2**, t_R 15 min, 1.0 mg) and a

mixture of apramide G (**1.3**) and micromide A (**1.4**, t_R 41 min). This fraction was further purified by a linear gradient of 80 to 100 % aqueous MeOH [YMC-AQ ODS, 250 x 10 mm, flow rate 3 mL/min, PDA detection] to afford the former (**1.3**, t_R 14.2 min) and micromide A (**1.4**, t_R 15.9 min) in yields of 1.8 and 1.7 mg, respectively. The Sephadex fraction eluting between 180 and 200 mL was purified by RP-HPLC with a linear gradient of 65 to 75 % aqueous CH_3CN over 30 min [YMC-AQ ODS, 250 x 10 mm, flow rate 3 mL/min, PDA detection] to afford 1.7 mg of micromide B (**1.9**, t_R 23 min).

Extraction and Isolation of VP643 – Lipophilic Extract. The freeze-dried cyanobacterium (300 g) was thrice extracted with a 4:1 mixture of CH_3CN-CH_2Cl_2 to provide a total of 2.67 g of lipophilic extract. After partitioning between hexane and 80 % aqueous methanol the aqueous residue was loaded on to a Si flash column and was eluted with increasing amounts of MeOH in CH_2Cl_2. The 8 % fraction (50 mg) was passed over a C_8 column and the 50 % aqueous CH_3CN residue (9.2 mg) was subsequently rechromatographed on a cyanopropyl column [Econosil CN, 250 x 10 mm, solvent system a linear gradient from 30 to 70 % CH_3CN in H_2O over 40 min. flow rate 3 mL/min, PDA detection] to give a 6.0 mg fraction (t_R 8.0 min). This fraction was further purified [YMC-AQ ODS, 250 x 10 mm, solvent system a MeOH:0.01 % TFA linear gradient from 65 to 100 % MeOH over 30 min, flow rate 3 mL/min, PDA detection] to provide 2.1 mg of tasiamide A (**1.11**) (t_R 15.3 min).

The 5 % fraction from the initial Silica column was loaded onto a Sephadex LH-20 column (50 x 2.5 cm) and eluted with 4:1 CH_2Cl_2:MeOH. The samples eluting between 120 and 180 mL were again separated by Sephadex LH-20 using 5 % MeOH in CH_2Cl_2. The fraction eluting between 180 and 240 mL was concentrated and separated by

repeated RP-HPLC [1. Ultracarb ODS 30, 250 x 10 mm, 60 % aqueous CH_3CN, flow rate 3 mL/min, t_R 34.2 min; 2. Ultracarb ODS 30, 70 % aqueous MeOH, flow rate 3 mL/min, t_R 27.0 min; 3. Ultracarb ODS 30, 85 % aqueous MeOH, flow rate 3 mL/min, t_R 12.0 min; 4. Ultracarb ODS 30, 70 % aqueous CH_3CN, flow rate 3 mL/min, t_R 19.6 min] to yield tasihalide A (**1.15**, 0.9 mg).

Extraction and Isolation of VP643 – Aqueous Extract. The cyanobacterium (300 g), which had already been extracted with 4:1 CH_3CN:CH_2Cl_2, was exhaustively extracted with 30 % aqueous EtOH to give 2 g of extract. After partitioning between *n*-BuOH and water, the dry organic residue was loaded onto a Sephadex LH-20 column (50 x 2.5 cm) and eluted with 5 % MeOH in $CHCl_3$ (400 mL), 15 % MeOH (700 mL), and pure MeOH (500 mL). The 5 % fraction eluting between 100 and 140 mL was purified by C_{18} chromatography using increasing amounts of CH_3CN in H_2O. The 50 % fraction was then separated by RP-HPLC (t_R 10.5 min) [Ultracarb ODS 30, 250 x 10 mm, 45 % aqueous CH_3CN, flow rate 3 mL/min, detection 220 nm]. Final purification with 70 % aqueous MeOH [YMC-AQ ODS, 250 x 10 mm, flow rate 2 mL/min, detection at 254 nm] provided 2.6 mg of tasiamide B (**1.4**) (t_R 14.2 min).

The 5 % MeOH Sephadex fractions eluting between 80 and 140 mL were combined, loaded on a C_{18} column, and eluted with increasing amounts of aqueous MeCN. The 50 % and 60 % fractions were combined and subjected to reversed-phase HPLC [Ultracarb ODS 30, 250 x 10 mm, 45 % MeCN in H_2O, flow rate 3 mL/min, detection 220 nm] to give tasihalide B (**1.16**) (t_R 48 min), tasipeptin B (**1.14**) (t_R 48 min) and tasipeptin A (**1.13**) (t_R 55 min). Both **1.13** and **1.14** were subsequently repurified [YMC-AQ ODS, 250 x 10 mm, 50 % aqueous MeCN, flow rate 2.5 mL/min, detection at

220 nm] with to yield 2.2 mg (t_R 23 min) of **1.14** and 4.3 mg (t_R 48 min) of **1.13.** Tasihalide B (**1.16**) was purified by repeated HPLC [1. Ultracarb ODS 30, 250 x 10 mm, 60:40 CH_3CN: 0.0025M Na_2SO_4, flow rate 3 mL/min, detection at 220 nm, t_R 25 min; 2. YMC-AQ ODS, 250 x 10 mm, 80 % aqueous MeCN, flow rate 2.0 mL/min, detection at 220 nm, t_R 10.5 min; 3. Ultracarb ODS 30, 250 x 10 mm, 80 % aqueous MeOH, flow rate 3 mL/min, detection at 220 nm, t_R 14.2 min] to yield 0.8 mg.

1.5.3.2 Isolation of New *Lyngbya* Metabolites

Extraction and Isolation of VP417. The cyanobacterium was initially extracted and separated as previously described except the *n*-BuOH/H_2O partition was omitted.[5] The 5 % *i*-PrOH fraction contained lyngbyapeptin A (**1.37**), the 6 % apratoxin A, and the 8 % a mixture of apratoxin A, lyngbyastatin 2, lyngbyabellin A (**1.39**), **1.36**, and **1.38**. This 8 % fraction was separated by RP-HPLC [Ultracarb ODS 30, 250 x 10 mm, 80 % aqueous CH_3CN, flow rate 3 mL/min, detection at 220 nm] to provide a mixture of **1.36** and **1.38** (t_R 7.5 min). Further purification using 65 % aqueous CH_3CN afforded pure 15-norlyngbyapeptin A (**1.36**) (0.8 mg, t_R 14.2 min) and lyngbyabellin D (**1.38**) (0.8 mg, t_R 18.9 min).

Extraction and Isolation of VP680. The cyanobacterium was extracted with 1:1 CH_2Cl_2:MeOH to yield 1.49 g of lipophilic extract. This extract was then partitioned between hexane and 80 % MeOH. After drying the aqueous methanol layer, the residue was partitioned between water and *n*-butanol to afford 154 mg of material from the organic layer. Separation on a C_{18} column with increasing amounts of MeCN in H_2O resulted in the activity concentrated primarily in the 60 % MeCN in H_2O fraction (9 mg). Further purification on a RP column (50 %, 60 %, 70 % MeCN in H_2O) gave 4.7 mg of

material in the 60 % MeCN fraction that after semi-preparative RP HPLC [Ultracarb ODS 30, 250 x 10 mm, 65 % CH_3CN in H_2O, flow rate 3 mL/min, detected at 220 nm] afforded 1.6 mg of crude **1.48** (t_R 16 min). Final HPLC purification with 70 % MeOH (t_R 13.8 min) yielded 1.1 mg of pure obyanamide (**1.48**).

Extraction and Isolation of VP755. VP755 was extracted with 1:1 EtOAc:MeOH to yield 1.11 g of lipophilic extract that was subsequently partitioned between hexane and 80 % aqueous MeOH. After drying, the aqueous methanol residue was partitioned between water and *n*-butanol. Normal-phase flash chromatography of the organic layer with increasing amounts of methanol in dichloromethane resulted in the cytotoxicity concentrated primarily in the 5 % methanol fraction. Subsequent separation on a C_{18} column with increasing amounts of MeCN in H_2O resulted in the activity concentrated primarily in the 60 % MeCN in H_2O fraction. This sample was purified twice by RP-HPLC [Ultracarb ODS 30, 250 x 10 mm, flow rate 3 mL/min, detection at 220 nm], first with 70 % MeCN in H_2O (t_R 21 min) and then with 80 % MeOH in H_2O to yield 1.1 mg of ulongapeptin (**1.55**, t_R 25 min) and 2.8 mg of palau'amide (**1.61**, t_R 28 min).

Extraction and Isolation of NIH199, 154, and 143. The freeze-dried cyanobacterium (95.11 g) designated NIH199 was sequentially extracted with a 1:1 mixture of MeOH/CH_2Cl_2 and 30 % aqueous ethanol to afford 1.29 g of lipophilic and 4.60 g of aqueous extract. NIH154 (72.44 g) and NIH143 (45.42 g) were treated in a similar manner to provide 12.43 and 5.45 g of lipophilic extracts, respectively. These extracts were partitioned between hexane and 80 % MeOH, and then the aqueous residues were further partitioned between *n*-butanol and water. The organic fractions

were separated on silica gel eluting with CH_2Cl_2 and increasing amounts of *i*-PrOH. The biologically active fractions (5 and 8 %) were separated on a C_{18} column (2000 mg, Alltech) with increasing amounts of CH_3CN in H_2O. Final purification of the active fractions by RP-HPLC [Ultracarb ODS 30, 250 x 10 mm, 70 % aqueous CH_3CN, flow rate 3 mL/min, detection at 220 nm] afforded pure lyngbyastatin 3 (**1.63**, t_R 18 min). NIH199 yielded 10 mg and 15 mg of **1.63** from the lipophilic and aqueous extracts, respectively, while NIH154 and NIH143 gave 49 and 48 mg of **1.63** from the lipophilic extracts respectively.

Extraction and Isolation of NIH198. A 121.9 g sample of freeze-dried *Lyngbya majuscula* was extracted with a 1:1 mixture of ethyl acetate and methanol to give 2.5 g of lipophilic extract. The remaining cell mass was extracted with a 3:7 mixture of ethanol and water to give 13.5 g of aqueous extract. These extracts were purified as described above for NIH199. Final purification of the 5 and 8 % MeOH fractions [Ultracarb ODS 30, 250 x 10 mm, flow rate 3 mL/min, detection at 220 nm] using an isocratic system of 55 % aqueous acetonitrile afforded two active compounds, lyngbyastatin 1 (**1.64**) (t_R 40 min, 10 mg) and dolastatin 12 (**1.65**) (t_R 46 min, 20 mg) from the lipophilic extract. Purification of the aqueous extract in the same manner afforded 3.6 mg of **1.64** and 6.8 mg of **1.65**.

1.5.4 Physical Data

1.5.4.1 *Symploca* Metabolites

Micromide A (1.4) was obtained as an amorphous powder: $[\alpha]^{21}_D$ -28° (*c* 0.5, MeOH); UV (MeOH) λ_{max} (log ε) 201 (4.40), 225 (3.80), 274 (2.40) nm; IR (film) ν_{max} 3311, 1680, 1462, 1379 cm^{-1}; ^1H NMR, ^{13}C NMR, ^1H-^1H COSY, and HMBC data, see

Table 4; MALDI *m/z* $[M + Na]^+$ 926.5; HR-MALDI *m/z* $[M + Na]^+$ 926.5155 (calcd for $C_{49}H_{73}N_7O_7SNa$ 926.5184, 2.9 mDa error).

Micromide B (1.9) was obtained as an amorphous powder: $[\alpha]^{21}_D$ +6° (*c* 0.4, MeOH); UV (MeOH) λ_{max} (log ε) 201 (3.71) nm; IR (film) ν_{max} 3382, 1739, 1651, 1371, 1233, 1095 cm^{-1}; ^1H NMR, ^{13}C NMR, ^1H-^1H COSY, and HMBC data, see Table 5; FABMS *m/z* $[M + Na]^+$ 510; HR-FABMS *m/z* $[M + H]^+$ 488.3225 (calcd for $C_{25}H_{46}NO_6$ 488.3223, 0.2 mDa error).

Tasiamide A (1.11) was obtained as an amorphous powder: $[\alpha]^{21}_D$ +15° (*c* 0.4, $CHCl_3$); UV (MeOH) λ_{max} (log ε) 201 (4.27), 254 (2.52) nm; IR (film) ν_{max} 3311, 1737, 1643, 1453 cm^{-1}; ^1H NMR, ^{13}C NMR, ^1H-^1H COSY, and HMBC data, see Table 6; FABMS *m/z* (intensity) $[M + Na]^+$ 852 (15), $[M + H]^+$ 830 (16), 814 (8), 701 (56), 687 (13), 603 (6), 483 (10), 370 (71), 348 (4), 332 (6), 291 (46), 228 (43), 200 (66), 142 (20), and 128 (36); HR-FABMS *m/z* $[M + Na]^+$ 852.4833 (calcd for $C_{42}H_{67}N_7O_{10}Na$ 852.4841, 0.8 mDa error).

Tasiamide B (1.12) was obtained as an amorphous powder: $[\alpha]^{21}_D$ -28° (*c* 0.4, MeOH); UV (MeOH) λ_{max} (log ε) 201 (7.60) nm; IR (film) ν_{max} 3396, 3307, 1743, 1633, 1538, 1455, 1265, 1176 cm^{-1}; ^1H NMR, ^{13}C NMR, ^1H-^1H COSY, and HMBC data, see Table 7; MALDI *m/z* $[M + Na]^+$ 1002; HR-MALDI *m/z* $[M + Na]^+$ 1001.5347 (calcd for $C_{50}H_{74}N_8O_{12}Na$ 1001.5318, 2.9 mDa error).

Tasipeptin A (1.13) was obtained as an amorphous powder: $[\alpha]^{24}_D$ -23° (*c* 1.5, MeOH); UV (MeOH) λ_{max} (log ε) 202 (6.74) nm; IR (film) ν_{max} 3371, 3291, 1731, 1643, 1453 cm^{-1}; ^1H NMR, ^{13}C NMR, ^1H-^1H COSY, and HMBC data, see Table 9; HR-MALDI *m/z* $[M + Na]^+$ 892.5140 (calcd for $C_{45}H_{71}N_7O_{10}Na$ 892.5155, 1.5 mDa error).

Tasipeptin B (1.14) was obtained as an amorphous powder: $[\alpha]^{21}_{D}$ -13° (*c* 0.7, MeOH); UV (MeOH) λ_{max} (log ε) 202 (2.81) nm; IR (film) ν_{max} 3400, 3304, 1735, 1650, 1536, 1462, 1205 cm^{-1}; ^{1}H NMR, ^{13}C NMR, and HMBC data, see Table 10; MALDI *m/z* $[M + Na]^{+}$ 793; HR-MALDI *m/z* $[M + Na]^{+}$ 793.4454 (calcd for $C_{40}H_{62}N_6O_9Na$ 793.4475, 2.1 mDa error).

Tasihalide A (1.15) was obtained as an amorphous powder: $[\alpha]^{24}_{D}$ -18° (*c* 0.6, MeOH); UV (MeOH) λ_{max} (log ε) 207 (4.3), 253 (1.2) nm; IR (film) ν_{max} 3501, 1735, 1372, 1236, 1026, 977 cm^{-1}; ^{1}H NMR, ^{13}C NMR, and HMBC data, see Table 11; ESI *m/z* (relative intensity) $[M + Na]^{+}$ 707 and 709 (1:1); HR-ESI *m/z* $[M + NH_4]^{+}$ 702.1154 (calcd for $C_{26}H_{38}Br^{79}IO_8NH_4$ 702.1133, 2.1 mDa error).

Tasihalide B (1.16) was obtained as an amorphous powder: $[\alpha]^{23}_{D}$ -13° (*c* 0.4, MeOH); UV (MeOH) λ_{max} (log ε) 202 (3.1) 253 (1.3) nm; IR (film) ν_{max} 1735, 1372, 1236, 1026, 977 cm^{-1}; ^{1}H NMR, ^{13}C NMR, and HMBC data, see (Table 12); ESI *m/z* (relative intensity) $[M + Na]^{+}$ 744 and 746 (1:1); HR-ESI *m/z* $[M + NH_4]^{+}$ 744.1246 (calcd for $C_{28}H_{40}Br^{79}IO_9NH_4$ 744.1239, 0.7 mDa error).

1.5.4.2 *Lyngbya* Metabolites

15-Norlyngbyapeptin A (1.36) was obtained as a white powder: $[\alpha]^{22}_{D}$ -31° (*c* 0.4, MeOH); UV (MeOH) λ_{max} (log ε) 201 (4.20), 226 (4.02) nm; IR (film) ν_{max} 3367, 2849, 1635, 1456, 1338 cm^{-1}; ^{1}H NMR and ^{13}C NMR data, see Table 15; HR-FABMS *m/z* $[M + Na]^{+}$ 706.3649 (calcd for $C_{36}H_{53}N_5O_6SNa$ 706.3614, 3.5 mDa error).

Lyngbyabellin D (1.38) was obtained as a white powder: $[\alpha]^{25}_{D}$ +20° (*c* 0.4, MeOH); UV (MeOH) λ_{max} (log ε) 202 (7.31), 223 (6.81) nm; IR (film) ν_{max} 3365, 1731, 1650, 1538, 1455, 1232, 1097 cm^{-1}; ^{1}H NMR, ^{13}C NMR, ^{1}H-^{1}H COSY, and HMBC data,

see Table 16; HR-FABMS *m/z* $[M + Na]^+$ 918.2386 (calcd for $C_{38}H_{55}{}^{35}Cl_2N_3O_{13}S_2Na$ 918.2445, 5.9 mDa error).

Obyanamide (1.48) was obtained as a white powder: $[\alpha]^{27}{}_D$ +20° (*c* 0.4, MeOH); UV (MeOH) λ_{max} (log ε) 210 (5.20), 222 (4.32) nm; IR(film) ν_{max} 3315, 1734, 1628, 1551, 1521, 1458, 1279, 699 cm^{-1}; ^1H NMR, ^{13}C NMR, ^1H-^1H COSY, and HMBC data, see Table 17; FABMS *m/z* 622.4 $[M + Na]^+$; HR-FABMS *m/z* $[M + H]^+$ 600.2873 (calcd for $C_{30}H_{42}N_5O_6S$ 600.2859, 1.4 mDa error).

Ulongapeptin (1.55) was obtained as an amorphous powder: $[\alpha]^{21}{}_D$ -16° (*c* 0.4, MeOH); UV (MeOH) λ_{max} (log ε) 204 (3.84) nm; IR (film) ν_{max} 3336, 1727, 1654 (br), 1508, 1458, 1259, 1078 cm^{-1}; ^1H NMR, ^{13}C NMR, ^1H-^1H COSY, HMBC, TOCSY, and ROESY data, see Table 18; FABMS *m/z* 809.4 $[M + H]^+$; HR-MALDI *m/z* $[M + H]^+$ 809.5226 (calcd for $C_{44}H_{69}N_6O_8$ 809.5171, 4.5 mDa error).

Palau'amide (1.61) was obtained as a colorless oil: $[\alpha]^{23}{}_D$ -22° (*c* 0.4 MeOH); UV (MeOH) λ_{max} (log ε) 202 (4.54) nm; IR (film) ν_{max} 3444, 1737, 1713, 1644, 1455, 1414, 1247, 1094 cm^{-1}; ^1H NMR, ^{13}C NMR, ^1H-^1H COSY, HMBC, TOCSY, and ROESY data, see Table 19,Table 20, and Table 21; FABMS *m/z* $[M + Na]^+$ 874; HR-MALDI *m/z* 874.5003 (calcd for $C_{46}H_{69}O_{10}N_5Na$ 874.4942, 6.1 mDa error).

Lyngbyastatin 3 (*R*-Ibu-1.63) and Ibu-epilyngbyastatin 3 (*S*-Ibu-1.63) were obtained as a colorless oil: $[\alpha]^{27}{}_D$ -62° (*c* 0.12, $CHCl_3$); UV (MeOH) λ_{max} (log ε) 201 (4.23), 209 (3.98), 221 (3.87), 277 (3.45) nm; IR (film) ν_{max} 3386, 1729, 1637, 1513, 1466, 1248 cm^{-1}; FABMS *m/z* $[M + H]^+$ 1014, $[M + Na]^+$ 1036; HR-FABMS *m/z* $[M + H]^+$ 1013.6337 (calcd for $C_{52}H_{85}N_8O_{12}$ 1013.6399, 5.8 mDa error).

Lyngbyastatin 1 (*R*-Ibu-1.64) and Ibu-epilyngbyastatin 1 (*S*-Ibu-1.64) were obtained as a clear glassy oil: $[\alpha]^{27}_{D}$ -17° (*c* 0.3, MeOH); UV (MeOH) λ_{max} (log ε) 236 (3.15), 277 (2.80), 284 (2.75) nm; IR (film) ν_{max} 3320, 1791, 1673, 1637, 1525, 1461, 1402, 1279, 1161, 1079, 1008 cm^{-1}; HR-FABMS *m/z* 1021.5965 (calcd for $C_{51}H_{82}N_8O_{12}Na$ 1021.5944, 2.1 mDa error).

Dolastatin 12 (*S*-Ibu-1.65) and Ibu-epidolastatin 12 (*R*-Ibu-1.65) were obtained as a clear glassy oil: $[\alpha]^{27}_{D}$ -54° (*c* 0.7, MeOH); UV (MeOH) λ_{max} (log ε) 234 (2.70), 241 (3.00), 243 (3.66), 277 (2.24), 283 (2.24) nm; IR (film) ν_{max} 3316, 1791, 1672, 1637, 1525, 1461, 1402, 1278, 1161, 1078, 1008 cm^{-1}; HR-FABMS *m/z* 991.5818 (calcd for $C_{50}H_{80}N_8O_{11}Na$ 991.5839, 2.1 mDa error).

1.5.5 Synthesis of Standards.

1.5.5.1 Standards for Micromide A (1.4)

Chiral Separation of Methyl 3-Hydroxyhexanoate (1.5). A racemic mixture of methyl 3-hydroxyhexanoate was separated by chiral HPLC [OD gold, 15 % *i*-PrOH in hexane, 1 mL/min, PDA detection] to afford (*R*)- and (*S*)-**1.5** at 21.4 and 27.6 min with $[\alpha]^{23}_{D}$ of -22° and +23° (*c* 0.8, MeOH), respectively.[32]

Synthesis of 3(*R*)-Methoxyhexanoate (*R*-1.6). To 0.5 mL of methyl 3(*R*)-hydroxyhexanoate in 20 mL of petroleum ether (bp 40-60 °C) was added KOH (4 pellets), 14 μL of triethylamine, and 0.39 mL of dimethyl sulfate. The solution was allowed to stir at room temperature for 5 h before the solvent was removed under a stream of N_2. To this residue was then added 5 mL of 0.5 N NaOH and 5 mL of MeOH and the solution stirred overnight. The mixture was then acidified to pH 2 with 1 N HCl and extracted into diethyl ether. The organic layer was dried with $MgSO_4$ and

concentrated in *vacuo* to afford (*R*)-**1.6** in approximately 80 % yield. Treatment of racemic methyl 3-hydroxyhexanoate in a similar manner provided **1.6**. ^{1}H NMR of (*R*)-**1.6** ($CDCl_3$, 300 MHz) δ_H (integration, multiplicity; *J* in Hz) 3.64 (1H, p; 5.9), 3.39 (3H, s), 2.53 (2H, d; 5.9), 1.61 (1H, m), 1.49 (1H, m), 1.40 (2H, m), 0.93 (3H, t; 7.3).

Mandelate Derivatives. To 10 mg of (*R*)-**1.6** in 0.2 mL of CH_2Cl_2 were added 2 mg of DMAP, 12 mg of methyl D-mandelate and 70 μL of 1 M DCC in CH_2Cl_2. The mixture was stirred at room temperature for 3 h before filtration and evaporation. The crude residue was purified by silica chromatography eluting with a mixture of 6:1 hexane:*i*-PrOH to afford **1.7** in 85 % yield. The racemic mixture **1.6** was treated in the same manner to afford **1.8** as a mixture of 3*R*- and 3*S*-(methyl D-mandelate) methoxyhexanoate. ^{1}H NMR of (*R*)-**1.7** ($CDCl_3$, 300 MHz) δ_H (integration, multiplicity; *J* in Hz) 7.46 (5H, m), 5.95 (1H, s), 3.72 (3H, s), 3.70 (1H, m), 3.34 (3H, s), 2.67 (1H, dd; -15.3, 7.3), 2.57 (1H, dd; -15.3, 5.6), 1.6-1.4 (4H, m), 0.88 (3H, t; 6.5).

1.5.5.2 Standards for Lyngbyabellin D (1.38).

Synthesis of α,β-Dihydroxy-β-methylpentanoic Acid (Dhmp 1.46, 1.47). A 3:1 mixture of the unsaturated ethyl ester[108] (**1.44**, 100 mg) was heated to 60 °C for 12 h in 7 mL of pyridine and 11 mL of 5% aqueous NaOCl. The mixture was thrice partitioned between EtOAc and H_2O, the organic layers combined, dried over $MgSO_4$ and the solvent removed in *vacuo*. This mixture was then stirred with 300 mg of $Ba(OH)_2$ in 0.5 mL of methanol at room temperature overnight before the addition of 1 % H_2SO_4 till the pH was 3. The cloudy solution was allowed to stir overnight, before the $BaSO_4$ was pelleted by centrifugation. The supernatant was removed by a stream of N_2 to yield a

mixture of all four diastereomers (**1.46, 1.47**), in a ratio of approximately 3:1:1:3 as determined by chiral HPLC.

Asymmetric Synthesis of α,β-Dihydroxy-β-methylpentanoic Acids (*ent*-1.46). A round bottom flask with 700 mg of AD mix-α was stirred at room temperature with 10 mL of a 1:1 mixture of *t*-BuOH and water till the organic layer was yellow.[109] To this was added 50 mg of methanesulfonamide and the mixture cooled to 0 °C before the addition of 50 mg of the **1.44**. After 18 h at 0 °C, 700 mg of sodium sulfite was added and the solution allowed to warm to room temperature over 30 min. This was then partitioned between EtOAc and water, the organic layer dried over $MgSO_4$, and the solvent removed to yield the pure dihydroxy ester. Subsequent saponification with $Ba(OH)_2$ and acid workup followed by centrifugation provided the enantiomerically pure (2*R*,3*S*)-**1.46** from the supernatant. Dihydroxylation of **1.44** with AD mix-β produced the corresponding enantiomer by the same procedure.

(2*R*,3*S*)-2,3-Dihydroxy-3-methylpentanoic Acid [(2*R*,3*S*)-1.46]: $[\alpha]_D^{24}$ -8° (*c* 1.23, H_2O, Lit $[\alpha]_D^{20}$ -16)[160], $[\alpha]_D^{24}$ -14° (*c* 2.00, 0.1 N HCl, Lit $[\alpha]_D^{20}$ -16)[161]; ^1H NMR (D_2O, 300 MHz) δ_H (multiplicity, integration; *J* in Hz) 0.70 (t, 3H; 7.5), 0.99 (s, 3H), 1.35 (dq, 1H; -13.8, 7.5), 1.45 (dq, 1H; -13.8, 7.5), 3.87 (s, 1H).[160]

(2*S*,3*R*)-2,3-Dihydroxy-3-methylpentanoic Acid [(2*S*,3*R*)-1.46]: $[\alpha]_D^{24}$ +7° (*c* 1.23, H_2O), $[\alpha]_D^{21}$ +13° (*c* 2.30, 0.1 N HCl, Lit $[\alpha]_D^{20}$ +16);[161,162] ^1H NMR (D_2O, 300 MHz) δ_H (multiplicity, integration; *J* in Hz) 0.70 (t, 3H; 7.5), 0.99 (s, 3H), 1.35 (dq, 1H; -13.8, 7.5), 1.45 (dq, 1H; -13.8, 7.5), 3.87 (s, 1H).

1.5.5.3 Standards for Obyanamide (1.48).

Synthesis of 3-Aminopentanoic Acid Standards: (*R*)-*N*-Boc-2-aminobutanol (1.50).[163] To a 5 mL vial containing 100 μL of (*R*)-2-aminobutanol was added 50 mg of NaOH (1 mol eq.) in 1 mL of water and 750 μL of *tert*-butanol. Next, 230 mg of di-*tert*-butylcarbonate was added and the cloudy solution stirred overnight at room temperature. The next day, the pH of the solution was adjusted to 7 with 6 N HCl and the solution partitioned between ethyl acetate and water. The organic phase was dried over $MgSO_4$ and the solvent removed in *vacuo* to yield 151 mg (69 %) of compound **1.50**. ^{1}H NMR ($CDCl_3$, 300 MHz) δ_H (carbon position, multiplicity; *J* in Hz) 0.80 (4, t; 7.9), 1.30 (7/8/9, s), 1.42 (3, m), 3.38 (2, m), 3.42 (1, m), 5.07 (OH, br s); ^{13}C NMR δ_C 64.0 (1), 53.8 (2), 24.3 (3), 10.2 (4), 156.7 (5), 79.6 (6), 28.2 (7/8/9).

(*R*)-*N*-Boc-2-aminobutanol Tosylate (1.51).[164] Compound **1.50** (151 mg) was dissolved in 1 mL of freshly distilled pyridine and the solution was stirred at 0 °C while 293 mg of *p*-toluenesulphonyl chloride (2 mol eq.) was slowly added. The reaction mixture was stored at -4 °C for 3 days and then poured over 30 mL of ice in a 60 mL separatory funnel and extracted with 30 mL of diethyl ether. The organic layer was subsequently washed with 6 N HCl, followed by saturated aq. $NaHCO_3$ and saturated aq. sodium chloride. The organic layer was dried over $MgSO_4$ and evaporated to yield 263 mg (100 %) of **1.51**. ^{1}H NMR ($CDCl_3$, 300 MHz) δ_H (carbon position, multiplicity; *J* in Hz) 0.79 (4, t; 7.3), 1.32 (7/8/9, s), 1.40 (3, m), 2.36 (16, s), 3.49 (2, m), 3.94 (1, m), 7.70 (12/14, d; 7.1), 7.23 (11/15, d; 7.8); ^{13}C NMR δ_C (carbon position) 71.3 (1), 65.9 (2), 24.4 (3), 10.4 (4), 155.3 (5), 79.6 (6), 28.5 (7/8/9), 145.0 (10), 128.0 (11/15), 130.0 (12/14), 158.3 (13), 21.8 (16).

(*R*)-*N*-Boc-3-amino-pentanitrile (1.52). To 250 mg of **1.51** in 2 mL of wet DMSO was added 43 mg of NaCN with stirring. The reaction was left at room temperature overnight and then partitioned between diethyl ether and water. The ether layer was evaporated and the residue chromatographed on silica gel using 10:1 hexane to ethyl acetate to afford 66 mg (44 %) of **1.52**. ^{1}H NMR ($CDCl_3$, 300 MHz) δ_H (carbon position, multiplicity; *J* in Hz) 0.90 (5, t; 7.3), 1.39 (8/9/10, s), 1.49 (4, m), 2.46 (2, dd; -16.1, 5.1), 2.68 (2, dd; -16.1, 4.6), 3.62 (3, m); ^{13}C NMR δ_C (carbon position) 117.4 (1), 40.9 (2), 49.0 (3), 23.5 (4), 10.4 (5), 155.3 (6), 79.9 (7), 28.4 (8/9/10).

(*R*)-3-Aminopentanitrile (1.53). A solution of 66 mg (0.3 mmol) of **1.52** in 1 mL of concentrated trifluoroacetic acid was stirred for 10 minutes. Evaporation of the solvent under N_2 and partitioning of the residue between EtOAc and water yielded 30 mg (92 %) of **1.53** from the aqueous phase. ^{1}H NMR (MeOH-d_4, 300 MHz) δ_H (carbon position, multiplicity; *J* in Hz) 1.09 (5, t; 7.6), 1.85 (4, m), 2.98 (2, d; 5.6), 3.51 (3, m); ^{13}C NMR δ_C (carbon position) 115.8 (1), 25.4 (2), 49.3 (3), 20.3 (4), 8.5 (5).

(*R*)-3-Aminopentanoic Acid Hydrochloride (*R*)-(1.54). A solution of 30 mg of **1.53** in 1 mL of 6 N HCl was refluxed overnight. Purification of the residue over DOWEX 50 resin eluting with 1 M HCl resulted in 40 mg (87 %) of **1.54**. IR (Nujol) ν_{max} 3415, 3300, 3100, 1712 cm^{-1}; H NMR (MeOH-d_4, 300 MHz) δ_H (carbon position, multiplicity; *J* in Hz) 0.98 (5, t; 7.8), 1.72 (4, m), 2.69 (2, dd; -17.3, 4.7), 2.84 (2, dd; -17.3, 8.3), 3.6 (3, m), 7.01, 7.19, 7.36 (NH_3).

(*S*)-3-Aminopentanoic Acid Hydrochloride (*S*)-1.54. The *S* enantiomer was synthesized in the same manner as described for (*R*)-3-aminopentanoic acid, but starting with (*S*)-2-aminobutanol.

L- and D-Lactic Acid.[152] A solution of L-Ala in 1 mL of 4 N HCl at 4 °C was treated with excess sodium nitrite (500 mg in 1 mL of water) and left to stir overnight. The mixture was repeatedly extracted with ethyl ether and evaporated to dryness to give L-lactic acid. D-Lactic acid was prepared in the same manner from the enantiomer.

1.5.5.4 Standards for Ulongapeptin (1.55).

Synthesis of 3-Amino-2-methyloctanoic Acid (1.60). To 15 mL of THF in a 100 mL flask under N_2 was added trimethyl phosphonoacetate (**1.56**) (5.5 mmol) and *n*-BuLi (5.6 mmol). After stirring at -78 °C for 1 h, this mixture was cannulated into 20 mL of THF containing hexanal (5.5 mmol). The reaction was allowed to warm to room temperature overnight and then the solvent was removed. After the residue was partitioned between diethyl ether and water, the organic layer was dried over $MgSO_4$ and evaporated. Purification of this residue, dissolved in a 20:1 mixture of petroleum ether:diethyl ether, by silica chromatography yielded pure methyl oct-2(*E*)-enoate (**1.57**). This α,β-unsaturated ester was then treated according to Davies' procedure,[144] except the diastereomers were not separated after methylation. The C-2 diastereomers were instead separated by HPLC as their FDLA derivatives after deprotection.

D-FDLA + (2*R*, 3R)-3-Amino-2-methyloctanoic Acid (1.60). ^{1}H NMR (acetone-d_6, 500 MHz) δ_H (integration, multiplicity; *J* in Hz) 9.11 (1H, s), 8.93 (1H, d;9.2), 8.55 (1H, d; 6.4), 7.55 (1H, br s), 6.63 (1H, br s), 6.11 (1H, s), 4.26 (1H, m), 3.99 (1H, m), 2.96 (1H, m), 1.86 (2H, m), 1.68 (1H, m), 1.40 (2H, m), 1.30 (6H, m), 1.23 (3H, d; 6.3), 1.01 (3H, d; 5.9), 0.93 (3H, d; 5.7), 0.85 (3H, t; 7.2).

L-FDLA + (2*R*, 3*R*)-3-Amino-2-methyloctanoic Acid (1.60). ^{1}H NMR (acteone-d_6, 500 MHz) δ_H (integration, multiplicity; *J* in Hz) 9.11 (1H, s), 8.91 (1H, d; 8.9), 8.61 (1H, d; 6.3), 7.54 (1H, br s), 6.73 (1H, br s), 6.11 (1H, s), 4.26 (1H, m), 3.98 (1H, m), 2.93 (1H, m), 1.89 (2H, m), 1.68 (1H, m), 1.44 (2H, m), 1.31 (6H, m), 1.20 (3H, d; 7.3), 1.02 (3H, d; 6.2), 0.94 (3H, d; 6.1), 0.85 (3H, t; 7.9).

D-FDLA + (2*S*, 3*R*)-3-Amino-2-methyloctanoic Acid (1.60). ^{1}H NMR (acteone-d_6, 500 MHz) δ_H (integration, multiplicity; *J* in Hz) 9.10 (1H, s), 8.54 (1H, d; 8.9), 8.52 (1H, d; 5.5), 7.71 (1H, br s), 6.64 (1H, br s), 6.20 (1H, s), 4.35 (1H, m), 4.25 (1H, m), 2.92 (1H, m), 1.84 (2H, m), 1.68 (1H, m), 1.40 (2H, m), 1.30 (6H, m), 1.23 (3H, d; 7.0), 1.02 (3H, d; 6.0), 0.94 (3H, d; 6.2), 0.83 (3H, t; 7.0).

L-FDLA + (2*S*,3*R*)-3-Amino-2-methyloctanoic Acid (1.60). ^{1}H NMR (acteone-d_6, 500 MHz) δ_H (integration, multiplicity; *J* in Hz) 9.11 (1H, s), 8.93 (1H, d; 9.2), 8.55 (1H, d; 6.4), 7.55 (1H, br s), 6.63 (1H, br s), 6.11 (1H, s), 4.30 (1H, m), 4.11 (1H, m), 2.85 (1H, m), 1.86 (2H, m), 1.70 (1H, m), 1.47 (2H, m), 1.27 (6H, m), 1.22 (3H, d; 7.1), 1.04 (3H, d; 5.7), 0.95 (3H, d; 5.9), 0.85 (3H, t; 8.0).

1.5.5.4 Standards for Lyngbyastatin 3 (1.63).

Synthesis of 3-Amino-2-methylhexanoic Acid Standards: (3*R*,7*R*)-Ethyl-*N*-(α-methylbenzyl benzyl)-3-aminohexanoate (1.78). A solution of (*R*)-(+)-*N*-benzyl-*N*-α-methylbenzylamine (3.2 mmol) in THF (10 mL) was cooled to -78 °C prior to the slow addition of *n*-BuLi (3.0 mmol). The resulting pink solution was stirred for 30 min before the slow addition of ethyl *trans* 2-hexenoate (2 mmol) in 2 mL of THF. After the solution was stirred for 2 h at -78 °C, the reaction was quenched with saturated aqueous NH_4Cl. The solution was warmed to room temperature and partitioned between diethyl ether and

water. Chromatography of the organic residue on silica with petroleum ether (bp 40-60 °C) and diethyl ether (20:1) resulted in 504 mg (50 %) of **1.78**.

(2*SR*,3*R*,7*R*)-Ethyl-*N*-(α-methylbenzyl benzyl)-3-amino-2-methylhexanoate (1.79). A solution of **1.78** (0.3 mmol) in 2 mL of THF was added dropwise to a solution of KHMDS (0.5 mmol) in 10 mL of THF. The reaction mixture was stirred for 1 h before the addition of neat iodomethane (5 mmol). The mixture was warmed to room temperature over 16 h and then partitioned between diethyl ether and water to afford the crude product (52 mg, 50 %) as a 3:1 *anti*:*syn* mixture of C-2 diastereomers that was used without further purification.

(2*SR*,3*R*)-3-Amino-2-methylhexanoic Acid Hydrochloride (1.80). To the C-2 epimeric mixture of **1.79** (25 mg total) in 6 mL of glacial acetic acid was added 14 mg of 20 % Pd/C. After 16 h under approximately 5 atm of H_2 the mixture was filtered through a pad of celite and the solvent removed under N_2. Half of this sample was dissolved in 6 N HCl and refluxed for 18 h at 118 °C to yield 5.1 mg of **1.80** (100 %).

Synthesis of (4*S*,3*RS*)-4-Amino-3-hydroxy-2,2,dimethylpentanoic Acid. (4*S*)-Benzyl *N*-Boc-4-amino-3-oxo-pentanoate (1.89). This reaction was carried out as described by Bates in the synthesis of dolastatin 11,[136] except that the solution of the enolate of benzyl acetate was stirred for only 5 min before the addition of the acyl imidazole solution. Purification as described afforded **1.89** in a yield of 57 %. ^{1}H NMR ($CDCl_3$, 300 MHz) δ_H (integration, multiplicity; *J* in Hz) 7.38 (5, s), 5.18 (2, s), 5.08 (1, d; 7.0), 4.36 (1, p; 7.0), 3.64 (1, d; -16.0), 3.57 (1, d; -16.0), 1.43 (9, s), 1.32 (3, d; 7.0).

(4*S*)-Benzyl *N*-Boc-4-amino-3-oxo-2,2-dimethylpentanoate (1.90). To a solution of 150 mg of **1.89** in THF with 9 eq. MeI was added 1 eq. of NaH (65 %

dispersion). The solution was stirred for 1 h before the addition of one more equivalent of NaH and 9 more equivalents of MeI. After 16 h, 100 mL of diethyl ether was added and the mixture was sequentially partitioned with sodium thiosulfate and brine. The organic layer was dried over $MgSO_4$ and rotovaped to dryness. Purification over silica with 6:1 hexane:EtOAc yielded 60 mg (53 %) of (4*S*)-*N*-Boc-2,2,4-trimethyl-3-oxo-γ-lactam (**1.91**) followed by 33 mg of **1.90** (20 %). ^{1}H NMR ($CDCl_3$, 300 MHz) δ_H (integration, multiplicity; *J* in Hz) 7.33 (5, m), 5.15 (2, s), 4.89 (1, d; 7.9), 4.63 (1, p; 7.9), 1.59 (3, s), 1.44 (3, s), 1.41 (9, s), 1.18 (3, d; 7.9); **1.91**: ^{1}H NMR ($CDCl_3$) δ_H (integration, multiplicity; *J* in Hz) 4.35 (1, q; 6.9),1.56 (9, s), 1.52 (3, d; 7.0), 1.30 (3, s), 1.28 (3, s).

(4*S*,3*SR*)-Benzyl *N*-Boc-4-amino-3-hydroxy-2,2-dimethylpentanoate (1.92). A solution of **1.90** (33 mg) in methanol was added to 4 eq. of $NaBH_4$ at 0 °C. The mixture was stirred for 30 min until TLC gave a negative result with to treatment 2,4-dinitrophenylhydrazine, and then quenched with 1 N HCl. It was subsequently partitioned between EtOAc and brine, and concentrated to dryness to yield 20 mg (62 %) of **1.92.**

(4*S*,3*SR*)-4-Amino-3-hydroxy-2,2-dimethylpentanoic Acid (1.93). The benzyl group of **1.92** (20 mg) was removed by hydrogenation over 30 % Pd/C in methanol at room temperature over 12 h. The suspension was filtrered through celite and evaporated to dryness. The residue was dissolved in TFA for 15 min before removing the acid under a stream of nitrogen to afford 6 mg (68 %) of **1.93**. The ^{1}H NMR of the major diastereomer in the mixture: (MeOH-d_4, 300 MHz) δ_H (integration, multiplicity; *J* in Hz) 3.85 (1, d; 1.8), 3.51 (1, qd; 6.0, 1.8), 1.25 (3, s),[165] 1.24 (3, d; 6.0), 1.18 (3, s) and the minor diastereomer: 3.67 (0.67, d; 5.6), 3.39 (0.68, qd; 6.5, 5.6), 1.30 (2, s), 1.27 (2, s), 1.24 (2, d; 6.5).[26]

1.5.6 Degradations of Natural Products.

Saponification of Micromide B (1.10). To 0.5 mg of **1.9** was added 5 eq. of $Ba(OH)_2$ in 0.5 mL of methanol. The solution was stirred at room temperature overnight. The next day, after removing the solvent, the residue was resuspended in 0.2 mL of water and the pH adjusted to 2 with cold 1 % H_2SO_4. The barium sulfate which precipitated was filtered and the solvent removed to yield **1.10**. ^{1}H NMR values were determined by 1D TOCSY experiments on the 3,4-dihydroxy-2-methylpentanoic acid unit (CD_3CN, 500 MHz) δ_H (position, multiplicity; *J* in Hz) 4.09 (γ-methine, dq; 7.7, 6.2), 3.60 (β-methine, dd; 9.5, 7.7), 2.52 (α-methine, dq; 9.5, 7.2), 1.35 (δ-methyl, d; 6.2), and 1.18 (α-methyl, d; 7.2).

Dihydro-majusculamide C (1.81). A solution of 2 mg of **1.66** in 0.2 mL of methanol was added to 4 mg of $NaBH_4$. After stirring 25 min, another aliquot of $NaBH_4$ was added and the solution stirred for another 25 min before quenching with 1 N HCl. The mixture was partitioned between ethyl acetate and water and the combined organic residue purified by C_{18} HPLC [Phenomenex Ultracarb 30, 250 x 10 mm, 60 % aqueous CH_3CN, 3 mL/min, detection at 220 nm] to afford a single product (**1.81**, t_R 39 min) with no sign of **1.66** (t_R 50 min). ^{13}C NMR ($CDCl_3$, 500 MHz) δ_C 176.7, 173.4, 172.4, 170.50, 170.45, 170.0, 169.8, 169.7, 167.7, 158.6, 130.4, 128.7, 114.2, 80.3,[166] 77.9, 61.4, 61.0, 58.0, 55.3, 50.2, 47.5, 45.2, 44.4, 42.3, [166] 41.3, [166] 40.5, 37.5, 35.2, 32.7, 29.9, 29.5, 29.3, 27.1, 26.8, 25.6, 24.7, 23.6, 22.4, 18.33, 18.26, 15.48, 15.44, 14.6, 13.8, 11.7, 10.9, 10.7, 8.9; HR-MALDI *m/z* 1009.5991 [calcd for $C_{50}H_{82}N_8O_{12}Na$ 1009.5944, 4.7 mDa error].

Dihydro-lyngbyastatin 3 (1.82, 1.83). A sample of **1.63** (6 mg) was reduced as described for **1.66** and purified by C_{18} HPLC (62 % CH_3CN) to afford the minor (**1.82**, t_R

31 min) and the major reduction products (**1.83**, t_R 37 min) in a ratio of 1:2. **1.82**: HR-MALDI *m/z* 1037.6273 [calcd for $C_{52}H_{86}N_8O_{12}Na$ 1037.6257, 1.6 mDa error]. **1.83**: ^1H and ^{13}C NMR, see Table 23; HR-MALDI *m/z* 1037.6310 [calcd for $C_{52}H_{86}N_8O_{12}Na$ 1037.6257, 5.3 mDa error].

Dihydro-lyngbyastatin 1 (1.84, 1.85). A sample of **1.64** (4 mg) was reduced as described for **1.66** and purified by HPLC to afford the minor (**1.84**, t_R 37 min) and major reduction products (**1.85**, t_R 45 min) in a ratio of 1:4. **1.84**:[167] HR-MALDI *m/z* 1023.6057 [calcd for $C_{51}H_{84}N_8O_{12}Na$ 1023.6101, 4.4 mDa error]. **1.85**:[167] HR-MALDI *m/z* 1023.6078 [calcd for $C_{51}H_{84}N_8O_{12}Na$ 1023.6101, 2.3 mDa error].

Dihydro-dolastatin 12 (1.86, 1.87). A sample of **1.65** (4 mg) was reduced as described for **1.66** and purified by HPLC to afford the minor (**1.86**, t_R 44 min) and the major reduction products (**1.87**, t_R 55 min) in a ratio of 1:4. **1.86**:[167] HR-MALDI *m/z* 993.6040 [calcd for $C_{50}H_{82}N_8O_{11}Na$ 993.5995, 4.5 mDa error]. **1.87**: ^1H NMR, ^{13}C NMR, ^1H-^1H COSY, and HMBC data, see Table 24; HR-MALDI *m/z* 993.5944 [calcd for $C_{50}H_{82}N_8O_{11}Na$ 993.5995, 5.1 mDa error].

1.5.7 Determination of the Absolute Stereochemistry

The absolute configurations of the α-amino and α-hydroxy acid-derived units were determined by chiral HPLC analyses of the acid hydrolyzates by comparing the retention times of the components of the hydrolyzates with authentic standards. To liberate amino acids where the carboxy terminus was incorporated into a thiazole ring, ozonolysis was performed prior to acid hydrolysis. To liberate the γ-stereocenter in γ-amino-β-hydroxyacids, the acid hydrolyzate was ozonized and subjected to oxidative workup. The stereochemistry of the α-methyl-β-amino acids was determined by

advanced Marfey analyses.[128] The stereochemistry of the secondary alcohols was elucidated through their MPA derivatives.[46] The solvents for the chiral HPLC were as follows: Solvent A = 85:15 2 mM aqueous $CuSO_4$:CH_3CN; Solvent B = 90:10 2 aqueous mM $CuSO_4$:CH_3CN; Solvent C = 95:5 2 aqueous mM $CuSO_4$:CH_3CN; Solvent D = 2 aqueous mM $CuSO_4$; Solvent E = 1 aqueous mM $CuSO_4$; Solvent F = 0.5 aqueous mM $CuSO_4$; Solvent G = 0.25 aqueous mM $CuSO_4$. Acid hydrolysis was carried out with 0.3 mL of 6 N HCl. The specific details are given below using the following format [mg of natural product, temp (°C), time (h)] with the numbers in brackets referring to the acid hydrolysis conditions.

1.5.7.1 Micromide A (1.4)

Ozone was bubbled through a solution of 0.3 mg of **1.4** in 3 mL CH_2Cl_2 for 15 min until a blue color persisted. The solvent was then removed and the residue hydrolyzed [0.3, 118, 24]. After removal of the acid under a stream of N_2, the residue was dissolved in 10 % aqueous methanol and passed over a small C_{18} column. This solution was then analyzed by chiral HPLC [Chirex Phase 3126, flow rate 0.8 mL/min]. The retention times of the amino acid components of the hydrolyzate were L-Val (20.3), *N*-Me-D-Val (19.2), *N*-Me-L-Ile (28.1), *N*-Me-L-Phe (33.4), and L-Phe (41.0), as confirmed by co-injection. The retention times of the standards were L-Val (20.3), D-Val (27.1), *N*-Me-L-Val (14.0), *N*-Me-D-Val (19.2), *N*-Me-L-allo-Ile (27.0), *N*-Me-L-Ile (28.1), *N*-Me-D-Ile (42.0), *N*-Me-D-allo-Ile (42.1), *N*-Me-L-Phe (33.4), *N*-Me-D-Phe (36.2), L-Phe (41.0), and D-Phe (42.5). The solvents were as follows: Solvent A for *N*-Me-Phe; Solvent C for the other standards.

Mandelate Derivatization of the Hydrolyzate of Micromide A (1.4). [0.5, 118, 24] After removal of the acid under a stream of N_2, the residue was dissolved in water and exhaustively extracted with CH_2Cl_2. The organic extracts were combined, dried over $MgSO_4$ and the solvent removed. This residue was then dissolved in 0.1 mL of CH_2Cl_2 and to this was added 1 crystal of DMAP, 1.2 mg methyl D-mandelate in 0.5 mL of CH_2Cl_2, and 0.02 mL of 1 M DCC. After stirring for 3 h, the mixture was purified by HPLC [Bondclone Si, 250 x 10 mm, a linear gradient of 1 to 15 % *i*-PrOH in hexane, flow rate 2 mL/min, PDA detection]. The fraction eluting between 9 and 10 min was then analyzed by HPLC [Phenosphere Silica, 150 x 4.6 mm, 0.5 % *i*-PrOH in hexane, 0.75 mL/min, PDA detection]. The retention times of the derivatized standards were 24.1 and 27.3 min for (*S*)- and (*R*)-3-methoxyhexanoic acid respectively, while the hydrolyzate contained (*R*)-methoxyhexanoate (27.3 min).

1.5.7.2 Micromide B (1.9)

MPA derivatives of 1.9: (*R*)-MPA-1.9. To 0.5 mg of **1.9** in 0.3 mL of CH_2Cl_2 was added 1 crystal of DMAP, 4 mg of (*R*)-methoxyphenylacetic acid, and 4 mg of 1-[3-(dimethylamino)propyl]-3-ethylcarbodiimide hydrochloride. The solution was stirred at room temperature overnight and then quenched with cold 1 N HCl (0.4 mL). The resulting mixture was partitioned between ethyl acetate and water and the organic layer was dried over $MgSO_4$. The organic residue was dissolved in 20 % EtOAc in hexanes and applied to a prepacked silica column (500 mg). (*R*)-MPA-**1.9** eluted in the 40 % EtOAc in hexane fraction (4 mL) after 2 mL of hexane and 2 mL of 25 % EtOAc had passed through the column. ^1H NMR ($CDCl_3$) δ_H (position, multiplicity; *J* in Hz) 7.47 to 7.37 (Ph-MPA), 5.29 (NH, t; 6.2), 5.31 (H-3, ddd, 6.4, 3.7, 1.5), 5.15 (H-7, dd; 7.1, 5.6), 4.93

(H-8, qd; 6.6, 5.6), 4.78 (α-MPA, s), 3.65 (H-22, s), 3.45 (H-3_L, ddd; -13.9, 6.2, 3.7), 3.25 (H-3_H, dt; -13.9, 6.2), 3.42 (OMe-MPA, s), 2.60 (H-2, d; 1.5), 2.26 (H-11, t; 7.5), 2.18 (H-6, p; 7.1), 2.08 (H-25, s), 1.51 (H-12, m), 1.28 (H-13 to H-20, m), 1.15 (H-9, d; 6.6), 0.98 (H-23, d; 7.1), 0.88 (H-21, t; 6.9).

(*S*)-MPA-1.9. This derivative was prepared in the same manner as (*R*)-MPA-**1.9** except using (*S*)-methoxyphenylacetic acid. ^{1}H NMR ($CDCl_3$) δ_H (position, multiplicity; *J* in Hz) 7.44 to 7.32 (Ph-MPA), 6.01 (NH, t; 6.4), 5.31 (H-3, ddd; 6.4, 4.4, 1.2), 5.24 (H-7, dd; 7.1, 4.7), 4.98 (H-8, qd; 6.5, 5.5), 4.79 (α-MPA, s), 3.55 (H-3_L, ddd; -13.4, 6.4, 4.4), 3.47 (H-3_H, dt; -13.4, 6.4), 3.42 (OMe-MPA, s), 3.40 (H-22, s), 2.53 (H-2, d; 1.2), 2.43 (H-6, p; 7.1), 2.27 (H-11, t; 7.4), 2.10 (H-25, s), 1.51 (H-12, m), 1.28 (H-13 to H-20, m), 1.20 (H-9, d; 6.6), 1.10 (H-23, d; 7.1), 0.88 (H-21, t; 6.5).

1.5.7.3 Tasiamide A (1.11)

[0.3, 118, 16] The amino acids in the hydrolyzate were determined by analysis on the CHIRALPAK MA(+) column [flow rate 0.8 mL/min], except for *N*-Me-Glu which was detected on the Chirex Phase 3126 (D) [flow rate 0.8 mL/min]. The retention times (t_R, min) of the authentic standards were L-Pro (11.6), D-Pro (6.2), L-Ile (34.8), L-allo-Ile (26.0), D-Ile (16.8), D-allo-Ile (13.5), L-Leu (33.0), D-Leu (15.8), *N*-Me-L-Phe (32.2), *N*-Me-D-Phe (26.1), L-2-hydroxy-3-methylvaleric acid (65.3), L-allo-2-hydroxy-3-methylvaleric acid (52.8), D-2-hydroxy-3-methylvaleric acid (40.1), D-allo-2-hydroxy-3-methylvaleric acid (33.8), *N*-Me-L-Glu (48.2), and *N*-Me-D-Glu (22.9). The retention times of the amino acid components of the hydrolyzate were L-Pro (11.6), L-Leu (33.0), L-Ile (34.8), *N*-Me-D-Phe (26.1), *N*-Me-L-Glu (48.2), and L-2-hydroxy-3-methylvaleric

acid (65.3). The solvents were as follows: Solvent A for 2-hydroxy-3-methylvaleric acid; Solvent B for *N*-Me-Phe, *N*-Me-Glu; Solvent D for Leu, Ile and Pro.

1.5.7.4 Tasiamide B (1.12)

[0.3, 118, 24] The residue from the acid hydrolyzate was suspended in 10 mL of methanol and ozone was bubbled through the solution for 2 h. The solvent was then removed. The hydrolyzate was dissolved in a 2:1 mixture of concentrated formic acid and 30 % H_2O_2, stirred overnight, and then refluxed for 1 h at 80 °C. Analysis by chiral HPLC [Chirex Phase 3126 (+), flow rate 0.8 mL/min] established stereocenters derived from L-Asp (11.9), L-Ala (20.1), L-Pro (28.3), L-Leu (32.5), L-Val (37.8), *N*-Me-L-Phe (38.2), L-lactic acid (46.5), and *N*-Me-L-Glu (73.0). The retention times of the enantiomers not present in the hydrolyzate were D-Asp (15.1), D-Ala (29.0), D-Pro (60.2), D-Leu (36.8), D-Val (64.3), *N*-Me-D-Phe (42.0), D-lactic acid (62.4), and *N*-Me-D-Glu (36.2). The solvents were as follows: Solvent A for *N*-Me-Phe; Solvent B for Leu, *N*-Me-Glu; Solvent C for Asp; Solvent D for Pro, Val, and lactic acid; Solvent G for Ala.

1.5.7.5 Tasipeptins A (1.13) and B (1.14).

To 0.3 mg of **1.13** in 0.1 mL of CH_2Cl_2 was added 2 mL of dry CH_2Cl_2 containing 2 mg of pyridinium chlorochromate. The reaction was stirred overnight before being partitioned between methylene chloride and water. The organic layer was removed under a stream of N_2 and sample hydrolyzed [0.3, 118, 18]. The hydrolyzate was analyzed by chiral HPLC [Chirex Phase 3126 (D), flow rate 0.8 mL/min]. The retention times of the standards were L-Thr (12.0), L-allo-Thr (14.9), D-Thr (15.0), D-allo-Thr (20.0), L-Val (21.8), D-Val (30.2), L-Leu (61.5), D-Leu (80.2), L-Glu (83.3), D-Glu (93.4), *N*-Me-L-Phe (38.1), and *N*-Me-D-Phe (40.6). The retention times of the components of the hydrolyzate

of **1.13** were L-Thr (12.0), L-Val (21.8), L-Leu (61.5), L-Glu (83.3), and *N*-Me-L-Phe (38.1). The acid hydrolyzate of **1.14** after PCC oxidation as described above was found to contain L-Thr (12.0), L-Val (21.8), L-Leu (61.5), L-Glu (83.3), and *N*-Me-L-Phe (38.1). The solvents were as follows: Solvent D for Thr; Solvent C for Val, Leu and Glu; Solvent A for *N*-Me-Phe.

1.5.7.6 Tasihalides A (1.15) and B (1.16)

To 0.7 mg of tasihalide A (**1.15**) was dissolved in 0.2 N NaOMe and stirred at room temperature for 48 h. The mixture was then quenched with cold 1 N HCl and the solvent removed under a stream of nitrogen to yield **1.17**.

The residue was then dissolved in 2 mL of pyridine and added to a vial containing 4 mg of anisoyl chloride and 1 mg of dimethylaminopyridine. The resulting mixture was stirred at room temperature for 2 days and then quenched with 0.1 mL of 3-(dimethylamino)propylamine. After the solvent was removed, then residue was applied to a 500 mg prepack silica column and eluted with increasing amount of ethyl acetate in hexane. The 100 % hexane and 20 % EtOAc in hexane fractions were subsequently purified by normal phase HPLC [Bondclone, 300 x 7.80 mm, 10 min at 10% *i*-PrOH in hexane and then a linear gradient to 50% over the next 30 min, flow rate 2.5 mL/min, PDA detection]. The recovered starting material **1.17** eluted at 21.4 min.

A second attempt following the same procedure as above except for heating the reaction mixture to 70 °C for 2 days, resulting in recovered **1.17** after purification as described.

1.5.7.7 15-Norlyngbyapeptin A (1.36)

A solution of 0.1 mg of **1.36** in CH_2Cl_2 was ozonized at -78 °C for 15 minutes. The solvent was evaporated and the residue hydrolyzed [0.1, 90, 16]. The acid was removed under a stream of nitrogen and the sample passed over a 100 mg C_{18} pre-packed column, eluting with 1 mL of 10 % methanol before analysis by chiral HPLC [Chirex phase 3126 (D), flow rate 0.8 mL/min]. The hydrolyzate contained peaks for L-Pro (13.0), *N*-Me-L-Ile (32.0), *N*-Me-L-Leu (57.2), and *N*-Me-L-Tyr (14). The retention times of the standards were L-Pro (13.0), D-Pro (21.7), *N*-Me-L-allo-Ile (30.4), *N*-Me-L-Ile (32.0), *N*-Me-D-Ile (41.0), *N*-Me-D-allo-Ile (41.1), *N*-Me-L-Leu (57.2), *N*-Me-D-Leu (87.5), *N*-Me-L-Tyr (14), and *N*-Me-D-Tyr (16). The solvents were as follows: Solvent A for *N*-Me-Tyr; Solvent C for the all other amino acids

1.5.7.8 Lyngbyabellin D (1.38)

A solution of 0.1 mg of **1.38** in CH_2Cl_2 was ozonized and saponified as previously described for lyngbyabellin A (**1.39**).[96] The resulting mixture was analyzed by chiral HPLC [CHIRALPAK MA(+), (4.6 x 50 mm), 0.8 mL/min]. The retention times (min) with Solvent C of the α,β-dihydroxy-β-methylpentanoic acid standards (**1.46, 1.47**) prepared by the diastereoselective route were (2*R*,3*R*)-Dhmp (29.2), (2*R*,3*S*)-Dhmp (32.1), (2*S*,3*R*)-Dhmp (42.3), and (2*S*,3*S*)-Dhmp (53.5) in a ratio of approximately 3:1:1:3. The retention times of the standards prepared by asymmetric dihydroxylation with the AD-α and -β mixes were (2*R*,3*S*)-Dhmp (32.1) and (2*S*,3*R*)-Dhmp (42.3), respectively. The base hydrolyzate was found to contain (2*R*,3*S*)-Dhmp (32.1), which was confirmed by co-injection of the appropriate standard. Glyceric acid was determined on the CHIRALPAK MA (+) with solvent F. Commercially available D-glyceric and L-

glyceric acid eluted in 12.0 and 8.6 min, while the hydrolyzate contained a peak for D-glyceric acid at 12.0 min.

A solution of 0.1 mg of lyngbyabellin D (**1.38**) in CH_2Cl_2 was ozonized, the solvent was removed, and the residue hydrolyzed at 118 °C for 24 h in 6 N HCl. The acid was removed under a stream of N_2 and the residue ozonized for 30 min in 2 mL of methanol at -78 °C. After removal of the solvent, the residue was dissolved in 2:1 98 % formic acid: 30 % H_2O_2 and stirred overnight before the solution was refluxed for 1 h at 100 °C.[168] The solvent was removed and the sample eluted over a small C_{18} column with 10 % aqueous methanol. Comparison of authentic standards of L-Val (20.3) and D-Val (34.5) by chiral HPLC [CHIRALPAK MA, flow rate 0.8 mL/min, solvent B] with the components of the hydrolyzate established the presence of L-Val (20.3 min).

1.5.7.9 Obyanamide (1.48)

For analysis, 0.2 mg of **1.48** was dissolved in 1 mL of CH_2Cl_2 and ozonized for 15 minutes. After hydrolysis [0.2, 110, 16] the solvent was evaporated and the sample was passed over a C18 column (100 mg) with 10 % CH_3CN. The mixture was analyzed by Chiral HPLC, comparing the retention times of the components of the hydrolyzate with those of authentic standards [Chirex Phase 3126 (D), flow rate 1 mL/min, except alanine flow rate 0.8 mL/min]. The retention times of the amino acid components of the hydrolyzate were (*S*)-3-aminopentanoic acid (8.0), L-Ala (11.8), L-lactic acid (18.5), *N*-Me-L-Val (20.5) and *N*-Me-L-Phe (28.3).The retention time (t_R, min) of the standards were L-Ala (11.8), D-Ala (16.8), *N*-Me-L-Val (20.5), *N*-Me-D-Val (26.5), L-lactic acid (18.5), D-lactic acid (31.5), *N*-Me-L-Phe (28.3), *N*-Me-D-Phe (29.9), (*S*)-3-aminopentanoic acid (8.0), and (*R*)-3-aminopentanoic acid (13.0). The identities of the

peaks were also confirmed by co-injection. The solvents were as follows: Solvent D for Ala and *N*-Me-Val; Solvent C for lactic acid and 3-aminopentanoic acid; Solvent A for *N*-Me-Phe.

Chiral TLC Analysis on the Hydrolyzate of Obyanamide (1.48). The acid hydrolyzate of **1.48** was subjected to TLC analysis on Chiralplate (Macherey-Nagel) using 1:9 MeOH/CH_2Cl_2 as the developing solvent. With V_2O_5 spray reagent[169] the lactic acid was visualized as an intense blue spot. Authentic L-lactic acid and D-lactic acid had R_f values of 0.63 and 0.60, respectively. The L-lactic acid in the hydrolyzate had an R_f of 0.63.

1.5.7.11 Ulongapeptin (1.55)

Ulongapeptin - Amino Acid-Derived Units. A 0.3 mg sample of **1.55** was dissolved in 0.5 mL of methanol and added to a 1 mL vial along with 1 mg of 30 % Pd/C. The solution was stirred under an atmosphere of H_2 for 18 h at room temperature. The reaction mixture was filtered through a pad of Celite that was flushed with methanol. After removal of the solvent, the residue was hydrolyzed [0.3, 90, 18]. The acid was removed under a stream of nitrogen and the hydrolyzate analyzed by chiral HPLC, comparing the retention times of the components of the hydrolyzate with those of authentic standards [Chirex Phase 3126 (D), flow rate 1 mL/min]. The retention times of the components of the hydrolyzate were L-lactic acid (18.5), L-Val (30.3), *N*-Me-L-Val (23.4), *N*-Me-D-Val (41.8), and *N*-Me-D-Phe (33.5). The retention time of the standards were L-Val (30.3), D-Val (54.5), *N*-Me-L-Val (23.4), *N*-Me-D-Val (41.8), L-lactic acid (18.5), D-lactic acid (31.5), *N*-Me-L-Phe (31.2), and *N*-Me-D-Phe (33.5). The solvents

were as follows: Solvent A for *N*-Me-Phe; Solvent C for lactic acid; Solvent D for the remaining amino acids.

Ulongapeptin - 3-Amino-2-methyloctynoic Acid. The hydrogenated hydrolyzate was derivatized with L-FDLA by the standard procedure[128] and compared with the derivatized synthetic standards. The analysis was carried out by RP-HPLC [YMC-Pack AQ-ODS 10 x 250 mm, 50 % MeCN in 0.01 N TFA, flow rate 2.5 mL/min, PDA detection]. The retention times (min) of the L-FDLA derivatized standards were (2*R*,3*S*)-**1.60** (25.7), (2*S*,3*S*)-**1.60** (26.7), (2*R*,3*R*)-**1.60** (45.6), and (2*S*,3*R*)-**1.60** (54.1)[170] with the retention times of L-FDLA+(2*R*,3*S*)-**1.60** and L-FDLA-(2*S*,3*S*)-**1.60** being inferred from the retention times of D-FDLA+(2*S*,3*R*)-**1.60** and D-FDLA+(2*S*,3*S*)-**1.60** respectively. The retention time of the β-amino acid in the hydrolyzate was 26.7 min (2*S*,3*S*), which was confirmed by co-injection of (2*S*, 3*S*)-**1.60**. The previously identified amino acids appeared at 12.0 (L-Val), 15.1 (*N*-Me-L-Val), and 20.5 minutes (N-Me-D-Val).

1.5.7.12 Palau'amide (1.61)

[0.3, 90, 16] The amino acid components of the hydrolyzate were analyzed by chiral HPLC [Chiral Phase 3126 (D), flow rate 0.8 mL/min]. The hydroxy acid was analyzed on the CHIRALPAK MA(+) column [flow rate 0.7 mL/min]. The retention times of the amino acids in the hydrolyzate were L-Ala (14.8), *N*-Me-L-Ala (18.2), D-2-hydroxyisocaproic acid (28.4), L-Ile (54.5), and *N*-Me-D-Phe (57.3). The retention times of the standards not present in the hydrolyzate were D-Ala (19.2), *N*-Me-D-Ala (21.2), L-2-hydroxyisocaproic acid (35.8), L-allo-Ile (38.2), D-allo-Ile (58.0), D-Ile (76.2), and *N*-Me-L-Phe (49.5). The solvents were as follows: Solvent E for *N*-Me-Ala and Ala; Solvent C for Ile; Solvent A for the remaining standards.

1.5.7.13 Lyngbyastatin 3 (1.63)

Chiral GC/MS Analysis of Lyngbyastatin 3 (1.63). [1, 118, 18] The acid was removed under N_2 and the dry hydrolyzate was treated at 100 °C for 45 min with a mixture of 0.3 mL of 2-propanol and 50 μL of acetyl chloride. The excess reagent was removed under N_2 and the residue treated at 100 °C for 15 min with 50 μL of a 1:1 solution of $(CF_3CF_2\ CO)_2O/CH_2Cl_2$. After the mixture had cooled to room temperature, the excess reagent was removed and the resulting mixture of isopropyl esters and *N*-(pentafluropropionyl) amino acids was dissolved in 50 μL of MeOH and analyzed by GC-MS [Chirasil-Val column, 25 μm x 0.25 m, Alltech; 12 psi initial pressure, temperature gradient of 40 to 120 °C with a heating rate of 3 °C/min]. Derivatized (2*S*,3*R*)-3-amino-2-methylpentanoic acid (**1.68**) had a t_R of 18.6 min: *m/z* (intensity) 319 (5), 290 (25), 260 (42), 248 (40), 230 (50), 204 (100). Lyngbyastatin 3 (**1.63**) showed derivatized 3-amino-2-methylhexanoic acid (**1.69**) with a t_R of 21.0 min: *m/z* (intensity) 333 (2), 290 (20), 274 (45), 248 (38), 230 (40), 218 (85), 204 (70), 176 (80).

Absolute Stereochemistry of the Amino Acid-derived Units. [0.5, 90, 24] The hydrolyzate was analyzed by chiral HPLC and the retention times compared with authentic standards ([Chirex Phase 3126 (D), flow rate 0.8 mL/min] except 2-hydroxy-3-methylvaleric acid which was determined on the CHIRALPAK MA(+) [flow rate 0.8 mL/min]). The retention times of the amino acid components of the hydrolyzate were Gly (7.1), *N*-Me-L-Ala (9.0), *N*-Me-L-Val (14.1), *N*-Me-L-Leu (52.1), L-2-hydroxy-3-methylvaleric acid (66.2), and *N,O*-diMe-L-Tyr (81.5). The retention times of the standards were Gly (7.1), *N*-Me-L-Ala (9.0), *N*-Me-D-Ala (9.8), *N*-Me-L-Val (14.1), *N*-Me-D-Val (19.2), *N*-Me-L-Leu (52.1), *N*-Me-D-Leu (79.0), *N,O*-diMe-L-Tyr (81.5), *N,O*-

diMe-D-Tyr (87.1), D-2-hydroxy-3-methylvaleric acid (40.1), D-allo-2-hydroxy-3-methylvaleric acid (34.1), L-allo-2-hydroxy-3-methylvaleric acid (52.0), and L-2-hydroxy-3-methylvaleric acid (66.2). The solvents were as follows: Solvent A was used for 2-hydroxy-3-methylvaleric acid; Solvent B for *N,O*-diMe-Tyr; Solvent C for the remaining amino acids.

Advanced Marfey Analysis. [1, 118, 16] After removal of the acid, the residue was twice dissolved in 25 % aqueous triethylamine and evaporated to dryness. The hydrolyzate was resuspended in 50 µL of water, and then 20 µL of 1 M $NaHCO_3$ and 50 µL of 1 % FDLA (either the L- or DL-mixture as required) were added. The reaction was maintained at 80 °C for 3 min until the yellow solution turned orange. After cooling to room temperature 20 µL of 1 N HCl was added and the yellow solution was diluted with 810 µL of CH_3CN. A portion of the sample (25 µL) was analyzed by RP-HPLC [Bondclone 10 C_{18}, 300 x 7.80 mm, Phenomenex, a linear gradient of 20 to 80 % CH_3CN with 0.01 M TFA over 50 min, flow rate 3 mL/min, PDA detection]. The retention times of the L-FDLA derivatized amino acids in the hydrolyzate were Gly (21.5), *N*-Me-L-Ala (22.1), *N*-Me-L-Val (25.8), *N,O*-diMe-L-Tyr (26.5), *N*-Me-L-Leu (28.2), and (2*S*,3*R*)-**1.80** (31.2). The retention times of the D-FDLA derivatized amino acids in the DL-mixture were Gly (21.5), *N*-Me-L-Ala (22.9), (2*S*,3*R*)-**1.80** (26.5), *N*-Me-L-Val (29.2), *N,O*-diMe-L-Tyr (30.3), and *N*-Me-L-Leu (30.7). The retention times of L-FDLA-**1.80** were (2*R*,3*R*)-**1.80** (30.3) and (2*S*,3*R*)-**1.80** (31.3), while the D-FDLA derivatized standards were detected at (2*R*,3*R*)-**1.80** (26.7) and (2*S*,3*R*)-**1.80** (27.2).

LC-MS Analysis of the β-Amino Acid. The separations of the L- and DL-FDLA derivatives were performed on a Hydrobond-ODS [100 x 3.0 mm, a linear gradient of 20

to 80 % CH_3CN with 0.01 M TFA over 50 min, flow rate 0.3 mL/min, detection at 342 nm]. The mass spectra were collected in the negative mode and had an ESI voltage of 4.6 kV with the auxiliary and sheath gas pressure set at 5 units and 70 psi, respectively, and the capillary heated to 200 °C. A mass range of *m/z* 438 to 440 was covered. The retention times of L-FDLA derivatized *N*-Me-DL-Leu were 32.3 and 35.3 minutes for the L- and D-derivatized amino acid respectively. The L-FDLA derivatized hydrolyzate of **1.63** gave peaks for *N*-Me-L-Leu (32.3) and (2*S*,3*R*)-**1.80** (35.8), while the DL-FDLA derivatized hydrolyzate gave two additional peaks, (2*S*,3*R*)-**1.80** (30.6) and *N*-Me-L-Leu (35.3).

Marfey Analysis of the Reduction Products. The samples were hydrolyzed for 24 h in 6 N HCl and after removal of the acid the residues were derivatized with L-FDLA before HPLC analyses [YMC-AQ ODS, 250 x 10 mm, a linear gradient of 40 to 50 % aqueous CH_3CN with 0.1 % TFA (pH 4.13) over 60 min, flow rate 2.5 mL/min, PDA detection]. The retention time of L-FDLA-(3*SR*,4*S*)-**1.93** was 20.3 min, while D-FDLA-(3*SR*,4*S*)-**1.93** eluted at 22.6 min. The reduction product (**1.81**) of majusculamide C (**1.66**) contained L-FDLA-(3*SR*,4*S*)-**1.93** (20.3). The minor reduction products **1.82**, **1.84**, and **1.86** derived from **1.63**, **1.64**, and **1.65**, respectively, also contained L-FDLA-(3*SR*,4*S*)-**1.93** (20.3), which was confirmed by co-injection of the appropriate standard and by comparison of the UV spectra. The stereochemistry of Ibu units in the major reduction products **1.83**, **1.85**, and **1.87** were determined by LC-MS due to overlap in the HPLC trace.

LC-MS on the Reduction Products. The separations of the L- and DL-FDLA derivatives were performed on a Hydrobond-ODS [100 x 3.0 mm, a linear gradient of 40

to 50 % CH_3CN with 0.25 % acetic acid over 60 min, flow rate 0.3 mL/min, detection at 342 nm]. The mass spectra were collected in the positive mode and had an ESI voltage of 4.6 kV with the auxiliary and sheath gas pressure set at 5 units and 70 psi, respectively, and the capillary heated to 200 °C. A mass range of *m/z* 455.4 to 456.4 was covered. The retention times of L-FDLA-(3*SR*,4*S*)-**1.93** were 18.2 min. Under this system D-FDLA-(3*R*,4*S*)-**1.93** and D-FDLA-(3*S*,4*S*)-**1.93** were resolved, with the major and minor reduction products eluting at 20.0 and 24.8 min, respectively. While the relative stereochemistry of **1.93** was not conclusively established, reduction of similar γ-amino-β-hydroxyesters generally proceed via a chelation control mechanism to produce the 3*R**,4*S** diastereomer as the major product.[152] The major reduction products **1.83**, **1.85**, and **1.87** contained peaks for D-FDLA-(3*R*,4*S*)-**1.93** (20.0 min) indicating *R* configurations in the Ibu units of these natural products. The minor reduction products (**1.82**, **1.84**) of lyngbyastatin 3 and 1 were also analyzed by LC-MS and contained peaks of the correct mass that co-eluted with L-FDLA-(3*SR*,4*S*)-**1.93** (18.2), confirming the *S* configurations in these natural products.

1.6 APPENDIX: ^{1}H AND ^{13}C NMR SPECTRA

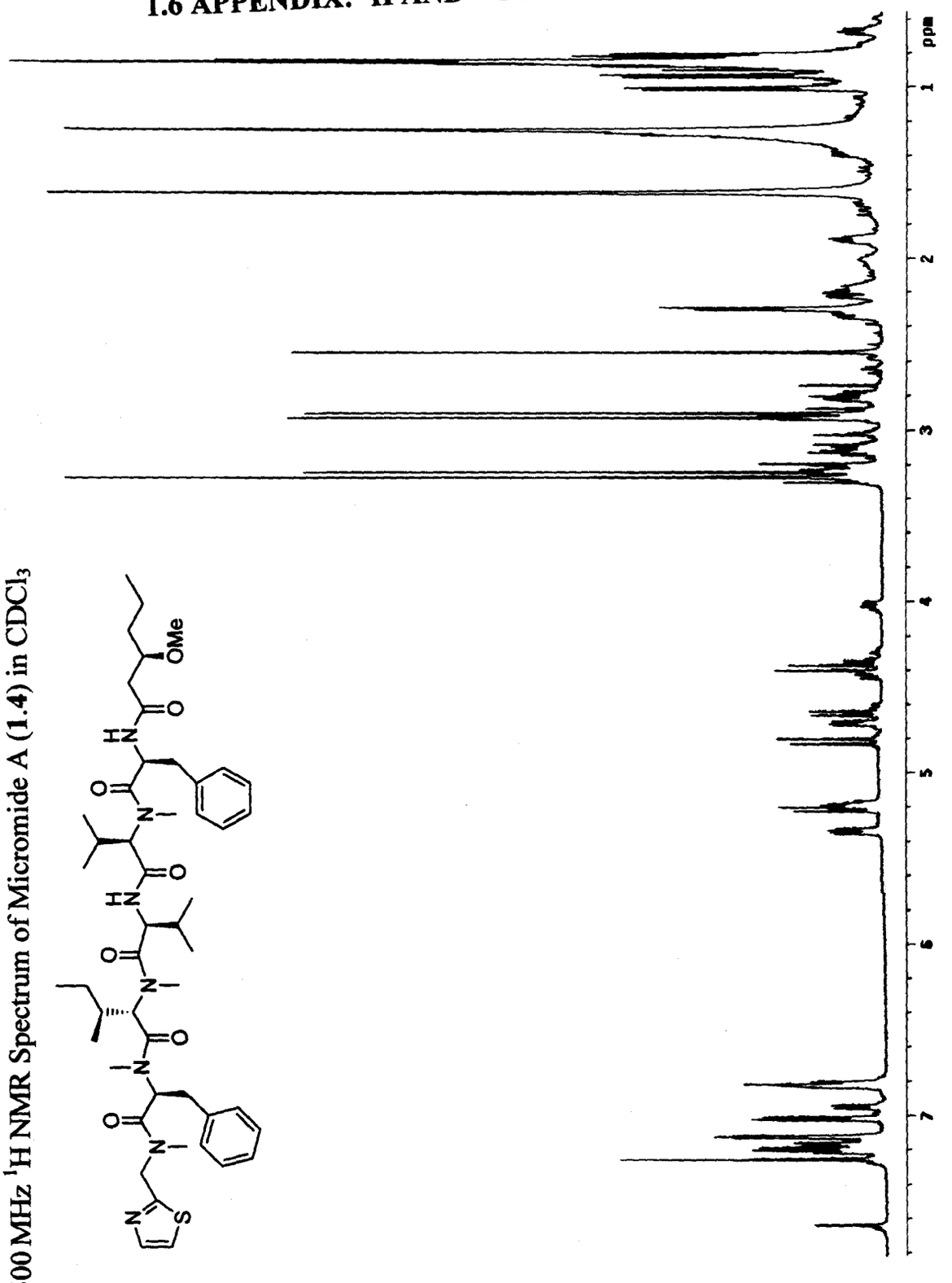

500 MHz ^{1}H NMR Spectrum of Micromide A (**1.4**) in $CDCl_3$

125 MHz ^{13}C NMR Spectrum of Micromide A (**1.4**) in $CDCl_3$

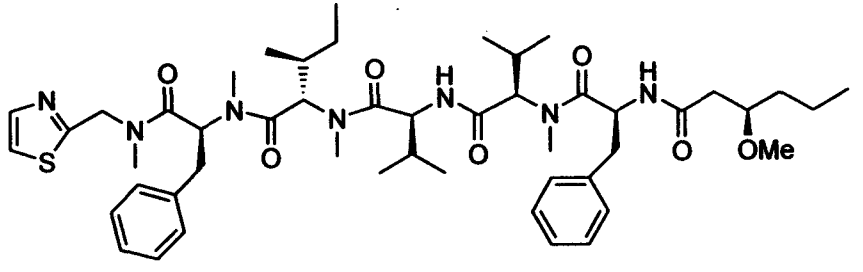

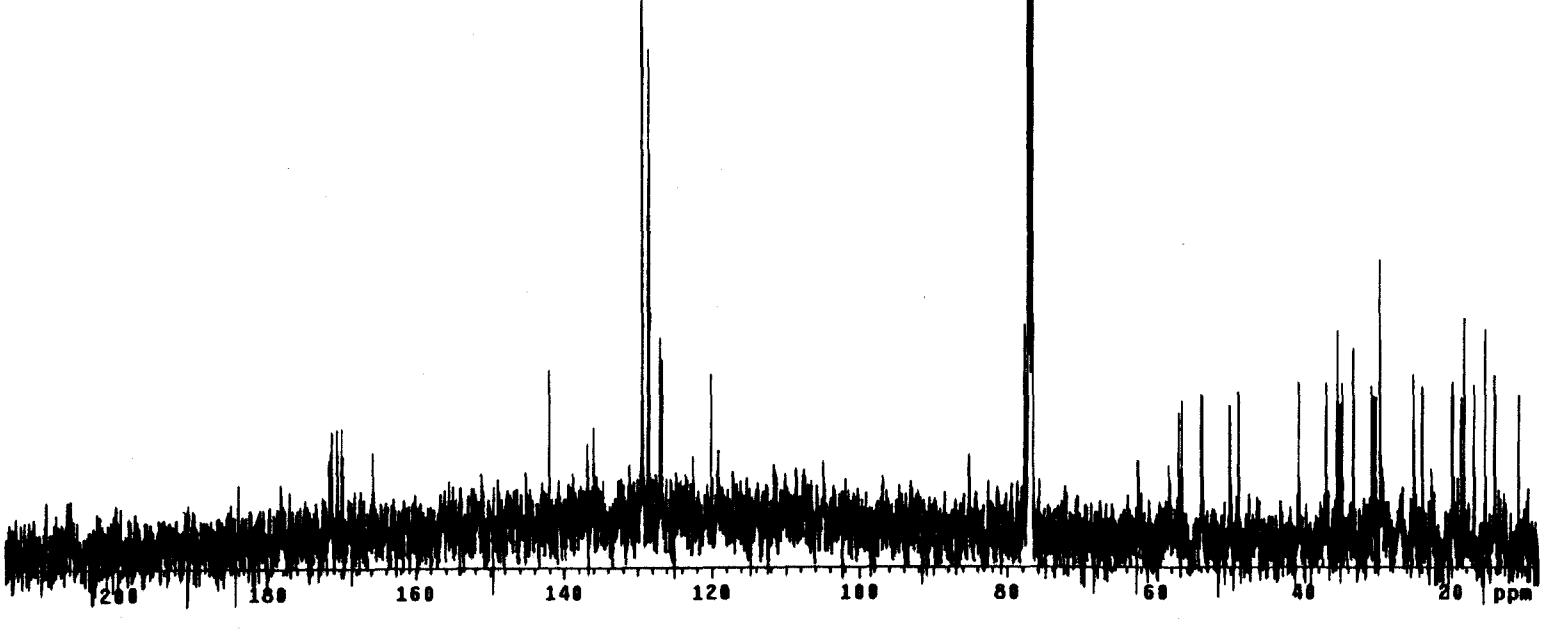

500 MHz ^{1}H NMR Spectrum of Micromide B (**1.11**) in $CDCl_3$

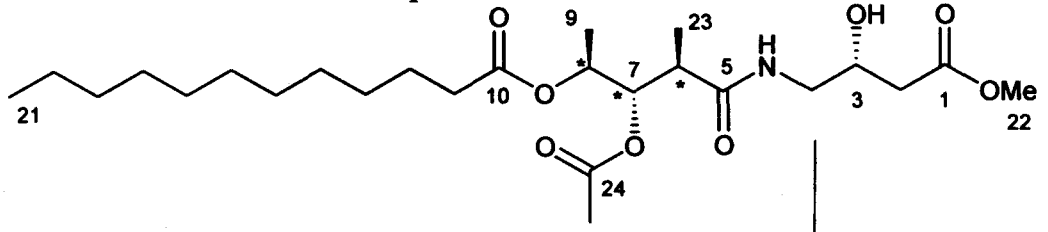

125 MHz ^{13}C NMR Spectrum of Micromide B (**1.9**) in $CDCl_3$

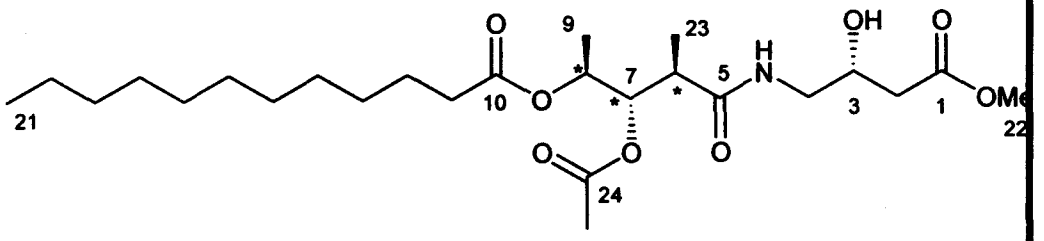

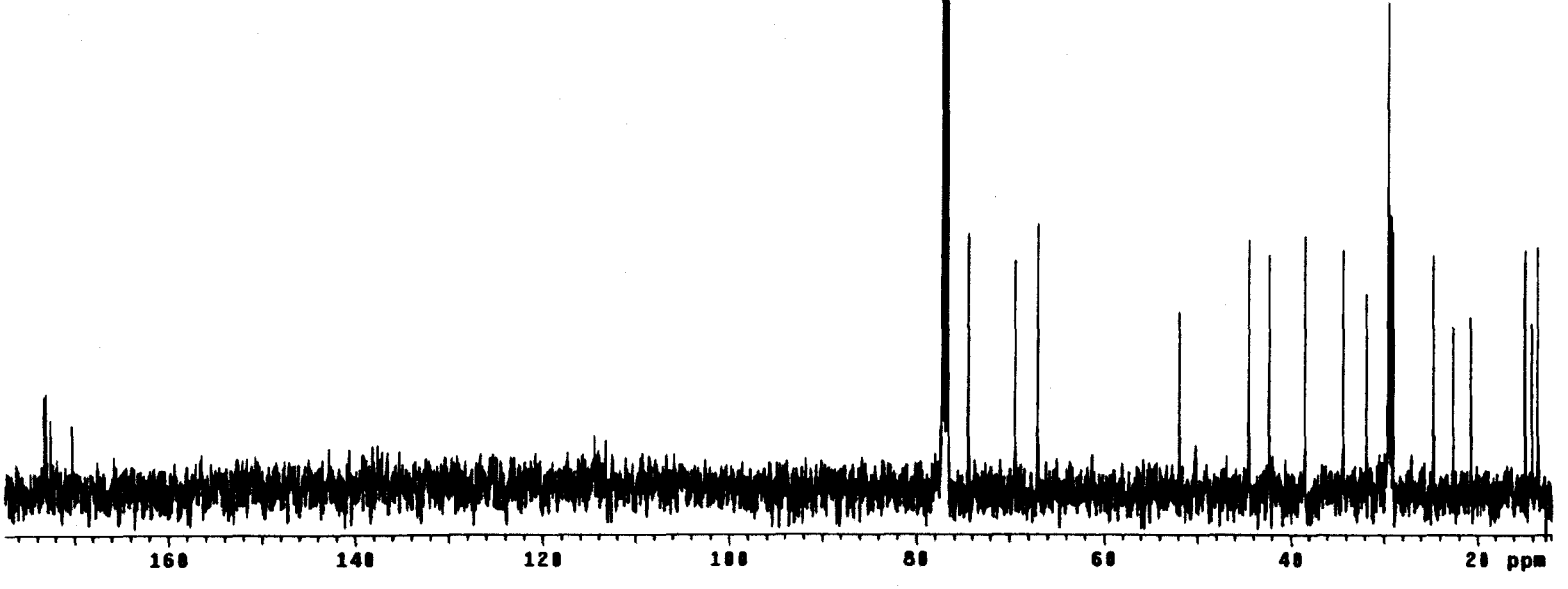

500 MHz ^{1}H NMR Spectra of Tasiamide A (**1.11**) in $CDCl_3$

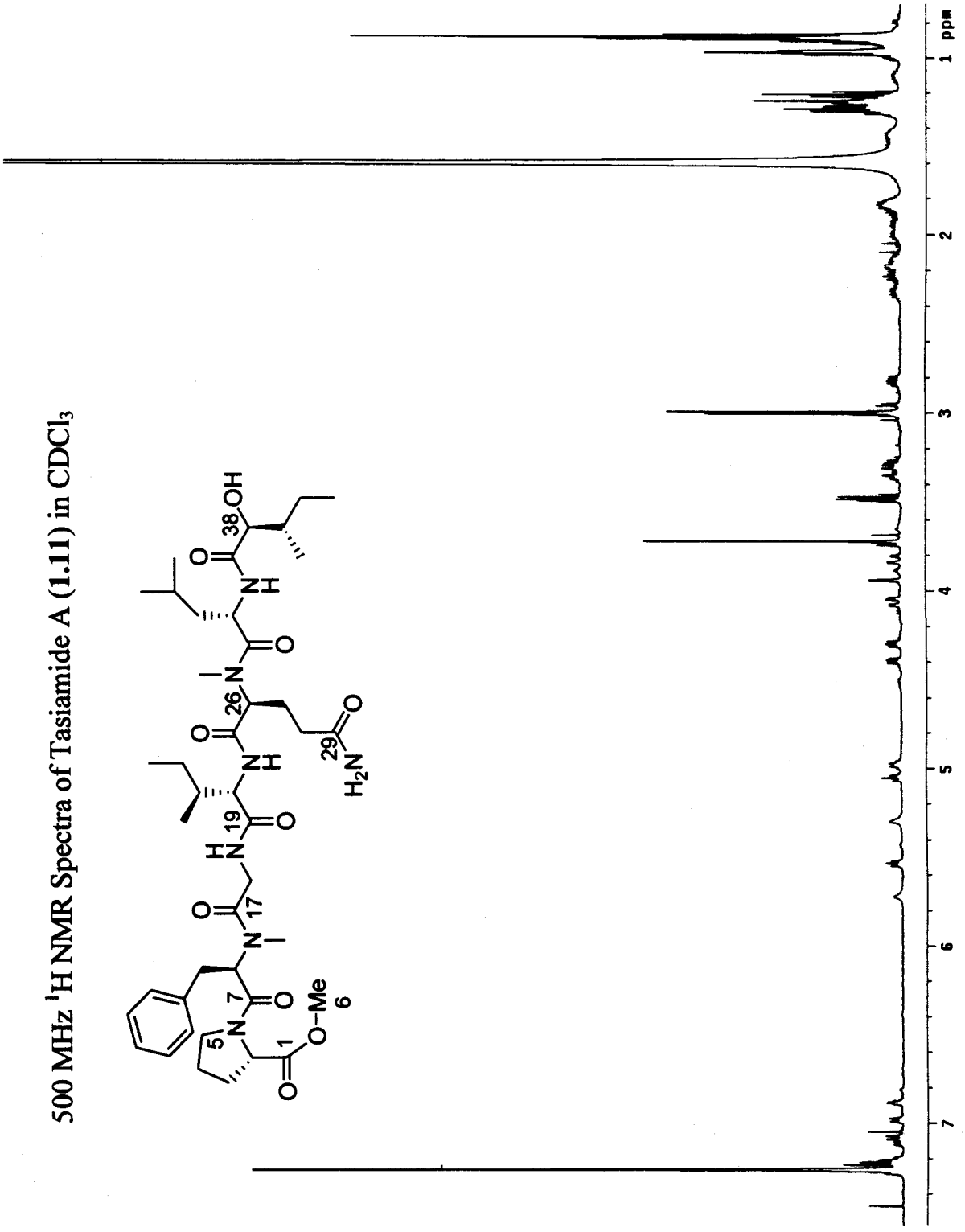

125 MHz ^{13}C NMR Spectrum of Tasiamide A (**1.11**) in $CDCl_3$

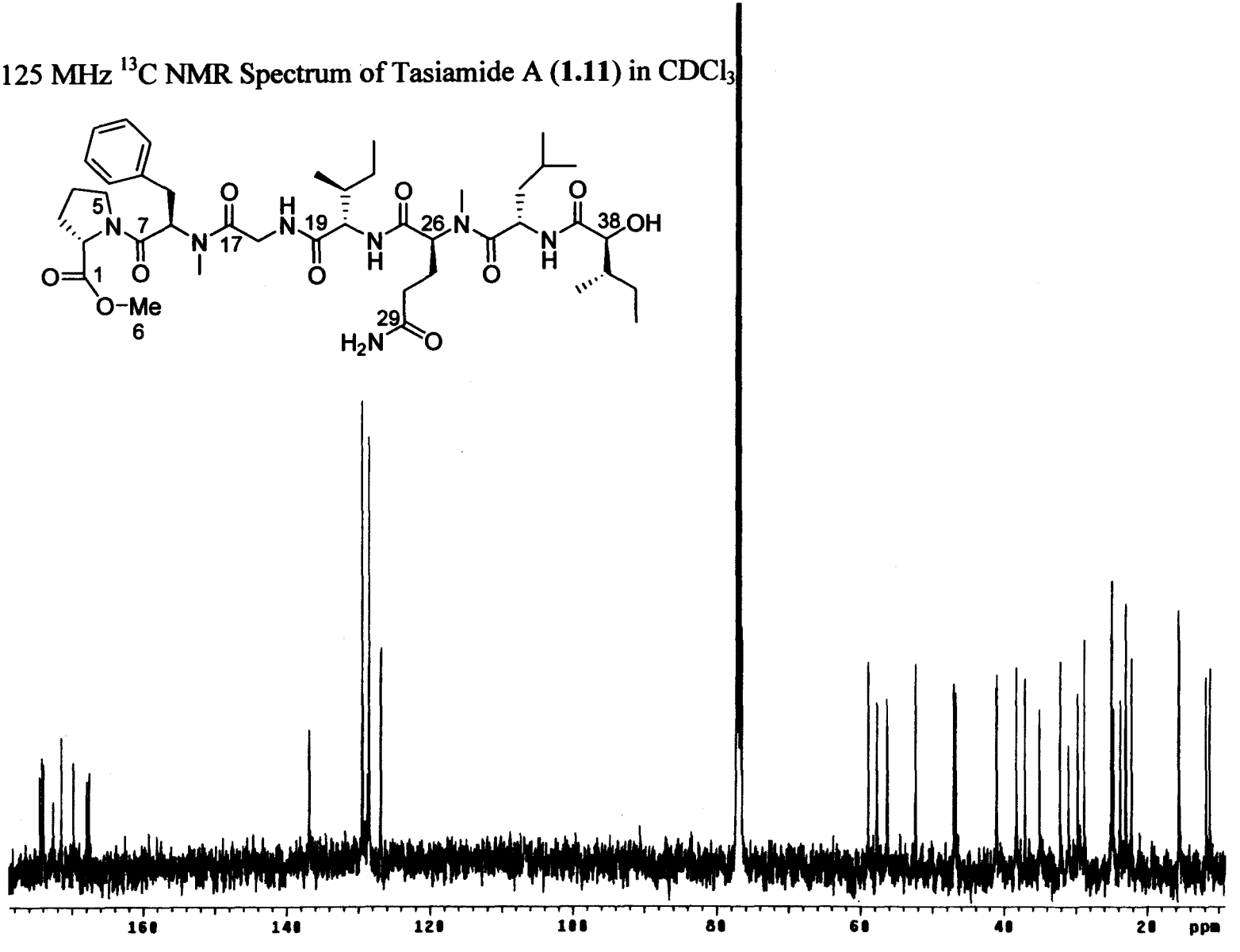

500 MHz ^{1}H NMR Spectrum of Tasiamide B (**1.12**) in $CDCl_3$

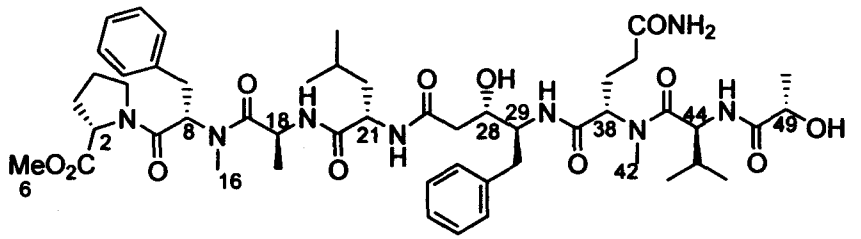

125 MHz ^{13}C NMR Spectrum of Tasiamide B (**1.12**) in $CDCl_3$

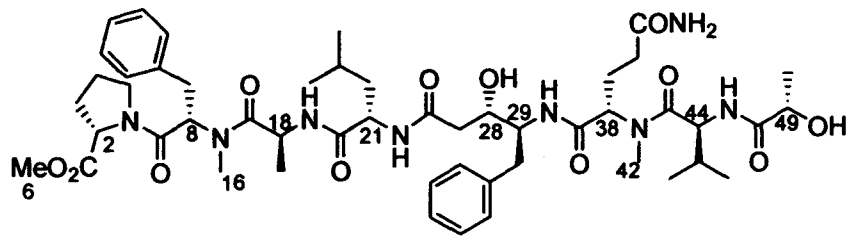

500 MHz ^{1}H NMR Spectrum of Tasipeptin A (**1.13**) in $CDCl_3$

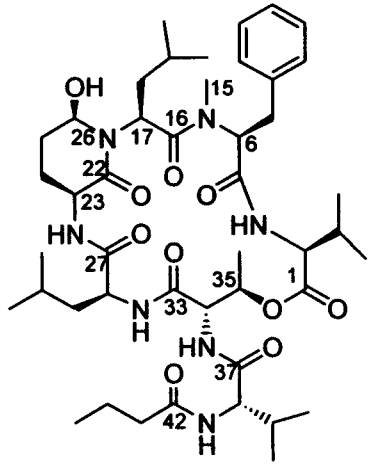

125 MHz ^{13}C NMR Spectrum of Tasipeptin A (**1.13**) in $CDCl_3$

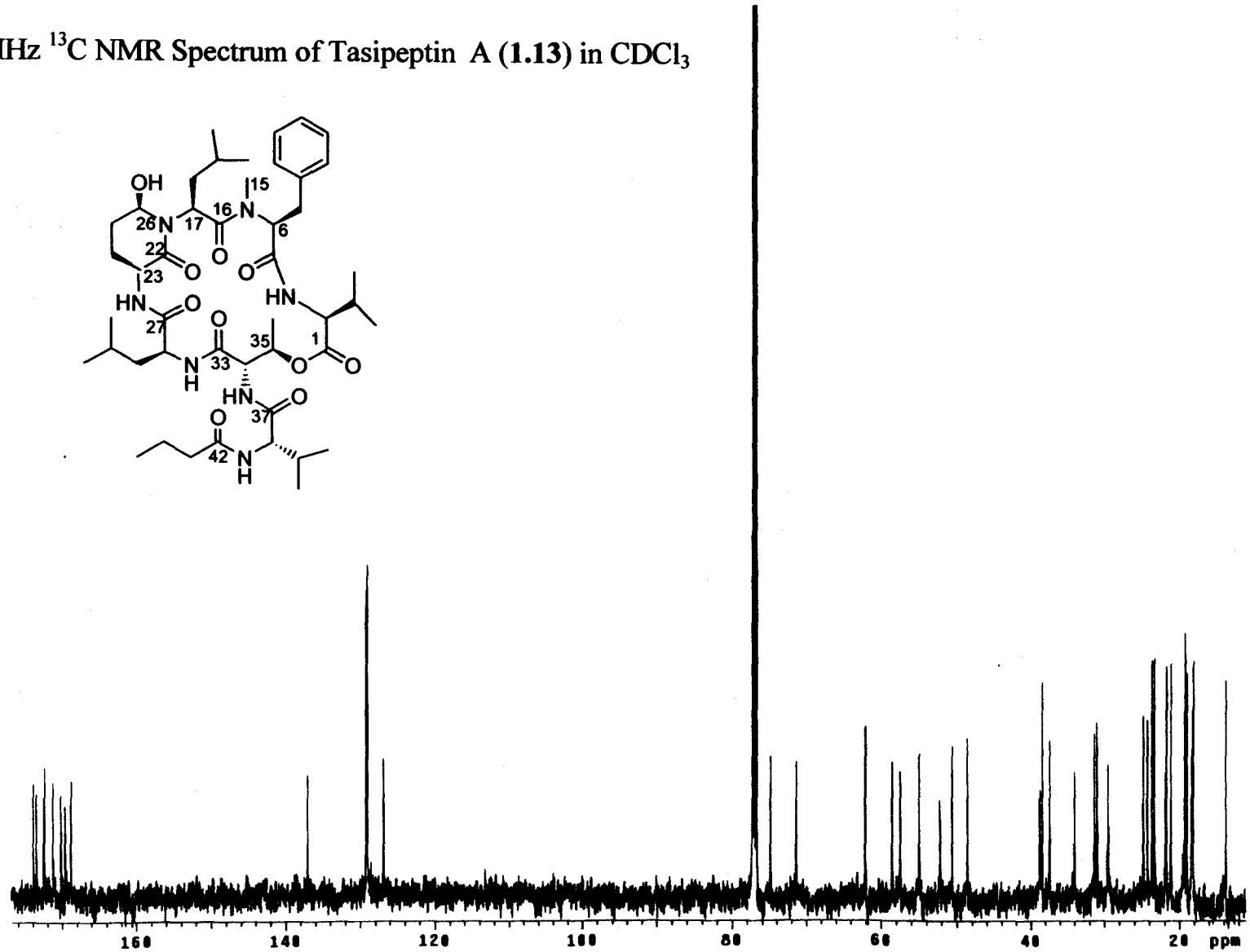

500 MHz ^{1}H NMR Spectrum of Tasipeptin B (**1.14**) in $CDCl_3$

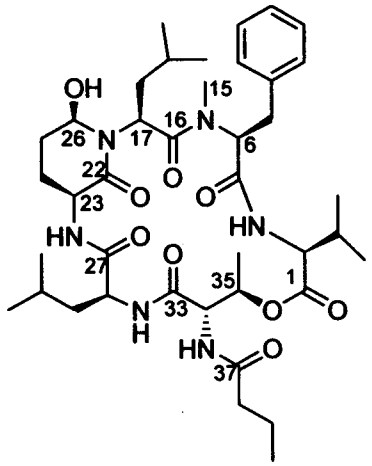

125 MHz ^{13}C NMR Spectrum of Tasiapeptin B (**1.13**) in $CDCl_3$

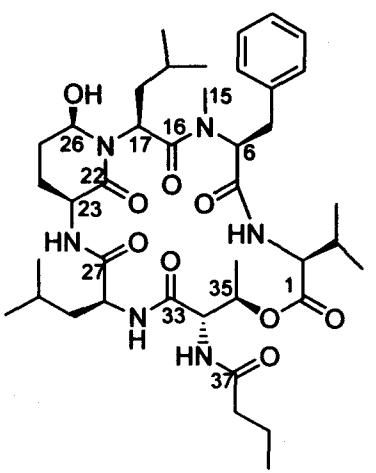

500 MHz ^{1}H NMR Spectrum of Tasihalide A (**1.15**) in $CDCl_3$

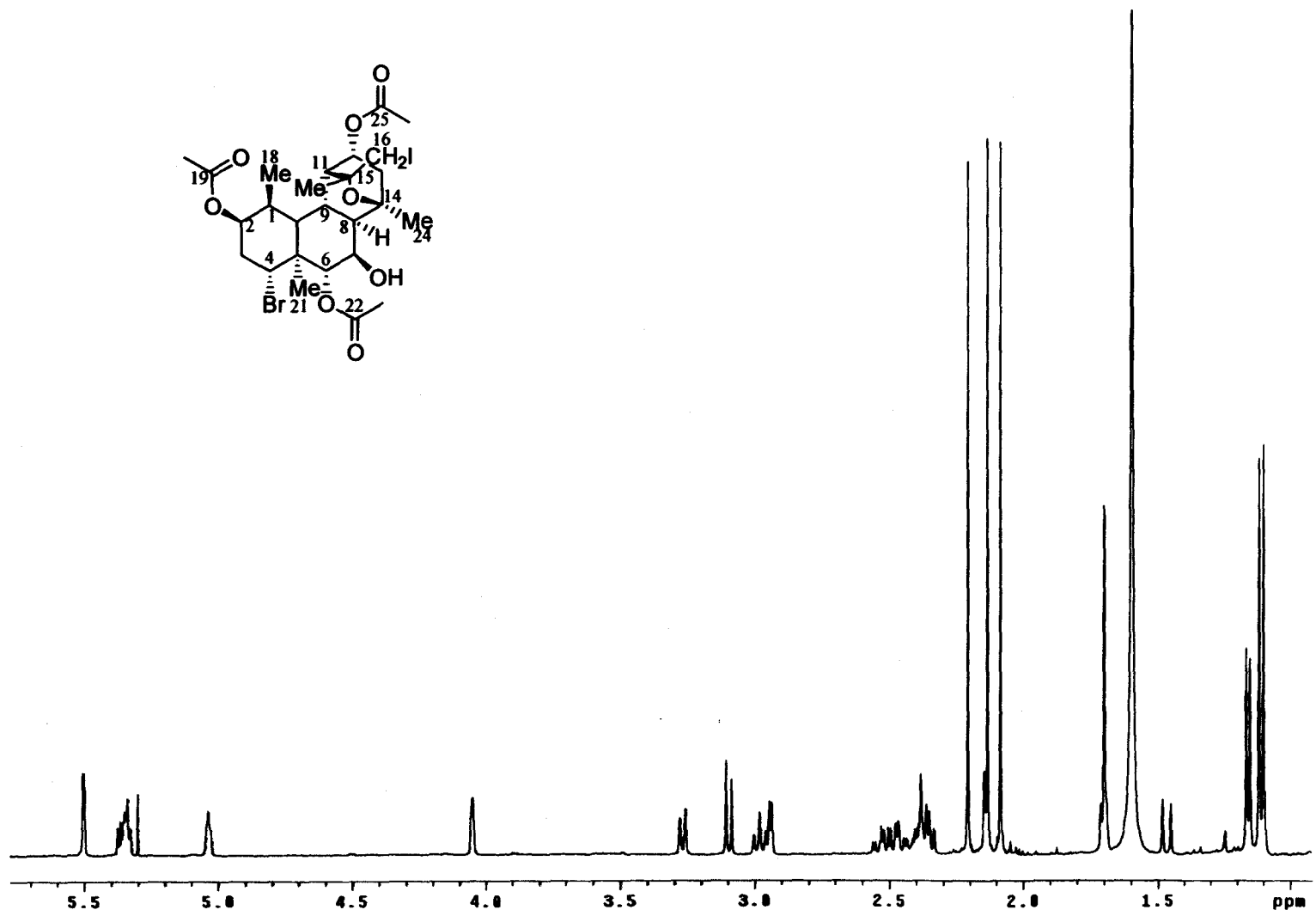

125 MHz ^{13}C NMR of Tasihalide A (**1.15**) in $CDCl_3$

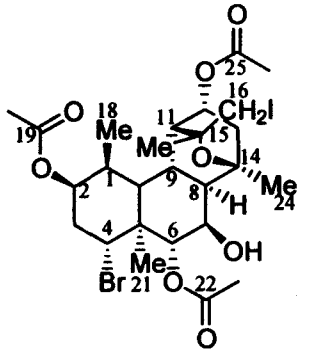

500 MHz ^{1}H NMR Spectrum of Tasihalide B (**1.16**) in $CDCl_3$

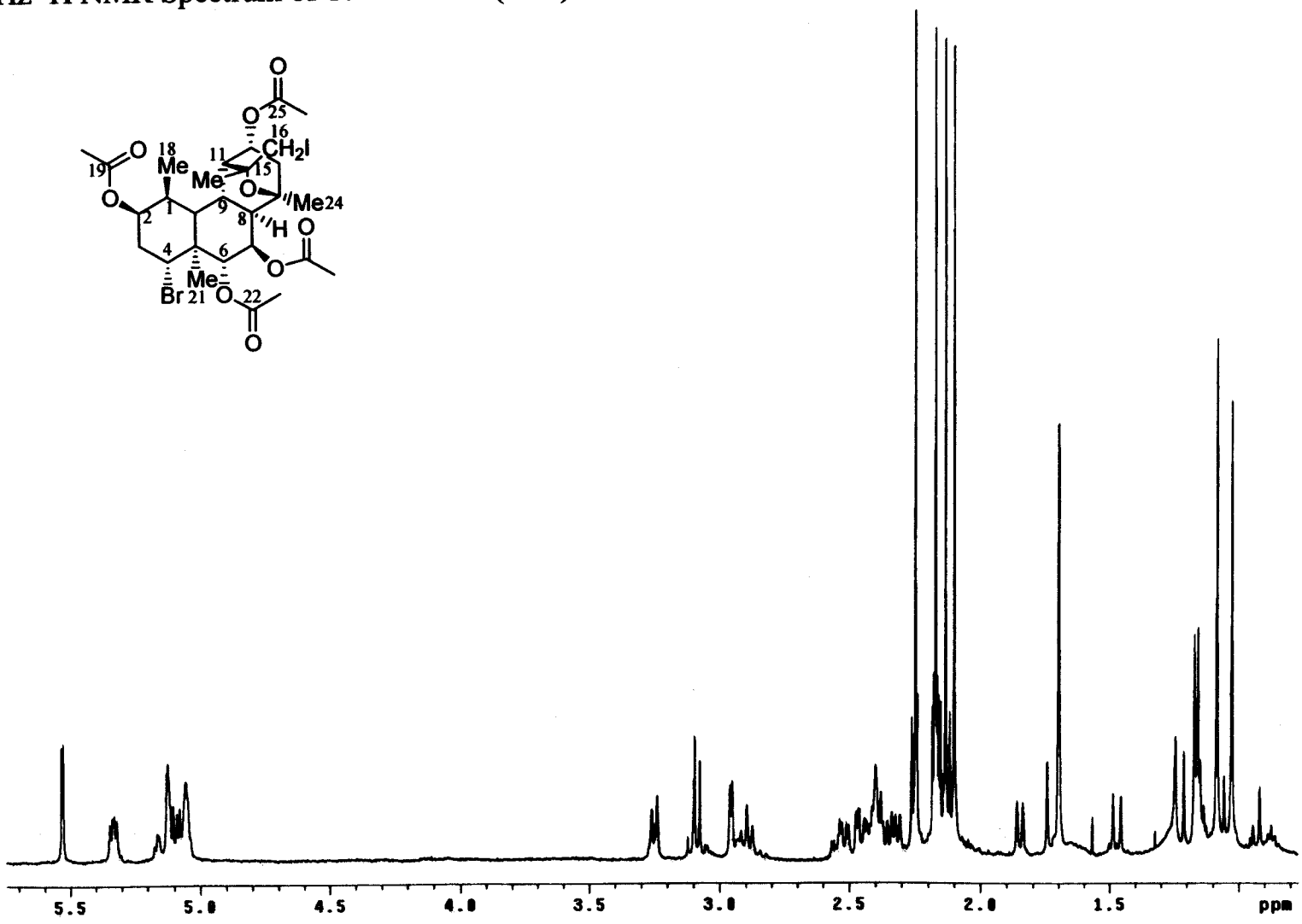

125 MHz ^{13}C NMR Spectrum of Tasihalide B (**1.16**) in $CDCl_3$

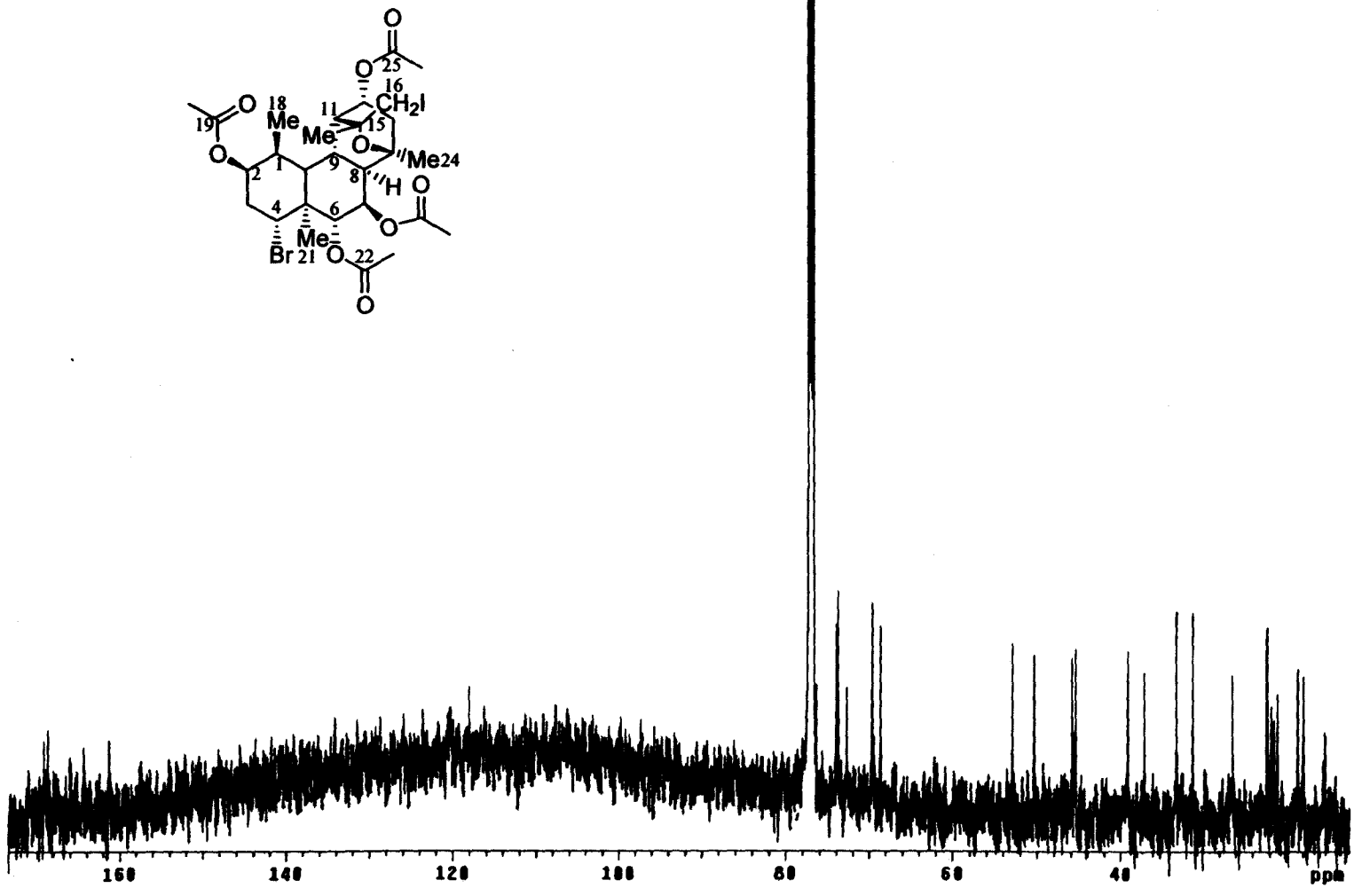

500 MHz ^{1}H NMR Spectrum of 15-NorLyngbyapeptin A (**1.36**) in $CDCl_3$

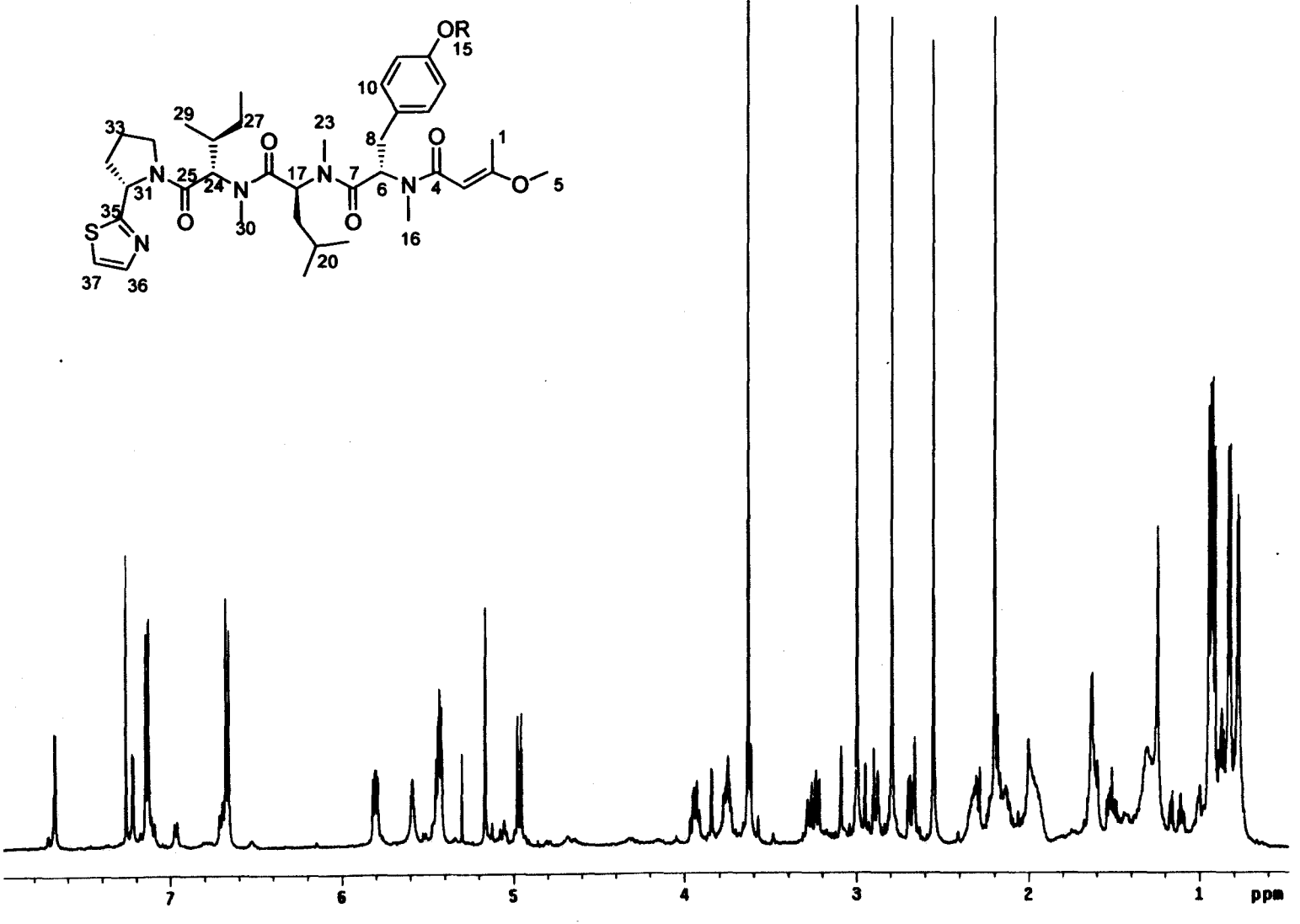

125 MHz ^{13}C NMR of 15-Norlyngbyapeptin A (**1.36**) in $CDCl_3$

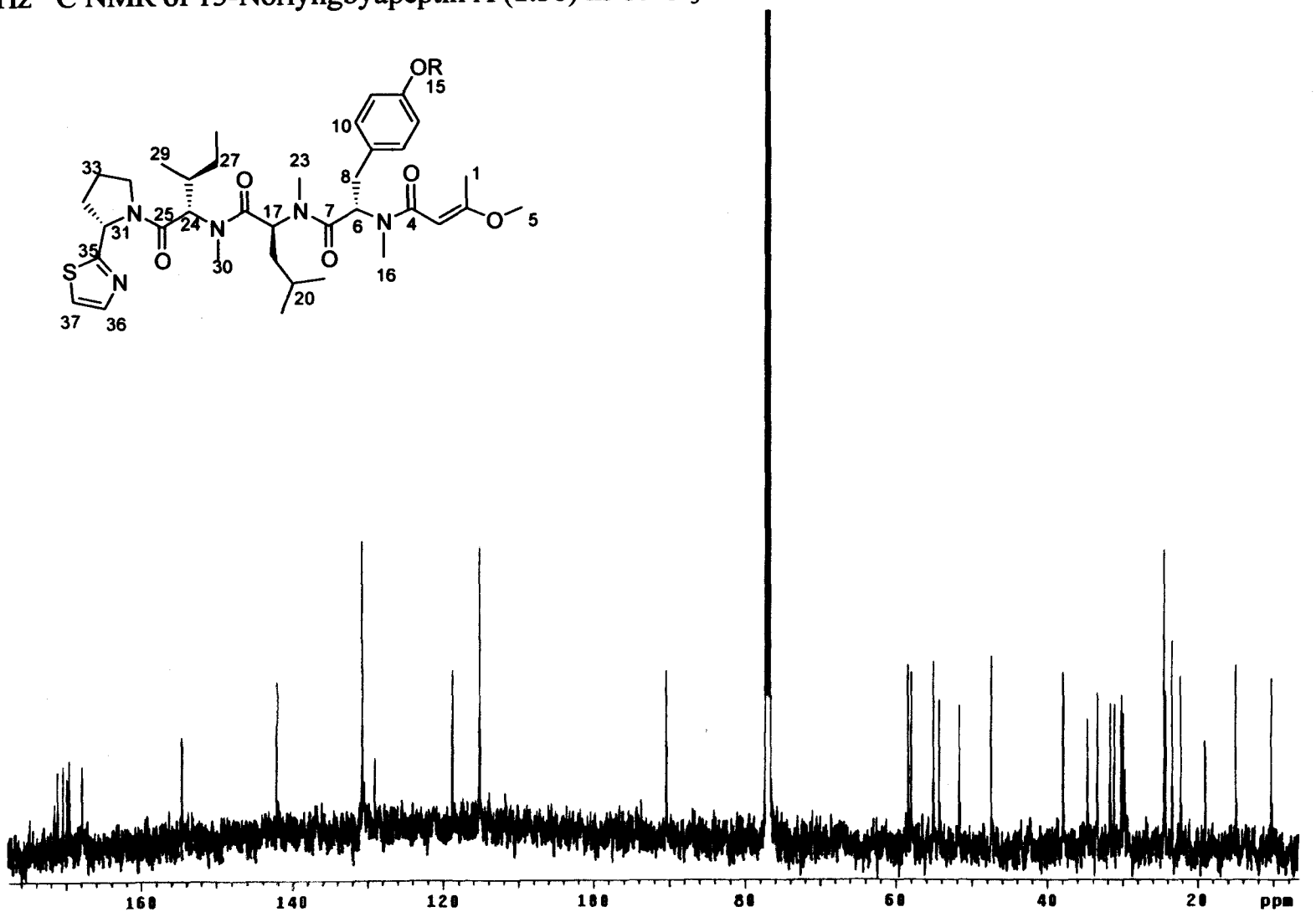

500 MHz ^{1}H NMR Spectrum of Lyngbyabellin D (**1.38**) in $CDCl_3$

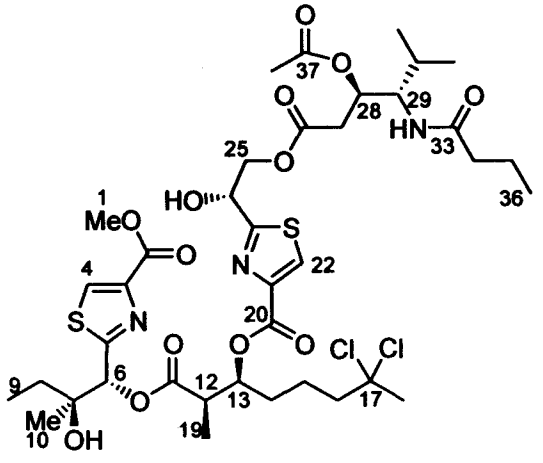

125 MHz ^{13}C NMR Spectrum of Lyngbyabellin D (**1.38**) in $CDCl_3$

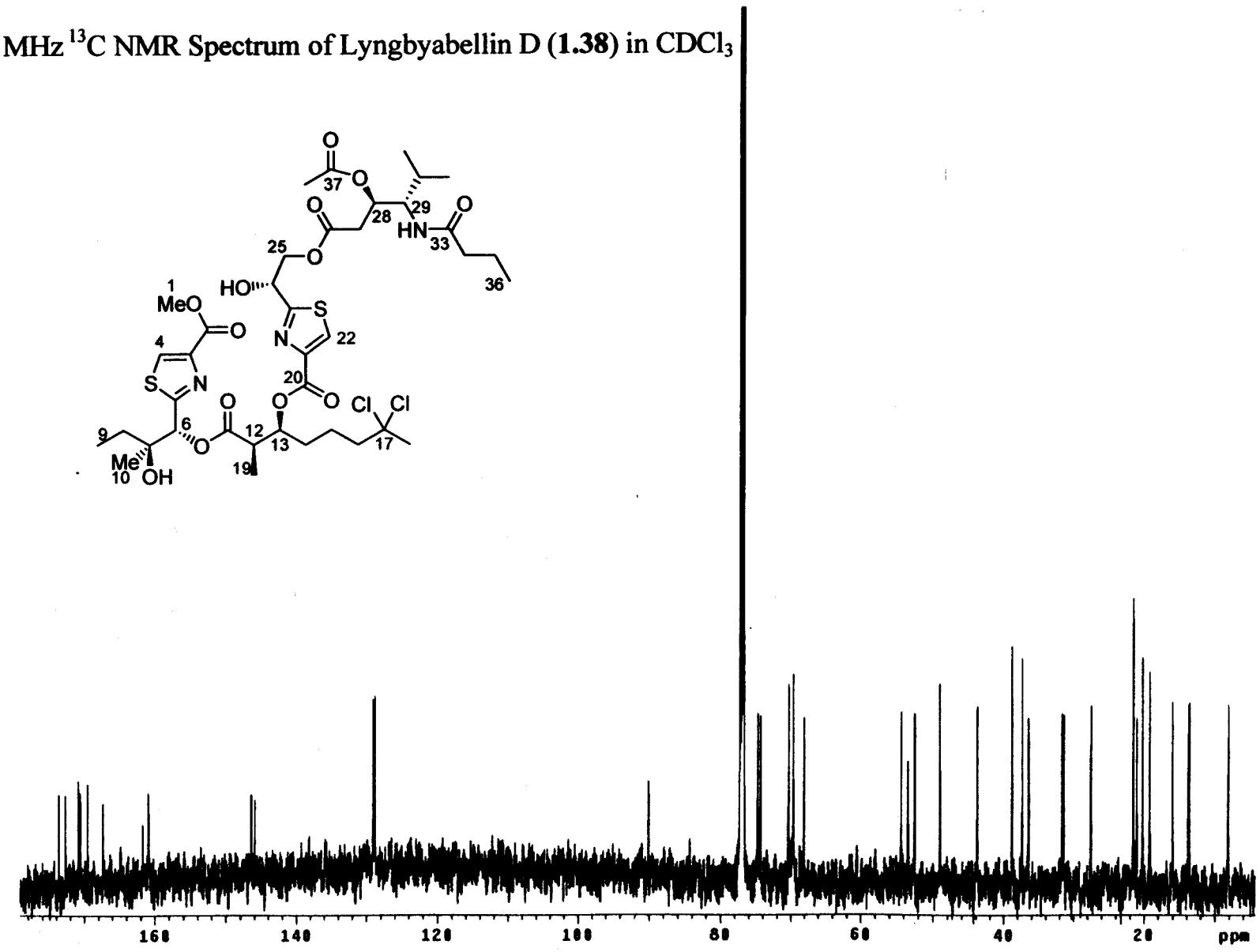

500 MHz ^{1}H NMR Spectrum of Obyanamide (**1.48**) in $CDCl_3$

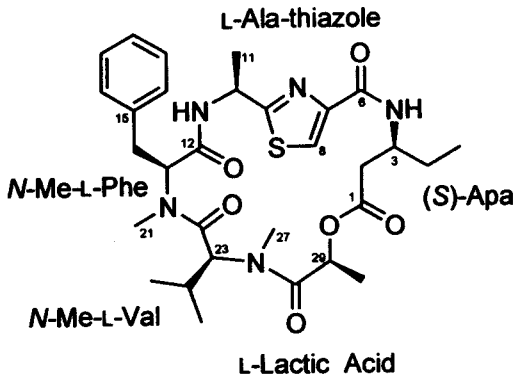

125 MHz ^{13}C NMR Spectrum of Obyanamide (**1.48**) in $CDCl_3$

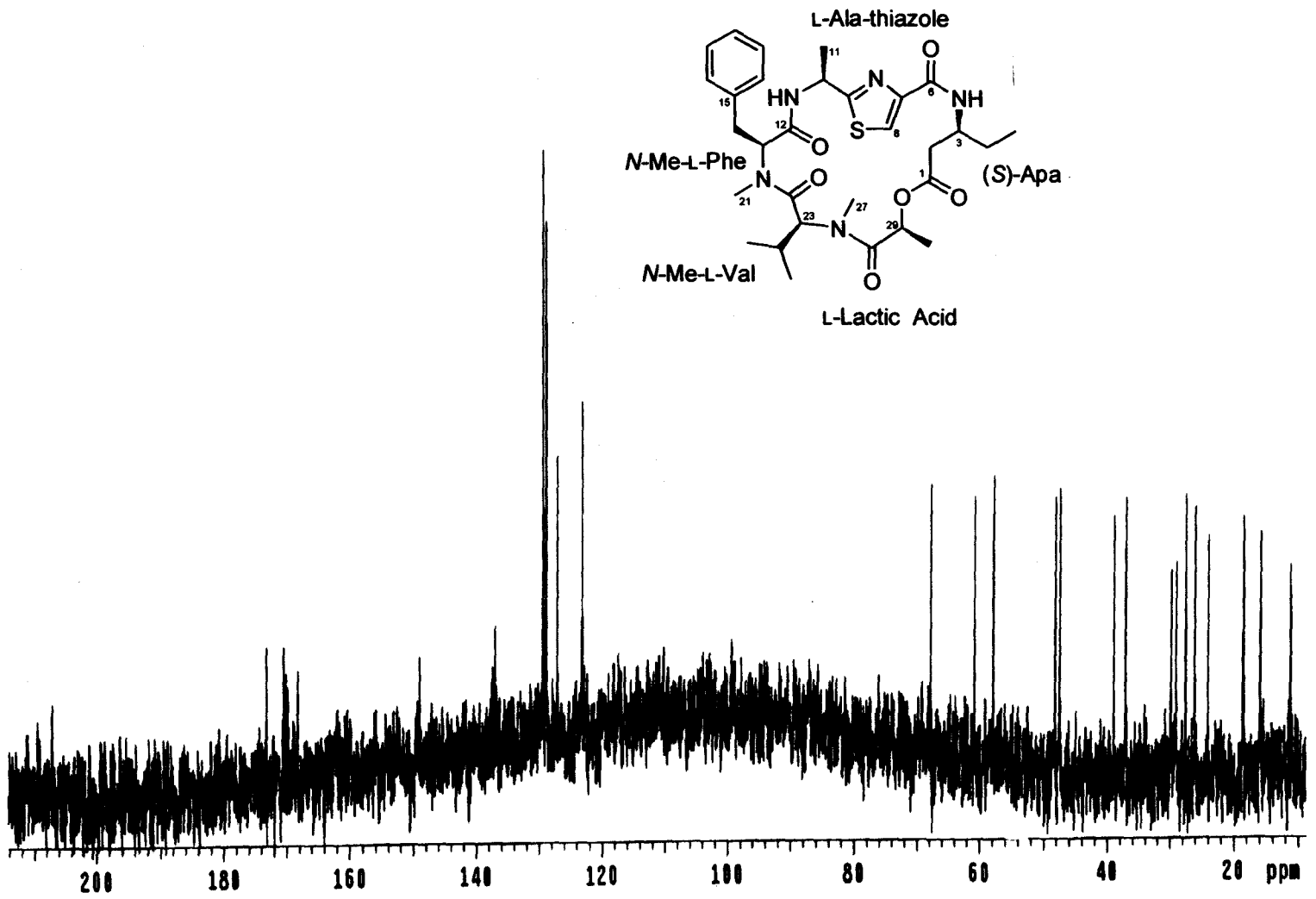

500 MHz ^{1}H NMR Spectrum of Ulongapeptin (**1.55**) in $CDCl_3$

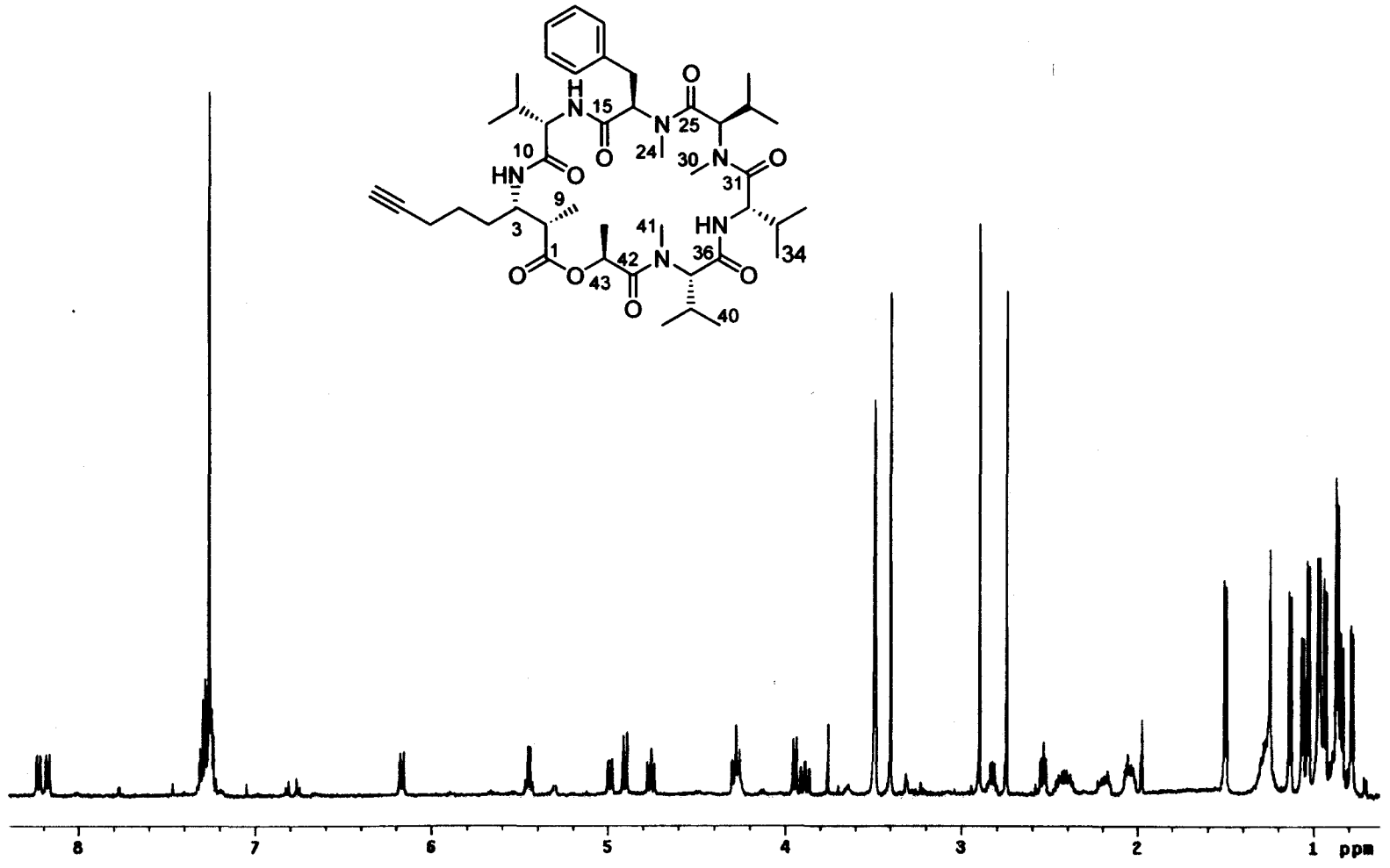

125 MHz ^{13}C NMR Spectrum of Ulongapeptin (**1.55**) in $CDCl_3$

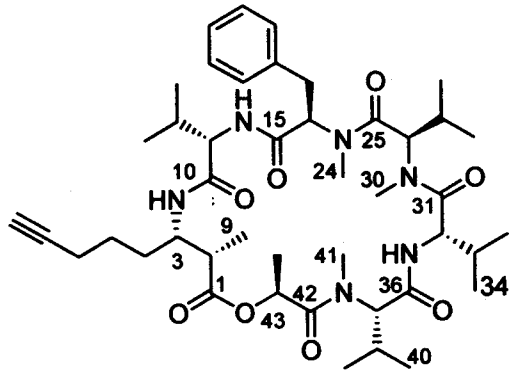

500 MHz ^{1}H NMR Spectrum of Palau'amide (**1.61**) in $CDCl_3$

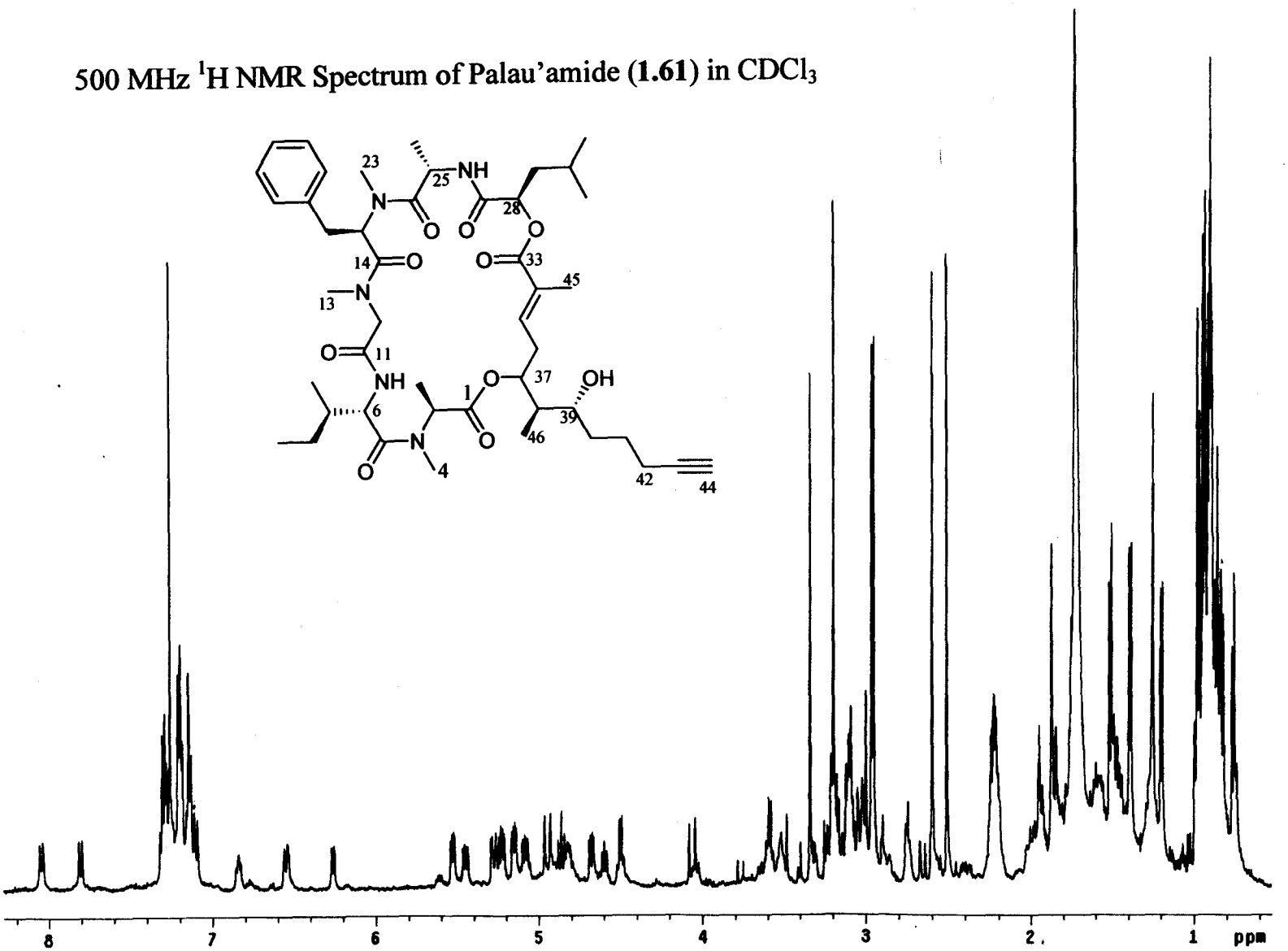

125 MHz ^{13}C NMR Spectrum of Palau'amide (**1.61**) in $CDCl_3$

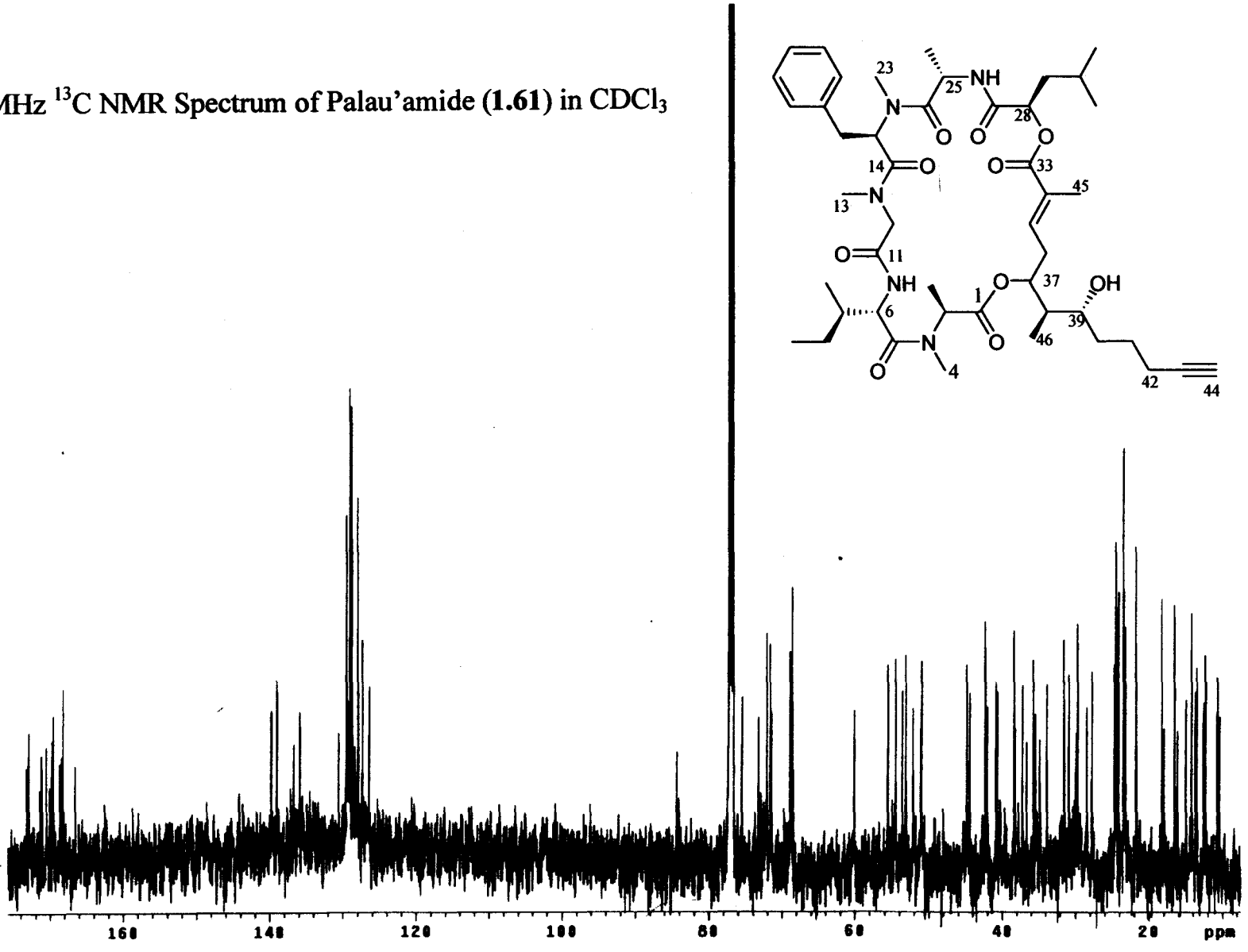

500 MHz ^{1}H NMR Spectra of Palau'amide (**1.61**) in MeOH-d_3

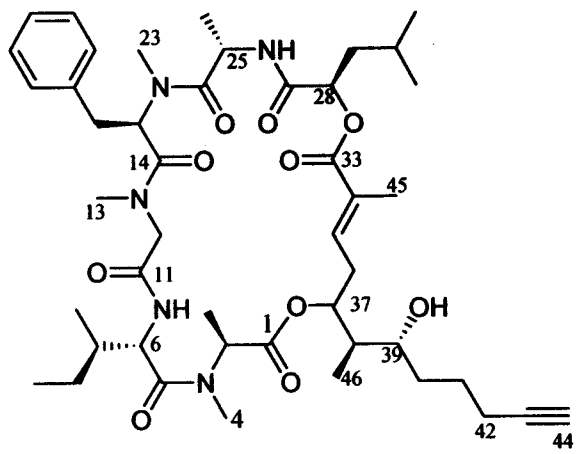

125 MHz ^{13}C NMR Spectra of Palau'amide (**1.61**) in MeOH-d_3

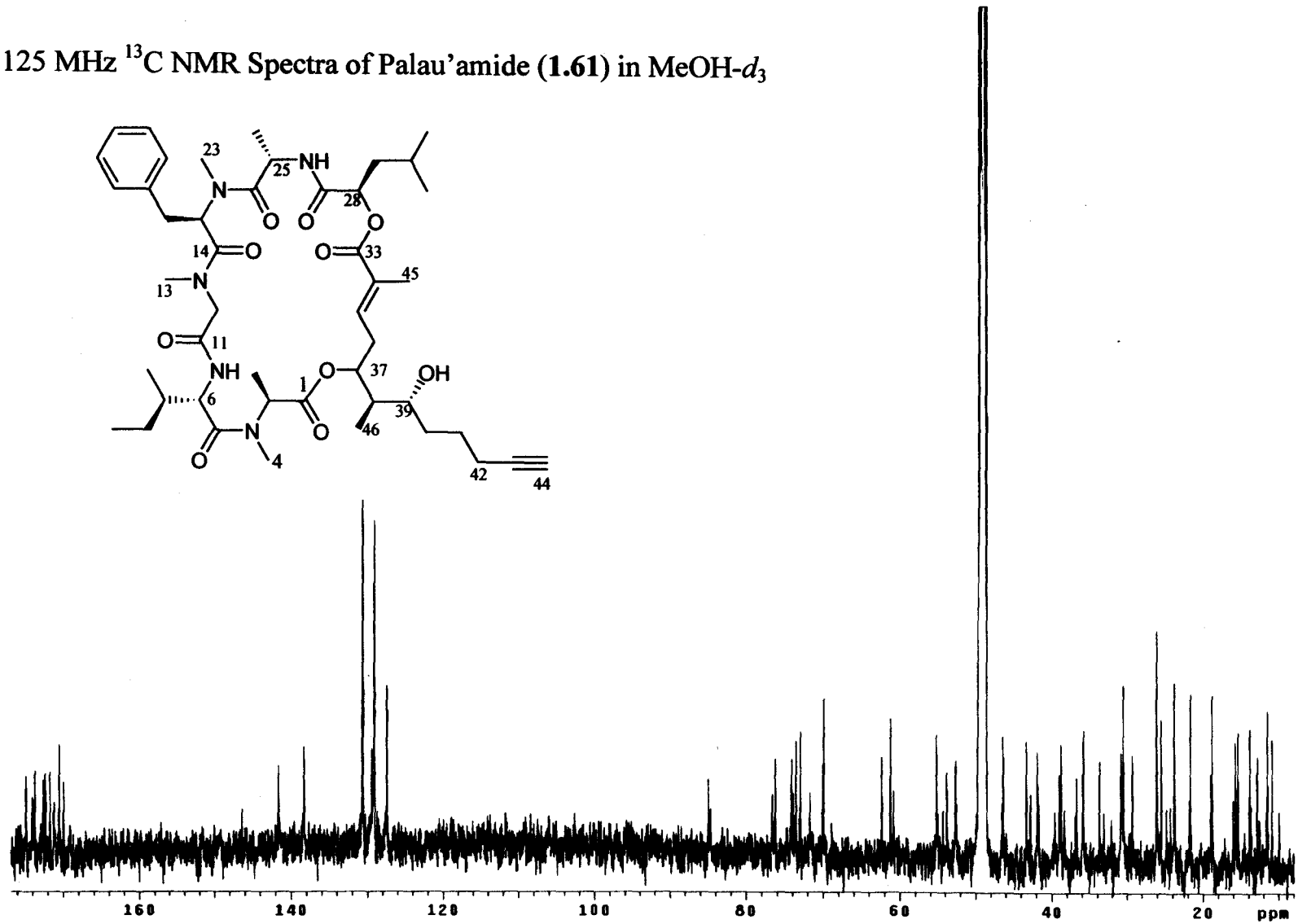

400 MHz ^{1}H NMR Spectrum of Lyngbyastatin 3 (**1.63**) at 70 °C in CD_3CN

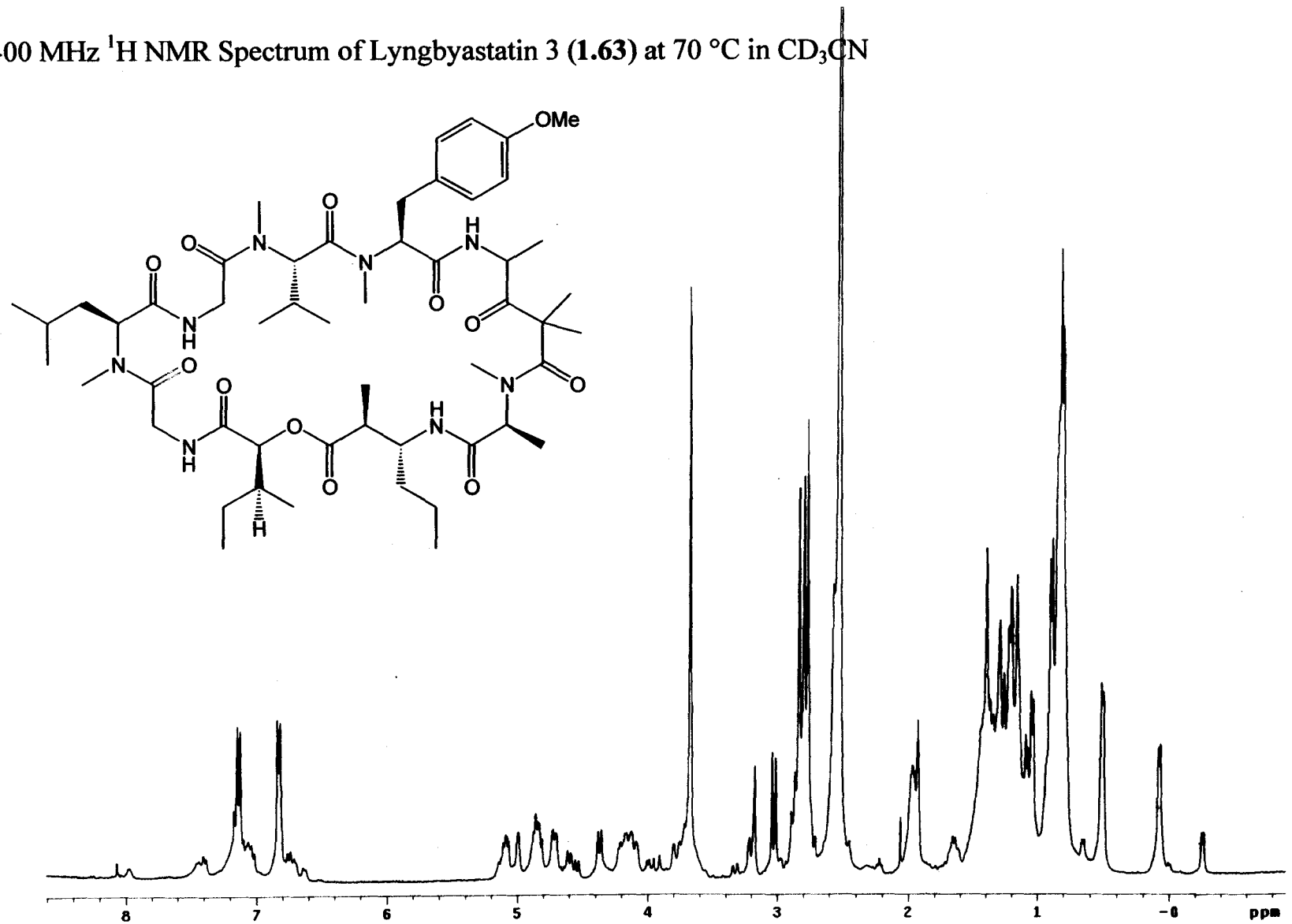

100 MHz ^{13}C NMR Spectrum of Lyngbyastatin 3 (**1.63**) at 70 °C in CD_3CN

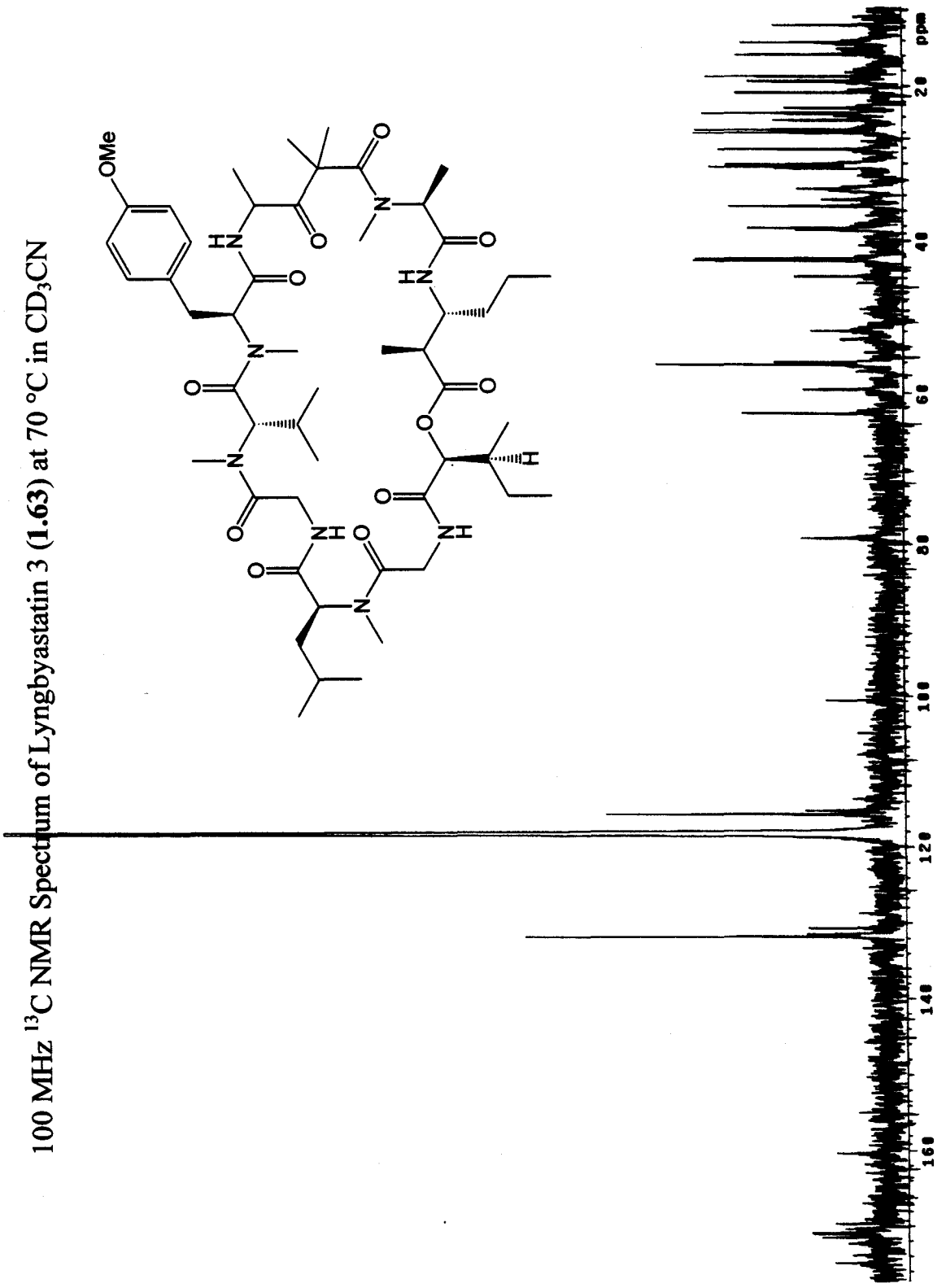

400 MHz ^{1}H NMR Spectrum of Lyngbyastatin 1 (**1.64**) at 70 °C in CD_3CN

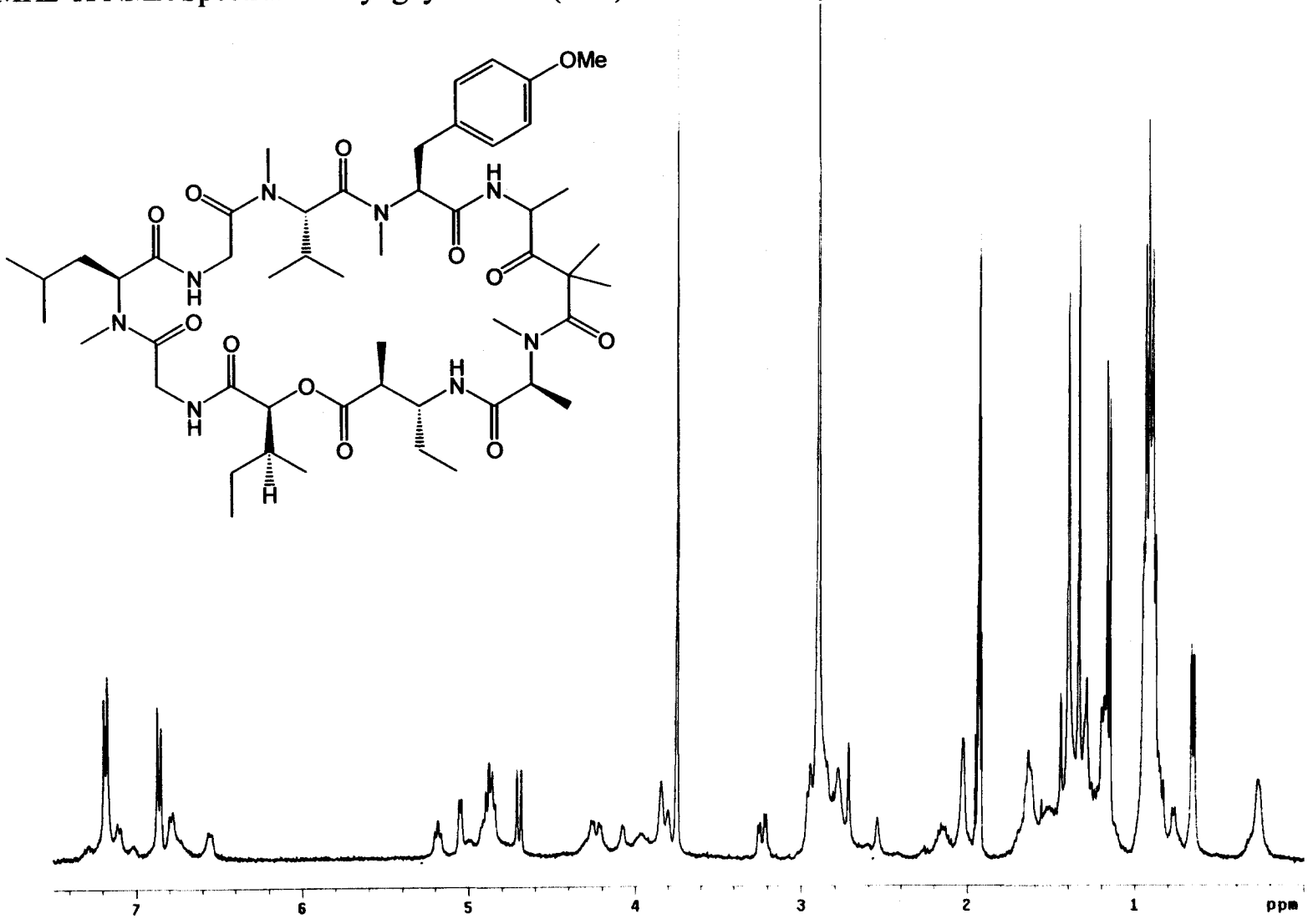

100 MHz ^{13}C NMR Spectrum of Lyngbyastatin 1 (**1.64**) at 70 °C in CD_3CN

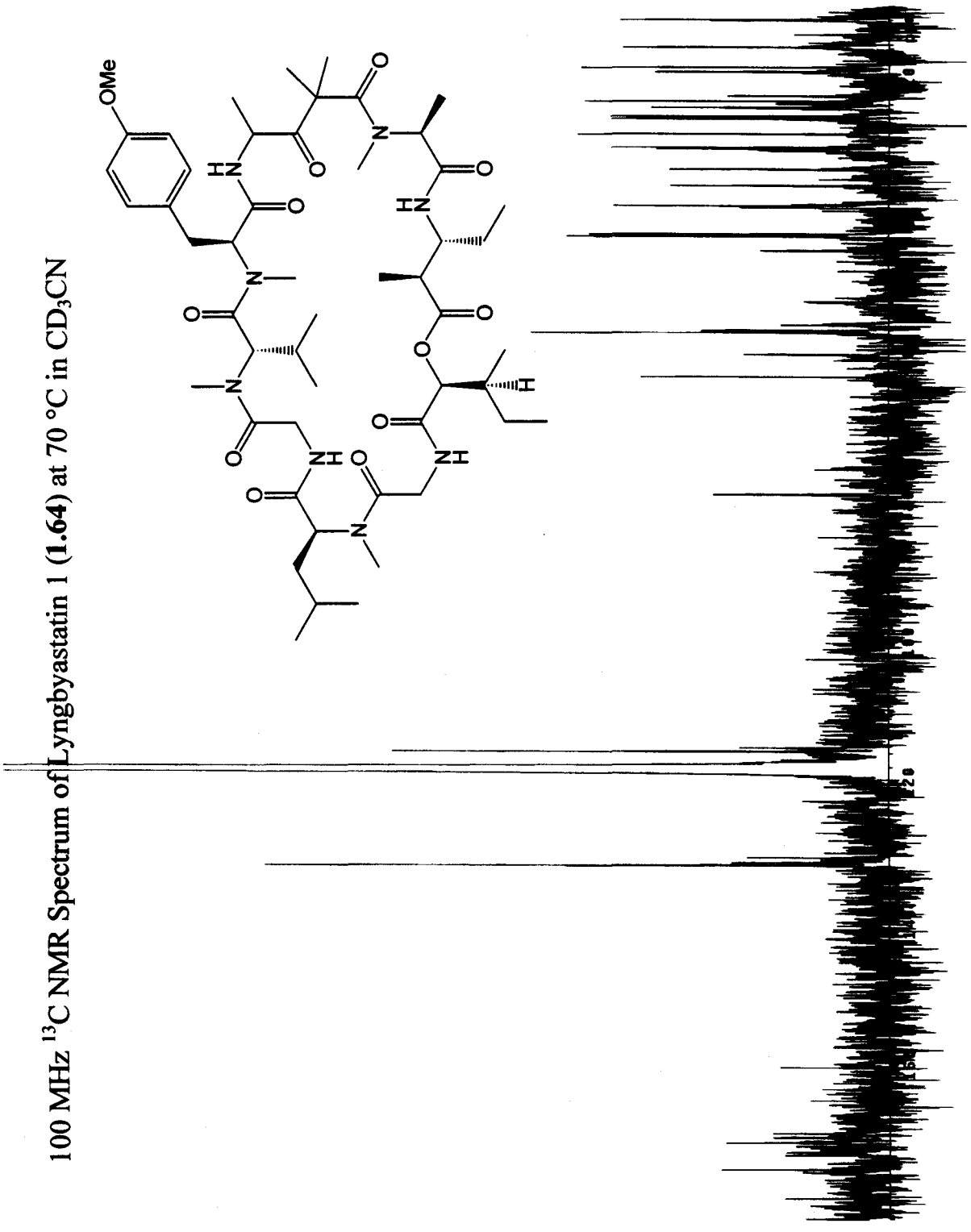

400 MHz ^{1}H NMR Spectrum of Dolastatin 12 (**1.65**) at 70 °C in CD_3CN

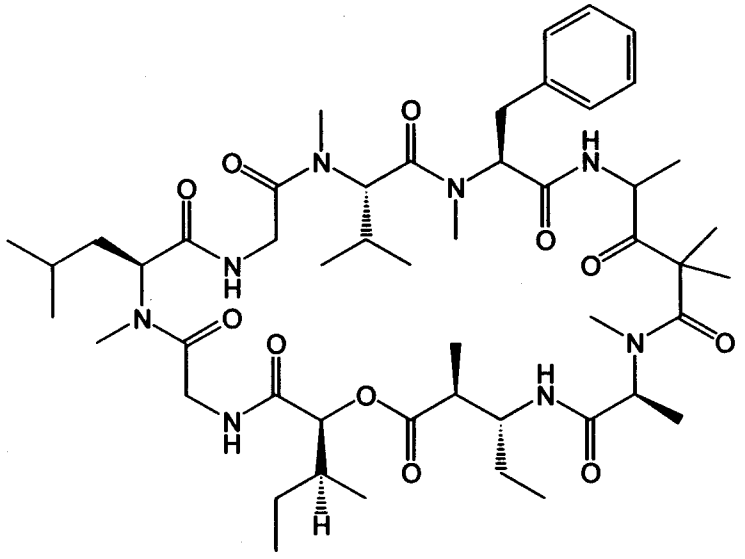

100 MHz ^{13}C NMR Spectrum of Dolastatin 12 (**1.65**) at 70 °C in CD_3CN

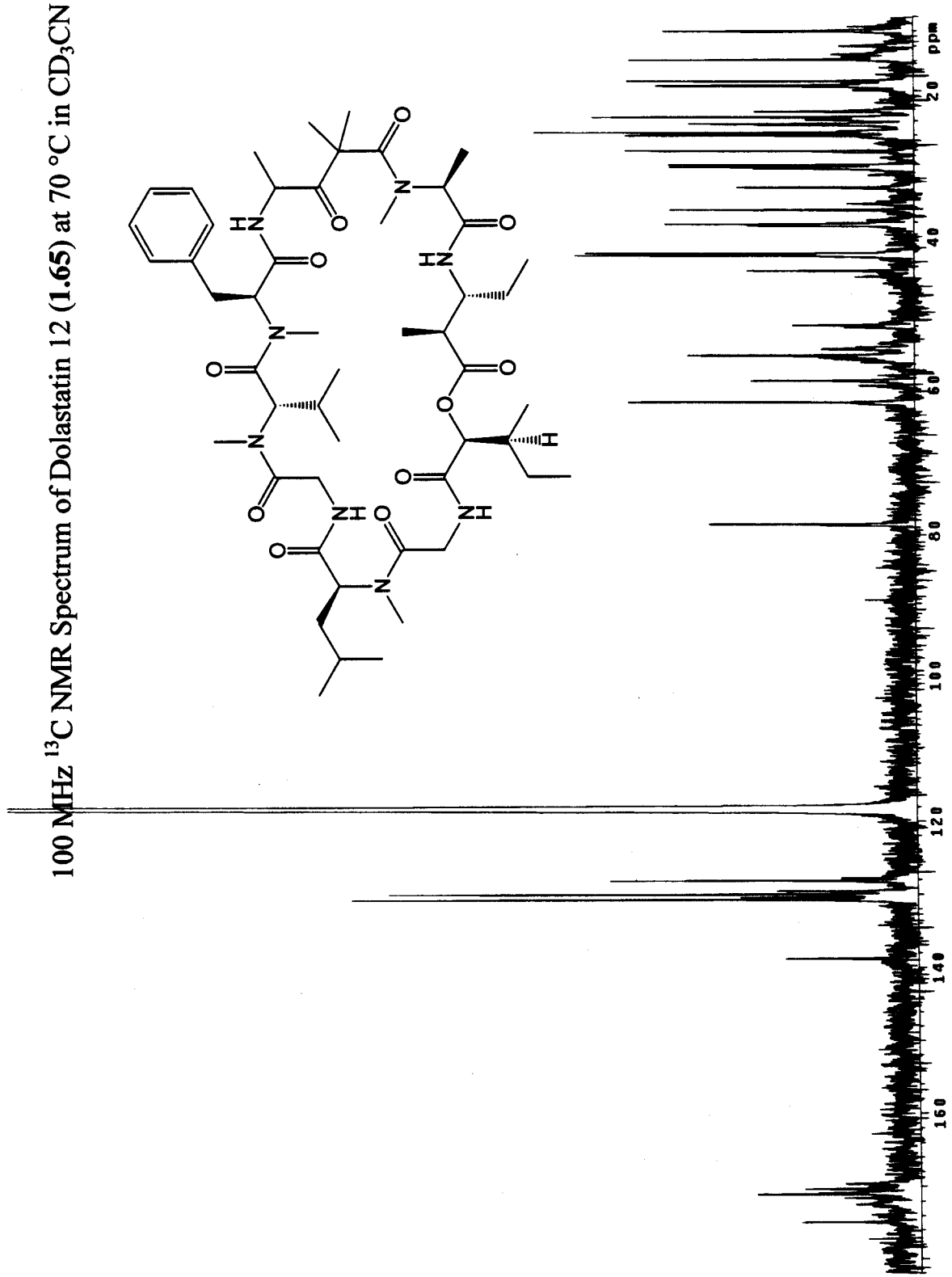

500 MHz ^{1}H NMR Spectrum of **1.81** in $CDCl_3$

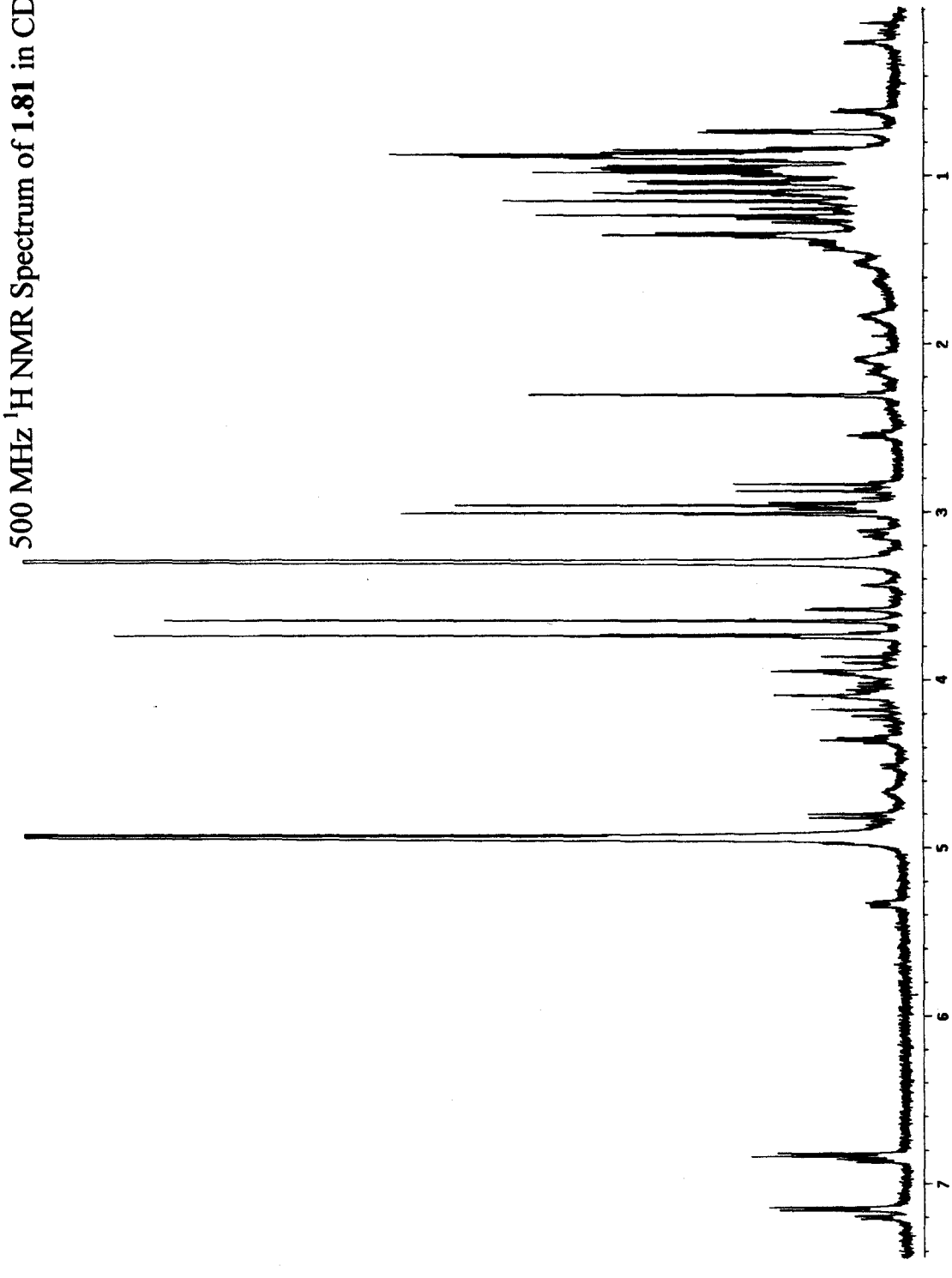

125 MHz ^{13}C NMR Spectrum of **1.81** in $CDCl_3$

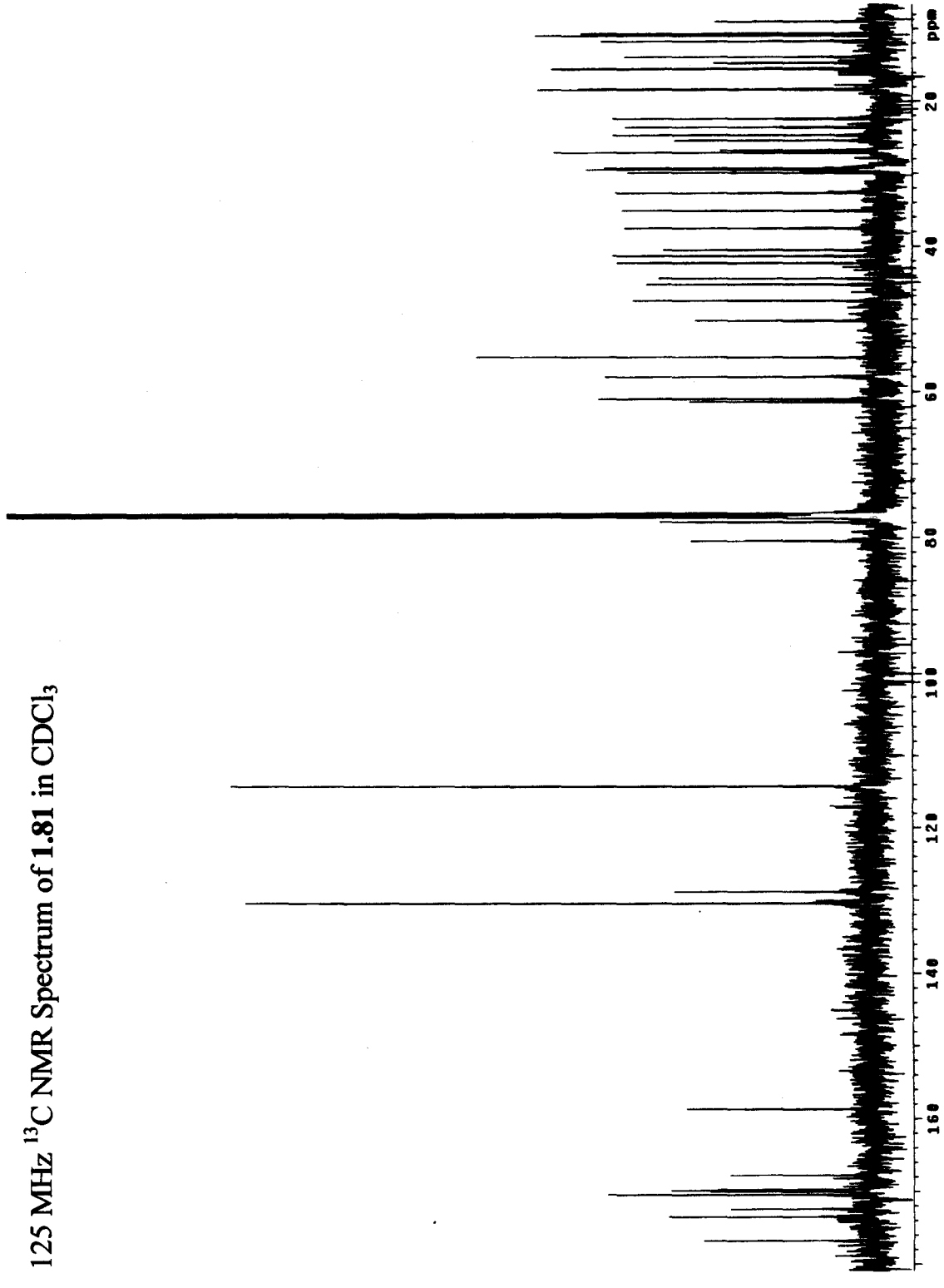

500 MHz ^{1}H NMR Spectrum of **1.82** in $CDCl_3$

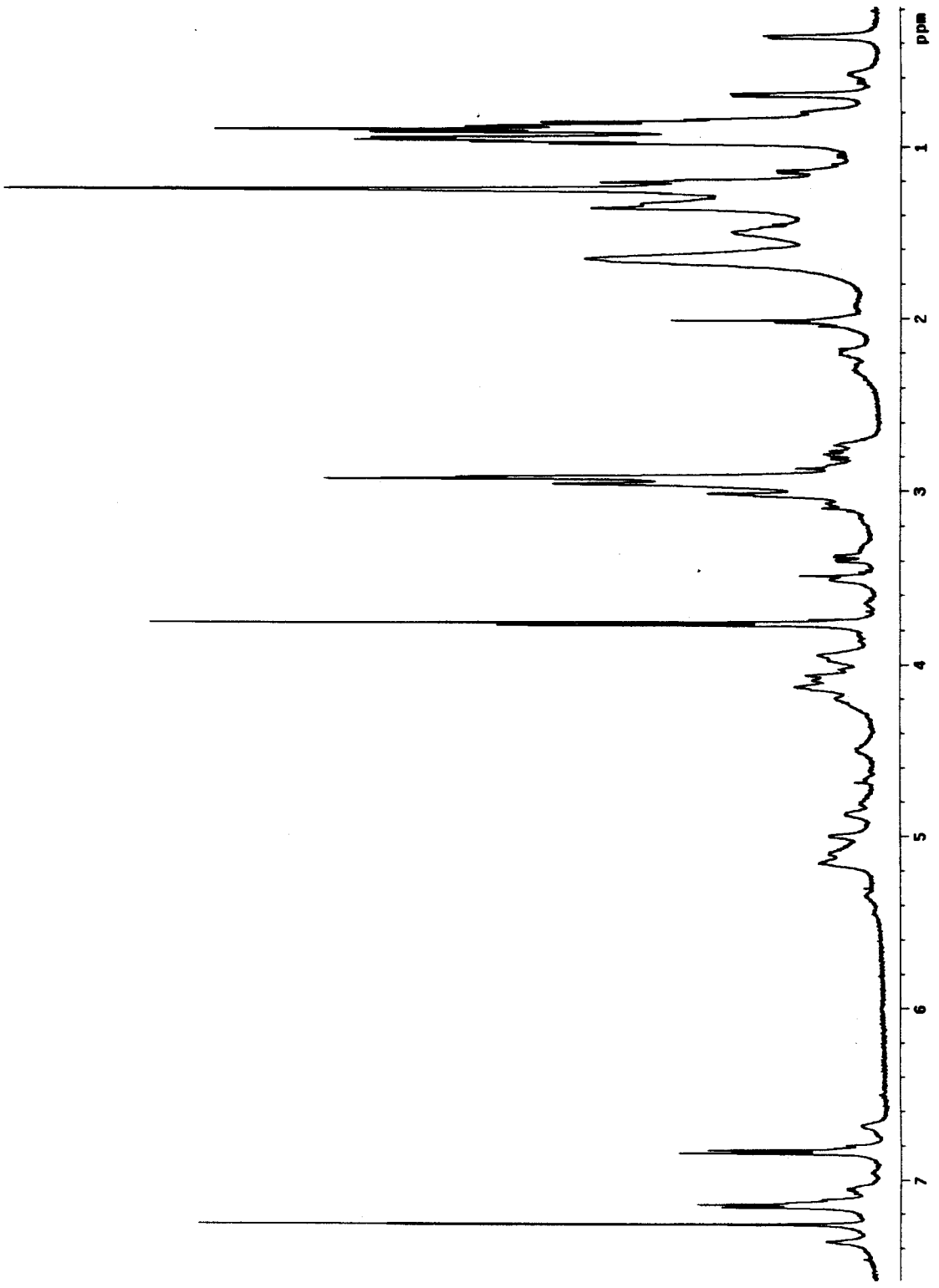

500 MHz ^{1}H NMR Spectrum of **1.83** in $CDCl_3$

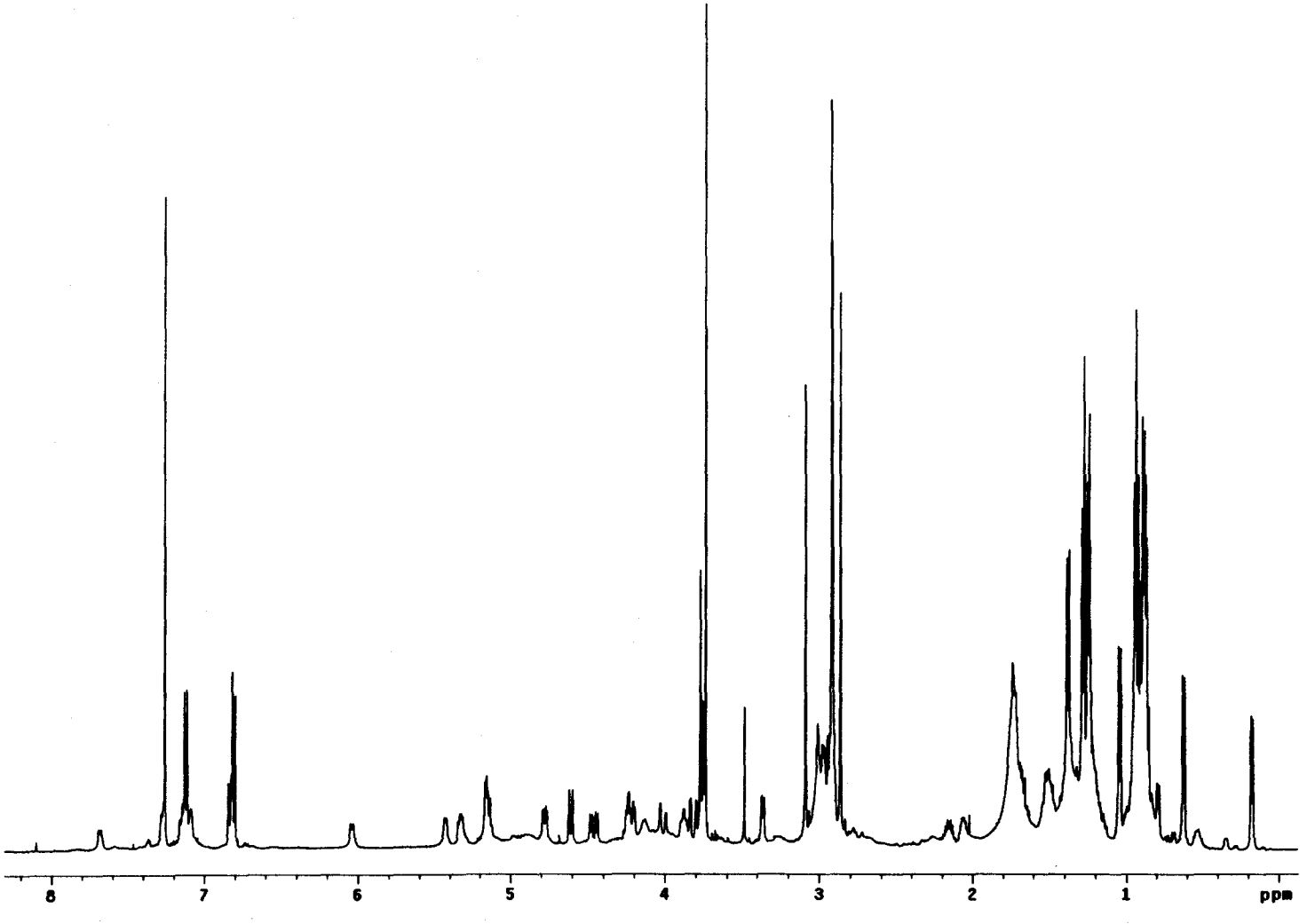

125 MHz ^{13}C NMR Spectrum of **1.83** in $CDCl_3$

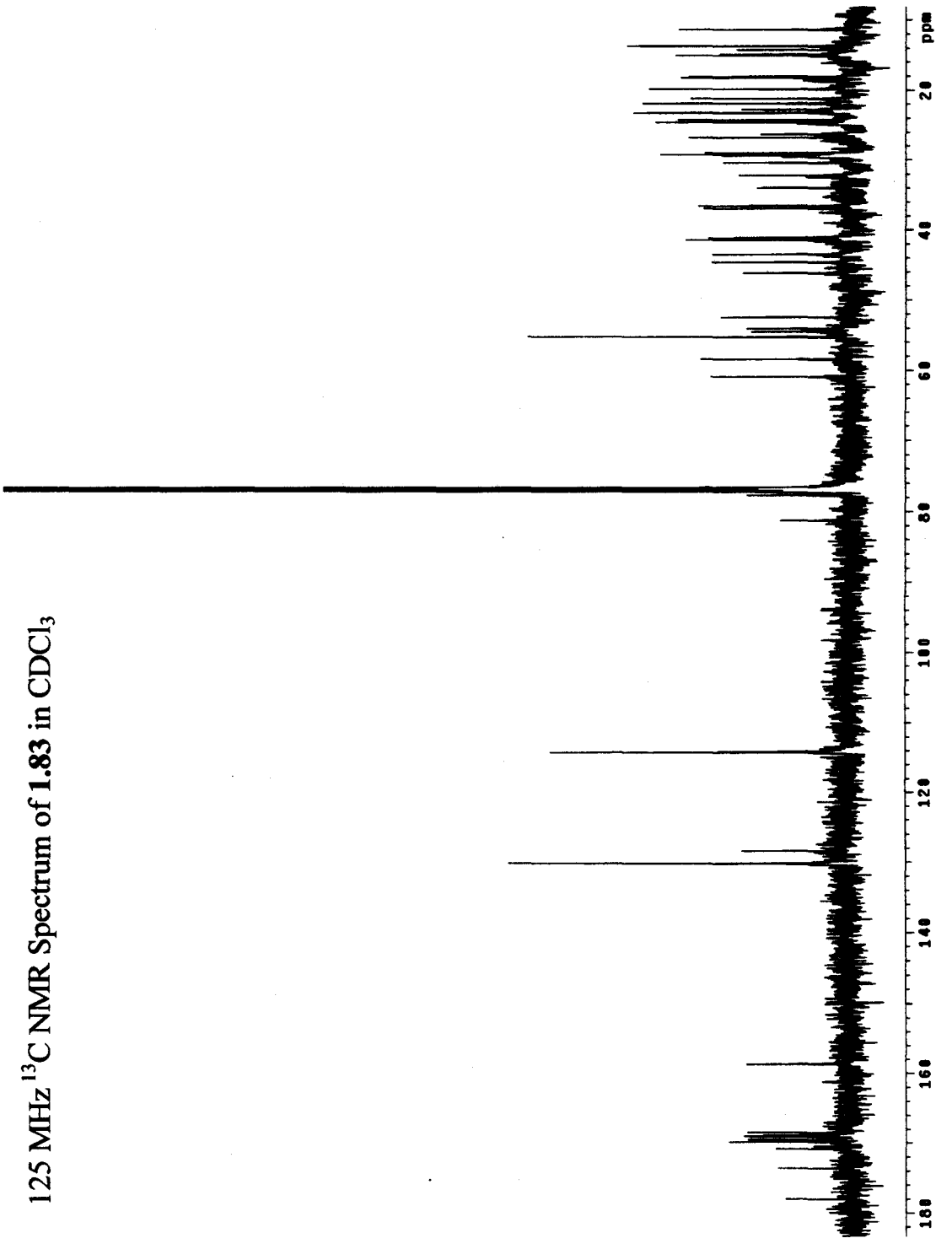

500 MHz ^{1}H NMR Spectrum of **1.84** in $CDCl_3$

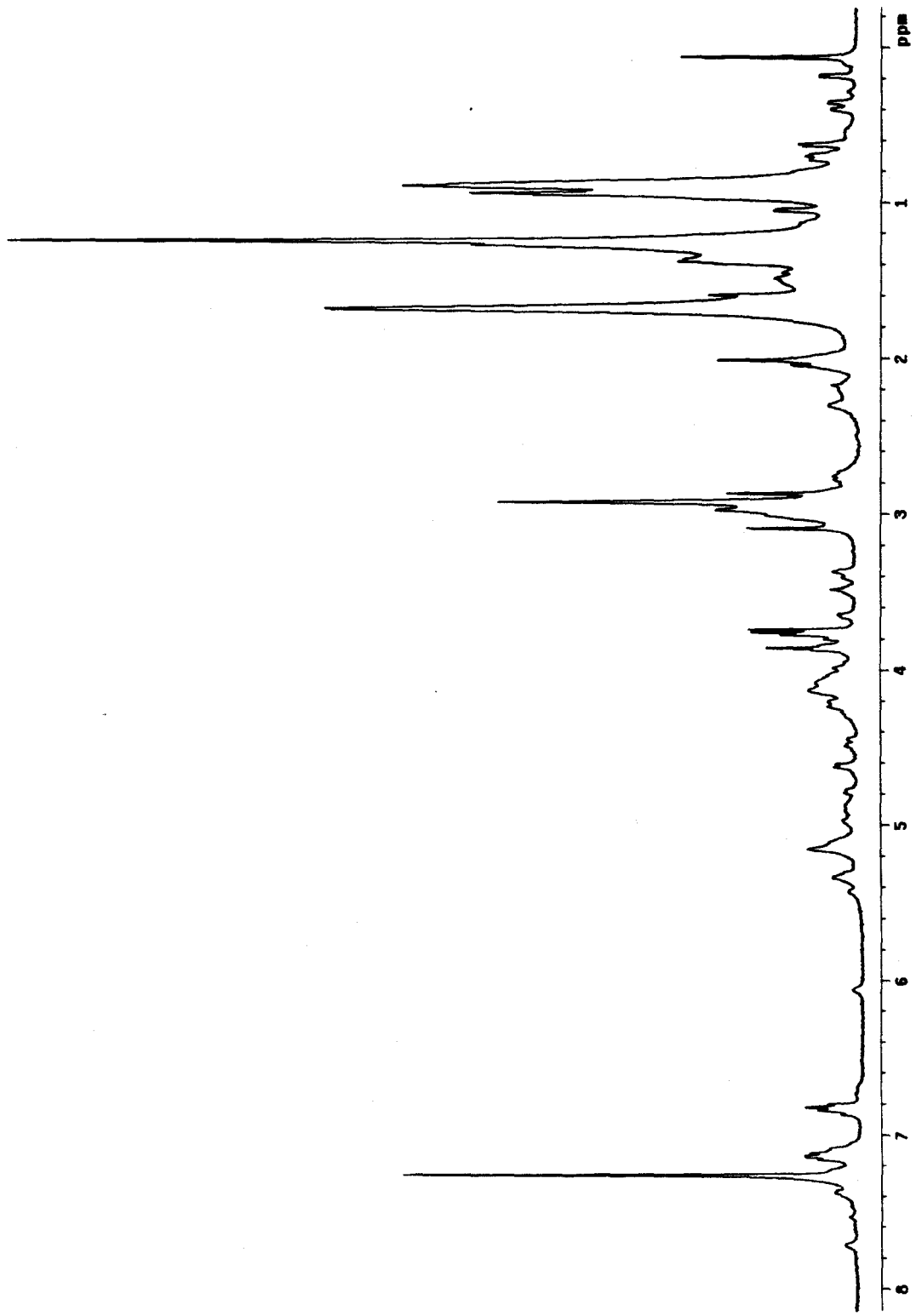

500 MHz ^{1}H NMR Spectrum of **1.85** in $CDCl_3$

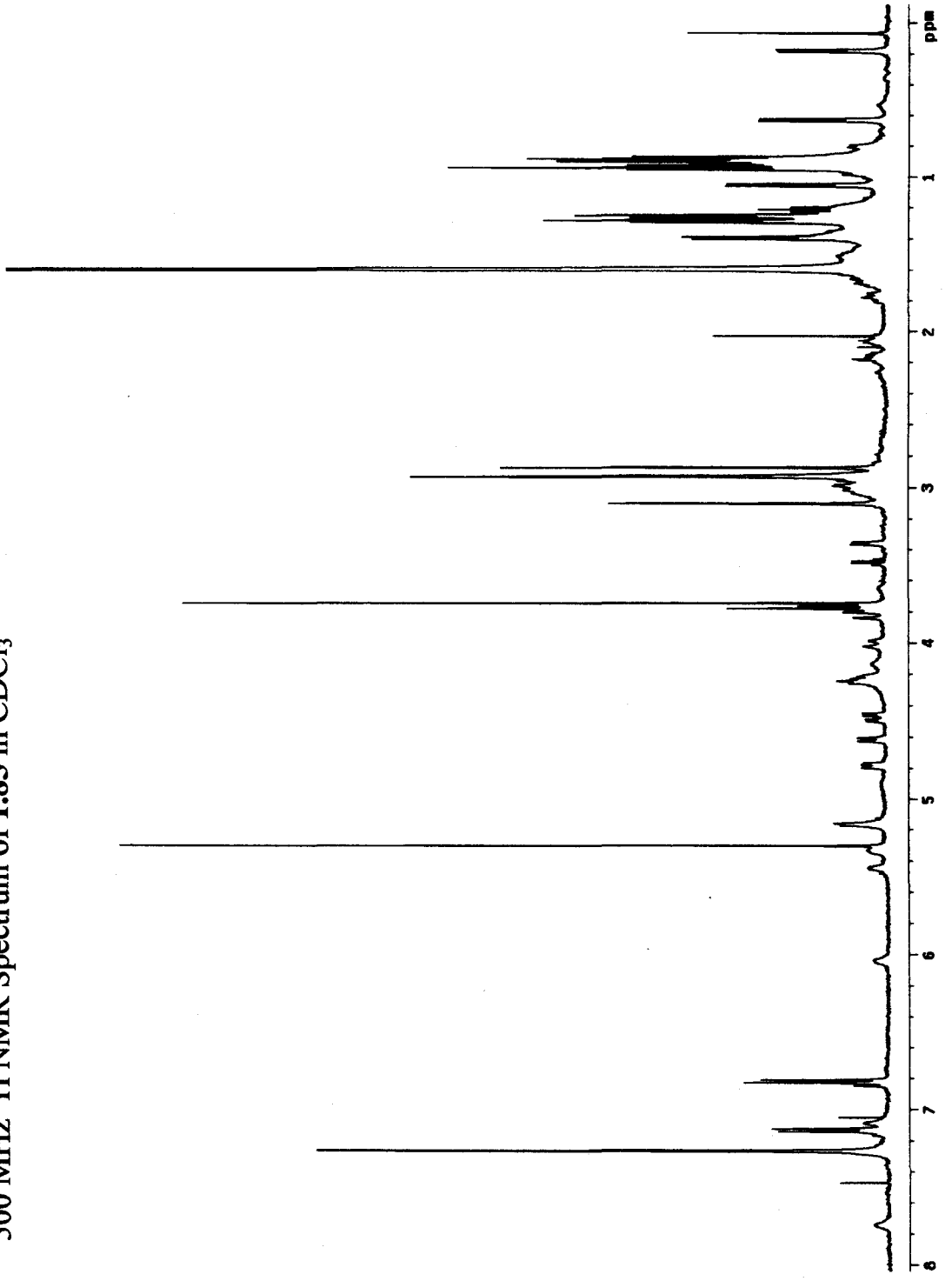

500 MHz ^{1}H NMR Spectrum of **1.86** in $CDCl_3$

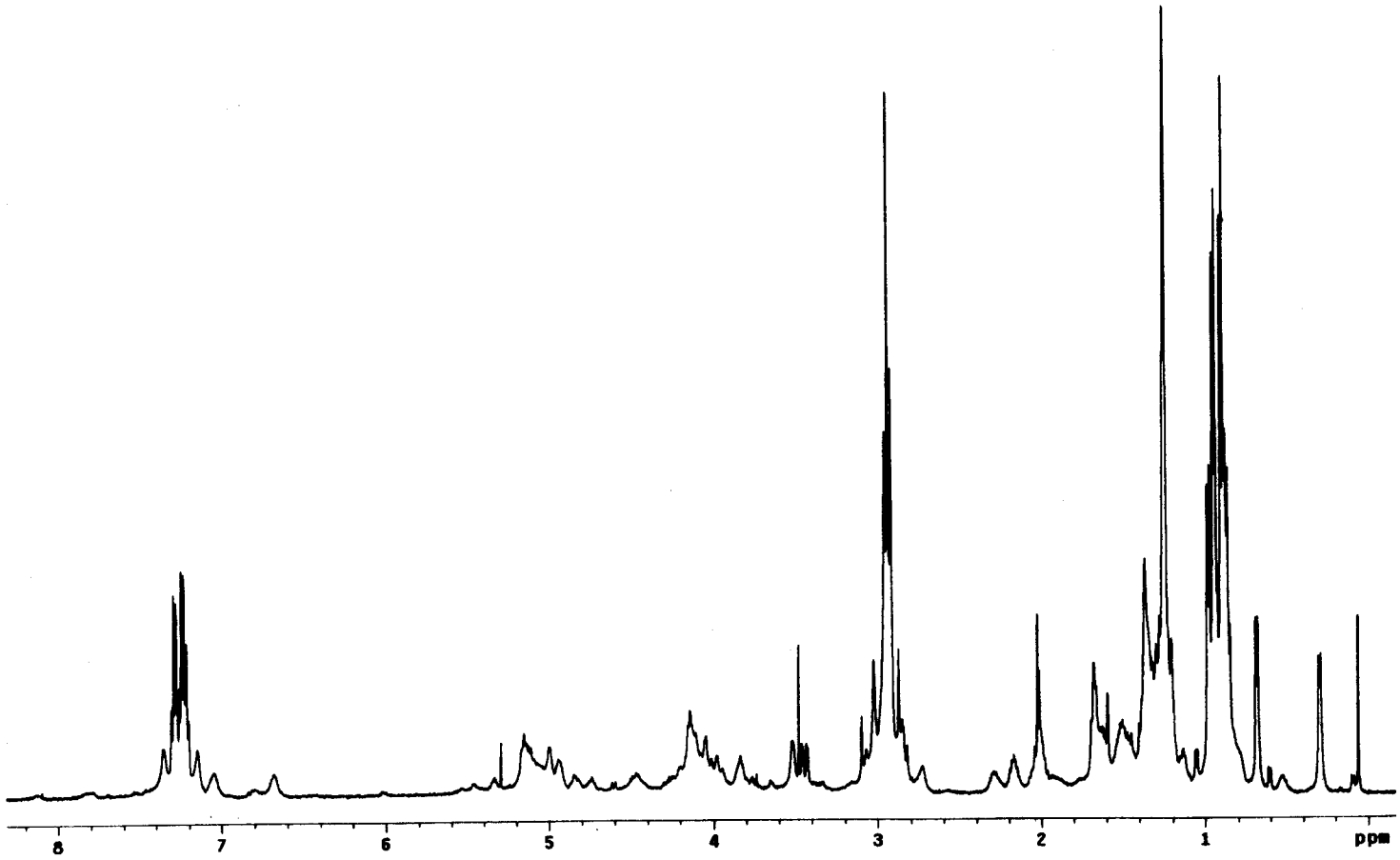

500 MHz ^{1}H NMR Spectrum of **1.87** in $CDCl_3$

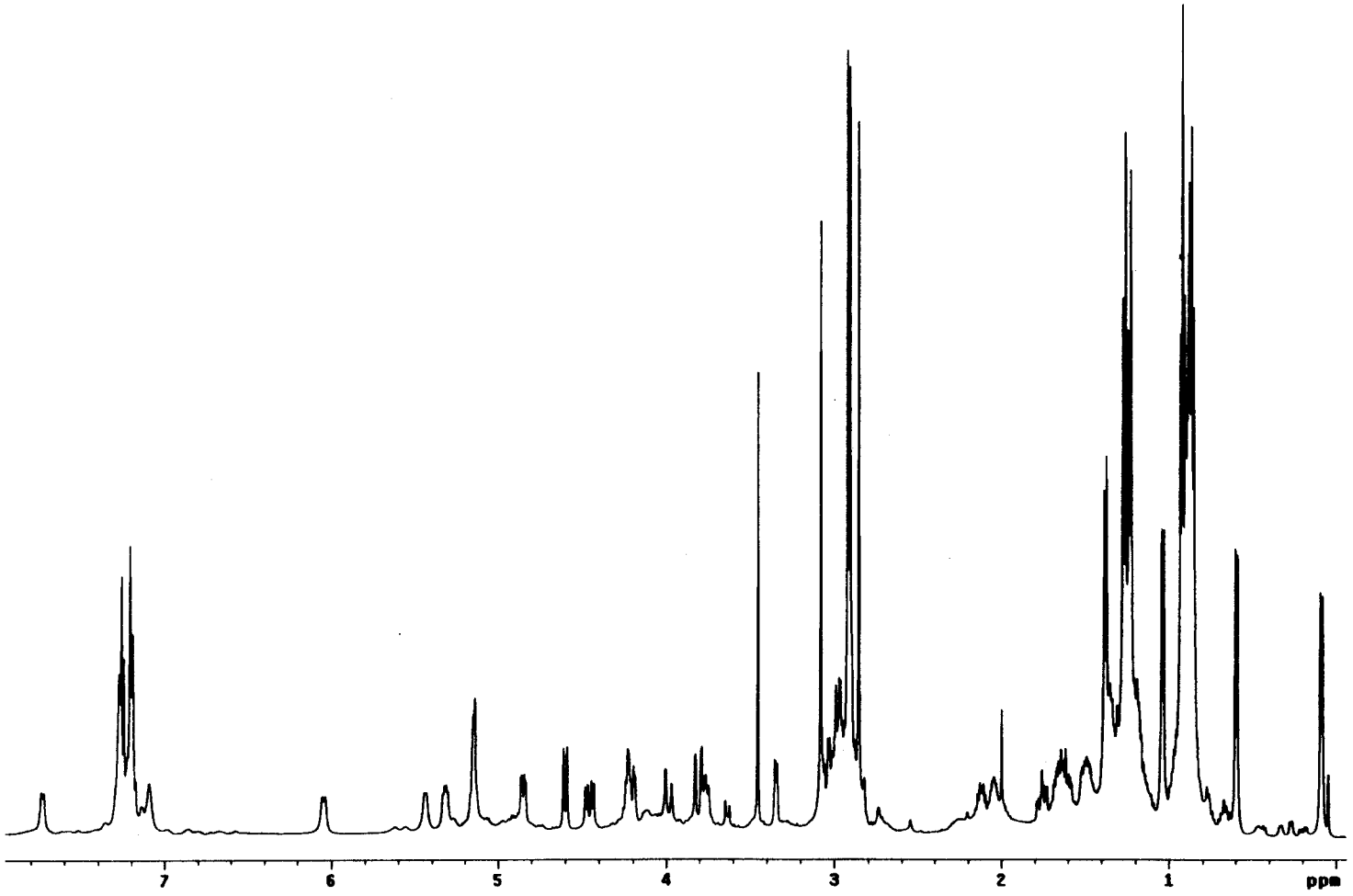

125 MHz ^{13}C NMR Spectrum of **1.87** in $CDCl_3$

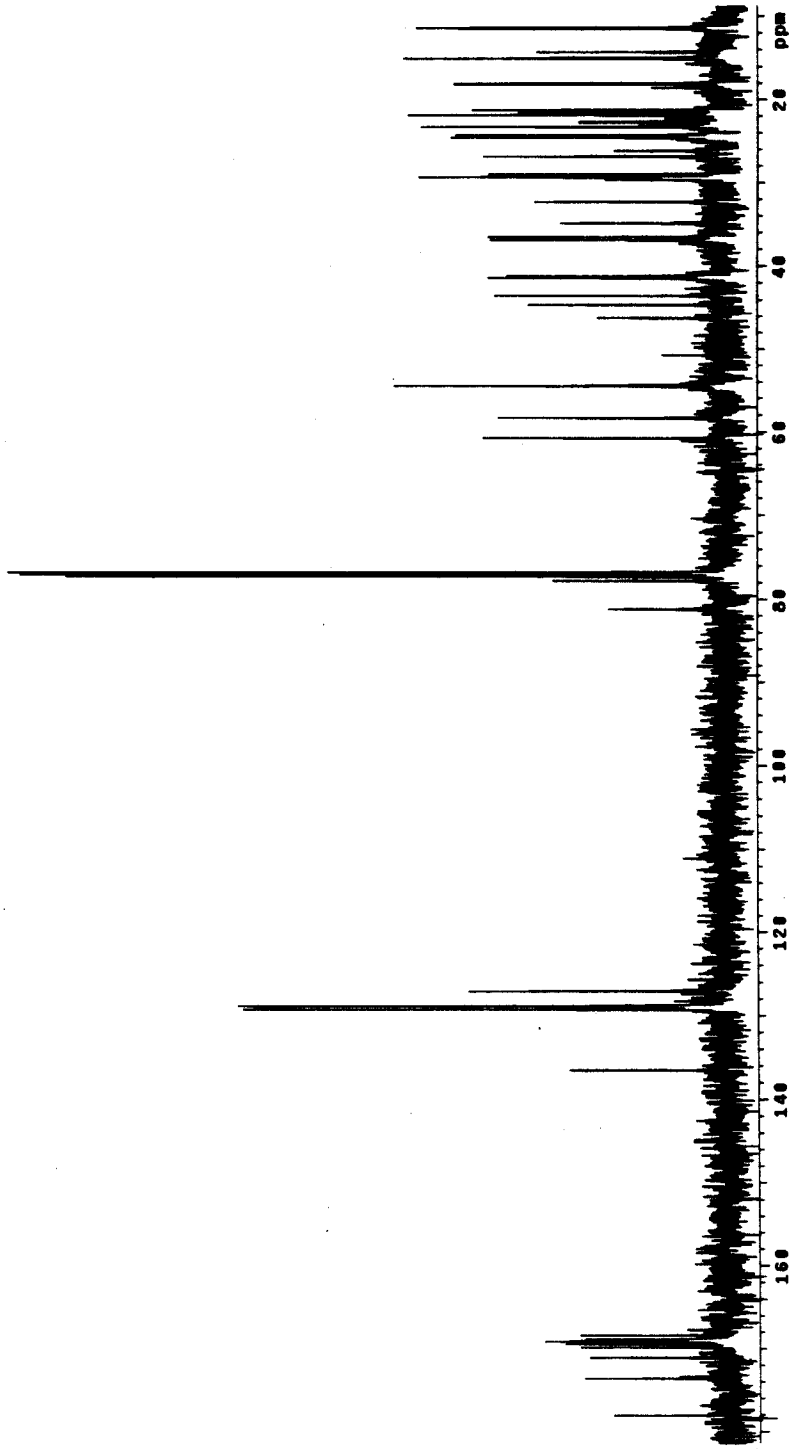

1.7 REFERENCES

(1) Cragg, G. M.; Newman, D. J. *Cancer Invest.* **1999**, *17*, 153-163.

(2) Bergmann, W.; Burke, D. C. *J. Org. Chem.* **1955**, *20*, 1501-1507.

(3) Schwartsmann, G.; Brondani da Rocha, A.; Berlinck, R. G. S.; Jimeno, J. *Lancet Oncol.* **2001**, *2*, 221-225.

(4) Burja, A. M.; Banaigs, B.; Abou-Mansour, E.; Burgess, J. G.; Wright, P. C. *Tetrahedron* **2001**, *57*, 9347-9377.

(5) Proksch, P.; Edrada, R. A.; Ebel, R. *Appl. Microbiol. Biotechnol.* **2002**, *59*, 125-134.

(6) (a) Luesch, H.; Harrigan, G. G.; Goetz, G.; Horgen, F. D. *Curr. Med. Chem.* **2002**, *9*, 1791-1806. (b) Bewley, C. A.; Faulkner, D. J. *Angew. Chem. Int. Ed.* **1998**, *37*, 2162-2178.

(7) Of course, there are exceptions. One case of particular interest in Hawaii is kahalalide F, which is sequestered by the sea hare *Elysia rubefescens* from its algal food source *Bryopsis* sp. Yields of kahalalide F from the sea hare are significantly greater than from the green algae. It is believed the high concentration of the compound in the *Elysia* functions as a feeding deterent towards the sea hare's predators. Becerro, M. A.; Goetz, G.; Paul, V. J.; Scheuer, P. J. *J. Chem. Ecol.* **2001**, *27*, 2287-2291.

(8) Pettit, G. R.; Kamano, Y.; Herald, C. L.; Fujii, Y.; Kizu, H.; Boyd, M. R.; Boettner, F. E.; Doubek, D. L.; Schmidt, J. M.; Chapuis, J.-C. *Tetrahedron* **1993**,

49, 9151-9170. One ton of the sea hare *Dolabella auricularia* was collected to isolate a milligram of dolastatin 10.

(9) Staley, J. T.; Castenholz, R. W.; Colwell, R. R.; Holtz, J. G.; Cane, M. D.; Pace, N.R.; Salyers, A. A.; Tiedje, J. M. The Microbial World: Foundation of the Biosphere, a report from The American Acadamey of Microbiology, 1997.

(10) Gerwick, W. H.; Tan, L. T.; Sitachitta, N. In *The Alkaloids*; Cordell, G. A., Ed.; Academic Press: San Diego, 2001; Vol. 57, pp 75-184.

(11) Stone, M. J.; Williams, D. H. *Mol. Microbiol.* **1992**, *6*, 29-34.

(12) Moore, R. E. *Pure & Appl. Chem.* **1982**, *54*, 1919-1934.

(13) Pietra, F. *A Secret World: Natural Products of Marine Life*; Birkhäuser: Basel, Switzerland, 1990.

(14) Paul, V. J. (University of Guam), personal communication.

(15) Moore, R. E.; Corbett, T. H.; Patterson, G. M. L.; Valeriote, F. A. *Current Pharmaceutical Design* **1996**, *2*, 317-330.

(16) Goldie, J. H.; Coldman, A. J. *Drug Resistance in Cancer: Mechanism and Models*; Cambridge University Press: Cambridge, 1998; p 59.

(17) Göker, E.; Gorlick, R.; Bertino, J. R. In *Drug Resistance in the Treatment of Cancer*; Pinedo, H. M.; Giaccone, G., Ed.; Cambridge University Press: Cambridge, 1998; Chapter 1, p 1.

(18) Lewis, R. *FDA Consumer* **1995**, *27*, http://www.fda.gov/fdac/795_toc.html

(19) Goldie, J. H.; Coldman, A. J. *Drug Resistance in Cancer: Mechanism and Models*; Cambridge University Press: Cambridge, 1998; p 12.

(20) Corbett, T. H.; Valeriote, F. A.; Polin, L.; Panchapor, C.; Pugh, S.; White, K.; Lowichik, N.; Knight, J.; Bissery, M.-C.; Wozniak, A.; LoRusso, P.; Biernat, L.; Polin, D.; Knight, L.; Biggar, S.; Looney, D.; Demchik, L.; Jones, J.; Jones, L.; Blair, S.; Palmer, K.; Essenmacher, S.; Lisow, L.; Mattes, K. C.; Cavanaugh, P. F.; Rake, J. B.; Baker, L. H. In *Cytotoxic Anticancer Drugs: Models and Concepts for Drug Discovery and Development;* Valeriote, F. A., Corbett, T. H. , Baker, L. H., Eds.; Kluwer Academic Publishers: Norwell, 1992; pp 35-87.

(21) Valeriote, F. A.; Moore, R. E.; Patterson, G. M. L.; Paul, V. J.; Scheuer, P. J.; Corbett, T. H. In *Developments in Oncology*; Valeriote, F. A., Corbett, T. H., Baker, L. H., Eds.; Kluwer Academic Publishers: Norwell, 1994; pp 1-26.

(22) Mynderse, J. S.; Moore, R. E.; Kashiwagi, M.; Norton, T. R. *Science* **1977**, *196*, 538-540.

(23) Kashiwagi, M.; Mynderse, J. S.; Moore, R. E.; Norton, T. R. *J. Pharm. Sci.* **1980**, *69*, 735-738.

(24) Slater, G. P.; Blok, V. C. *Wat. Sci. Technol.* **1983**, *15*, 181-190.

(25) Tanaka, T.; Yamasaki, K.; Kohda, H.; Tanaka, O.; Mahato, S. B. *Planta Med.* **1980**, (Suppl), 81-83.

(26) Horgen, F. D.; Yoshida, W. Y.; Scheuer, P. J. *J. Nat. Prod.* **2000**, *63*, 461-467.

(27) Harrigan, G. G.; Luesch, H.; Yoshida, W. Y.; Moore, R. E.; Nagle, D. G.; Paul, V. J. *J. Nat. Prod.* **1999**, *62*, 655-658 and references therein.

(28) Da Rocha, A. B.; Lopes, R. M.; Schwartsmann, G. *Curr. Opin. Pharmacol.* **2001**, *4*, 364-369.

(29) Luesch, H.; Moore, R. E.; Paul, V. J.; Mooberry, S. L.; Corbett, T. H. *J. Nat. Prod.* **2001**, *64*, 907-910.

(30) Luesch, H.; Yoshida, W. Y.; Moore, R. E.; Paul, V. J. *J. Nat. Prod.* **2000**, *63*, 1106-1112.

(31) Bhatt, M. V.; Kulkarni, S. U. *Synthesis* **1983**, *4*, 249-282.

(32) Lemieux, R. U.; Giguere, J. *Can. J. Chem.* **1951**, *29*, 678-90.

(33) Fafadia, N. J.; Wakankar, D. M.; Nambudiry, M. E. N. *Chem. Ind.* **1988**, *6*, 203-204.

(34) Seco, J. M.; Latypov, S. K.; Quiñoá, E.; Riguera, R. *J. Org. Chem.* **1997**, *62*, 7569-7574.

(35) Harrigan, G. G.; Luesch, H.; Yoshida, W. Y.; Moore, R. E.; Nagle, D. G.; Biggs, J.; Park, P. U.; Paul, V. J. *J. Nat. Prod.* **1999**, *62*, 464-467.

(36) Rablen, P. R.; Lockman, J. W.; Jorgensen, W. L. *J. Phys. Chem. A.* **1998**, *102*, 3782-3797. Adopting this conformation induces a *syn*-pentane interaction between the methyl C-9 and C-23. The added stabilization predicted for the bidentate chelation of the hydroxy group on C-7 (*ca.* 9 kcal/mol) should offset the cost of this steric interaction (*ca.* 1-3 kcal/mol). March, J. *Advanced Organic Chemistry*;

John Wiley & Sons: New York, 1985; pp 121-122. The last value is derived from the difference between the *syn* and antiperiplanar conformers of butane (4 to 6 kcal/mol) and corresponding values for ethane (*ca.* 3 kcal/mol).

(37) Unfortunately, no NOEs could be obtained to verify or refute this assertion as too little material was available even to detect a NOE correlation between H-9 and H-8 that should be observed regardless of the conformation.

(38) Di Marzo, V.; Bisogno, T.; De Petrocellis, L.; Melck, D.; Martin, B. R. *Curr. Med. Chem.* **1999**, *6*, 721-744.

(39) Luesch, H. The Search for New Anticancer Drugs from Marine Cyanobacteria and Investigation on the Biosynthesis of Cyanobacterial Metabolites. Ph.D. Thesis, University of Hawaii, Honolulu, HI, 2002, p 174.

(40) Witanowski, M; Webb, G. A. *Nitrogen NMR*; Plenum Press: New York, 1973; pg 188.

(41) Laxaphycin B: Bonnard, I.; Rolland, M.; Francisco, C.; Banaigs, B. *Lett. Pept. Sci.* **1997**, *4*, 289-292. Lobocyclamide B: MacMillan, J. B.; Molinski, T. F. *Org. Lett.* **2002**, *4*, 1883-1886.

(42) Trogen, G. B.; Annila, A.; Eriksson, J.; Kontteli, M.; Meriluoto, J.; Sethson, I.; Zdunek, J.; Edlund, U. *Biochemistry*, **1996**, *35*, 3197-3205.

(43) Rinehart, K. L.; Sakai, R.; Kishore, V.; Sullins, D. W.; Li, K. M. *J. Org. Chem.* **1992**, *57*, 3007-3013.

(44) Ozonolysis of the dehydration product 4-amino-5-phenyl-pent-2-enoic acid produces phenylalanine which after prolonged ozonolysis affords aspartic acid. Mori, M.; Chiba, N. *Liebigs Annalen der Chime* **1989**, *10*, 957-962.

(45) The (*R*)-MPA derivative was formed by DCC coupling and purified by silica chromatography with increasing amounts of ethyl acetate in hexane. The (*S*)-adduct was formed by EDCI coupling and after partitioning between cold 1 N HCl and CH_2Cl_2, the organic layer provided a derivative clean enough to be analyzed.

(46) Latypov, S. K.; Seco, J. M.; Quiñoá, E.; Riguera, R. *J. Am. Chem. Soc.* **1998**, *120*, 877-882.

(47) García, R.; Seco, J. M.; Vázquez, S. A.; Quiñoá, E.; Riguera, R. *J. Org. Chem.* **2002**, *67*, 4579-4589.

(48) A similar phenomenon has been observed for β-hydroxy ketones derived from the aldol reactions of chiral aldehydes see: Roush, W. R.; Bannister, T. D.; Wendt, M. D.; VanNieuwenhze, M. S.; Gustin, D. J.; Dilley, G. J.; Lane, G. C.; Scheidt, K. A.; Smith, W. J., III *J. Org. Chem.* **2002**, *67*, 4284-4289.

(49) While no exceptions were found for Ahppa containing compounds, this trend was not observed in all other amino acid-derived 4-amino-3-hydroxyacids. Exceptions were most common when a polar (e.g. OH) or a bulky group was directly adjacent to the γ-stereocenter.

(50) If this hydrogen bonding occurs within the Ahppa unit of **1.12** then the concerns outlined in Matsumori, N.; Kaneno, D.; Murata, M.; Nakamura, H.; Tachibana, K. *J. Org. Chem.* **1999**, *64*, 866-876 regarding the use of NOE correlations to determine the relative stereochemistry of vicinal center that have a small proton-proton coupling would not be valid.

(51) Andrés, J. M.; Pedrosa, R.; Pérez, A.; Pérez-Encabo, A. *Tetrahedron* **2001**, *57*, 8521-8530.

(52) Palomo, C.; Miranda, J. I.; Linden, A. *J. Org. Chem.* **1996**, *61*, 9196-9201.

(53) Liang, B.; Richard, D. J.; Portonovo, P. S.; Joullie, M. M. *J. Am. Chem. Soc.* **2001**, *123*, 4469-4474.

(54) Bonini, B. F.; Comes-Franchini, M.; Fochi, M. I.; Laboroi, F.; Mazzanti, G.; Ricci, A.; Varchi, G. *J. Org. Chem.* **1999**, *64*, 8008-8013.

(55) Doi, T.; Kokubo, M.; Yamamoto, K.; Takahashi, T. *J. Org. Chem.* **1998**, *63*, 428-429.

(56) Ina, H.; Kibayashi, C. *J. Org. Chem.* **1993**, *58*, 52-61.

(57) Metabolites containing an analogous *O*-Me-Tyr unit have been isolated from marine bacteria SANK70992. Oosumi, H.; Kaneko, I.; Minekura, H.; Takamatsu, Y.; Maruyama, Y.; Kinoshita, T. Jpn. Kokai Tokkyo Koho 95-157406. 1996.

(58) Stratmann, K.; Burgoyne, D. L.; Moore, R. E.; Patterson, G. M. L.; Smith, C. D. *J. Org. Chem.* **1994**, *59*, 7219-7226.

(59) Sato, T.; Shibazaki, M.; Yamaguchi, H.; Abe, K.; Matsumoto, H.; Shimizu, M. *J. Antibiotics* **1994**, *47*, 588-590.

(60) Ōmura, S.; Imamura, N.; Kawakita, K.; Mori, Y.; Yamazaki, Y.; Masuma, R.; Takahashi, Y.; Tanaka, H.; Huang, L. Y.; Woodruff, H. B. *J. Antibiotics* **1986**, *39*, 1079-1085.

(61) Harrigan, G. G.; Luesch, H.; Yoshida, W. Y.; Moore, R. E.; Nagle, D. G.; Paul, V. J.; Mooberry, S. L.; Corbett, T. H.; Valeriote, F. A. *J. Nat. Prod.* **1998**, *61*, 1075-1077.

(62) Reshef, V.; Carmeli, S. *Tetrahedron* **2001**, *57*, 2885-2894.

(63) Fujii, K.; Sivonen, K.; Naganawa, E.; Harada, K. *Tetrahedron* **2000**, *56*, 725-733.

(64) Fujii, K.; Sivonen, K.; Nakano, T.; Harada, K. *Tetrahedron* **2002**, *58*, 6863-6871 and references therein.

(65) Okino, T.; Qi, S.; Matsuda, H.; Murakami, M.; Yamaguchi, K. *J. Nat. Prod.* **1997**, *60*, 158-161.

(66) Bonjouklian, R.; Smitka, T. A.; Hunt, A. H.; Occolowitz, J. L.; Perun, T. J., Jr.; Doolin, L.; Stevenson, S.; Knauss, L.; Wijayaratne, R.; Szewcyzk, S.; Patterson, G. M. L. *Tetrahedron* **1996**, *52*, 395-404.

(67) Matern, U.; Oberer, L.; Falchetto, R. A.; Erhard, M.; König, W. A.; Herdman, M.; Weckesser, J. *Phytochemistry* **2001**, *58*, 1087-1095.

(68) Nogle, L. M.; Williamson, R. T..; Gerwick, W. H. *J. Nat. Prod.* **2001**, *64*, 716-719.

(69) Nakanishi, I.; Fujikawa, A.; Imai, K.; Sato, A. *J. Peptide Res.* **2000**, *55*, 120-128.

(70) This position is often modified, i.e. chlorination or O-methylation, and a few examples exist with tryptophan in this position. Murakami, M.; Kodani, S; Ishida, K.; Matsuda, H.; Yamaguchi, K. *Tetrahedron Lett.* **1997**, *38*, 3035-3038.

(71) Ishida, K.; Matsuda, H.; Murakami, M. *Tetrahedron* **1998**, *54*, 5545-5556.

(72) Itou, Y.; Ishida, K.; Shin, H. J.; Murakami, M. *Tetrahedron* **1999**, *55*, 6871-6882.

(73) Ishida, K.; Murakami, M.; Matszuda, H.; Yamaguchi, K. *Tetrahedron Lett.* **1995**, *36*, 3535-3538.

(74) Lee, A. Y.; Smitka, T. A.; Bonjouklian, R.; Clardy, J. *Chemistry & Biology* **1994**, *1*, 113-117.

(75) Silverstein, R. M.; Bassler, C. G.; Morrill, T. C. *Spectrometric Identification of Organic Compounds*; Wiley & Sons: New York, 1981; pg 269.

(76) Gribble, G. W. *J. Nat. Prod.* **1992**, *55*, 1353-1395.

(77) Butler, A.; Walker, J. V. *Chem. Rev.* **1993**, *93*, 1937-1944.

(78) This number excludes the iodine-containing thyroid hormones.

(79) Gribble, G. W. *Acc. Chem. Res.* **1998**, *31*, 141-152.

(80) Gribble, G. W. *Prog. Chem. Org. Nat. Prod.* **1996**, *68*, 1-423.

(81) Coleman, J. E.; Van Soest, R.; Andersen, R. J.; Kelsey, R. G. *J. Nat. Prod.* **1999**, *62*, 1137-1141.

(82) Kazlauskas, R.; Murphy, P. T.; Wells, R. J.; Baird-Lambert, J. A.; Jamieson, D. D. *Aust. J. Chem.* **1983**, *36*, 165-170.

(83) Yoshida, W. Y.; Lee, K. K.; Carroll, A. R.; Scheuer, P. J. *Helv. Chim. Acta* **1992**, *75*, 1721-1725.

(84) Zein, N.; Sinha, A. M.; McGahren, W. J.; Ellestad, G. A. *Science* **1988**, *240*, 1198-1201.

(85) Shpatov, A. V.; Shakirov, M. M.; Raldugin, V. A. *Russ. J. Org. Chem.* **2000**, *36*, 1127-1138.

(86) Carter-Franklin, J. N.; Parrish, J. D.; Tschirret-Guth, R. A.; Little, R. D.; Butler, A. *J. Am. Chem. Soc.* **2003**, *125*, 3688-3689.

(87) Ishihara, J.; Shimada, Y.; Kanoh, N.; Takasugi, Y.; Fukuzawa, A.; Murai, A. *Tetrahedron* **1997**, *53*, 8371-8382.

(88) Electrophilic halogenations are assumed in the biosynthetic schemes since it is well established that terpenoids cyclize by cationic mechanisms. Radical halogenations cannot be excluded though, as the placement of the halides is consistent with both reaction manifolds.

(89) For other examples of marine natural products containing *cis*-decalin systems see: a) Iwagawa, T.; Kaneko, M.; Okamura, H.; Nakatani, M.; Van Soest, R. W. M. *J. Nat. Prod.* **1998**, *61*, 1310-1312. b) Gavagnin, M.; Ungur, N.; Castelluccio, F.; Cimino, G. *Tetrahedron* **1997**, *53*, 1491-1504.

(90) Since the chair conformation is usually 19-23 kJ/mol more stable than the twist-boat conformation and a 1,3-synaxial interaction between methyl groups only offsets approximately 16 kJ/mol, other factors must contribute to the formation of

the *cis*-ring junction. Thermodynamic values from Eliel, E. L.; Wilen, S. H. *Stereochemistry of Organic Compounds*; Wiley & Sons, Inc: New York, 1994; pp 689-707.

(91) For examples of proven 1,3-hydride shifts see Arigoni, D. *Pure & Appl. Chem.* **1975**, *41*, 219-245.

(92) With the A-ring in a twist-boat conformation a 1,3-migration would result in the hydride in the correct axial position, but the vacant *p* orbital in **1.13** would be parallel to the σ bonded hydrogen in this conformation.

(93) For examples of successive 1,2-hydride migrations, e.g. fusiccocin biosynthesis, see MacMillan, J.; Beale, M. H. In *Comprehensive Natural Products Chemistry*; Barton, D., Nakanishi, K., Meth-Cohn, O., Cane, D. E., Eds; Elsevier Science, Ltd.: Exeter, UK, 1999; Vol. 2, pp 217-243.

(94) Serdula, M.; Bartolini, G.; Moore, R. E.; Wiebenga, N.; Gooch, J. *Hawaii Med. J.* **1982**, *41*, 200-201.

(95) Moore, R. E.; Blackman, A. J.; Cheuk, C. E.; Mynderse, J. S.; Matsumoto, G. K.; Clardy, J.; Woodard, R. W.; Cymerman, C. J. *J. Org. Chem.* **1984**, *49*, 2484-2489.

(96) Luesch, H.; Yoshida, W. Y.; Moore, R. E.; Paul, V. J. *Tetrahedron* **2002**, *58*, 7959-7966 and references therein.

(97) *Alpheus frontalis*

(98) Luesch, H.; Yoshida, W. Y.; Moore, R. E.; Paul V. J. *Bioorg. Med. Chem.* **2002**, *10*, 1973-1978 and references therein.

(99) (a) Isolation: Klein, D.; Braekman, J.-C.; Daloze, D.; Hoffmann, L.; Castillo, G.; Demoulin, V. *Tetrahedron Lett.* **1999**, *40*, 695-696. (b) Stereochemistry: Luesch, H.; Yoshida, W. Y.; Moore, R. E.; Paul, V. J. *J. Nat. Prod.* **2000**, *63*, 1437-1439.

(100) The apramides, originally isolated from an earlier re-collection of VP417,[30] are another example of compounds that contains an Thz-Pro unit.

(101) Stachelhaus, T.; Mootz, H. D.; Marahiel, M. A. *Chem. Biol.* **1999**, *6*, 493-505.

(102) Challis, G. L.; Ravel, J.; Townsend, C. A. *Chem. Biol.* **2000**, *7*, 211-224.

(103) The simplest modifications would be as follows: GGG (Gly) to ATG (Met); GCA (Ala) to GAA (Gln) or GCG (Ala) to GAG (Gln); TGT (Cys) to CAT (His) or TGC (Cys) to CAC (His).

(104) Sone, H.; Kondo, T.; Kiryu, M.; Ishiwata, H.; Ojika, M.; Yamada, K. *J. Org. Chem.* **1995**, *60*, 4774-4781.

(105) Luesch, H.; Yoshida, W. Y.; Moore, R. E.; Paul V. J. *J. Nat. Prod.* **2000**, *63*, 611-615.

(106) (a) Isolation: Marquez, B. L.; Watts, K. S.; Yokochi, A.; Roberts, M. A.; Verdier-Pinard, P.; Jimenez, J. I.; Hamel, E.; Scheuer, P. J.; Gerwick, W. H. *J. Nat. Prod.* **2002**, *65*, 866-871. (b) Synthesis: Cetusic, J. R. P.; Green, F. R., III; Graupner, P. R.; Oliver, M. P. *Org. Lett.* **2002**, *4*, 1307-1310.

(107) Yang, N. C.; Finnegan, R. A. *J. Am. Chem. Soc.* **1958**, *80*, 5845-5848.

(108) Zimmerman, H. E.; Robbins, J. D.; McKelvey, R. D.; Samuel, C. J.; Soussa, L. R. *J. Am. Chem. Soc.* **1974**, *96*, 4630-4643.

(109) Andersson, P. G.; Sharpless, K. B. *J. Am. Chem. Soc.* **1993**, *115*, 7047-7048.

(110) The anti diastereomer, suspected in homohydroxydolabellin, has a coupling.of approximately 4 Hz

(111) Matsumori, N.; Kaneno, D.; Murata, M.; Nakamura, H.; Tachibana, K. *J. Org. Chem.* **1999**, *64*, 866-876.

(112) Methanol was excluded from the isolation procedure until it was apparent from the ^{1}H NMR that lyngbyabellin D contained a methyl ester. Therefore it is also unlikely lyngbyabellin D arises from methanolysis of a C-1/C-24 linkage.

(113) Harborne, J. B. *Nat. Prod. Rep.* **2001**, *18*, 361-379.

(114) After NMR characterization, FABMS indicated that a second compound was present in the sample (FABMS *m/z* = 1408). Further HPLC purification using MeOH yielded pure obyanamide (**1.48**) as described above, but it was this other minor compound which was responsible for most of the activity. Too little material was isolated (<200 μg) for characterization of the compound which exhibited cytotoxicity <1 μg/ml against the KB cell line.

(115) For representative examples see: (a) Sone, H.; Kigoshi, H.; Yamada, K. *Tetrahdron* **1997**, *53*, 8149-8154.; (b) Luesch, H.; Yoshida, W. Y.; Moore, R. E.; Paul, V. J.; Mooberry, S. L. *J. Nat. Prod.* **2000**, *63*, 611-615.; (c) Pettit, G. R.; Kamano, Y.; Brown, P.; Gust, D.; Inoue, M.; Herald, C. L. *J. Am. Chem. Soc.*

1982, *104*, 905-907.; (d) Ojika, M.; Nemoto, T.; Nakamura, M.; Yamada, K. *Tetrahedron Lett.* **1995**, *36*, 5057-5058.

(116) Golakoti, T.; Ogino, J.; Heltzel, C. E.; Husebo, T. L.; Jensen, C. M.; Larsen, L. K.; Patterson, G. M. L.; Moore, R. E.; Mooberry, S. L.; Corbett, T. H.; Valeriote, F. A. *J. Am. Chem. Soc.* **1995**, *117*, 12030-12049.

(117) Carter, D. C.; Moore, R. E.; Mynderse, J. S.; Niemczura, W. P.; Todd, J. S. *J. Org. Chem.* **1984**, *49*, 236-241.

(118) Pettit, G. R.; Kamano, Y.; Kizu, H.; Dufresne, C.; Herald, C. L.; Bontems, R. J.; Schmidt, J. M.; Boettner, F. E.; Nieman, R. A. *Heterocycles* **1989**, *28*, 553-558.

(119) Harrigan, G. G.; Yoshida, W. Y.; Moore, R. E.; Nagle, D. G.; Park, P. U.; Biggs, J.; Paul, V. J.; Mooberry, S. L.; Corbett, T. H.; Valeriote, F. A. *J. Nat. Prod.* **1998**, *61*, 1221-1225.

(120) Pettit, G. R.; Xu, J.; Hogan, F.; Williams, M. D.; Doubek, D. L.; Schmidt, J. M.; Cerny, R. L.; Boyd, M. R. *J. Nat Prod.* **1997**, *60*, 752-754.

(121) Sone, H.; Nemoto, T.; Ishiwata, H.; Ojika, M.; Yamada, K. *Tetrahedron Lett.* **1993**, *34*, 8449-8452.

(122) (a) MacMillan, J. B.; Ernst-Russell, M. A.; de Ropp, J. S.; Molinski, T. F. *J. Org. Chem.* **2002**, *67*, 8210-8215. (b) MacMillan, J. B.; Molinski, T. F. *Org. Lett.* **2002**, *4*, 1883-1886.

(123) Luesch, H.; Williams, P. G.; Yoshida, W. Y.; Moore, R. E.; Paul, V. J. *J. Nat. Prod.* **2002**, *65*, 996-1000.

(124) Two HMBC experiments optimized for $^{3}J_{CH}$ = 7 and 4 Hz respectively failed to show any correlation between C-1 and H-43.

(125) It should be noted that the assignment of the ROESY correlation to the methyl group of the lactic (Table 18) from the δ_H 0.87 proton signal is tentative since the proton signals for H-44 and H-34 overlap. Analysis of models suggests that H-40 is responsible for this correlation to the lactic acid unit rather than H-34. Unfortunately, too little material remains to establish conclusively by NMR studies in other solvents, which methyl group showed a ROESY correlation to H-44.

(126) Agami, C.; Cheramy, S.; Dechoux, L.; Melaimi, M *Tetrahedron* **2001**, *57*, 195-200.

(127) The methylation occurs predominantly from the *re* face of the enolate to yield the anti α-methyl-β-amino acid as the major product. cf. Davis (1994).

(128) (a) Fujii, K.; Ikai, Y.; Oka, H.; Suzuki, M.; Harada, K. *Anal. Chem.* **1997**, *69*, 5146-5151. (b) Fujii, K.; Ikai, Y.; Mayumi, T.; Oka, H.; Suzuki, M.; Harada, K. *Anal. Chem.* **1997**, *69*, 3346-3352.

(129) Fernandez-Suarez, M.; Munoz, L.; Fernandez, R.; Riguera, R. *Tetrahedron: Asymmetry* **1997**, *8*, 1847-1854 and references within.

(130) The coupling constant was measured from the $^{1}J_{CH}$ satellites in the HMBC spectrum.

(131) The elevated temperature was necessary to shift the proton signal for the residual water away from the acyl oxy methine proton signals so they could be irradiated in TOCSY experiments.

(132) Smith, A. B., III; Wood, J. L.; Wong, W.; Gould, A. E.; Rizzo, C. J.; Barbosa, J.; Funayama, S.; Komiyama, K.; Ōmura, S. *J. Am. Chem. Soc.* **1996**, *118*, 8308-8315.

(133) Salomon, C. E.; Williams, D. H.; Lobkovsky, E.; Clardy, J. C.; Faulkner, D. J. *Org. Lett.* **2002**, *4*, 1699-1702.

(134) Boger, D. L.; Patane, M. A.; Zhou, J. *J. Am. Chem. Soc.* **1994**, *116*, 8544-8556.

(135) Conformer A has a ROESY correlation between H-13 and H-15, while conformer B between H-12 and H-15.

(136) Bates, R. B.; Brusoe, K. G.; Burns, J. J.; Caldera, S.; Cui, W.; Gangwar, S.; Gramme, M. R.; McClure, K. J.; Rouen, G. P.; Schadow, H.; Stessman, C. C.; Taylor, S. R.; Vu, V. H.; Yarick, G. V.; Zhang, J.; Pettit, G. R.; Bontems, R. *J. Am. Chem. Soc.* **1997**, *119*, 2111-2113.

(137) Bai, R.; Bates, R. B.; Hamel, E.; Moore, R. E.; Nakkiew, P.; Pettit, G. R.; Sufi, B. A. *J. Nat. Prod.* **2002**, *65*, 1824-1829.

(138) Kofron, J. L.; Kuzmic, P.; Kishoe, V.; Gemmecker, G.; Fesik, S. W.; Rich, D. H. *J. Am. Chem. Soc.* **1992**, *114*, 2670-2675.

(139) Econosil C_{18}, 250 x 10mm, linear gradient 20 % CH_3CN in H_2O to 100 % CH_3CN over 20 min then 100 % for 40 min, flow rate 2 mL/min, detection at 220 nm; **1.63** (t_R 25.4 min), **1.64** (t_R 24.5 min).

(140) Hartmut, F.; Nicholson, G. J.; Bayer, E. *J. Chrom. Sci.* **1977**, *15*, 174-176.

(141) Provided by Robert Bates at the University of Arizona.

(142) Kimura, J.; Takada, Y.; Inayoshi, T.; Nakao, Y.; Goetz, G.; Yoshida, W. Y.; Scheuer, P. J. *J. Org. Chem.* **2002**, *67*, 1760-1767.

(143) This procedure had been used to synthesize (2*S*,3*R*)-MAP hydrochloride. Davies, S. G.; Walters, I. A. S.; Ichihara, O. *Synlett* **1994**, *2*, 117-118.

(144) Davies, S. G.; Walters, I. A. S. *J. Chem. Soc. Perkin Trans. 1* **1994**, *9*, 1129-1139.

(145) The diastereomeric ratio was based on the ^{1}H NMR integration of the methyl protons in accordance with Davis, S. G.; Ichihara, O. *Tetrahedron: Asymmetry* **1991**, *2*, 183-186.

(146) Prepared according to Marfey, P. *Carlsberg Res. Commun.* **1984**, *49*, 591-596 with the appropriate amino amide.

(147) It should be noted that our proposed elution order [*ent*-(2*S*,3*S*), *ent*-(2*R*,3*S*), (2*S*,3*R*), (2*R*,3*R*)] of the DL-FDLA derivatives differs from that reported for the L-FDAA derivatives [(2*R*,3*R*), (2*S*,3*R*)].[142] Comparison of the DL-FDLA derivatized hydrolyzate of **1.63** established that our 2nd and 3rd standards were present [ent-(2*R*,3*S*), (2*S*,3*R*)], as confirmed by coinjection, and not the 2nd and 4th as would be expected from the FDAA derivatives elution order. In Ulongamide F,[121] which

contains (2*R*,3*R*)-Amha, the 1st and 4th standards were present in the DL-hydrolyzate, not the 1st and 3rd. Apparently the side chain of the amino amide has some effect on the elution order.

(148) The same elution order with respect to C-3 (3*S* elutes before 3*R*) was seen when synthetic MAP units were derivatized with the commercially available Marfey reagent (1-fluoro-2, 4-dinitrophenyl-L-alanamide, L-FDAA). In this instance the C-2 diastereomers could not be separated. See Williams, D. E.; Burgoyne, D. L.; Rettig, S. J.; Andersen, R. J.; Faith-Afshar, Z. R.; Allen, T. M. *J. Nat. Prod.* **1993**, *56*, 545-551.

(149) FDLA derivatized *N*-Me-Leu was also detected at *m/z* 438 in the hydrolyzate. The DL-mixture showed peaks at 32.3 and 35.3 minutes while the L-mixture contained a peak at 32.3 minutes. The identities of these peaks were confirmed by coinjection of an authentic standard.

(150) Reductive deoxygenation using *p*-toluenesulfonyl hydrazide and sodium cyanoborohydride resulted in reduced **1.63**. A second reaction of **1.63** and *p*-toluenesulfonyl hydrazide in CH_2Cl_2 failed to yield any tosylhydrazone.

(151) That the successful synthetic route to lyngbyastatin 1 (**1.64**) employed *N*,*N*-diBoc-L-Ala suggests the same problem with lactam formation (**1.91**) was encountered. (cf. Bai, R. *et al* 2002)

(152) (a) Maibaum, J.; Rich, D. H. *J. Org. Chem.* **1988**, *53*, 869-873. (b) Schuda, P. F.; Greenlee, W. J.; Chakravarty, P. K.; Eskola, P. *J. Org. Chem.* **1988**, *53*, 873-875.

(153) HPLC analysis of the final product (**1.93**) indicated that approximately 15 % epimerization had occurred at C-4 during the synthesis.

(154) Under the HPLC analysis conditions, the C-3 diastereomers of derivatized **1.93** were not resolved, i.e. only a single peak was detected when the mixture of L-FDLA derivatized (3*R*,4*S*)- and (3*S*,4*S*)-**1.93** was injected. Likewise, when the D-FDLA derivatized mixture was analyzed on the Bondclone C_{18} column the standards equivalent to (3*S*,4*R*)- and (3*R*,4*S*)-**1.93** appeared as a single peak, but when these samples were submitted for LC-MS analysis on a different C_{18} column the standards equivalent to (3*S*,4*R*)- and (3*R*,4*S*)-**1.93** resolved into two peaks.

(155) In general the stereochemical outcome (Cram vs. Anti-Cram) of the reductions of the natural products was irrelevant to our analysis.

(156) On average the ratio of the two signals was 61 and 53 % for the minor reduction product obtained from MeOH-d_4 and MeOH respectively. The theoretical calculated ratio of $(M+1+H)^+/(M+H)^+$ is 61 % for $C_{50}H_{82}N_8O_{11}$.

(157) The samples of **1.63** from NIH199, 153, and 143 were combined before the stereochemistry of the Ibu unit was known. This precluded determining if each collection had the same ratio of epimers as might be expected if the diastereomers were artifacts of the isolation procedure and not due to biosynthetic differences in the strains.

(158) Fusetani, N. In *Drugs from the Sea;* Fusetani, N., Ed.; Karger, New York, 2000; pp 1-5.

(159) Similar to Van Draanen, N. A.; Arseniyadis, S.; Crimmins, M. T.; Heathcock, C. H. *J. Org. Chem.* **1991**, *56*, 2499-2506.

(160) Kinoshita, M.; Hamazaki, H.; Awamura, M. *Bull. Chem. Soc. Jpn* **1978**, *51*, 3595-3598.

(161) Crout, D. H. G.; Whithouse, D. *J. Chem. Soc. Perkins Trans. 1* **1997**, *5*, 544-549.

(162) The erythro diastereomer 2*S*,3*S* has an $[\alpha]^{23}_{D}$ value of +23° (*c* 2.30, 0.1 N HCl). Crout, D. H. G.; Whithouse, D. *J. Chem. Soc. Perkins Trans. 1* **1997**, *5*, 544-549.

(163) Kocienski, P. S. *Protecting Groups;* Gutmann & Co. GmbH: New York, 1994; pp 193-195.

(164) Tietze, L. *Reactions and Synthesis in the Organic Chemistry Laboratory*; University Science Books: California, 1989; pp 437-438.

(165) These three signals overlapped significantly and had a combined integration of 11 relative to the other observed signals.

(166) This signal is not present in the starting material.

(167) Insufficient material was available to obtain a ^{13}C NMR spectrum that showed all expected carbon signals.

(168) Ackman, R. G.; Retson, M. E.; Gallay, L. R.; Vandenheuvel, F. A. *Can J. Chem.* **1961**, *39*, 1956-1963.

(169) Klaus, R.; Fisher, W. *Chromatographia* **1989**, *23*, 137-140.

(170) The elution order of (2*R*,3*R*) vs (2*S*,3*R*) and *ent*-(2*S*,3*R*) vs *ent*-(2*R*,3*R*) was assigned based on the relative integration of the HPLC peaks after derivatization

with L- and DL-FDLA. The major peaks were assigned as (2*R*,3*R*) and *ent*-(2*R*,3*R*).